A NOVEL FRAMEWORK FOR ENHANCING MARINE DUAL FUEL ENGINES ENVIRONMENTAL AND SAFETY PERFORMANCE VIA DIGITAL TWINS

Sokratis Stoumpos

A thesis presented in fulfilment of the requirements for the degree of
Doctor of Philosophy

University of Strathclyde

Department of Naval Architecture, Ocean and Marine Engineering

Glasgow

June 2020

Declaration of Authenticity and Author's Rights

This thesis is the result of the author's original research. It has been composed by the author and has not been previously submitted for examination, which has led to the award of a degree.

Signed: Sokratis Stoumpos

Date: 4 June 2020

To my beloved father, Evangelos

“Ἓν οἶδα ὅτι οὐδὲν οἶδα”

Σωκράτης, 470 π.Χ - 399 π.Χ.

“the one thing I know is that I know nothing”

Socrates, 470 BC – 399 BC

ACKNOWLEDGEMENTS

First and foremost, I would like to express my gratitude to my advisor, Dr. G. Theotokatos, for giving me the opportunity to acquire my PhD diploma though this research study and for his support and willingness to enlighten me with his vast knowledge throughout these years. His guidance and support advanced my engineering perspective and assisted me interpret complex procedures and ideas in a comprehensive and simplistic manner.

Furthermore, I would like to thank my family for their support, the inspiration and guidance they unconditionally offered me. Based on his long years' experience on the role of marine engineer on-board vessels, my dear father vastly assisted me through his long talks on numerous everyday challenges, which affected my engineering understanding. Through his life difficulties, these unforgettable lessons helped me form my perception not only on a discipline level but also on a life aspect. Thank you pops for the good things you given me, and may God rest your soul. Equally, through her constant care, her concerns and trust on me, my beloved mother offered my endless courage and support to keep committing in my studies despite all the difficulties, thus holding a unique place in my heart. Thank you both for your patience, courage and valuable lessons learned.

Lastly, I would like to thank my friends and colleagues from the University of Strathclyde Maritime Research Safety Center (MSRC) and Lloyd's Register for their patience and support through the hard times.

Gamma Technologies Suite© support is greatly acknowledged by the author.

RESEARCH OUTPUT

The outcome of this research dissertation is associated to both research and industrial/commercial practices. Hence, during this investigation and development, dissemination activities were performed, including journal articles and conference proceedings publications, as follows.

Journal Publications

Stoumpos S., Theotokatos G., Mavrelos C., Boulougouris E. (2020). Towards Marine Dual Fuel Engines Digital Twins – Integrated Modelling of Thermodynamic Processes and Control System Functions. Journal of Marine Science Engineering 2020, 8(3), 200; https://doi.org/10.3390/jmse8030200

Theotokatos G., Stoumpos S., Bolbot V. and Boulougouris E. (2019). Simulation-based investigation of a marine dual fuel engine. Journal of Marine Engineering & Technology, 19:sup1, 5-16, https://doi.org/10.1080/20464177.2020.1717266

Stoumpos, S., Theotokatos, G., Boulougouris, E., Vassalos, D., Lazakis, I. and Livanos, G. (2018). Marine dual fuel engine modelling and parametric investigation of engine settings effect on performance-emissions trade-offs. Ocean Engineering, 157, 376-386. ISSN 0029-8018, https://doi.org/10.1016/j.oceaneng.2018.03.059

Conference Publications

Theotokatos G., Stoumpos S., Bolbot V., Boulougouris E. and Vassalos D. (2018). Marine Dual Fuel Engine Control System Modelling and Safety Implications Analysis. In: 14th International Naval Engineering Conference and Exhibition. IMarEST, London. http://doi.org/10.24868/issn.2515-818X.2018.064

Theotokatos G., Stoumpos S., Lazakis I. and Livanos G. (2016). Numerical study of a marine dual-fuel four-stroke engine. In: Maritime Technology and Engineering III. CRC Press, London, pp. 777-783. ISBN 9781498795937. https://doi.org/10.1201/b21890-100

Theotokatos G., Stoumpos S., Ding Y., Xiang L. and Livanos G. (2015). Computational investigation of a large dual fuel marine engine. In: Shipping in Changing Climates Conference 2015 - SCC2015, Glasgow, UK.

TABLE OF CONTENTS

LIST OF FIGURES

LIST OF TABLES

LIST OF APPENDICES

ABBREVIATIONS

0D	Zero-dimensional
1D	One-dimensional
3D	Three-dimensional
A/C	Air Cooler
ABP	Air Bypass System
ABS	American Bureau of Shipping
AI	Artificial Intelligence
AMS	Alarms and Monitoring System
ANN	Artificial Neural Networks
ATEX	Atmospheres Explosibles – "Explosive Atmospheres"
BDC	Bottom Dead Center
BMEP	Brake Mean Effective Pressure
BSEC	Brake Specific Energy Consumption
BSFC	Brake Specific Fuel Consumption
CA	Crank Angle
CAPEX	Capital Expenditure
CFD	Computational Fluid Dynamics
CI	Compression Ignition
CNG	Compressed Natural Gas
CO	Carbon Monoxide
CO_2	Carbon Dioxide
CPS	Cyber-Physical System
CRM	Current Running operating Mode
DD	Data-Driven model
DF	Dual Fuel
DNV-GL	Det Norske Veritas - Germanischer Lloyd
DoE	Design of Experiments
DT	Digital Twin
DTG	Diesel to Gas mode switching
EA	Evolutionary Algorithms
EC	European Commission
ECA	Emission Control Area
EDS	Engine Diagnostics System
EEDI	Energy Efficiency Design Index
EEOI	Energy Efficiency Operational Indicator
EGCS	Exhaust Gas Cleaning System
EGR	Exhaust Gas Recirculation

EMSA	European Maritime Safety Agency
ES	Expert Systems
ESS	Engine Safety System
ETA	Event Tree Analysis
EWG/WG	Exhaust Waste Gate
FMEA	Failure Mode, Effects, and Analysis
FMECA	Failure Mode, Effects & Criticality Analysis
FOS	Faulty Operation Simulator
FTA	Fault Tree Analysis
GAV	Gas Admission Valve
GHG	Greenhouse Gasses
GT	Gamma Technologies
GTD	Gas to Diesel mode switching
GVU	Gas Valve Unit
HAZID	Hazard Identification
HAZOP	Hazard and Operability
HC	Hydrocarbons
HCCI	Homogeneous Charge Compression Ignition
HFO	Heavy Fuel Oil
HP-EGR	High Pressure Exhaust Gas Recirculation
HRR	Heat Release Rate
IACS	International Association of Classification Societies
IEC	International Electrotechnical Commission
IGC	International Code of the Construction and Equipment of Ships Carrying Liquefied Gases in Bulk
IGF	International Code of Safety for Ships Using Gases or Other Low-Flashpoint Fuels
IIoT	Industrial Internet of Things
IMEP	Indicated Mean Effective Pressure
IMO	International Maritime Organization
IoT	Internet of Things
LFO	Light Fuel Oil
LHV	Lower Heating Value
LNG	Liquefied Natural Gas
LP-EGR	Low Pressure Exhaust Gas Recirculation
LPG	Liquefied Petroleum Gas
LR	Lloyd's Register
LSFO	Low Sulphur Fuel Oil
MARPOL	International Convention for the Prevention of Marine Pollution
MCR	Maximum Continuous Rating

MEPC	Marine Environment Protection Committee
MGO	Marine Gas Oil
MIMO	Multiple Input–Multiple Output
MISO	Multiple Input–Single Output
ML	Machine Learning
MOGA	Multi-objective Genetic Algorithm
MVEM	Mean Value Engine Model
NDA	Non-Disclosure Agreement
NG	Natural Gas
NN	Neural Networks
NSGA	Non-dominated Sorting Genetic Algorithm
OPEX	Operational Expenses
PHA	Preliminary Hazard Analysis
PI	Proportional–Integral controller
PID	Proportional–Integral–Derivative controller
PM	Particulate Matter
RPN	Risk Priority Number
SCR	Selective Catalytic Reduction
SEEMP	Ship Energy Efficiency Management Plan
SFOC	Specific Fuel Oil Consumption
SHD	Engine Shutdown
SLD	Engine Slowdown
SOI	Start of Injection
SOLAS	International Convention for the Safety of Life at Sea
T/C	Turbocharger
TDC	Top Dead Center
UDS	Unified Digital System
UEC	Unified Engine Controls
ULSFO	Ultra-Low Sulphur Fuel Oil
UNIC	Unified Controls
US EPA	United States Environmental Protection Agency
VGT	Variable Geometry Turbocharger
VLSFO	Very-Low Sulphur Fuel Oil
WFE	Water Fuel Emulsification

NOMENCLATURE

A	Pipe cross-sectional flow area	m^2
AFR_{st}	Stoichiometric equivalence ratio	kg/kg
C_f	Friction factor	—
C_x	Stikei constants	—
D	Pipe diameter	m
dp	Pressure differential acting across dx	Pa
dx	Discretization length	m
e	Total specific internal energy	J/kg
$E_{f,total}$	Total fuel energy	J
FF	Weight of Wiebe function	—
H	Total specific enthalpy	J/kg
H_2O	Water	—
H_x	Hydrogen	—
k	Reaction rates constants	m^3/kmol/s
K_p	Pressure loss coefficient	—
LHV	Lower heating value	J/kg
m	Mass / Wiebe function parameter m	kg / —
$\dot{m}$	Mass flow rate	kg/s
$\dot{m}_{charge\ air}$	Charge air mass flow rate	kg/s
m_d	Diesel fuel mass	kg
$\dot{m}_{EGR}$	EGR exhaust gas mass flow rate	kg/s
m_f	Burnt fuel amount	kg
m_g	Gas fuel mass	kg
m_p	Pilot fuel mass	kg
NO_x	Nitrogen Oxides	—
N_x	Nitrogen	—
OH	Hydroxide	—
O_x	Oxygen	—
p	Pressure	Pa
$\dot{Q}_{ht}$	Heat flow rate	W
$\dot{Q}_b$	Combustion heat release rate	W
T	Temperature	K
u	Velocity	m/s
V	Volume	m^3
Feedforward Neural Networks		
f(x)	Activation function of output layer	—
g(x)	Activation function of 2nd hidden layer	—

h(x)	Activation function of 1st hidden layer	—
k_1, k_2	Objective coefficients	—
SSE	Sum of square errors	—
SSW	Sum of square weights	—
u	Input in the feedforward NNs	—
v, a	Weights and biases of 1st hidden layer	—
w, c	Weights and biases of output layer	—
y	Neural network output	—
z, b	Weights and biases of 2nd hidden layer	—
Greek letters		
a	Wiebe function parameter	—
$\dot{x}_b$	Fuel burning rate	—
$\Delta\theta_{g,i}$	Combustion duration	° / deg
θ	Crank angle	° / deg
θ_{SC_i}	Start of combustion	° / deg
λ	Air−fuel equivalence ratio	—
ϱ	Density	kg/m^3
τ_{ID}	Ignition delay	s

ABSTRACT

The Internet of Things (IoT) advent and digitalisation has enabled the effective application of the digital twins (DT) in various industries, including shipping, with expected benefits on the systems safety, efficiency and environmental footprint. The present research study establishes a novel framework that aims to optimise the marine DF engines performance-emissions trade-offs and enhance their safety, whilst delineating the involved interactions and their effect on the performance and safety. The framework employs a DT, which integrates a thermodynamic engine model along with control function and safety systems modelling. The DT was developed in GT-ISE© environment. Both the gas and diesel operating modes are investigated under steady state and transient conditions. The engine layout is modified to include Exhaust Gas Recirculation (EGR) and Air Bypass (ABP) systems for ensuring compliance with 'Tier III' emissions requirements. The optimal DF engine settings as well as the EGR/ABP systems settings for optimal engine efficiency and reduced emissions are identified in both gas and diesel modes, by employing a combination of optimisation techniques including multi-objective genetic algorithms (MOGA) and Design of Experiments (DoE) parametric runs. This study addresses safety by developing an intelligent engine monitoring and advanced faults/failure diagnostics systems, which evaluates the sensors measurements uncertainty. A Failure Mode Effects and Analysis (FMEA) is employed to identify the engine safety critical components, which are used to specify operating scenarios for detailed investigation with the developed DT. The integrated DT is further expanded, by establishing a Faulty Operation Simulator (FOS) to simulate the FMEA scenarios and assess the engine safety implications. Furthermore, an Engine Diagnostics System (EDS) is developed, which offers intelligent engine monitoring, advanced diagnostics and profound corrective actions. This is accomplished by developing and employing a Data-Driven (DD) model based on Neural Networks (NN), along with logic controls, all incorporated in the EDS. Lastly, the manufacturer's and proposed engine control systems are combined to form an innovative Unified Digital System (UDS), which is also included in the DT. The analysis of marine (DF) engines with the use of an innovative DT, as presented herein, is paving the way towards smart shipping.

Keywords: *marine dual fuel (DF) engines, GT-Suite©, 0D/1D simulation model, data-driven model, digital twin, cyber-physical system, engine control functional systems, emissions, performance-emissions trade-offs, optimisation, safety, actuators/sensors faults/failures detection and diagnosis, sensors measurements uncertainty.*

1 INTRODUCTION

1.1 Chapter outline

This Chapter presents the background information and motivation for this thesis. A brief introduction of the environmental challenges and solutions is provided, and the maritime future trends are presented. The research question, the aim and the objectives of the undertaken research, are discussed. Finally, the structure of this thesis is described.

1.2 Background and Motivation

1.2.1 Current status

Marine diesel engines gaseous emissions have been steadily increasing throughout the last years, with the maritime industry currently accounting for 3.5% to 4% of all greenhouse gas emissions, primarily carbon dioxide (CO_2) emissions (Walker et al., 2019). Comparing Walker et al. (2019) findings to the respective CO_2 levels reported in Bows–Larkin et al. (2014), an increase of 1% to 1.5% in gaseous emissions is noted from 2014 until 2019. According to the International Maritime Organization (IMO), the CO_2 emissions projected from shipping were equal to 2.2% of the global human-made emissions in 2012, and are expected to rise 50% to 250% by 2050 if no action is taken (IMO, 2014b). Therefore, for controlling gaseous emissions and air pollution as well as reducing the environmental impact of the maritime industry, various international and national regulatory bodies such as IMO, European Maritime Safety Agency (EMSA) and

United States Environmental Protection Agency (US EPA) have adopted a series of regulations for limiting the non-greenhouse gaseous emissions including nitrogen oxides (NO_x) and sulphur oxides (SO_x,) as well as the greenhouse gaseous emissions; mainly CO_2, as presented by IMO (2019f), EMSA (2015) and EPA (2010).

Indicatively, IMO, as part of the International Convention for the Prevention of Pollution from Ships (MARPOL) Annex VI (IMO, 2019d), introduced progressive reductions in the NO_x emissions from marine diesel engines installed on ships, as described by IMO 'Tier II' and 'Tier III' limits. Sulphur Oxides (SO_x) and fuel requirements are correlated, and have been progressively controlled by the IMO, requiring lower maximum sulphur content in fuel oil. Worldwide, as of 1st January 2020, ships not equipped with an Exhaust Gas Cleaning System (EGCS) are required to limit to their maximum sulphur content of fuel oil to 0.50% m/m, whereas ships equipped with approved EGCSs, should demonstrate compliance to the requirements.

As a first step to reduce GHG emissions from shipping, IMO introduced the Energy Efficiency Design Index (EEDI), the Energy Efficiency Operational Indicator (EEOI) as well as the Ship Energy Efficiency Management Plan (SEEMP) and, in 2016, further amended SEEMP requirements under MARPOL Annex VI (IMO, 2019a), to collect and report verified annual data on CO_2 emissions and other relevant information. The intent of this regulations is to provide an incentive for ship owners, through the monitoring of CO_2 emissions, to improve efficiency whilst reducing CO_2 emissions and ultimately reduce the fuel consumption throughout the ship lifetime, leading to minimised operating costs (Theotokatos and Tzelepis, 2015).

1.2.2 Decarbonisation Strategy

As part of the commitment for Greenhouse Gases (GHG) reduction from the shipping industry, the IMO Marine Environment Protection Committee (MEPC) adopted in 2018, an Initial Strategy on the reduction of greenhouse gas emissions from ships (IMO, 2018). This Initial Strategy envisages for the first time a reduction in total GHG emissions from international shipping, defining 'Levels of ambition', 'Guiding principles' and possible 'Candidate measures' to achieve the GHG reduction commitment.

The levels of ambition directing the Initial Strategy take into account technological innovation and the global introduction of alternative fuels and energy sources for international shipping, which will be integrated to achieve the overall ambition. The levels of ambition directing the Initial Strategy are: (a) carbon intensity of the ship to decline through the implementation of further phases of the EEDI (already a mandatory requirement) for new ships; (b) to reduce CO_2 emissions per transport work, as an average across international shipping, by at least 40% by 2030 and; (c) to peak GHG emissions from international shipping as soon as possible and to reduce the total annual GHG emissions by at least 50% by 2050, compared to 2008.

The Initial Strategy is established by the guiding principles, including the developed instruments of the IMO regulatory framework, the MARPOL Annex VI and other IMO Conventions. The high-level listed potential candidate measures to reduce GHG emissions from ships are categorised to: (a) short-term measures (2018 to 2023) oriented towards tightened statutory requirements; (b) medium-term measures (2023 to 2030), oriented towards alternatives and innovation and; (c) long-term measures (beyond 2030), oriented towards pursuing the development and provision of zero-carbon or fossil-free fuels.

1.2.3 Alternative fuels – Liquified Natural Gas (LNG)

From the previous discussion, it can be inferred that the imposed regulatory framework is currently pressing the shipping industry towards short and medium-term measures. As the greenhouse and non-greenhouse emissions reduction is amongst the high priority issues that the shipping industry has to endure on account for the imposed stricter environmental standards (IMO, 2019d), the use of alternative fuels including natural gas (NG), methanol and bio-fuels have been proposed for improving the environmental sustainability of the maritime operations (Brynolf et al., 2014). Indicatively, the percentage of ship operators selecting LNG as an fuel type is estimated up to 66%, whereas low sulphur fuel oil (LSFO) or marine gas oil (MGO) options follow with 30% of the market (Gunton, 2019).

As it is discussed in Livanos et al. (2014) and Hegab et al. (2017), natural gas is the greenest fossil fuel that forms a well proven and feasible solution for ships propulsion.

Whilst the conventional diesel fuels will remain the main preference for the majority of the existing vessels in the near future, the commercial opportunities of the natural gas are attractive for new-built vessels. The price of liquified natural gas (LNG) is becoming more and more attractive; about 60% of the heavy fuel oil (HFO) price. The sulphur content of the natural gas is almost zero (about 0.004% by mass), which is well below the 0.1% limit required for Emission Control Areas (ECAs), and therefore the SO_x emissions of the engines operating in gas mode are very limited. Thus, the natural gas as a fuel, has proven to be a viable solution for vessels operating both inside and outside the ECAs. In specific, this is mainly attributed to the rapid development of the global LNG infrastructure (Livanos et al., 2014) and the lower LNG fuel price levels (US-DOE, 2017) when compared to other fossil fuels (Abadie and Goicoechea, 2019). Furthermore, the clean nature of lean combustion achieved by the LNG usage (Karim, 2015), leads to considerable NO_x and CO_2 emissions reduction (due to the low carbon to hydrogen ratio), and almost elimination of particulate matters (PM) and SO_x emissions. The economic and environmental benefits of using LNG as an alternative fuel, led the engine manufacturers to develop dual fuel (DF) versions of both the large two-stoke slow-speed engines and the four-stroke medium and high-speed engines (Woodyard, 2009).

1.2.4 Dual fuel engines performance and safety

Responding to the imposed regulatory framework and considering the utilisation of alternative fuels, the engine manufacturers such as MAN (2012b) and Wärtsilä (2015b), as well as Classification societies, e.g. ABS (2013), have conducted studies aiming the gaseous emissions reduction. The undergone efforts focused on innovative dual fuel (DF) engine development as well as the conversion of existing marine engines, enabling them the utilisation of alternative fuels. The main goals that drive these initiatives are primarily the improvement of the combustion characteristics, thus the engines efficiency, and secondly, the reduction of fuel consumption, which eventually leads to engines gaseous emissions minimisation (Jean-Michel, 2012, Hendrik et al., 2016, Bouman et al., 2017).

Dual fuel engines can achieve high output by combining fuel flexibility, low emissions, and high efficiency and reliability. The dual fuel engines can operate on either in the natural gas (gas mode) by employing natural gas as the main fuel and light fuel oil (LFO) as the pilot fuel, or the diesel mode by employing light fuel oil (LFO) or heavy fuel oil (HFO) as the main fuel (for this reason are also called tri-fuel engines (Wärtsilä, 2009)). In addition, the engine can operate in a third mode (shared fuel mode), where both gas and diesel fuels can be used in defined percentages as per the engine manufacturer. The engine can smoothly shift between fuels whilst operating, without loss of power or speed, providing the same output regardless of the fuel. Therefore, due to fuel flexibility the dual fuel engines are currently becoming the industry standard not only for LNG carriers but also for all the LNG-fuelled vessels, as noted by WinGD (2017) and DNV-GL (2019).

The marine DF engines typically run under steady state conditions using the same fuel type, although relatively slight power demand fluctuations may occur due to the vessel weather conditions changes. More considerable power demand changes may occur due to alteration in the operating conditions (sailing, manoeuvring, at port), interactions with other ship power systems or by the operator request. Switching to a different fuel mode needs to be implemented either when the vessel approaches or leaves ECAs or when a failure is present in the fuel systems and their components, i.e. pressure loss of the natural gas fuel supply (Wärtsilä, 2019b). In this respect, the engine manufacturers assess the behaviour of the engine and understand the interactions between the engine components during both steady and transient conditions, including operating modes switching, to ensure smooth and reliable operation.

Consequently, apart from ensuring DF engines highest efficiency and the lowest emissions, it is a prerequisite to ascertain the engine safe operation. Safety is defined as the state where a system operates without causing any harm to humans, environment and assets (Vincoli, 2014). When considering marine engines safety, it can be inferred that the environmental aspect is related to the airborne emissions generated from the marine engines, whereas the human safety aspect can be jeopardised either by exposure to engine emissions or to hazards owing to faulty engine/components operation. The NO_x and PM emissions generated during the combustion process have proven to be as

harmful for human health, thus increasing the potential for human deceases in the area of operation (Attfield et al., 2012). On the other hand, asset-related risks may also have a negative impact to human safety, due to the potential hazards the human may be exposed considering the additional hazards induced in DF engines, when the safe operation is not ensured (e.g. fire, explosive environment, gases leakages etc.).

Hence, industrial standards (IACS unified requirements (IACS, 2019), IGF (IMO, 2019b) and ICG (IMO, 2019c) Code , IEC (2019), European Commission directive (ATEX) (EC, 2019) and SOLAS Convention (IMO, 2019e)) have been established to ensure that the engine manufacturers develop environmentally sound, reliable and safe engines by taking into account all the potential hazards that may occur during engine operation. The identification and qualitative or quantitative assessment of risks therefore is crucial. Moreover, the additional risks introduced by gas fuel utilisation in DF engines, are addressed by supplementary assessments, mainly described in the gas safety concept reports (WinGD, 2019).

Nevertheless, the DF engines operate at acceptable safety levels and demonstrate satisfactory reliability. However, there is space for further improvement of the engines safety system by accommodating cutting-edge technological advancements and their application benefits, as discussed in the following chapters.

1.2.5 Future marine industry trends

It is beyond any doubt that a new era of forthcoming technological developments has commenced in the maritime industry. Several state-of-the-art technologies have been identified as the top drivers for the commercial shipping industry over the next few years. These include new shipbuilding technologies, fuel-efficient propulsion and powering technologies, smart ships, advanced materials, big data analytics, robotics, sensors and communications (Meier et al., 2019). All are linked to or influenced directly or indirectly by digital and communication technologies. On a modern ship, most of the installed machinery and systems are already monitored and controlled by supervisory control and monitoring systems. These systems transfer data from sensors to processing units that control electrical, mechanical, hydraulic components and actuators.

The computer-based technology used by ship's control systems, is shared by other systems on-board. In other words, the navigation, propulsion, steering and power management, dynamic positioning, cargo handling, bilge and ballast, and safety systems use the same or similar processing unit technologies as the ship's internal and external communications, ventilation and conditioning, lighting and other systems (Meier et al., 2019).

Dual fuel engines consist an enormous technological advancement that behind them lies a profound complexity of interconnected systems that include the engine individual components. This renders applicable the use of term 'cyber-physical systems' (CPS) when referring to engines in general, and specifically to DF engines, as they consist of both elements that are used to control and monitor physical processes required for power generation, and physical components which are affected by the control elements.

Therefore, the dawn of this new era that shipping is currently experiencing (fourth industrial revolution or Industry 4.0), is mainly governed by artificial intelligence (AI) practices involving big data analytics and machine learning (ML) techniques, as described by Vuollet et al. (2019) and Meier et al. (2019). In essence, industry 4.0 is the trend towards automation and data exchange in manufacturing technologies and processes which include cyber-physical systems (CPS), the internet of things (IoT), industrial internet of things (IIOT), cloud computing, cognitive computing and artificial intelligence.

Furthermore, the implementation of AI capabilities has shed new light in the development of cyber-physical systems and the detailed process modelling of engines; by employing Digital Twins (DT), (Meier et al., 2019, Stoumpos et al., 2020). Examples of this advent are already met in other industries, such as automotive, aviation etc., demonstrating considerable benefits in the modelled systems performance and safety. Therefore, shipping industry is also expected to adapt to this trend. Processing algorithms are capable of swift data processing, and as machine learning algorithms gain greater levels of intelligence, ship owners who have invested in AI will find competitive advantages. The real value, however, derives from obtaining valuable information from data, which can assist to effective asset performance management. Mathematical simulation models in conjunction with big data technologies, including machine learning

techniques, allow for the benchmarking of generated data sets. Machine learning systems and their algorithms are capable of churning through distinct data points from operations history, to reveal key relationships between variables that can be used to predict future outcomes (Wingrove, 2019).

There are numerous applications that this kind of capability can be used in maritime industry. Indicatively, amongst them are: (a) the ability to optimise voyages in real-time, which can lead to increased revenue for operators; (b) the predictive vessel management and maintenance, spotting the signs in the build-up to a preventable event and stepping in before it disrupts operations; (c) engine monitoring and real-time engine performance parameters optimisation; and (d) improved engine faults/failures diagnosis and prediction. Whilst the voyage management has rapidly gained interest by the maritime industry, the remaining engine-oriented applications have just started gaining attention, however, they are yet to be adopted by the marine engine manufacturers. This is mainly attributed to the Internet of Things (IoT) that recently allowed these techniques to become cost-effective. However, a potential AI integration to the existing engine control and safety system of the marine (DF) engines could see vast benefits; namely: (a) high-level engine performance; (b) detailed diagnostics of engine faults along with recommended actions; (c) advanced sensors diagnostics and sensors measurement uncertainty minimisation; (d) deviations from engine healthy state for a number of measured parameters; (e) in-cylinder processes analysis; and (f) effective analysis on a number of engine parameters (Vuollet et al., 2019), (Meier et al., 2019). In this respect, the engine performance optimisation, the control of measurement uncertainties as well as the engine risk mitigation (or safety enhancement) can be obtained.

1.3 Research Question

The aforementioned discussion dictates the apparent need of a practicable and feasible solution in the maritime industry, to be adopted by the engine manufacturers and/or the operators, in order to enhance the environmental and safety performance of the marine engines. Digitalisation can be seen as the technological opportunity to increase the engine and ship efficiency as well as to improve the asset availability by evolving the fault/failure diagnosis and reducing the potential safety implications during operation.

Therefore, the problems that are discussed in this thesis are summarised in the following question:

How can the dual fuel engines be further improved/enhanced in terms of performance and safety, considering future environmental regulatory requirements and digitalisation capabilities?

1.4 Aim and objectives

The main aim of the present research study is to develop a novel framework for enchaining environmental and safety performance of marine dual fuel engines by employing digital twins. In this way, the marine (DF) engines performance-emissions trade-offs will be optimise and the safety will be enhanced, whilst delineating the involved interactions and their effects on the performance and safety. This framework for both new and existing marine engines.

The objectives identified to achieve the set aim are given below.

Objective no.1: Perform a comprehensive literature review on the DF engines performance, emissions and safety context for revealing the research gaps

This objective includes the review of: (a) the marine dual fuel engines categories, technology and operation modes; (b) the previous numerical and experimental investigations and state-of-the-art industry/commercial developments in marine engines related to the performance optimisation and/or emissions reduction; (c) the previous investigations related to the application of the EGR as an exhaust after-treatment system on marine engines; (d) the existing investigations on engine control systems related to the fuel functional control and EGR and/or air bypass system (ABP) systems control; (e) the research studies addressing the engine operational limitations and safety implications along with the evaluation methodologies/tools used; and (f) investigations focusing on engine safety systems related to faults/failures detection and diagnosis.

Objective no.2: Research approach development

This objective encompasses the research approach to be followed during this study is developed at this stage. The research approach entails the selection of the reference

cyber-physical system (CPS) under investigation as well as the development of a novel framework. The conceived framework is divided into two methodologies: (a) performance improvement and emissions reduction methodology; and (b) safety enhancement methodology. The former methodology (performance improvement and emissions reduction) comprises combination and utilisation of state-of-the-art technologies, methods and tools for performance improvement and emissions reduction in both DF engine operating modes, whilst considering the engine design and operational limitations. This methodology is anticipated to result to compliance with the 'Tier III' emissions requirements. The latter methodology (safety enhancement) entails the development of a dynamic Engine Diagnostics System (EDS), by combining and utilising state-of-the-art methods and tools (e.g. Neural Networks (NNs), Data-Driven (DD) models), as well as advance diagnosis methods, considering engine safety critical components and sensors measurements uncertainty. Therefore, this methodology elaborates on the DF engine safety enhancement.

Objective no.3: Reference cyber-physical system (CPS) Digital Twin (DT) development

This objective entails the analysis and mapping of the investigated cyber-physical system (i.e. marine DF engine) along with its sub-systems/components including the Unified Engine Controls (UEC). The reference CPS digital twin is developed and validated against available data.

Objective no.4: Digital Twin development with integrated Unified Digital System (UDS)

This objective involves the development of the extended digital twin, considering the developed framework. This includes the integration of the manufacturer's Unified Engine Controls (UEC) with the proposed and developed Engine Diagnostics System (EDS) in a novel UDS for engine performance improvement, emissions reduction and safety enhancement. The developed state-of-the-art digital twin will then be employed to investigate the proposed framework.

Objective no.5: Case studies design – optimisation/ verification

This objective covers the design of the case studies for addressing: (a) the reference CPS response during transients and the identifications of the engine design and operational

limitations; (b) the framework verification to improve the engine performance and reduce emissions; (c) the identification of the most critical DF engine systems, examination of potential safety implications and evaluation of the engine manufacturer failure diagnosis method; and (d) the verification the UDS response and framework verification for safety performance enhancement. These case studies are also expected to demonstrate the applicability as well as the benefits thought their implementation.

1.5 Terminology

The terms used in this thesis are defined below.

i. The use of term 'cyber-physical systems' (CPS), when referring to DF engines, is based on the principle that the embedded ECS controls the physical processes, with feedback loops where physical processes affect computations and vice versa. Therefore, the CPSs are integrated complex systems representing computational, networking, and physical processes (NSF, 2020, Tay et al., 2018).

ii. The 'Digital Twin' or DT is "a realistic digital representation of assets, processes or systems in the built or natural environment" (Bolton et al., 2018). In this thesis, the developed DT provides a realistic digital representation of a marine four-stroke DF engine that is capable of consistently and accurately representing and predicting the physical system actual response under different boundary conditions. The term 'Digital Twin' is therefore used to refer to the virtual model of the investigated DF engine as a CPS (i.e. the detailed engine thermodynamic model along with its integrated control systems).

iii. The fourth Industrial revolution or 'Industry 4.0' introduces concepts and technologies of the combination of cyber-physical systems (CPS) and the Internet of Things (IoT) (Tay et al., 2018). This thesis contributes towards 'Industry 4.0' in the maritime industry by developing and investigating a state-of-the-art DT of a CPS such as the investigated marine four-stroke DF engine.

iv. The term 'sensors measurements uncertainty' in this thesis is used to describe the abnormalities of the sensors signals/measurements (including drift, offset and gain).

1.6 Research focus

The research focus and boundaries are presented in below.

i. In this thesis, the marine engines, as CPS, is the focus of investigation.

ii. The marine dual fuel engine performance investigation focuses on both the diesel and the gas operating modes for the DF engine settings optimisation that will result to compliance with the 'Tier III' emissions requirements.

    a. Whilst the gas operating mode offers compliance against the airborne emission limitations, an investigation is performed to examine the effect of the engine settings on the performance-emissions trade-offs, considering the engine operational limitations.

    b. For the diesel operating mode, the investigation focuses on the Exhaust Gas Recirculation (EGR) systems, as the most suitable technology.

    c. The engine shared fuel operating mode is not included under the scope of this study, due to the fact that this operating mode is optional on the investigated marine DF four-stroke engine. Furthermore, if applicable, the shared fuel mode operation is found to be limited.

    d. The EGR system investigation for the engine gas mode is considered out of the scope, as the engine gas operating mode can achieve compliance with the respective requirements.

    e. The author acknowledges the existence of other exhaust after-treatment technologies for compliance with the imposed requirements, such as Selective Catalytic Reduction (SCR), however, SCR is mostly designed and designated for diesel engines, therefore is considered out of the scope in the present research study.

iii. This research study covers the marine four-stroke DF engine control systems mainly from a system functional process perspective, in order to enable the investigation of the engine transient simulations. Therefore, the control systems design and development employ basic modelling principles. The sensors bias (signals delays and drift) is not taken into account in this study.

iv. This thesis investigates the marine engines safety in terms of system design and operational limitations, safety implications and faults/failure detection and diagnosis. The advanced faults/failures diagnosis is limited to the valves' actuators and engine sensors. The faults/failures prediction as well as the maintenance-wise aspect of this subject is not considered under the scope of this study, therefore it is not discussed. Moreover, the present study does not consider faults/failures diagnosis of the engine mechanical components.

v. Finally, the systems capital expenditure (CAPEX) and operational expenses (OPEX) or any other related costs as well as systems' volume and mass footprint are not considered in this work. In specific, the impact that the selected technologies have on the cargo capacity, the machinery space design and the structural ship design are not discussed.

1.7 Dissertation layout

The present thesis consists of eight chapters, as outlined in Figure 1.1. The illustrated outline is designed to briefly inform the reader on the chapter contents and research tasks distribution as well as to assist on efficient information tracking. Each chapter includes a summary section highlighting key achievements and novelties.

Chapter 1. Introduction: The first Chapter sets out the essence of the thesis by introducing the background as well as the motivation for this proposed and developed research work and sets the main aim that will be achieved through the performed research and the objectives reflecting the foremost study aim.

Chapter 2. Critical review: The research background through an extensive critical review is presented in this Chapter. The key points derived from the presented literature review are summarised and finally, the gaps in the existing literature are discussed.

Chapter 3. Research approach: This Chapter focuses towards the theoretical framework, the methodological approach, the research methods and tools that were employed during this research thesis and the methodological steps to address the identified research gaps in the literature.

Chapter 4. Reference cyber-physical system (CPS): The identification and description of the reference CPS along with its sub-systems is presented in this Chapter. A detailed description of the engine components, controls and safety systems currently adopted by the manufacturer are presented and discussed.

Chapter 5. Engine digital twin modelling and validation: This Chapter presents the discrete stages the modelling process was conceived. The considered and developed tools and methods are demonstrated by introducing the modelling philosophy and principles. The functionality and novelties of the methodology are explained in depth by clarifying design assumptions. Validation of the developed system for different operating profiles (steady state and transient) are reported.

Chapter 6. Case studies: The designed case studies for the engine performance, emissions and safety investigation as well as the verification of the developed system are presented in this Chapter. Tools for identifying the critical case studies are reported.

Chapter 7. Results and discussion: This Chapter reports the results that were derived from the case studies simulation. In-depth discussion of the findings and the system verification is presented.

Chapter 8. Final remarks and research conclusions: A summary of the key learning points of this research are presented in this Chapter. This Chapter also provides the research reflections, and proposals for future research.

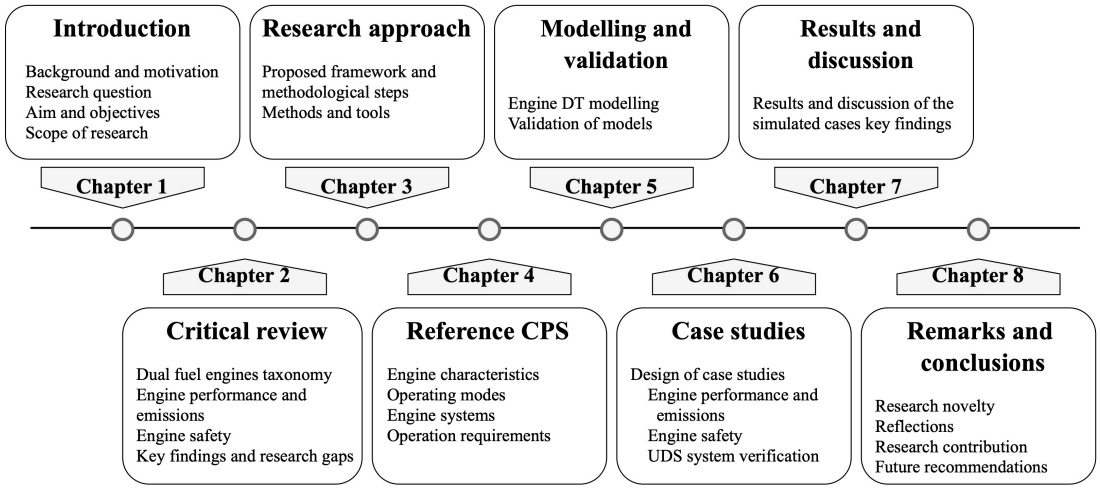

Figure 1.1 Layout of thesis Chapters

1.8 Chapter summary

In this Chapter, a brief introduction of the maritime industry impact to human and the environment was provided. The established regulatory framework as well as the latest technological developments in marine DF engines, the so called 'edge' of technology, including the AI applications in the maritime sector, were reported. Lastly this Chapter set the aim achieved through this work and the objectives reflecting the overall study aim. In the following Chapter, a critical review of the research area is presented, and the research gaps are identified and discussed.

2 CRITICAL REVIEW

2.1 Chapter outline

A comprehensive literature review is presented in this Chapter, focusing on the marine dual fuel engines investigations and the state-of-the-art industry developments, related to the performance optimisation and emissions reduction. In addition, the literature survey addresses investigations related to the application of the EGR as exhaust after-treatment system on marine engines. Engine control systems related to the fuel functional control as well as EGR systems are reported and discussed. The literature is further expanded to cover research studies on the engine operational limitations, safety implications, evaluation methodologies and tools as well as investigations focusing on engine safety systems related to fault detection and diagnosis. Lastly, the key findings from the critical review along with the research gaps identified are presented and discussed.

2.2 Taxonomy of DF engines

The marine DF engines are primarily categorised based on their operating cycle to four-stroke and two-stroke engines, likewise the conventional diesel engines. Each engine type is further divided into two sub-categories depending on the concept that fuels are delivered. In specific, when DF engines operate in diesel mode, diesel (LFO or HFO) is used as main fuel. When operating in the gas mode, DF engines run with a small amount of pilot diesel fuel; approximately 1% as reported by Wärtsilä (2009) for

initiating combustion, and natural gas as the main fuel. However, natural gas in DF engines can be delivered in different ways. With regards to the marine four-stroke DF engines, gas fuel delivery can be attained in two ways. The first approach entails the premixed combustion concept at low gas pressure (5-7 bar) (Wärtsilä, 2015b), with the natural gas injected in the inlet ports during the cylinder induction phase, as described by Menage et al. (2013) and Aaltonen et al. (2016). The second approach encompasses the gas direct injection concept at high gas pressure (around 350 bar) with the natural gas injected within the cylinders during the compression phase after the pilot fuel injection. Both sub-categories can achieve typical brake mean effective pressure (BMEP) of around 25 bar. Typical example of the first type is the Wärtsilä 50DF engine, whereas the Wärtsilä 32 GD and 46 GD engines are classified under the second type (Jarf and Sutkowski, 2009). Similarly, there are two types of two-stroke DF engines differing in the gas injection and combustion concept. The first operates at high fuel gas pressure (around 300-350 bar) with the gas injected during the combustion phase and burnt according to the diffusive combustion concept as described by Kindt and Sørensen (2016) and MAN (2015). The second operates in low fuel gas pressure (around 7 bar) with the gas injected into the engine cylinder during the compression phase and burnt based on the premixed combustion concept as explained by Nylund and Ott (2013).

2.3 Engine performance and emissions

The continuous engine design development and optimisation procedures in terms of engine performance and emissions, employ a number of techniques including experimentation, design, prototyping and engine mathematical modelling that are essential to the marine industry, as discussed by Kyrtatos et al. (2016a). Modelling and simulation, however, are considered the most cost-effective methods for obtaining a better understanding of the engine operation and the involved interactions between the engine sub-systems/components as well as predicting the engine performance and emission characteristics (Geertsma et al., 2018, Stoumpos et al., 2018). Therefore, simulation tools of various complexities (zero-dimensional (0D) to three-dimensional (3D)) (Singh et al., 2004, Merker et al., 2005, Coble et al., 2011, Christen and Brand, 2013, Xu et al., 2014, Ritzke et al., 2016, Stoumpos et al., 2018, Mavrelos and Theotokatos, 2018, Theotokatos et al., 2020, Stoumpos et al., 2020) have been used for

investigating the DF engine steady state performance and transient response. For analysing marine engines and ship propulsion systems, various model types have been also used as described by Benvenuto et al. (2014), Theotokatos and Tzelepis (2015), Baldi et al. (2015), Cichowicz et al. (2015) and Bondarenko and Fukuda (2020).

2.3.1 Dual fuel (DF) engines

As it is reported by Mavrelos and Theotokatos (2018), a limited number of studies have been published focusing on the experimental and/or numerical analysis of marine DF engines.

García Valladolid et al. (2017) experimentally studied a marine DF engine at steady state conditions complemented by a liquid fuel injection model for obtaining a better understanding of the local combustion conditions. Li et al. (2015) experimentally investigated a small marine four-stroke DF engine for comparing the engine performance/emissions characteristics in the diesel and the gas operating modes. Boeckhoff et al. (2010) presented the experimental investigation of a large marine four-stroke DF engine of the premixed combustion type at both steady state conditions (studying the effect of the engine and fuel parameters variations on the engine performance and emissions) and transient conditions (with fuel switching) reporting the engine operational experience. Banck et al. (2016) conducted an experimental analysis of a large DF four-stroke engine optimised for marine applications discussing the engine load acceptance at various load ramp slopes and the engine operational requirements at the low load range. Portin (2010) reported the development of DF four-stroke engines for offshore applications and presented experimental data for the engine load acceptance test from 40% to 80% load for the gas mode. Mohr and Baufeld (2013) experimentally investigated a large size four-stroke single-cylinder engine at steady state conditions and discussed the influence of the engine settings variation on the engine performance and emissions.

Previous investigations reported that DF engines encounter operational limitations in marine and offshore applications due to the expected considerable transient loading requirements. In specific, during the load increase phase of premixed combustion DF engines running in the gas mode, the engine delivered power initially increases due to

the injection of additional amount of gas fuel, whilst the amount of combustion air increases more slowly due to the turbocharger lag effect. Thus, the engine runs temporarily with a rich gas fuel−air mixture until the turbocharger delivers the required air flow. In principle, the same takes place in a diesel engine, but due to the different combustion process, the load acceptance is subject to different limitations. Thus, over-fuelling a gas engine leads to a rich combustion (i.e. lower air−fuel ratio), which at low loads improves the engine combustion efficiency (Portin, 2010), whereas at higher loads, over-fuelling causes the engine operating point to shift towards the knocking limit as the range between the misfiring and knocking borderlines becomes narrower at higher engine loads (García Valladolid et al., 2017). In contrast, over-fuelling a diesel engine at low loads reduces the combustion efficiency and leads to black smoke, if not controlled. However, at higher loads, the turbocharger faster response improves the diesel engine load acceptance.

Considering the size, complexity and cost of the marine DF engines, experimental studies require significant resources. Thus, engine modelling as well as simulation is employed as one of the most effective methods for obtaining a better understanding of the engine operation and components interactions as well as predicting the engine performance and emission characteristics. Mavrelos and Theotokatos (2018) investigated a large marine DF two-stroke engine of the premixed combustion type with the aim to simultaneously reduce the CO_2 and NO_x emissions based on a steady state 0D model developed in the GT-ISE software. Ritzke et al. (2016) proposed a combined 0D/1D and computational fluid dynamics (CFD) 3D approach for modelling a four-stroke DF marine engine in the AVL Boost and FIRE software tools. The 0D/1D engine model was used to generate information regarding the initial and boundary conditions, and subsequently these conditions were used for the 3D CFD model.

Pirker et al. (2010) and Sixel et al. (2016) reported a physical model for modelling the premixed combustion process of marine DF engines. The latter author integrated the developed model with the engine 0D/1D model developed in the GT-ISE software. The model was used for the investigation of two engines (a single-cylinder engine and a large marine four-stroke DF engine) operation at steady state conditions considering both natural gas and methanol as the main fuel. Based on the comparison with

experimental data, the developed model accuracy was considered adequate for allowing its usage at the design phase of dual fuel or gas-diesel engines. Kyrtatos et al. (2019) focused on the development and validation of the dual-fuel combustion model using the test data from the H35DF dual-fuel medium-speed engine, employing double Vibe function to calculate the heat release rate with the aim to find the appropriate correlations between Vibe and engine parameters using linear methods chosen amongst empirical methods. Furthermore, Masaki et al. (2019) numerically investigated and experimentally validated a premixed charge compression ignition DF combustion strategy for the DF engine gas mode, aiming to increase engine thermal efficiency. Černík (2018) developed and validated (via available engine shop trials data) a phenomenological simulation methodology for combustion modelling of both liquid (quasi-dimensional model) and gaseous (phenomenological combustion model) fuels for large low speed 2-stroke marine engines operating under both steady and transient operation conditions. The aim of this study was to investigate the engine performance where the author concluded that the proposed method enables the computationally effective optimization of complex propulsion systems. Wenig et al. (2019) developed a quasi-dimensional phenomenological combustion model to calculate the burning rate of a lean premixed mixture marine DF two stroke engine with pre-chamber. Following model constants calibration based on a set of experimental data, it was concluded that the model provided sufficient accuracy for a wide range of engine operating conditions.

In addition, a limited number of studies investigating the transient operation (including load and fuel changes) of small vehicles or heavy-duty DF engines by using simulation tools have been published. Xu et al. (2014) developed a one-dimensional (1D) model of an automotive four-stroke dual fuel engine in the GT-ISE software to study and improve the engine transient response by optimising the engine fuel injection. This model was validated against a comprehensive set of experimental data, from which a lag in the engine power delivery under transient loading with dual fuel operation was identified, and subsequently was applied to generate the required insight and to design control strategies for smooth torque delivery under dynamic conditions. For modelling the combustion process, a triple-Wiebe function was employed, the constants of which were correlated with the engine indicated mean effective pressure based on the acquired experimental data, as reported by Xu et al. (2016). Barroso et al. (2013) modelled a

heavy-duty DF compression ignition (CI) engine by employing an 1D model in GT-ISE; the model was calibrated by using engine mapping experimental data and used in both steady state and transient conditions. Georgescu et al. (2016) investigated the transient behaviour of gas and DF engines running on natural gas by employing two mean value dual cycle models. The first model was used to gain insight into the DF engine in-cylinder combustion process, whilst the second was used to simulate the entire engine system. The simulation results were used to discuss the engine limitations and transient response. Mayr et al. (2017) developed and implemented a methodology for simulating the transient response of large gas engines on a single-cylinder engine test bed. Simple and fast models and algorithms based on lookup tables were employed to provide the boundary of the investigated engine components conditions. The simple model results were compared with the results from an 1D model developed in the GT-ISE software demonstrating sufficient accuracy.

Additional research efforts on dual fuel engines (both experimental and numerical), along with a review of the operation principles and practices, are reported in (Karim, 2015).

2.3.2 Exhaust Gas Recirculation (EGR) system

Exhaust after-treatment technologies, such as Exhaust Gas Recirculation (EGR) and Selective Catalytic Reduction (SCR) are the main options for the engine manufacturers to ensure compliance of the diesel or DF engines (operating in diesel mode) with the current and future environmental requirements. However, these technologies are associated with a number of challenges on their initial cost, efficiency, operability and space requirements.

The SCR is an exhaust gas after-treatment system that utilises urea solution to neutralize the NO_x emissions (Pakarinen, 2012). Although the SCR technology is a highly effective method to reduce the NO_x emissions, the system is associated with considerable volume footprint requirements (for the SCR unit urea and storage tanks), additional weight, increased capital cost (Rudrabhate and Chaitanya, 2017) as well as engine thermal and pressure drop issues. Moreover, the SCR technology efficiency is highly dependent on the exhaust temperature inlet and system maintenance.

The EGR system affects the combustion process by recirculating an amount of the exhaust gas to reduce the oxygen concentration at the working medium entering the engine cylinders, thus decreasing the maximum combustion temperature (MAN, 2012c, EGCSA, 2014). However, its implementation leads to the engine fuel efficiency deterioration and increases the soot emissions. As indicated in the tests conducted by MAN (Tsalaptis, 2015), the IMO 'Tier III' NO_x emissions levels can be satisfied by employing an EGR rate (mass fraction) in the range of 30-40%.

Based on the review of the pertinent literature, the EGR system is considered to be a cost-effective technology for rendering the diesel mode operation in DF engines compliant with the regulatory requirements. On the other hand, as the SCR system is mostly designed and employed for diesel engines, it is considered out of the scope in this study.

The investigation and implementation of the EGR technology in diesel engines, either alone or combined with other technologies, has mainly been studied in applications of the automotive industry (Ladommatos et al., 2000, Maiboom and Tauzia, 2011, Gautier et al., 2009, Zamboni and Capobianco, 2013, Samokhin et al., 2014, Castillo Buenaventura et al., 2015, Thangaraja and Kannan, 2016). The investigation of the EGR system in marine engines has recently become an area of focus by the engine manufacturers. A considerable number of studies focused on the two-stroke diesel engines with EGR systems installed, whereas only a limited number of studies focused on the marine four-stroke diesel engines. Therefore, an apparent lack of investigations is noted for the marine four-stroke DF engines.

The effects of the EGR system on the marine two-stroke diesel engines are examined in a number of studies. Hiraoka et al. (2016a) (2016b) experimentally investigated a low-pressure EGR (LP-EGR) system installed on a marine two-stroke engine aiming to verify the long-term reliability and durability of the system by sea trials and monitoring in actual ship operation. Kaltoft and Preem (2013) numerically investigated a high-pressure EGR (HP-EGR) system for a marine two-stroke engine and examined the percentage distribution of exhaust gases in the turbocharger unit and the EGR system aiming to identify the EGR rate for IMO 'Tier III' compliance. Higashida et al. (2013) studied an HP-EGR system in conjunction with a VGT system and a water fuel

emulsification (WFE) system on a two-stroke engine, in order to minimise the fuel consumption penalty due to the decrease of the cylinders combustion pressure. Raptotasios et al. (2015) conducted a theoretical analysis on a marine two-stroke engine by using a validated multi-zone combustion model to identify the EGR rate for compliance with the IMO 'Tier III' requirements and examine the impact of EGR system on the engine fuel consumption. Feng et al. (2016) examined a marine two-stroke engine in-cylinder working process by employing the AVL Boost software and investigated the effects of the EGR system combined with a two-stage turbocharger and Miller timing. Sun et al. (2017) numerically investigated a marine two-stroke engine with an EGR system by using a CFD model and examined the NO_x emissions reduction for different EGR rates as well as the impact of advanced start of injection (SOI) on the engine fuel consumption. Ji et al. (2019) numerically investigated a low-speed two-stroke diesel engine and examined the effects of Miller cycle, the EGR system and the intake air humidification coupled with fuel injection strategies on the engine performance using CONVERGE CFD software.

Previous investigations demonstrated that the marine two-stroke diesel engines equipped with an EGR system are capable of complying with IMO 'Tier III' requirements, with or without use of alternative technologies, for EGR rates varying from 20% to 40%. The alternative technologies used in combination with the EGR system can partially compensate the EGR system effects on the engine, yet the achieved emissions reduction was associated with a brake specific fuel oil consumption (BSFC) increase ranging from 1% to 6% from their reference values. This is attributed to the reduced combustion cylinder pressure due to lower oxygen concentration of the charge air, which, in turn, results in lower engine power output; therefore, a fuel increase is needed, so that the engine retains its power output. Finally, there is a limited number of studies proposing the use of the air bypass system (ABP) along with the EGR system (on two-stroke engines only) (Nielsen et al., 2018, Wang et al., 2017) to improve the engine performance and reduce complexity in comparison with the two-stage turbocharging layout.

The EGR system effects on the marine four-stroke diesel engines were investigated by Ludu et al. (2007), Tinschmann et al. (2010), Wirth (2010), Millo et al. (2013), Fiedler et

al. (2013), Park et al. (2013), Pueschel et al. (2013), Rickert et al. (2016), Kyrtatos et al. (2016b), Kaario et al. (2016) and Stork et al. (2019). Ludu et al. (2007) experimentally investigated the operation of a single-cylinder engine with HP-EGR and developed a multi-cylinder four-stroke engine model in AVL Boost for numerically studying the EGR rates satisfying the IMO 'Tier III' requirements as well as the EGR system impact on the soot and smoke emissions as well as the engine fuel consumption. Tinschmann et al. (2010) presented a comparison of the internal and external mechanisms to reduce the NO_x emissions by using a single-cylinder engine model approach and investigating the EGR system along with Miller timing and two-stage turbocharging. Park et al. (2013) numerically examined the effects of an EGR system on a four-stroke engine and its combination with charge air humidification aiming to achieve compliance with to the IMO 'Tier III' NO_x levels. Pueschel et al. (2013) numerically investigated the combination of post-injection strategies on a four-stroke engine equipped with a LP-EGR system, in order to decrease the soot emissions. The EGR system was capable of providing EGR rates up to 20% controlled by a pneumatic valve, whereas an EGR blower was activated to achieve EGR rates up to 40%. Furthermore, Rickert et al. (2016) numerically examined a four-stroke engine equipped with a two-stage turbocharger and an EGR system with main focus to reduce soot emissions by employing a post-injection strategy. Kyrtatos et al. (2016b) experimentally examined an HP-EGR configuration on a two-stage turbocharged, 6-cylinder medium-speed diesel engine, in combination with the water fuel emulsification (WFE) system to reduce soot emissions. Kaario et al. (2016) experimentally investigated the EGR system on a single cylinder of a medium-speed engine with EGR rates up to 30%, whereas advanced SOI was also examined to optimise the engine fuel consumption by using a 1D simulation model set up in GT-ISE.

From the preceding studies discussion, it can be summarised that the four-stroke engines require EGR rates ranging from 15% up to almost 40% to satisfy the IMO 'Tier III' requirements. In addition, these studies findings demonstrated that the use of an EGR system is associated with a BSFC penalty ranging from 3% to 10% due to the delayed start of combustion and the slower combustion, as well as with high soot and smoke emissions, which are attributed to the flame temperature reduction (Fabio et al., 2015, Kaario et al., 2016). Effective solutions to improve the engine BSFC when EGR

systems are used include varying the fuel injection profile, implementing two-stage turbocharging and, retarding the intake valve timing. The use of the two-stage turbocharging as suggested by Rickert et al. (2016), or the variable geometry turbine (VGT) are proposed as a viable option for IMO 'Tier III' compliance, due to the lowest fuel consumption observed. In addition, early SOI with high EGR rates was identified as the most effective solution according to Pueschel et al. (2013) for improved engine efficiency, whereas the fuel injection pressure increase and WFE system was proposed by Tinschmann et al. (2010) and Kyrtatos et al. (2016b) to reduce soot emissions. To overcome the increased smoke emissions, Tinschmann et al. (2010) suggested an increase in the charge air pressure or the fuel injection pressure.

For DF four-stroke engines, the EGR technology was studied by Kumaraswamy and Prasad (2012), Yasin et al. (2015), Singh and Subramanian (2016), Wu et al. (2018), Duan et al. (2019) and Li et al. (2019). Kumaraswamy and Prasad (2012) converted a single-cylinder four-stroke diesel engine to DF and investigated the effects of various diesel–Liquefied Petroleum Gas (LPG) substitution ratios, engine speeds and loads on the engine BSFC and emissions with the operation of the EGR system in the diesel and gas modes. Yasin et al. (2015) conducted experiments on a single-cylinder DF engine by testing the diesel and gas operating modes with and without the EGR system operating, with the aim to examine the impact of the EGR system on the CO and CO_2 emissions. Furthermore, Singh and Subramanian (2016) tested a single-cylinder DF four-stroke engine under dual fuel operation at constant speed for EGR rates up to 30% in order to investigate the CO, NO_x, hydrocarbon (HC) and smoke emissions trade-offs. Finally, Wu et al. (2018) used a four-cylinder DF four-stroke engine equipped with a LP-EGR system to investigate its effects on the CO, NO_x and HC emissions, for EGR rates up to 20%. Duan et al. (2019) developed a detailed 1D simulation model of a hydrogen-enriched natural gas SI engine and validated it against the experimental data, with the aim to investigate the engine performance and emissions under different EGR systems layouts, including a low-pressure and high-pressure EGR systems separately and combined. Li et al. (2019) performed a quantitative experimental investigation of the effects of compression ratio, EGR and spark timing strategies on performance, combustion and NO_x emissions characteristics on a four-stroke SI natural gas engine

fuelled with 99% methane content. The compression ratio was modified by replacing pistons with different bowl volumes.

The previous investigations indicated that DF engines equipped with EGR systems demonstrated a 70% reduction in the NO_x emissions at the diesel mode, for EGR rates ranging from 20% to 30%. With regard to the CO and HC emissions, the findings of the literature studies vary, as different operating conditions were investigated. Kumaraswamy and Prasad (2012) reported a decrease in CO and HC emissions with the EGR system operation in the diesel-LPG mode, whereas and Wu et al. (2018) analysed how the addition of hydrogen with EGR system influences the performance and emissions of a diesel-hydrogen DF engine, reporting an increase in CO and HC emissions.

2.3.3 Engine control system(s)

For operating a marine DF engine in a broad envelope as well as accommodating the demands during the modes switching, the engine control system design as well as sufficient control strategies development is required. The available literature on the control systems during fuel mode transition of a marine DF engine are mainly focusing on experimental studies of marine DF engines and provide details of the engine settings and operation.

Wang et al. (2015) studied the design of a marine DF engine fuels control system to accommodate effective fuels transitions by employing a mean value model-based approach. It was concluded that a Multiple Input–Single Output (MISO) control system architecture with feedback corrections applied to both the gas and diesel fuels is advantageous compared with architectures that apply corrections to only one fuel command (either diesel or gas). Schmid (2016) focused on the marine four-stroke gas and DF engines cylinder individual combustion control by employing an anti-knock approach determining ways of combining combustion balancing (which is currently a challenging task due to the extreme sensitivity of the modern engines to the cylinder-to-cylinder variations) with conventional control functions. Ott et al. (2013) investigated the cylinder combustion individual feedback control of a four-stroke DF engine. The centre of combustion and maximum pressure rise were controlled by actuating the start

and duration of the pilot diesel fuel injection. Engine experimental analysis indicated that the proposed controller was able to compensate the influence of various disturbances. An applicable and comprehensive control strategy for an automotive natural gas/diesel engine was presented by Wang et al. (2016b). Roecker et al. (2016) demonstrated a method for controlling the diesel fuel injection in DF four-stroke engine in order to overcome the shortcomings of the natural gas port injection and improve the engine transient performance and implemented the developed control in two vehicles engines. Fathi et al. (2017) discussed the homogeneous charge compression ignition (HCCI) engine control structure in order to effectively control these engines and obtain acceptable performance and emissions characteristics. However, the complete detailed modelling of the engine and its control system has not been reported in the pertinent literature.

In addition to the preceding studies, the introduction of the EGR systems in marine engines establishes a further need for the development and modelling of an appropriate control strategy. Similarly to the findings noted in the literature with regards to the EGR system application on marine engines, the EGR system control modelling in marine two-stroke engines have been addressed by a limited number of studies, whereas there is a noticeable gap of studies in the literature focusing on the EGR system controls on four-stroke diesel and DF engines.

The EGR system control development and modelling, with regards to the marine two-stroke engines is reported in a limited number of studies. Llamas and Eriksson (2014) investigated the optimal control of a heavy duty diesel engine with EGR and VGT during transients, where minimum time and fuel optimal control problems are defined. The same authors, conducted a similar study in 2018, using a mean value model of a large two-stroke marine diesel engine equipped with an EGR was used to capture the effects of changes in the fuel control inputs. Samokhin et al. (2014) developed a simplified control structure of an HP-EGR system installed on a two-stroke engine, which was represented by a set of non-linear differential equations. Alegret et al. (2015) used a mean value engine model (MVEM) of a marine two-stroke engine, consisting of seven control inputs (fuel mass flow, EGR blower speed, fuel injection time, fuel injection angle, exhaust valve closing angle, cut-out valve position, cylinder by-pass

valve position) to investigate the performance of the EGR system and validate it through measured data. Nielsen et al. (2018) investigated a large two-stroke marine engine equipped with an EGR system with two different EGR control methods. The first method was based on a measurement of the scavenge oxygen fraction, whereas the second method was based on a control-oriented model and a non-linear estimator. These methods were validated through MVEM simulations as well as on-board a vessel at actual operating conditions.

2.3.4 Engine performance and emissions optimisation

The optimisation studies literature review aims to identify the optimisation methodologies and tools used for addressing the defined optimisation objectives. In this respect, the objectives considered under the scope of this study include (a) the optimisation of the gas operating mode of the DF engine under investigation; and (b) the optimisation of the EGR system functional controls. Therefore, the optimisation studies review focuses on these two items.

Further to the studies presented in the previous sections, other research efforts on DF engines mainly dealt with the investigation and optimisation of the dual fuel engines emission characteristics (Srinivasan et al., 2006, Ozcan and Yamin, 2008, Papagiannakis et al., 2010, Zhang et al., 2016, Shinsuke et al., 2016, Wenzheng et al., 2019), the performance and heat release analysis (Krishnan et al., 2002), the development of methods for increasing the DF engines efficiency (Wang et al., 2016a, Banck et al., 2016, Moriyoshi et al., 2016), and the optimisation of the pilot fuel injection and gas substitution rate (Yang et al., 2015, Li, 2016, Cameretti et al., 2016). The optimisation methods to achieve single or multiple optimisation objectives reported in the literature, are mainly summarised in two categories respectively; (a) systematic or parametric investigation methods mostly by employing Design of Experiments (DoE); and (b) AI approaches. The latter mainly involves Artificial Neural Network (ANN) optimisation tools, and Evolutionary Algorithms (EAs), such as multi-objective genetic algorithms (MOGA).

The optimisation of the EGR system settings for automotive applications were examined in a number of studies. Hiroyasu (2004) carried out an optimisation study via

simulations for a single-cylinder truck engine by employing the Neighbourhood Cultivation Genetic Algorithm (NCGA) with the objective to minimise the NO_x and soot emissions along with the fuel consumption by controlling the fuel injection shape, the boost pressure, the EGR rate, the start of injection, the injection duration angle and the swirl ratio. The trade-off between fuel oil consumption and the NO_x emissions was identified and a linear correlation between the fuel consumption and the soot emissions was derived. Yin et al. (2014) experimentally studied in a four-cylinder automotive engine the effects of the split injection characteristics, the injection pressure and the EGR rate on the NO_x, soot and fuel consumption, identifying optimal settings, concluding that high levels of EGR and a late injection timing lead to simultaneous reduction of NO_x and soot with an associated fuel consumption increase. Amr and Saiful (2008) modelled an automotive four-stroke spark-ignition natural gas engine and optimised the engine compression ratio and ignition timing for obtaining the lowest fuel consumption accompanied with high power and low emissions. Ibrahim and Bari (2008) numerically investigated a four-stroke natural gas SI engine with a HP-EGR system by simulation, aiming to optimise the engine compression ratio and ignition timing for obtaining the lowest BSFC accompanied with high power and low emissions. Yin et al. (2014) experimentally investigated a four-cylinder automotive diesel engine and performed a multi-parameter parametric optimisation of the injection parameters to improve the trade-off between NO_x and soot emissions whilst maintaining fuel efficiency. Park et al. (2015) proposed a dual-loop EGR system for four-stroke diesel engines that combines the features of HP and LP EGR systems and investigated the system operation by simulation deriving a response surface model by employing Latin hypercube sampling as a fractional factorial DoE. Subsequently, a multi-objective Pareto analysis was employed to minimise the NO_x formation and fuel consumption through optimised engine settings. Jaliliantabar et al. (2019) numerically investigated a small single-cylinder four-stroke diesel engine equipped with an EGR system, aiming to optimise the EGR rate and the biodiesel fuel percentage using the multi-objective genetic algorithm NSGA-II. Jo et al. (2019) proposed an artificial neural network (ANN) using multiple combustion parameters, calculated from the in-cylinder pressure, to precisely estimate the LP-EGR rate of a turbocharged GDI engine. This ANN was trained and validated using experimental data at steady-state conditions. Ayhan et al.

(2020) experimentally investigated a single-cylinder four-stroke diesel engine performance and emissions characteristics aiming to optimise the proportions of corn oil methyl ester (COME) blends and EGR rates at variable engine loads and speed conditions, using the Taguchi method. Li et al. (2020) investigated a reactivity controlled compression ignition (RCCI) engine with EGR system with the objective to find effective ways of mitigating the high pressure rise rate in biodiesel and gasoline fuelled engines. A parametric (full factorial) optimisation as performed concluding that optimal conditions were obtained with advanced IVC timing and high EGR rate.

The EGR system settings optimisation in marine engines, as revealed from literature review, is limited. Lei et al. (2019) investigated a marine low-speed two-stroke diesel engine with HP-EGR system and its effects on the NO_x emissions and BSFC and proposed a cylinder air bypass system to optimise the engine BSFC.

2.4 Engine Safety

2.4.1 Safety implications

Comparing the marine DF engines with the conventional marine diesel engines, a number of additional components is introduced in order to allow the engine to operate and control the engine systems and process in both operating modes (diesel and gas). The new components and new functionalities do not constitute an issue, however, it may lead to new hazards and unpredicted hazardous interactions in systems, unless properly handled (Bolbot et al., 2019a, Bolbot et al., 2019b). In typical diesel engines, the hazardous situations include conditions such as high oil mist concentration in the engine crankcase, T/C compressor surging, diesel engine camshaft overloading, inadequate lubrication, cooling and fuel supply, increased or fluctuating thermal loading and sudden engine tripping, which under worst case scenario, may lead to deteriorated engine operating conditions (Xin, 2013, Theotokatos et al., 2018b). For instance, faults in the auxiliary systems of a diesel engine may lead to engine inappropriate cooling, lubricating and fuelling (Banks et al., 2001, Cicek et al., 2010). Other failures leading to hazardous situations include the engine components health deterioration, such as piston

rings, stuffing boxes, fuel injection system, and air filters (Hountalas, 2000, Banks et al., 2001, Cicek and Celik, 2013).

Furthermore, as every other system, a DF engine operates with inherent hazards; misfiring, knocking and T/C compressor surging may lead to considerable damage to the engine and its components/sub-systems (Theotokatos and Kyrtatos, 2003, Mavrelos and Theotokatos, 2018). In addition, deviations from the expected ranges of the engine performance parameters may trigger the engine safety functions rendering the engine temporarily unavailable. This may lead to system-level hazardous conditions including a ship position loss or a total blackout; both are associated with a potential for a collision, contact or grounding accidents (Bolbot et al., 2018). The storage and use of natural gas on-board ships increase the risk for fire and explosion accidents (Stefana et al., 2016, Jeong et al., 2017). Oil mist explosions can lead to hazards such as engine room fires, whilst they may also cause occupational accidents if occur in a close proximity to the vessel operational or maintenance personnel (Cicek and Celik, 2013). Therefore, it can be inferred that although the DF engines are considered vastly reliable, are still prone to faulty conditions due to either hardware or software deficiencies/issues (minor and rarely major issues) (Nylund, 2007, Portin, 2010).

2.4.2 Safety evaluation tools

The technological advancement of new systems, their complexity and high cost of their failures or downtime has led to the adoption of "identify and control" approach in safety engineering for dealing with hazards and accidents (Vincoli, 2014). A number of approaches can be used for the systematic identification of hazards in cyber-physical systems including Preliminary Hazard Analysis (PHA), Hazard and Operability study (HAZOP), System-Theoretic Process Analysis (STPA) and Failure Modes and Effects Analysis (FMEA) (Bolbot et al., 2019b). The implementation of the latter is considered as a pre-requisite for approval of the engine control systems (ECS) in marine engines (IACS, 2014).

In an effort to mitigate the safety implications and therefore the hazardous conditions, the engine designers are employing a number of methods and tools to identify, analyse and control all the safety concerns during the design phase (Dikis, 2017, WinGD, 2019).

The most common approaches for the marine engines safety assessment that the Classification societies (IACS, 2014) suggest are the Failure Mode Effects, and Analysis (FMEA) and the Failure Modes, Effects and Criticality Analysis (FMECA) (Ahmed and Gu, 2020). However, FMEA or FMECA is usually employed in combination with other tools including Fault Tree Analysis (FTA), Event Tree Analysis (ETA), HAzard IDentification (HAZID) and HAzard and OPerability (HAZOP) studies.

The FMEA implementation for engines safety assessment is also reported in a number of studies. In specific, Banks et al. (2001) applied a high level FMEA to a diesel engine for the purposes of development and assessment intelligent diagnosis techniques. Similarly, Cicek et al. (2010) employed FMEA to the marine engine fuel system to promote the application of preventative maintenance. Cicek and Celik (2013) applied FMEA to identify the potential causes leading to crankcase explosions on-board ships. Ling et al. (2012) performed FMEA for diesel engine cylinder with aim to propose new risk metrics. Lazakis et al. (2018) followed a combined approach of FMEA and FTA to identify the critical components in a typical diesel engine. Lastly, Vera-García et al. (2019) investigated the improvements of a failure database used for a four-stroke high-speed marine diesel engine. The developed database was assembled by considering FMEA, as well as an analysis of the symptoms obtained in an engine failure simulator. The FMEA was performed following the methodology of Reliability-Centered Maintenance (RCM), while the engine response against failures was obtained from a failure simulator based on a thermodynamic one-dimensional model, which was adjusted and validated with experimental data.

With regards to the ECS, the failure modes are associated with the failures either in sensors or actuators. Sensors can respond by giving erroneous measurements in terms of offset, drifting, biases and gain errors (Hountalas, 2000, Zidani et al., 2007, Heredia et al., 2008, Balaban et al., 2009, Gaeid et al., 2012) or by giving zero output. On the other hand, actuators can either become non-responsive to the control commands or have deteriorated response performance (Center, 2011).

2.4.3 Engine safety systems – faults/failure detection and diagnosis

The engine safety system(s) are considered crucial for ensuring the engine safe and smooth operation, especially in the case of the DF engines where gas-related hazards are present. The development of such system(s) is based on the manufacturers vast experience on faults and failure detection and diagnosis as well as the FMEA results (WinGD, 2019). Therefore, faults or failure detection and diagnosis of the marine engines forms a main area of interest with a considerable number of research studies.

Jung et al. (2018) used a data-driven model to compare the performance of classification algorithms for fault detection of fuel systems components (valves, pumps, injectors etc.) and fault isolation and demonstrate each method advantages and disadvantages. Chai et al. (2011) examined the effect of fault diagnosis on a marine engine, by using a comprehensive similarity method considering the faults of high pressure pumps wear, carbon formation of the fuel injector, breakage of piston ring and exhaust valves leakage. It was concluded that the fault diagnosis method of integrated similarity is capable of achieving higher rate diagnosis. Perera (2016a) and (2016b) investigated the sensor faults detection for the sensors used in energy efficiency analysis (shaft speed, fuel consumption etc.) and proposed a two-detection levels approach to identify faults in an on-board data acquisition system. The first fault detection level filtered the sensor values and if the sensor signals were not within a predefined range the sensor was deemed faulty. The in-range faults were detected by the second fault detection level by considering localized models where the respective data points were clustered by Gaussian mixture models with an expectation maximisation algorithm. Ntonas et al. (2020) developed a framework for turbomachinery and heat exchanger components fault simulation for predicting both turbocharger and diesel engine performance and operability by developing a marine four-stroke diesel engine simulation model validated against measured data.

Furthermore, Xi et al. (2018) examined the marine diesel engines faults detection by employing a machine learning classifier and proposed an improved methodology to avoid the human factors in the independent component analysis for vibration-source extraction. Experiments were performed for five different faults related to the inlet

valve, the outlet valve, the connection rod, the piston pin and the piston ring. The experimental data were acquired using a commercial diesel engine and were used to evaluate the performance of the proposed method. Moreover, Kowalski et al. (2017) developed a fully automatic machine learning-based system for fault diagnosis of marine four-stroke diesel engines, by monitoring engine sensors signals, and used them as an input for a pattern classification algorithm. Real-life datasets from actual engine operation were used addressing various faults (inlet and the exhaust valves leakage, uncalibrated fuel injector, fuel injection delay et. al) and a normal operation mode for comparison and error-correcting output from the developed system. The development and implementation of intelligent diagnostic methods using machine learning algorithms were also investigated by Tsaganos et al. (2018) focusing on the effective detection and diagnosis of sensors faults such as shaft speed, pressures, temperatures etc., for two-stroke slow-speed marine diesel engines. The proposed algorithm was experimentally evaluated concluding that it demonstrated superiority against the existing algorithms due to its predictive performance accuracy.

Tse and Tse (2014) focused on the diagnosis of the combustion-related faults (defective spark plug, oil leakage, defective valves, cylinder wear) in automobile engines by the use of low-cost sensors for the instantaneous angular speed method. It was concluded that this method could clearly reveal the differences between normal and abnormal engine combustion process and is capable of generating quality fault diagnostic results comparable with those obtained using expensive and conventional pressure sensors. Furthermore, Li et al. (2012) elaborated on the combustion-related faults detection of a marine diesel engine using the instantaneous angular speed. The authors performed numerical simulations using a 6-cylinder engine model and real instantaneous angular speed data measurements for evaluation purposes and concluded that the proposed fault detection method can offer improved detection rate with high accuracy.

Zhao et al. (2018) investigated the fault tracking control issues in ship propulsion systems and proposed a simple adaptive fault-tolerant PI tracking control scheme using an adaptive tuning law to adjust controller gains during operation. Simulations runs were performed on a case study ship propulsion system to demonstrate the effectiveness and advantages of the proposed control strategy. Jafarian et al. (2018) employed a statistical

approach to classify an automobile engine operation state and experimentally validated the fault diagnosis, including the misfire and valve clearance faults, using the vibration data captured by sensors. Jiang et al. (2017) examined the valve clearance fault detection based on the vibration signals measured on the engine cylinder heads and the feature extraction approach. Experiments were conducted for validation purposes on a twelve-cylinder ICE test rig and the results showed that the feature extraction approach is capable of extracting the commencement of valve closing impact accurately. Lastly, Hountalas and Kouremenos (1999) presented a method for marine two-stroke diesel engine fault diagnosis by processing measured engine data using a simulation model and demonstrated the application of the method for the case of the engine operation with high cylinder exhaust gas temperatures and low power output.

2.5 Key findings and research gaps

The expected outcome of the critical review is the identification of the key findings and research gaps related to the marine DF engines development and operation, in terms of performance, emissions and safety. Thereafter, this will lead to the appropriate research and development direction that should be adopted to cover this study aim and objectives.

The following key findings were identified from the preceding literature review:

- With regard to the marine DF engines optimisation, a limited number of studies experimentally optimising the performance and/or the engine emissions is noted, with no examination whatsoever on the marine four-stroke marine engines, especially when operating in gas mode. Furthermore, the numerical investigations of the marine DF engines available in the literature are limited only to the two-stroke engine type. The most relevant investigation identified on this area (Mavrelos and Theotokatos, 2018) focused on marine two-stroke DF engines whereas this study focuses on marine four-stroke DF engines.
- Similar to the above, the EGR system application is mainly oriented towards the diesel rather than the DF engines, where the conducted investigations are limited. With regards to the marine engines, the identified studies only focused

on the marine two-stroke diesel engines. The lack of studies on the EGR system effects in marine DF engines (both two-stroke and four-stroke engine types) is attributed to the DF engines capability to comply with the current emission requirements when operating in gas mode. The most relevant investigation identified on this area (Lei et al., 2019) focused on marine two-stroke diesel engines whereas this study focuses on marine four-stroke DF engines.

- The effects of the ABP system in combination with the EGR system on the marine engines have only been reported for marine two-stroke diesel engines.
- The studies conducted on the marine DF engine control, mainly focus on the fuel functional strategies and combustion controls via experiments either on marine two-stroke or four-stroke engines, whereas the EGR system controls have been investigated solely in marine two-stroke diesel engines.
- Due to the increased number of components, DF engines are considered more vulnerable to safety implications than the diesel engines. By employing well-established safety assessment tools (FMEA/FMECA in combination with ETA and/or FTA) and by including those additional parts (as reported in gas safety concept reports), the engine manufacturers are able to perform safety assessments and eventually mitigate potential hazards.
- Research awareness related to the AI and ML tools is mostly oriented towards the engine components faults diagnosis and prognosis with regards to the maintenance planning and tasks. The most relevant studies identified on this area have been conducted by Meier et al. (2019), Dimopoulos et al. (2014) and Zymaris et al. (2016). Meier et al. (2019) investigated a marine two-stroke DF engine using ML tools to improve the engine maintenance planning and costs associated. Dimopoulos et al. (2014) presented a software tool that can be used for assessment and optimisation of a vessels' systems design and operation, whereas Zymaris et al. (2016) presented a systems engineering methodology for the analysis and condition assessment of complex marine diesel-electric marine propulsion systems. The latter studies focus on the engine components faults diagnosis and prognosis assuming the sensors healthy operation, and they are focusing on the engine maintenance planning and tasks. The present study

differentiates from these investigations, as it focuses on the safety aspects of the actuators and sensors faults/failures detection. In addition, this study investigates the application of similar ML tools, however, on a different engine type; marine four-stroke DF engines.

- The studies conducted on the marine engines' failure diagnosis do not address the safety implications in engine operation due to faulty components/sensors. Moreover, safety investigations on marine DF engines are non-existent.
- Engine faults/failure detection and diagnosis have been thoroughly covered by a considerable number of research studies in the literature, also addressing the applicability of AI techniques in this field. The identified studies mainly investigated various faults/failure detection approaches on marine diesel engines, with primarily interest on two-stroke engine type. Sensors measurements uncertainty and its impact on the faults/failures diagnosis have not been investigated for marine DF engines.
- The AI and ML tools benefits in the marine DF engines, in terms of both performance and safety, are not addressed in the existing literature.

Considering the key findings, this thesis aims to address the following research gaps in scientific knowledge.

Gap no.1: A lack of a Digital Twin to adequately represent the marine four-stroke DF engines behaviour along with their control system functionalities.

Gap no.2: A lack of reporting the marine four-stroke DF engines processes during transient operations, including modes switching, as well as mapping the engine systems/components design and operational limitations.

Gap no.3: A lack of optimisation studies on DF engines to optimise performance-emissions trade-offs at gas mode operation, whilst considering the engine operational limitations.

Gap no.4: A lack of a methodology that aims to optimise the performance and emissions trade-off and consists the marine four-stroke DF engines operating in diesel mode, compliant with the IMO 'Tier III' requirements, whilst considering the systems/components design and operational limitations related to the EGR and ABP systems and their associated control system functionalities.

Gap no.5: A lack of a methodology that aims to enhance the marine four-stroke DF engines safety, by introducing ML capabilities to provide intelligent engine monitoring and advanced faults/failure detection, whilst considering safety implications and sensors measurements uncertainty.

2.6 Chapter summary

The research background through an extensive critical review was presented in this Chapter. In specific, the current literature on the analysis of the marine DF engines was discussed, including experimental and numerical investigations of performance and emissions, as well as control and functional strategies. The review was further expanded to safety-related investigations, covering engine safety implications, safety assessment tools as well as engine and control faults/failures detection and diagnosis. Summarising the key findings of this literature review and setting the ground for the proposed framework, the research gaps were discussed, and the research approach adopted in this thesis is presented in the following Chapter.

3 RESEARCH APPROACH

3.1 Chapter outline

In this Chapter, the proposed research approach and methodology framework to address the identified gaps is presented. The methods and tools selection to achieve the set objectives are discussed and justified. The methodological steps of this thesis, in reference to the set objectives, are deliberated and the followed research design framework is presented.

3.2 Research approaches and methodologies

As defined by Easterby-Smith et al. (2012), methodology is 'the combination of techniques used to inquire into a specific situation'. In other words, it is described as the way the methods and techniques are connected together in order to provide a 'coherent picture' and acquire knowledge.

The methodological approaches that the researchers adopt in order to acquire knowledge, are divided to deductive and inductive (Saunders et al., 2009). Deductive reasoning is based on an established theory or generalisation and aims to identify the applicability of this theory to specific cases. On the other hand, the inductive reasoning commences with observations of specific cases and seeks for generalisations of the under-investigation phenomenon and to find patterns. Therefore, the emphasis lies to whether the theory or data is first (deductive or inductive respectively) (Pathirage et al., 2007).

Research methods are defined as the techniques and procedures required to generate and analyse the research data (Saunders et al., 2009). The research methods are categorised to either qualitative or quantitative. The deductive approach is often used in quantitative research, whereas the inductive approach is applied in qualitative research (Saunders et al., 2009).

The present study aims to investigate the marine DF engine performance and emissions as well as marine DF engine safety. For the former part, the deductive methodological approach is adopted, due to the fact that generic methodologies followed in marine two-stroke engines design or in other industries are proposed and applied in the current research study to improve the investigated marine four-stroke DF engine performance and reduce emissions. Furthermore, the methodological approach embraced in this part of the research work is characterised as quantitative, since it is governed by the use of analytical mathematical modelling and the development of a digital twin for simulating the actual engine operation, as discussed in the following sections. On the other hand, the second part of this investigation (marine DF engines safety) seeks to make observations on specific cases and then generalise a methodology on marine four-stroke DF engines, employing the inductive methodological approach. Hence, the qualitative research method is the most suitable scheme to assess and conclude on the developed methodology and then generalise it.

3.3 Methodological steps

3.3.1 Literature review

The review of the published studies and research activities consists an essential task for a researcher enabling not only the classification of the existing methodologies or strategies (and possibly adopt or combine a number of them), but also to identify the research gaps and direct his development to eventually contribute to the existing knowledge on that subject or discipline. Likewise, the literature review in this study is driven by the aim and objectives set at the initial stage of this research study. In specific, this step addresses Objective no.1. Thus, the literature review is divided in two parts; the

engine performance and emissions as well as the engine safety, with in-depth focus on each category.

The reasoning behind the first part of the literature lies under the continuous efforts made towards more efficient vessel operations in maritime industry, whilst complying with the imposed regulatory airborne emissions requirements. Being a relatively recent development adopted by the marine industry, DF engines and their reported investigation, either numerical or experimental, is limited. Therefore, the preceding literature aimed to identify and review the available studies and state-of-the-art commercial developments on marine DF engines performance optimisation and emissions trade-offs, pinpoint the approaches and methods applied and overall note the level of DF engines development. Furthermore, as the engine response is governed by the engine control system, where the two systems are interconnected and interdependent, the literature had to be expanded to cover this area as well. This part is of vital importance, having in mind the latest development in marine (DF) engines and their recently introduced sub-systems that are electronically controlled. Lastly, as a mean for compliance to the imposed airborne emission limitations, the application of the EGR system combined with the ABP system in marine engines was one of the points addressed during the literature review to examine the effects and suitability of such an exhaust after-treatment system to the DF engines. The engine control system and its optimisation methods and tools employed on the marine engines development were critically reviewed to provide a detailed insight, to the extent possible, on the existing knowledge as well as to assist to the research gaps identification.

Moving to the second part of the literature, engine safety is one of the main factors affecting the engine operability. To gain a holistic understanding of the engine safety, studies focusing on the operational limitations and the safety implications are identified and reviewed. Moreover, to mitigate the hazardous conditions that can lead to safety implications, the safety evaluation methods and tools employed by the engine manufacturers during the engine design phase are identified. Yet, safety assessment is related to the engine critical system(s)/component(s) and the engine safety systems faults/failures detection and diagnosis methods. Hence, the literature was expanded to present and critically review the experimental and numerical investigations addressing

faults and failures identification and diagnosis methods and therefore, to provide an in-depth understanding on the existing work and the potential for development in this area, considering ML vast capabilities and benefits on engines safety.

3.3.2 Reference cyber-physical system (CPS) identification

In Chapter 2, the key findings identified in the open literature and the research gaps addressed in this research study were presented. To address all the gaps however, there is an apparent need for identifying a reference engine system for this investigation. From the available literature on the marine diesel/DF engines, it is obvious that marine four-stroke DF engines have faced a limited focus in-terms of performance, emissions and safety. This is attributed to the fact that two-stroke engines attain the majority percentage of engines in the maritime industry, as primer movers. Yet, a considerable number of vessels (mainly passenger and cruise ships) utilise four-stroke engines as their primary power generation for propulsion, whereas four-stroke engines remain the main option amongst ship owners for electricity generation on-board merchant vessels. Therefore, for addressing these gaps, the present study aims at the systematic investigation of a marine four-stroke DF engine processes and response by developing a digital twin that consists of a detailed engine thermodynamic model and its control systems. The selected reference CPS for this investigation is a marine four-stroke DF engine from Wärtsilä (W9L50DF).

The marine four-stroke DF engines consist of multiple sub-systems, interconnected and interdependent to each other. These are categorised to either the actual engine components or engine controls (including safety system), grouped under one UEC system. The understanding of these sub-systems operation is crucial in order to comprehend the functionality and the parameters governing the design and operation of these components. This allows for the determination of the engine design and operational limitations as well as the identification of the most critical components affecting the engine normal operation.

Furthermore, by acquiring the required operational and design information of the individual components, the detailed digital twin modelling of the cyber-physical system (i.e. the DF engine) becomes feasible. Thus, the development and validation of a novel

digital twin of the reference cyber-physical system can then allow the investigation of the proposed framework that aims towards the DF engine performance improvement, emissions reduction and safety enhancement. The reference CPS sub-systems are presented and described in-depth in Chapter 4. This task partially satisfies Objective no.2, whereas this objective completion is achieved in the Section 3.3.4.

3.3.3 Reference cyber-physical system (CPS) Digital Twin (DT) modelling and validation

This methodological step is interconnected with Objective no.3 and encompasses the development and validation of a state-of-the-art digital twin of the selected reference CPS along with its sub-systems, to address the research gaps no.1 and no.2 of a digital twin representing the marine four-stroke DF engines behaviour and map the engine components limitations and the control system requirements. However, further development of this model (enhanced model versions), was conducted throughout this research study. Prior to initiating the modelling stage of the digital twin though, there is a number of items to consider, including the reference CPS design information availability, the modelling assumptions, where appropriate, the software tools/suites available for this type of investigation (including UEC), the modelling approach adopted, the methods and tools employed, and lastly, the engine shop trials data availability for validation. The above information is briefly discussed herein and is thoroughly covered in Chapters 4 and 5.

One of the outputs of the previous methodological step, as part of the reference CPS identification, is the engine design information. This information is used as input in this step and includes data on the engine components dimensions/volumes, engine inertia etc., as well as engine operational data for discrete engine loads such as charge air (boost) pressure and temperature, cylinders firing order, intake and exhaust valves timing, turbocharger map etc. The manufacturer of the selected reference CPS (W9L50DF), shares (partially) engine design and operational information via the official website and the product guide (Wärtsilä, 2019b). The required information for setting up the DT, was obtained from a number of sources, including previous studies, pertinent literature and manufacturer sources.

The selected reference CPS digital twin is developed in the GT-ISE, a module of the Gamma Technologies Suite (GT, 2020). This software provides the tools, libraries and functionalities to address the inherent complexity of the engine and its control system modelling as well as the interfaces required for the programming of the controller logical functions. A similar implementation by using an in-house software would be more time-consuming. In addition, GT-ISE is a tool that has been extensively used in both academia and industry (GT, 2020) for modelling a considerable variety of engine types, sizes and fuels used. Amongst the main benefits of the software is that optimisation tools, neural network tool etc. are embedded in the GT-ISE module, eliminating the need to exchange information with another software.

Once the required information is collected and the software tool is determined, the modelling step can initiate. The modelling approach adopted for the engine model development (as part of the digital twin) in the present work, is characterised as thermodynamics-based modelling. Therefore, the digital twin reflects the physical relationships of all primary engine parameters (temperature, pressure, rotational speed) as well as the resultant values, (torque, fuel consumption, emissions) and the internal parameters (heat transfer, friction, etc.). The main reasoning behind the selection of this modelling approach is its offered capability to develop a digital twin generating results that represent the actual engine operation with high accuracy and fidelity. Nevertheless, this is associated with detailed engine information input and moderate simulation time, compared to other simpler modelling approaches (e.g. MVEM). Yet, the expected trade-off between accuracy and simulation time is acceptable under the scope of this study, whereas the software offers the advantage to convert at any time the developed detailed digital twin to real-time simulation model (and connect it to the actual engine), providing flexibility to the user (the level of accuracy against the detailed digital twin is user-controlled). For the thermodynamic engine model development, a 0D/1D modelling method is adopted for the different engine component (details presented in Chapter 5). The selected method was mainly preferred against the 3D modelling approach for the following reasons. The 0D/1D models require considerably lower computational power and time. Nevertheless, even in case the computational capacity is available for 3D (CFD) models to be used (instead of the 0D models), the increased volume of input data required (boundary conditions, design details etc.) required to

develop a Digital Twin may not be available, therefore 3D models are not considered suitable for the present DT development.

Furthermore, to enable the digital twin simulations in all operating modes and loads, the developed model must accommodate the engine functional fuels and cylinders controls, the EWG system control, the engine alarms and monitoring system (AMS) as well as the engine safety system (ESS) (e.g. gas valve unit (GVU)), all integrated in the UEC. These sub-systems are developed in parallel to the engine modelling, by primarily considering the expected engine response and operating parameters for transient operation and secondly the information (although limited) provided in the engine project guide (Wärtsilä, 2019b). In this respect, the modelling approach adopted for the UEC development is characterised by dynamic linear and nonlinear systems modelling, consisting of logical expressions, lookup tables and proportional-integral-derivative (PID) controllers adopting a closed loop/feedback or feed-forward control scheme. The UEC individual modules are developed adopting a multiple-input-single-output (MISO) modelling approach.

Part of the digital twin development is its calibration and validation; with regards to the engine thermodynamic model. The calibration process is conducted to address any model observed deviations from the measured data during shop trials by adjusting engine thermodynamic model parameters, such as fuel burning rate and the emissions weighting factor, as this information is not available (measured only on manufacturer research experimental investigations). Therefore, the digital twin calibration and validation provide the required confidence that the model is credible and can be used for the specified case studies investigation. Available engine shop test data of the reference CPS are used to calibrate and customise the digital twin response. In specific, the digital twin calibration is performed under steady state conditions, for discrete engine loads (100%, 85%, 75%, 50% and 25%) in both the diesel (DI) and gas (DF) operating modes. Furthermore, engine transient runs results of a similar engine available in the literature (18V50DF) (Olander, 2006) are used to validate the model under diesel to gas (DTG) and gas to diesel (GTD) mode switching.

Following the validation under steady state and transient conditions, the developed model is used for a systematic analysis of the engine response under the investigated

transient operating conditions. By comparing the engine performance parameters, the engine design and operational limitations are identified and discussed, providing valuable information for the understanding of the engine response and the control system design improvement.

3.3.4 Proposed framework

The outcome of the previous methodological step is the state-of-the-art digital twin of the investigated reference CPS. This methodological step aims to utilise and extend the developed digital twin by developing an appropriate framework and implementing it to either optimise engine settings (for gas mode) or develop additional sub-systems models (for diesel mode and safety enhancement) that will provide the desired outcome with regard to the set objectives of this thesis (Objective no.2 and no.4). In this respect, and in order to cover the respective research gaps (no.3, no.4 and no.5), the conceived framework is divided in two discrete methodologies; (a) performance improvement and emissions reduction methodology (divided into two phases); and (b) safety enhancement methodology (Figure 3.1).

3.3.4.1 Performance improvement and emissions reduction methodology

The research approach adopted in the first part of the established framework includes the development of a novel methodology by combining and utilising state-of-the-art technologies and methodologies for performance improvement and emissions reduction in both DF engine operating modes. For clarity reasons, the performance improvement and emissions reduction methodology is divided into two phases, as shown in Figure 3.1, based on the DF engine operating modes; i.e. the gas (phase 1) and diesel (phase 2) mode.

Both phases (gas and diesel operating modes) are studied by using one integrated version of the developed digital twin, accommodating all the required capabilities. The gas mode investigation is not related with any sub-system development, whereas for the diesel mode, the EGR and ABP systems along with their control systems are developed and integrated to the existing reference CPS digital twin. For the modelling of the EGR and ABP systems, a 0D/1D modelling approach is adopted; the basis for selecting this

method against 3D modelling approach is the same as mentioned in the previous methodological step (for the engine thermodynamic model). The optimisation methods and tools employed during the implementation of the performance improvement and emissions reduction methodology are described in the Section 3.3.6. The systems developed during the proposed framework implementation are thoroughly described in Chapter 5.

Phase 1 – DF engine gas mode operation

In the case of the gas operating mode (phase 1), the compliance against the existing airborne emission requirements is already achieved. Hence, this investigation focus is shifted towards the DF engine settings effect on the performance-emissions trade-offs, with main interest on the DF engine performance in steady state conditions as well as the NO_x and CO_2 emissions. Nevertheless, it is anticipated that the engine manufacturer has conducted an engine settings optimisation study, however, the engine design and operational limitations must be identified, whereas the generated results must validate the existing manufacturers engine settings. By analysing the derived results, the processes that affect the engine efficiency and gaseous emissions are revealed enabling the elaboration on possible ways to increase the engine efficiency and reduce emissions. Therefore, the purpose of this phase is to provide an in-depth understanding of the interconnections between the engine settings and their impact on the resulted emissions as well as to identify the optimal engine settings (in gas mode) whist considering the engine design and operational limitations that are identified in the previous methodological step. In this respect, this phase aims to address the research gap no.3.

Phase 2 – DF engine diesel mode operation

On the other hand, the reference CPS (W9L50DF) is not capable of complying to the IMO 'Tier III' limits in the diesel operating mode. To optimise the performance-emissions trade-off and eventually address this need and the respective research gap (no.4), this study introduces the second phase (phase 2) of the proposed performance improvement and emissions reduction methodology, to investigate the engine response with integrated EGR and ABP systems . The engine performance and emissions when employing the EGR and ABP systems are investigated under both steady state and

transient conditions; engine transient operation is mainly examined in terms of the EGR and ABP control systems development, considering the engine design and operational limitations.

3.3.4.2 Safety enhancement methodology

The second proposed methodology of the framework aims to address the research gap no.5 and enhance the safety of the marine DF engines operation by accommodating the sensors measurements uncertainty identification and advanced actuators/sensors faults/failures diagnosis (Figure 3.1). To achieve this, however, the conceived research approach adopts consecutive methodological steps, as described below, that ensure the required information exchange between the development stages.

First and foremost, as part of the safety aspect of the DF engines, a system failure mode effects and analysis (FMEA) is performed, where all the engine components are analysed to identify possible failure scenarios in the design that need to be handled. Primarily, the analysis focuses on the systems, the risk aspects and failure types of which differ from the ones of the conventional diesel engines. This step allows for the identification and assessment of the most critical DF engine systems (i.e. components) and the investigation of the safety implications imposed by the sensors measurements uncertainty and the faults diagnosis. In this respect, this step is essential for revealing and comprehending the interactions and effects of the engine critical components to the engine operation as well as for evaluating the existing failure diagnosis methods employed by the engine manufacturers. Moreover, the integrated digital twin previously developed (including the EGR and ABP systems), is further extended to permit the investigation (via simulations) of these possible engine faulty scenarios and capture the engine response under faulty conditions. In this respect, the faulty operation simulator (FOS) is designed and integrated in the UDS (described below), capable of reproducing the faulty components response and the sensors signal bias when activated.

The methodological steps described in the preceding paragraphs permit the implementation of the subsequent steps, which entail the development of an innovative engine diagnostics system (EDS). The research approach for this step consists the combination and utilisation of state-of-the-art tools such as neural networks (NNs) and

faults/failure diagnosis methods. Furthermore, the developed EDS consists of the intelligent engine monitoring system and the advanced faults/failures detection system. The former is realised in order to identify the sensors measurements uncertainty via a novel data-driven (DD) model in combination with classification thresholds and logic controls (i.e. logical expressions and conditions), whereas the latter system processes this information in a newly introduced set of faults/failures detection logical expressions and conditions, integrating the manufacturers current detection and diagnosis methods. The data-driven model, employing neural networks, was developed in the GT-ISE software. The NNs are trained to capture the engine healthy operational data generated for different boundary conditions via parametric simulations, utilising the DoE tool that is embedded in GT-ISE. Upon the NNs training completion, the DD model is validated against available DT data at each engine discrete load. Details on the EDS and its sub-systems modelling approach and the data-driven model validation are presented in Chapter 5.

3.3.5 Digital Twin Unified Digital System (UDS) integration

Having completed the above individual methodological steps, and considering this thesis aim, it is essential to incorporate the developed systems (EDS and FOS) in a unified digital system (UDS), as part of the integrated digital twin (Objective no.4). The integration goal is to establish a digital 'core' to monitor and control the engine operation as well as to evaluate the engine performance and safety with the required fidelity. To achieve this, the latest version of the digital twin (equipped with the FOS module) is further extended by introducing the EDS and incorporating all the engine control modules (including manufacturer control systems) in one main unit; the UDS. This model development is considered the final (integrated) digital twin version of this thesis and it is used to verify the UDS capabilities. The integrated UDS modelling approach is described Chapter 5.

3.3.6 Case studies design, optimisation and verification

The design of specific case studies is essential in order to study the reference CPS and verify the proposed framework, as reported in Objective no.5. Though the examined

case studies, the developed digital twins of each stage are used to simulate the actual engine operation and examine its response. Consequently, this methodological step involves the appropriate case studies design in order to: (a) examine the reference CPS response in transient conditions; (b) combine and implement state-of-the-art optimisation methods for improving the DF engine performance and reducing emissions; (c) identify the most critical DF engine systems, examine potential safety implications and evaluate engine manufacturer failure diagnosis method; and (d) evaluate the UDS response.

The investigation of the marine four-stroke DF engine response in transient conditions is examined under the diesel to gas (DTG) and gas to diesel (GTD) modes switching, the results of which are also used for the digital twin validation intransient conditions. The elaboration on these case studies assists to the in-depth understanding of the engine operating control functional processes required for the realisation of the mode switching, as well as the identification of the engine design and operational limitations.

With regard to the performance improvement and emissions reduction methodology, and specifically in the gas operating mode (phase 1), the adopted research approach encompasses a parametric investigation via design of experiments (DoE) in GT-ISE, for a number of engine settings (SOI, boost pressure and inlet valve timing), considering the engine operational and safety limitations (air−fuel equivalence ratio (or lambda) and charge air (boost) pressure. The parametric investigation (via DoE) is preferred against other optimisation methods, as this method can examine the investigated parameters for a predefined imposed range with specific increments, eventually leading to reduced simulation time. In addition, the parametric approach generates a set of engine settings, permitting the user to make their final selection, depending on the objective weighting factors each individual considers. Furthermore, for the diesel operating mode investigation (phase 2), the EGR and ABP system settings (ordered from the EGR and ABP control systems) are optimised in GT-ISE by initially employing the integrated MOGA optimiser and then the DoE tool. The reasoning behind the combination of the two optimisation approaches lies under the way the optimisation process was conceived. Initially, the MOGA optimiser aims to identify the EGR and ABP settings that will result to the optimal engine performance and emissions reduction to IMO 'Tier III'

levels, whereas the DoE parametric investigation is conducted to identify the SOI settings (for a given range) that will result to further optimisation of engine performance, as reported in the literature. Therefore, the optimisation process is discretised to EGR and ABP system settings optimisation (employing MOGA) and the engine performance optimisation (employing DoE). Details on the systems optimisation process are presented in Chapter 6.

On the other hand, the case studies related to the DF engine safety are designed to provide information on the most critical DF engine systems and the safety implications related to those systems as well as to evaluate the existing engine manufacturer failure diagnosis method and identify its weaknesses. In this respect, a DF engine safety assessment is performed by employing FMEA, to identify the critical DF engine components that can lead to hazardous scenarios, whilst the potential faulty engine operations are ranked, and the most critical cases are identified and simulated in GT-ISE using the developed digital twin of the reference CPS (W9L50DF) to investigate the engine response. For these simulations, the FOS system setup is appropriately adjusted for each case study to handle the engine signals (delay, offset etc.), based on the available sensors data retrieved from the pertinent literature review. The case studies simulation results are then assessed to deduct the required information and proceed with the EDS design. Moving to the final part of this methodological step, the integrated UDS verification is performed via the designed case studies. The UDS verification results from the simulated case studies (under faulty sensors response) in the diesel and the gas modes operation are qualitatively compared against the manufacturer reference CPS diagnosis system, and the respective FMEA scenarios considered for DT simulations reflecting these faults are re-evaluated to demonstrate the UDS applicability benefits.

3.4 Research design framework

Based on the proposed framework described in the preceding sections, the research design of this thesis is developed and presented in Figure 3.1. The illustrated plan includes all the methodological steps described in reference to the set thesis objectives, addressing the research gaps discussed in the critical review.

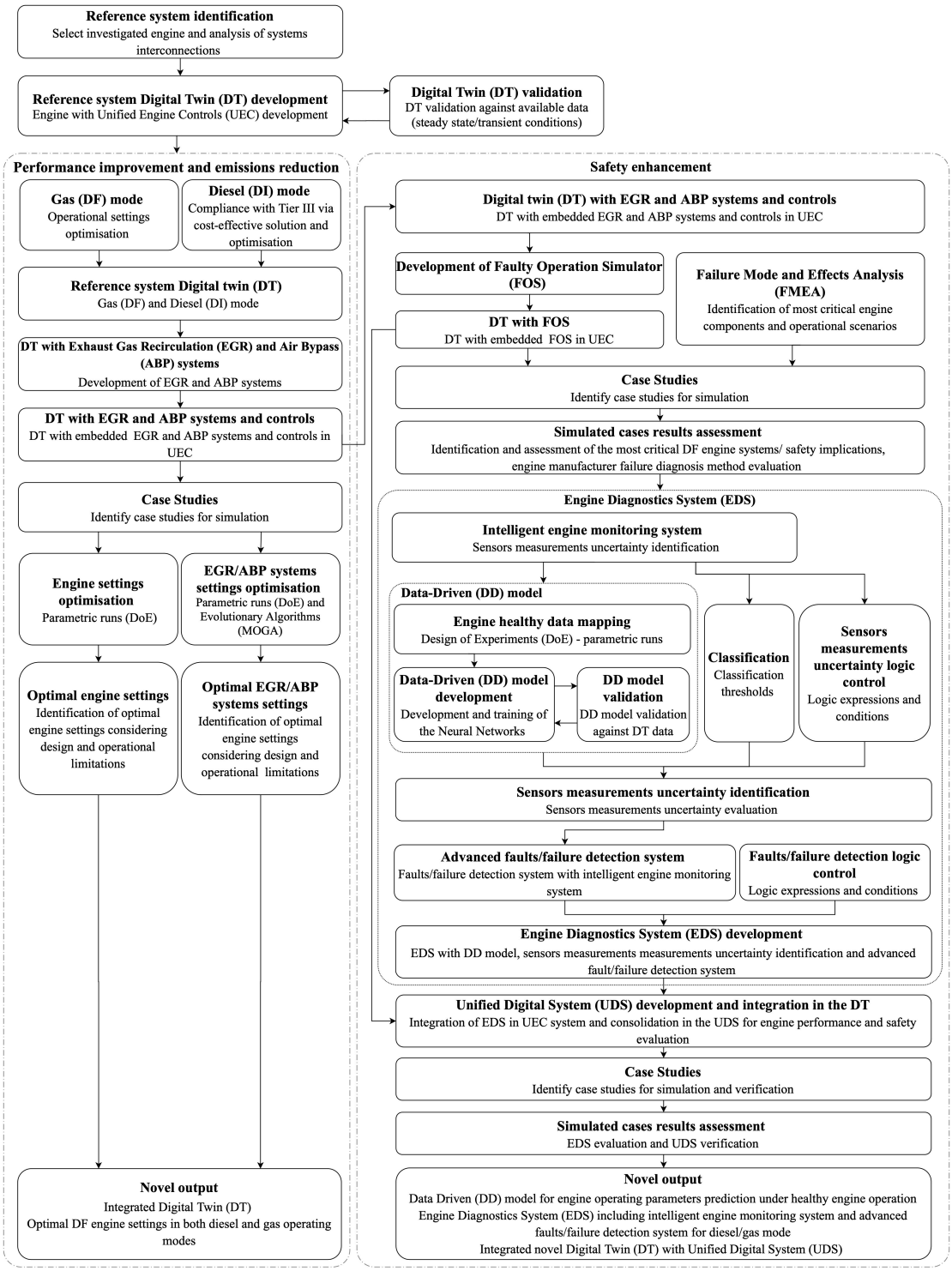

Figure 3.1 Research design framework

3.5 Chapter summary

This Chapter presented the adopted research approach for the development of the proposed methodology and discussed the methodological steps that were followed in this thesis to cover the identified research gaps. The methods and tools selection to achieve the set objectives are discussed and justified. In the following Chapters, the methodological steps are implemented, and the respective outcomes are discussed in detail.

4 REFERENCE CYBER-PHYSICAL SYSTEM (CPS)

4.1 Chapter outline

In this Chapter, the selected reference cyber-physical system (CPS) and its characteristics are presented. The components that entail the reference CPS along with their functionality are described in detail, whereas the reference CPS transient operational limitations identified by the manufacturer are reported. Lastly, the reference CPS parts as well as the additional systems considered during the modelling phase are defined.

4.2 Engine characteristics

In the present study, the reference CPS selected is a four-stroke, non-reversible, turbocharged and intercooled Wärtsilä 9L50DF engine is investigated (Wärtsilä, 2019b). The engine can operate in either the gas (DF) or diesel (DI) operating modes. The engine control system is capable of smoothly switching between operating modes. The engine high power output along with the fuel flexibility, the low emissions, the high efficiency and reliability, renders this engine an attractive solution either for electric power generation or ship propulsion (Wärtsilä, 2017). Its main advantage is the lean-burn combustion, which provides an increased engine efficiency with reduced in-cylinder peak temperatures, thus resulting in reducing the NO_x emissions and the engine

thermal loading. In this study, the selected engine was considered as a part of a generator set operating at a constant speed. The engine details are reported in the manufacturer product guide (Wärtsilä, 2019b), the main engine characteristics are illustrated in Table 4.1, whilst the engine layout and components are presented in Figure 4.1 and Figure 4.2.

Table 4.1 Engine main characteristics (Wärtsilä, 2019b)

	Parameter	**Unit**	
Operational	MCR power	[kW]	8775
	MCR speed	[r/min]	514
	BMEP at MCR	[bar]	20
	BSFC at MCR (Diesel mode)	[g/kWh]	190
	BSEC at MCR (Gas mode)	[kJ/kWh]	7300
Geometrical	Bore / Stroke	[mm]	500 / 580
	Connecting rod length	[mm]	1990
	TDC clearance height	[mm]	11
	Compression ratio (Schlick, 2014)	[-]	12:1
Other	No. of cylinders	[-]	9
	Turbocharger units	[-]	1

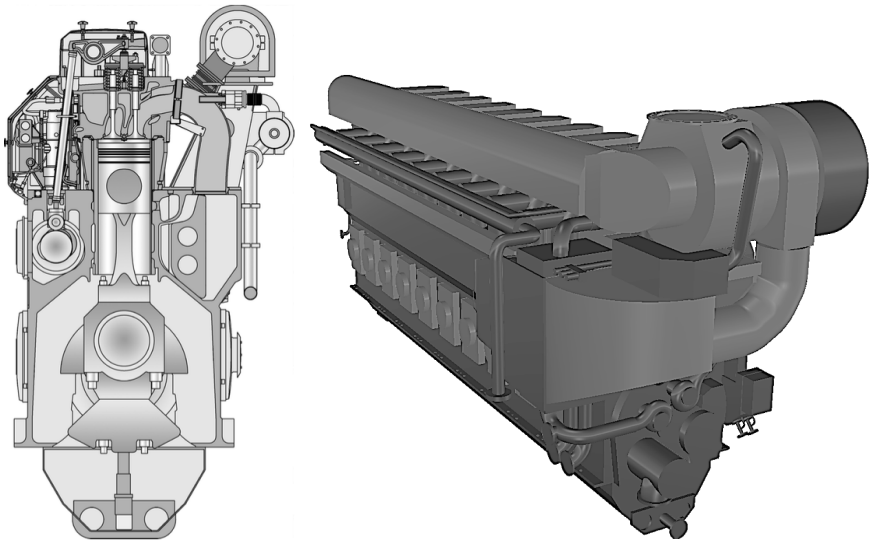

Source (Wärtsilä, 2019b)

Figure 4.1 Wärtsilä 9L50DF cross-section view (left) and 3D model (right)

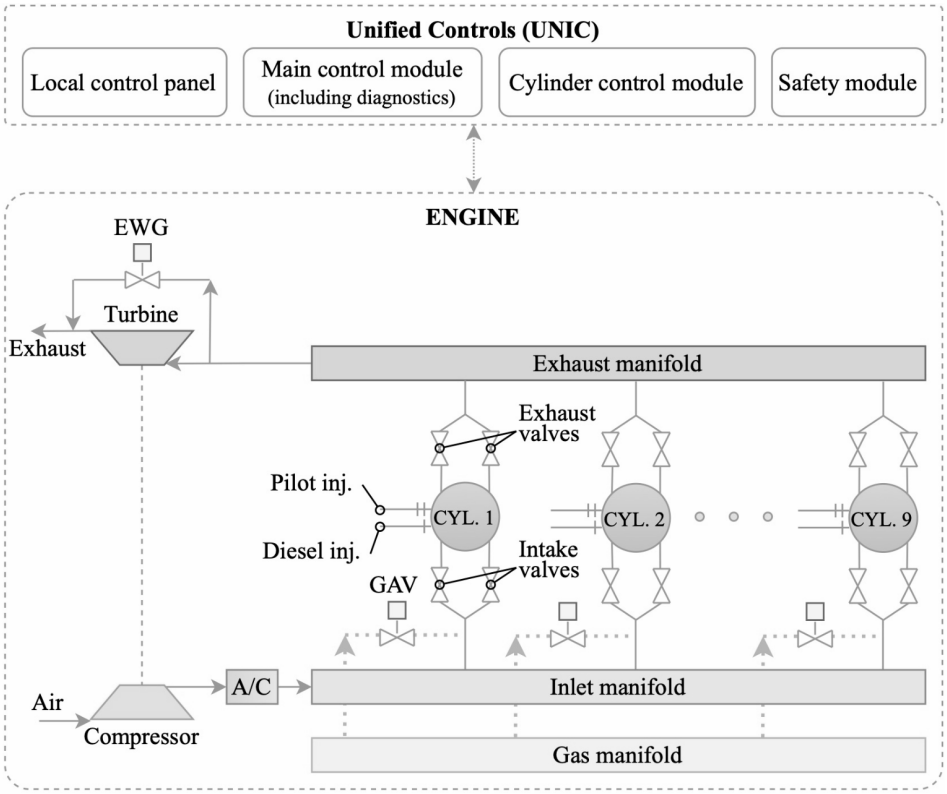

EWG: Exhaust waste gate; GAV: Gas admission valve

Figure 4.2 Reference CPS (Wärtsilä 9L50DF engine) layout

4.3 Operating modes and principles

As already mentioned, the engine is capable of operating in the following two distinct modes and one optional fuel shared mode: (a) the gas (DF) mode running on natural gas and light fuel oil (which is used as pilot fuel for initiating combustion); (b) the diesel (DI) mode, in which either HFO or LFO is used as the main fuel; and (c) the shared mode where both gas and diesel fuels are utilised based on a manufacturer imposed profile (shared mode is out of scope for this study as it is optional and, if applicable, is found to be limited).

Amongst the main benefits of the marine DF engines with low pressure admission when operating in the gas mode, is the radical emissions reduction compared to the diesel mode running in HFO. In specific, the SO_x emissions can be reduced up to 90-99% and the NO_x emissions up to 80-85%, as DF engines operate in the lean burn combustion concept. Furthermore, the CO_2 emissions can be decreased up to 20-30%,

due to the natural gas lower carbon to hydrogen ratio (Herdzik, 2011, MAN, 2012a, Jacobs, 2012), whereas the PM emissions are almost eliminated and there is no visible smoke during engine operation at gas mode.

Furthermore, as an option in Wärtsilä large bore DF engines (e.g. 46DF, 50DF), it is possible to operate the engine in fuel sharing mode (Wärtsilä, 2019b); the operator can set the gas/liquid fuel ratio preference depending on the amount of available gas and the power, based on an imposed fuel sharing as provided by the manufacturer. The investigated DF engine operating modes functional diagram is illustrated in Figure 4.3.

Lastly, the engine control and safety system can order the engine to run in the backup operating mode (i.e. conventional diesel fuel injection only). The engine will automatically switch from the gas mode to the diesel mode (gas trip) in several alarm situations (Wärtsilä, 2019b).

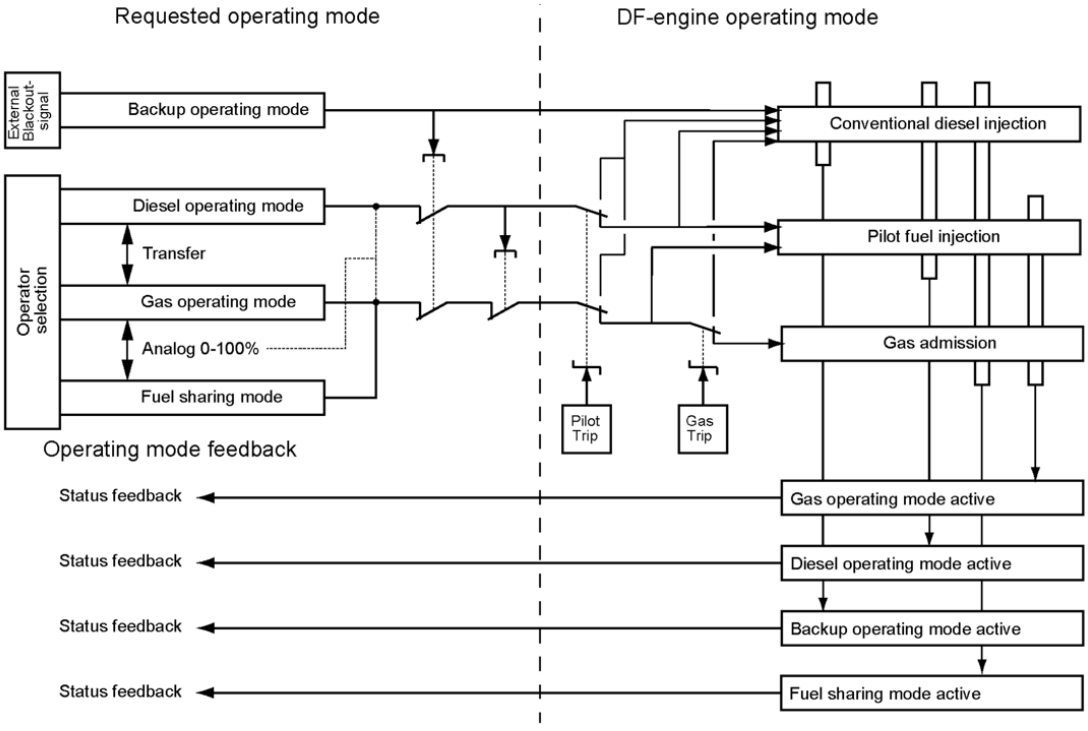

Source (Wärtsilä, 2019b)

Figure 4.3 DF engine operating modes functional diagram

Therefore, to allow for the engine smooth operation, an adequate control strategy for governing the injected fuels amount as well as their injection timing and duration has to

be implemented. This also includes the EWG control, which is essential to adjust the combustion air−fuel ratio by regulating the charge air (boost) pressure. The reference CPS control strategy is described in the following sections.

4.4 Engine fuel systems

Compared to the conventional marine diesel four-stroke engines, the number of components of the dual fuel engines is moderately increased in order to accommodate the utilisation of the secondary fuel, i.e. the natural gas. Therefore, some of the existing engine systems are slightly modified, whereas a number of new components is introduced, as presented hereafter.

4.4.1 Pilot fuel oil system

The pilot fuel high-pressure system main components include the pump unit, the common rail pipe, the feed pipes and the injection valves. The pump unit elevates the pilot diesel fuel pressure to the required level. It consists of an electric-driven or engine-driven high-pressure pump, a safety valve to protect against the system overpressure, the fuel filter(s) and a pressure control valve. In the case of the electric-driven pump, the pump unit is located in the DF engine room close to the engine. Pressurised pilot fuel is delivered from the pump unit into a common rail pipe. All high-pressure piping between the pump and the injectors are of the double wall type. Any leakage is collected from the annular space of the double wall pipe and lead to a collector with a leakage sensor. The common rail piping delivers the pilot fuel to each injection valve and also acts as a pressure accumulator to suppress the pressure pulses.

The Wärtsilä four-stroke large and medium bore DF engines utilise two-needle injection valves where the pilot fuel injector is integrated with the main diesel fuel injector (Figure 4.4). The bigger needle is for the main diesel fuel (used in diesel and backup operating modes) and the smaller needle serves the diesel pilot fuel (used in diesel and gas operating modes). In both cases, a solenoid valve operates the pilot fuel injection needle adjusting the injection timing and duration. The pilot fuel injection is also employed

when the DF engine runs in the diesel operating mode in order to keep the pilot fuel needles clean as well as to cool the injector parts.

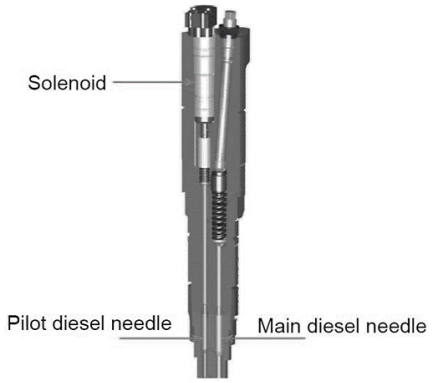

Source (Jacobs, 2012)

Figure 4.4 The pilot fuel twin needle injector

4.4.2 Gas Admission Valve (GAV)

The gas admission valves (GAV) (one per cylinder) are controlled by the engine Unified Controls (UNIC) system to adjust the amount of gas fed into each cylinder, thus regulating the engine power output and speed. Gas is injected by using solenoid valves at each cylinder inlet port (upstream the intake valves) (Figure 4.5) during the engine induction process. This design ensures that only air is present in the inlet manifold, and thus the risk for explosion in the engine charge air intake system is minimised. Since each GAV can be controlled independently of the corresponding cylinder inlet valves, the scavenging of this cylinder is possible without unburned gas escaping directly from the inlet to the exhaust manifolds.

The gas admission valve is an actuated digital solenoid valve. The valve is closed by a spring when no electrical signal is provided. The gas fuel inlet pressure at the gas (fuel) manifold is controlled over the whole engine load range by the pressure regulating valve that is adjusted by UNIC, in order to prevent the excessive forces from the gas (fuel) manifold pressure on the GAV, which could impact on the opening of the valve. It must be noted that the gas (fuel) manifold pressure is also regulated by considering the gas feeding system control and the GVU.

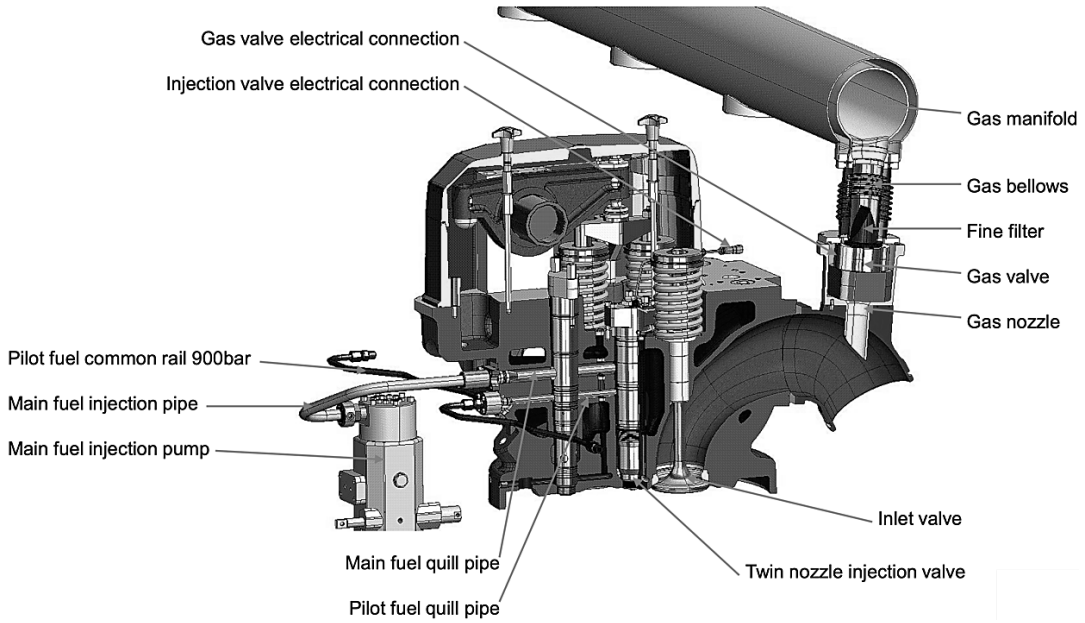

Source (Jacobs, 2012)

Figure 4.5 Layout of the engine pilot and gas fuelling systems

4.5 Engine intake and exhaust systems

The intake and exhaust systems are mainly passive components, with the exemption of the exhaust gas ventilation system and the air−fuel ratio control.

In order to achieve the optimal engine performance, it is essential to adjust the air−fuel ratio during varying operating conditions. For this purpose, the Wärtsilä small-bore engines use an ABP valve controlling the air−fuel ratio, whereas the Wärtsilä DF large and medium bore engines use an EWG valve.

The EWG valve allows part of the exhaust gases to bypass the turbocharger turbine. This valve operates as a regulator and adjusts the air−fuel ratio to the correct value regardless of varying ambient conditions (ambient temperature, humidity, etc.). The EWG is equipped with a feedback signal of the valve position to the UNIC.

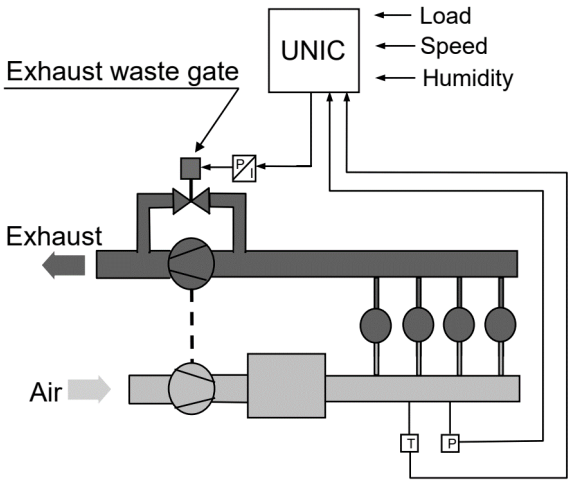

Source (Jacobs, 2012)

Figure 4.6 Exhaust waste gate (EWG) valve controls

4.6 Unified Controls (UNIC)

The UNIC automation system consists of a sophisticated network of multiple modules, exchanging information in order to ensure the efficient, smooth and safe engine operation. Consequently, the DF engine speed, power, combustion and safety functions are controlled by the UNIC to allow the optimal running conditions to be set, independently of the ambient conditions or the fuel type and properties. Its design allows the system to be directly mounted on the engine, which offers a compact design without components to be mounted in dispersed external cabinets or panels. The same automation system basis is used on all Wärtsilä DF engines (Vuollet et al., 2019).

Moreover, the system collects signals from various engine sensors at different locations on the engine. The sensors signals are processed and employed to control the engine settings that affect the combustion process. Thus, the gas feed pressure demand, gas admission duration and timing, pilot injection duration and timing, and air−fuel ratio are immediately adjusted to meet varying load demands or other conditions. The measured engine speed is, among many other functions, used for speed control, i.e. control of the fuel demand in order to achieve the ordered engine speed. For DF engines equipped with electronic fuel injection, the crank angle position is also important in order to correctly adjust the injection timing.

The UNIC is a physically distributed system (on the engine) that consists of the following main modules: main control module, cylinder control module, local control panel and engine safety module.

4.6.1 Main control module

This module contains diagnostic features as well as advanced I/O checks based on signal processing, like open/short circuit detection and sensor diagnostics.

The engine safety and steady operation is directly associated with the components failure, where failures can be categorised either as electrical (sensors, cables or control unit) or mechanical; the latter also referred to process failures (WinGD, 2019). At present, the engine manufacturers focus on the engine components diagnosis by employing a simplified approach, which is highly reliable, yet leaving space for further development; the components failure detection (i.e. actuators or sensors are non-responsive) is based on the expected values of each monitored parameter. Furthermore, in order to increase the engine reliability, where necessary, the manufacturer countermeasures are usually related to sensors redundancy, manual override and/or optical inspection. Thus, this approach may not be considered adequate, as in some cases the engine may switch from gas to diesel mode operation or even slowdown/ shutdown due to high sensors measurements uncertainty.

The manufactures approach employs a diagnostics module strategy based on the continuous engine supervision to detect a mechanical failure. In case where a component failure is detected, evaluation of the sensors input is performed (where appropriate), and the engine control system orders corrective actions (Figure 4.7).

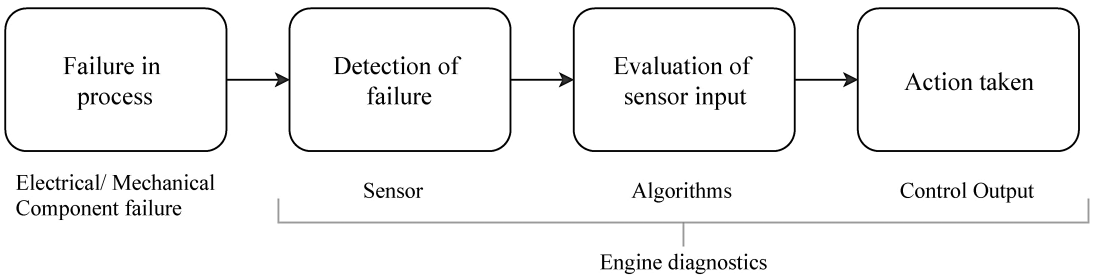

Figure 4.7 Current failure diagnostics strategy

The evaluation of the sensors input is based on algorithms that utilise the engine shop trials and testing measurements data that are recorded and stored in the UNIC diagnostic library.

Furthermore, in an effort to improve the DF engine reliability, the engine manufacturers have introduced three ways of sensors failure detection; (a) supervised sensors where the wiring is supervised, i.e. wire breakage or/and too high current signals (out of range) are detected; (b) double sensors, where it is possible to detect wire breakage as well as a drifting of a sensor; and (c) control-sensors feedback comparing; in case the expected sensor feedback is related to a control output, the validation of the sensor acquired signal is done by comparing the sensor input to the expected input when knowing the control output.

Notwithstanding the above, it must be mentioned that the sensors failure detection method currently employed by the manufacturer, detects sensor signals that are only out of range or drifting as well as non-operative actuators/sensors. Sensor measurements uncertainty is not considered under the current developments by the manufacturers.

4.6.2 Cylinder control principle

The cylinder control module handles all the injection and combustion monitoring of three (3) cylinders per sub-module. Exhaust gas temperature sensors and knock sensors are also connected to this module. The module processes locally functions related to fuel injection control and cylinder-specific measurements.

One of the key developments in the DF engines, is the combustion process control for each cylinder, to ensure knocking and misfiring-free operation in all conditions. The engine advanced automation system controls the engine functions accounting for the prevailing ambient conditions and the used fuel properties (fuel quality, methane number, etc.), so that optimal running conditions are obtained (Portin, 2010).

In specific, to achieve the required accurate combustion control, the gas admission valves as well as the diesel fuel injectors are electronically controlled (in the gas and diesel operating modes, respectively) to adjust the engine power output for maintaining

the ordered engine speed (Vuollet et al., 2019, Wärtsilä, 2019b). The injected pilot fuel amount depends on the engine operating mode and load. Moreover, to achieve stable combustion conditions, an air−fuel ratio operating window between the limits of misfiring and knocking combustion needs to be targeted, as shown in Figure 4.8. At higher engine loads, a lean air−fuel mixture is utilised to avoid knocking (Wärtsilä, 2019b). However, at high loads the misfiring limit is getting closer to knocking limit, which means that the useful operating window decreases. The engine cylinders air−fuel ratio is adjusted via an electronically controlled EWG, which bypasses a part of the exhaust gas along the turbocharger (TC) turbine (Wärtsilä, 2019b), as previously mentioned. Continuously monitored cylinders pressures by pressure sensors enables the accurate load evaluation and stable engine running. Knocking is detected by using a peak pressure sensor. Also monitoring of exhaust gas temperature is used to detect abnormal burning process and knocking situations.

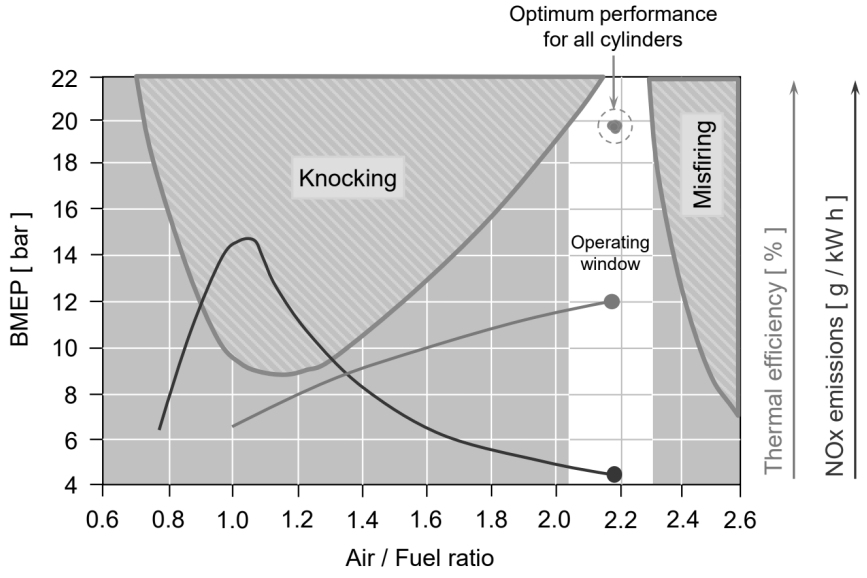

Source (Jacobs, 2012)

Figure 4.8 The lean burn operation window

4.6.3 Engine safety module

The engine safety module handles a number of speed measuring functions and it feeds these signals to the engine control and monitoring systems. Furthermore, this module is linked to the engine shutdown devices interface and local instruments.

4.7 Transient operation requirements

For ensuring the engine integrity and smooth running during transient operations, the UNIC needs to satisfy the engine response requirements as determined by the engine manufacturer (Wärtsilä, 2019b). With regard to the load transition, for load steps in the gas mode, the maximum acceptable step load increase is as illustrated in Figure 4.9 (left), whilst the maximum allowed step load decrease should be according to the following schedule: 100%-75%-45%-0% (for the intermediate engine loads, the nearest lower load threshold needs to be used). In addition, the recovery time (i.e. the time required for the engine to reach its steady-state operating point following a transient) should be less than 10 s, whilst the recommended time between consecutive load steps should be greater than 30 s. In the diesel mode, the maximum acceptable step load increase is as indicated in Figure 4.9 (left) and there are no limitations in terms of step load reductions. In this case, the recovery time after a load change decreases to 5 s, whereas the recommended time between consecutive load steps is greater than 10 s.

For ramp load changes in the gas mode, the engine control system must not permit a load reduction from 100% to 0% faster than 20 s prior to automatic transfer to the diesel mode. The maximum allowed ramp load increase for various engine operating conditions is shown in Figure 4.9 (right). The curve "preheated, normal gas" is used as the default ramp load increase for the gas mode, whereas the curve "max capacity gas" indicates the maximum allowed ramp load increase.

Furthermore, considering the fuel transition at any fixed load, the gas to diesel (GTD) mode switching needs to take place within 1 s at any load. The switching from the diesel mode to the gas mode (DTG) needs to be completed within 2 min for minimising disturbances to the gas fuel supply systems. In both cases, the maximum allowed speed drop is 10%. These manufacturer engine transient operation requirements are summarised in Table 4.2.

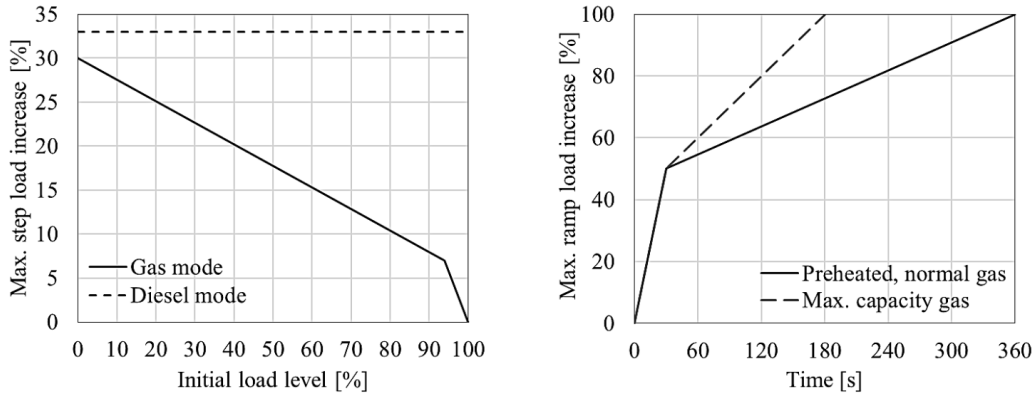

Source (Wärtsilä, 2019b)

Figure 4.9 Maximum allowed step load increase in percentage of MCR for the gas mode and the diesel mode (left); Maximum allowed ramp load increase for engine operating at nominal speed (right)

Table 4.2 Engine transient response requirements (Wärtsilä, 2019b)

Load Change	**Diesel Mode**	**Gas Mode**
Recovery time	≤ 5 s	≤ 10 s
Time between load steps	≥ 10 s	≥ 30 s
Maximum allowed speed drop	10%	10%
Maximum step-wise load increase	33% of MCR	shown in Figure 4.9
Maximum step-wise load decrease	No limitation	100 – 75 – 45 – 0 %
Mode switching	**Diesel to Gas**	**Gas to Diesel**
Time required for fuel change	2 min	1 s
Maximum allowed speed drop	10%	10%

4.8 Reference CPS modelling considerations

In the previous Sections, the reference CPS and its parts were described in detail. To proceed to the modelling phase however, the reference CPS sub-systems and components under consideration must be selected. This Section addresses this point by describing the reference CPS sub-systems to be modelled in the next Chapter, the EGR and ABP systems to be designed and integrated to the reference engine as well as the engine unified control modules to be considered. The reference CPS layout under consideration to be developed is illustrated in Figure 4.10.

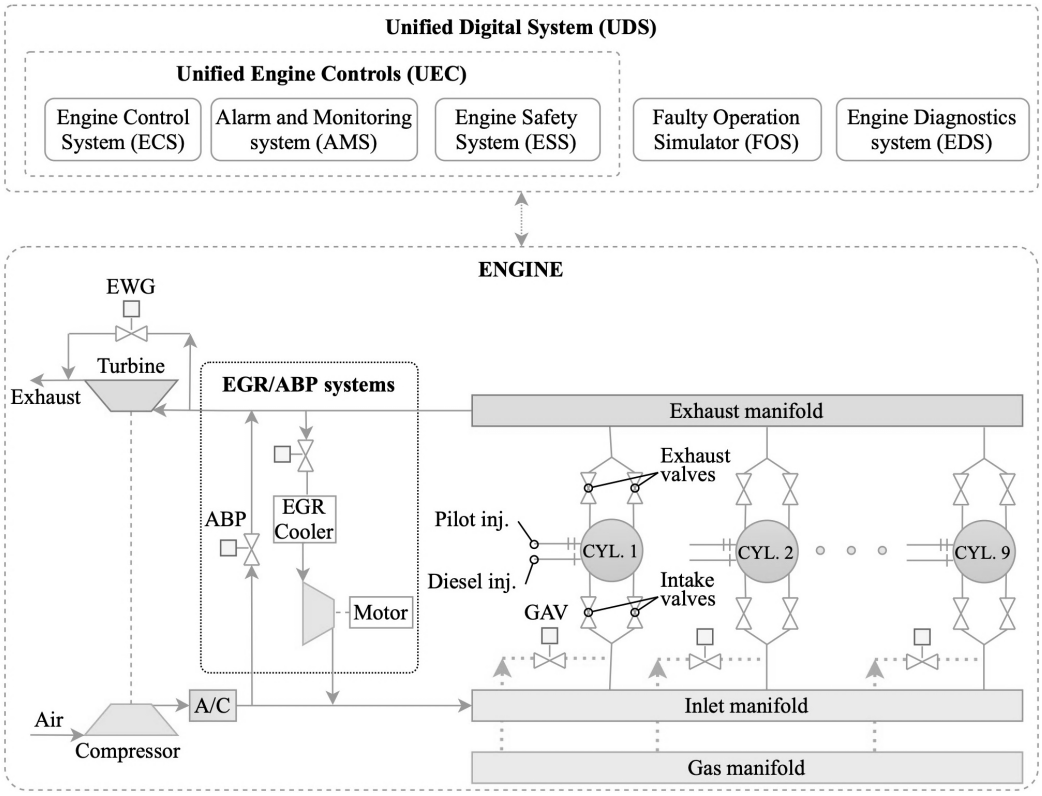

Figure 4.10 Reference CPS layout under consideration

4.8.1 Engine

For representing the actual engine operation during simulations, all the engine components, as presented in Figure 4.2, are considered. In this respect, the considered systems include the T/C with EWG, the A/C, the inlet and exhaust manifolds, the GAV, the diesel and pilot injectors and all the cylinders with their intake and exhaust valves.

4.8.2 EGR and ABP systems

According to the engine manufacturer, the W9L50DF engine is capable of accommodating an EGR system (Wärtsilä, 2019b). To determine the most suitable EGR system layout, the engine type, the fuel type (diesel/gas), the turbocharging system layout (single or two-stage turbocharging) and the turbine type (VGT, EWG) must be considered. Furthermore, due to the challenges and constrains for operating the engine in two modes (diesel and gas), the turbocharger needs to match both operating modes.

The EGR system investigated in this study is of the HP-EGR type, redirecting a controlled amount of exhaust gas from the exhaust manifold to the inlet manifold via the EGR system loop. The HP-EGR system, accompanied with a suitable control system, is considered the most efficient EGR design in terms of NO_x emissions reduction and fuel consumption trade-offs, as indicated in the literature for the specific application and engine type (Jeppesen, 2016, Grøne, 2016).

The EGR system is equipped with an EGR valve, controlled by the UEC and adjusts the recirculated exhaust gas amount to reduce the oxygen concentration of the inlet manifold working medium. Moreover, an exhaust gas cooler is fitted in the EGR system to reduce the exhaust gas temperature (which subsequently enters the EGR blower and the inlet manifold). Employing the HP-EGR blower along with EGR exhaust gas cooler, allows the working medium (air and exhaust gases) temperature in the inlet manifold to remain within the limits set by the engine manufacturer. Nevertheless, the inlet manifold working medium temperature limitation was considered during the EGR and ABP systems design stage.

Another essential part of the engine design with EGR system, is the air bypass system (ABP). The air bypass system is usually fitted in small-bore marine engines for preventing compressor surging of the turbocharger compressors in case of rapid engine load reduction (Wärtsilä, 2019a). The air bypass valve system is not commonly considered in the EGR design; the existing studies focused on either the two–stage turbocharged marine engines to directly reduce the NO_x emissions to the IMO 'Tier III' limits and optimise the engine fuel consumption or the single-stage turbocharged marine engines that use low EGR rate and supplementary technologies to achieve IMO 'Tier III' NO_x emissions limits. However, considering that the investigated engine in the present study is a marine DF engine, the turbocharger needs to match both the gas and diesel modes requirements. For that reason, the T/C matching is primarily performed in the diesel mode based on the targeted boost pressure, whereas the gas mode employs the EWG valve to adjust the boost pressure, thus realising the effective engine-turbocharger matching in both operating modes. Thus, considering that the EGR system operation is required in the diesel mode, the turbocharger matching proves to be a major challenge during the engine design stage. Furthermore, preliminary results of

this study indicated that the lack of the ABP system on a single-stage turbocharged engine that operates at high EGR rates can lead to an engine-turbocharger mismatch. This is attributed to the reduced turbine exhaust gases energy flow (due to the EGR system operation), which reduces the T/C shaft speed and thus the compressor mass flow and pressure ratio. Therefore, the compressor operating point (when the engine uses the EGR system) is shifted towards the compressor surge line. The ABP system application aims to avoid the matching and fitting of a new turbocharger unit, due to the engine and the existing T/C design operational limitations, that will lead to additional capital costs. This is achieved by redirecting a part of the charge air flow from the compressor outlet to the turbine inlet in order to keep the compressor operating point within the compressor normal operating region, thus avoiding instabilities.

Detailed description of the EGR and ABP systems and their respective controls as well as their modelling design approach is presented in the following Chapter.

4.8.3 Unified Engine Controls (UEC)

Whilst the conceived UEC system differentiates from the engine UNIC system, in terms of structure and modules definition, as it is described in the next Chapter, the main functionalities of both systems remain the same. In this respect, the considered ECS consists of the fuel control module, the cylinder control module, the EWG valve control as well as the EGR and ABP systems controls. The alarms and monitoring system (AMS) is responsible for monitoring the engine parameters (speed, pressure, temperature and other engine operating parameters) and activating the engine alarms, where appropriate. The engine safety system is similar to the manufacturer safety module, including the GVU controls, the gas leakage detection, the shutdown actions and local instruments related to the engine safety. Lastly, the engine diagnostics included in the main module; according to the engine manufacturer, are considered as a separate sub-system under a novel Engine Diagnostics System (EDS). Both Faulty Operation Simulator (FOS) and EDS form part of the proposed systems that are discussed in the following Chapter.

4.9 Chapter summary

In this Chapter, the reference CPS characteristics, the operating principles and transient operation limitations were presented. The engine sub-systems and components were described, whereas the reference CPS parts modelling considerations for the next development phase are presented.

5 ENGINE DIGITAL TWIN MODELLING AND VALIDATION

5.1 Chapter outline

This Chapter presents the modelling process of the identified reference CPS and its components as well as the developed models integration leading to investigated reference CPS digital twin. The modelling principles governing the engine operation as well as the UEC functional (logical/process) modelling are presented and discussed. Lastly, the developed digital twin is validated against steady state and transient conditions available data.

5.2 Engine Digital Twin

The present study focuses on the modelling of the investigated marine DF engine and its control system for studying the engine response at steady state and transient conditions by employing the GT-ISE, which is a widely used simulation program for engine modelling and analysis (GT, 2020). The complete digital twin was realised by using the following assemblies of the GT-ISE software: (a) the user input; (b) the 0D/1D engine model; (c) the unified digital system (UDS). The schematic representation of the assemblies is illustrated in Figure 5.1. In the developed model, the user can order a specific transient operation (i.e. load changes at either the gas or the

diesel modes, a mode switching at constant load, or extreme load changes that may result in a mode switching) by employing the user input assembly.

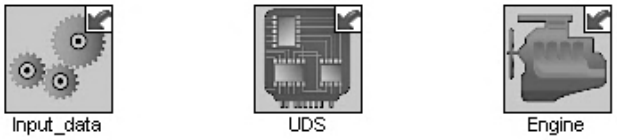

Figure 5.1 W9L50DF digital twin layout in GT-ISE environment

5.2.1 Engine model

The engine thermodynamic model uses a number of elements available in the GT-ISE software library, which are appropriately interconnected. The complete engine layout of the model in GT-ISE is presented in Figure 5.2.

The input data required to set up the engine thermodynamic model includes the engine geometric data, the cylinders valves profiles, the compressor and turbine maps, the EWG valve area, the constants of engine sub-models (combustion, heat transfer and friction), the ambient conditions as well as the engine load and mode time variation. Initial conditions need to be provided for the temperature, pressure and composition of the working medium contained in the engine cylinders, pipes and receivers. The input data was acquired from the engine manufacturer product guide and the three-dimensional (3D) engine drawings available by the engine manufacturer in (Wärtsilä, 2019b).

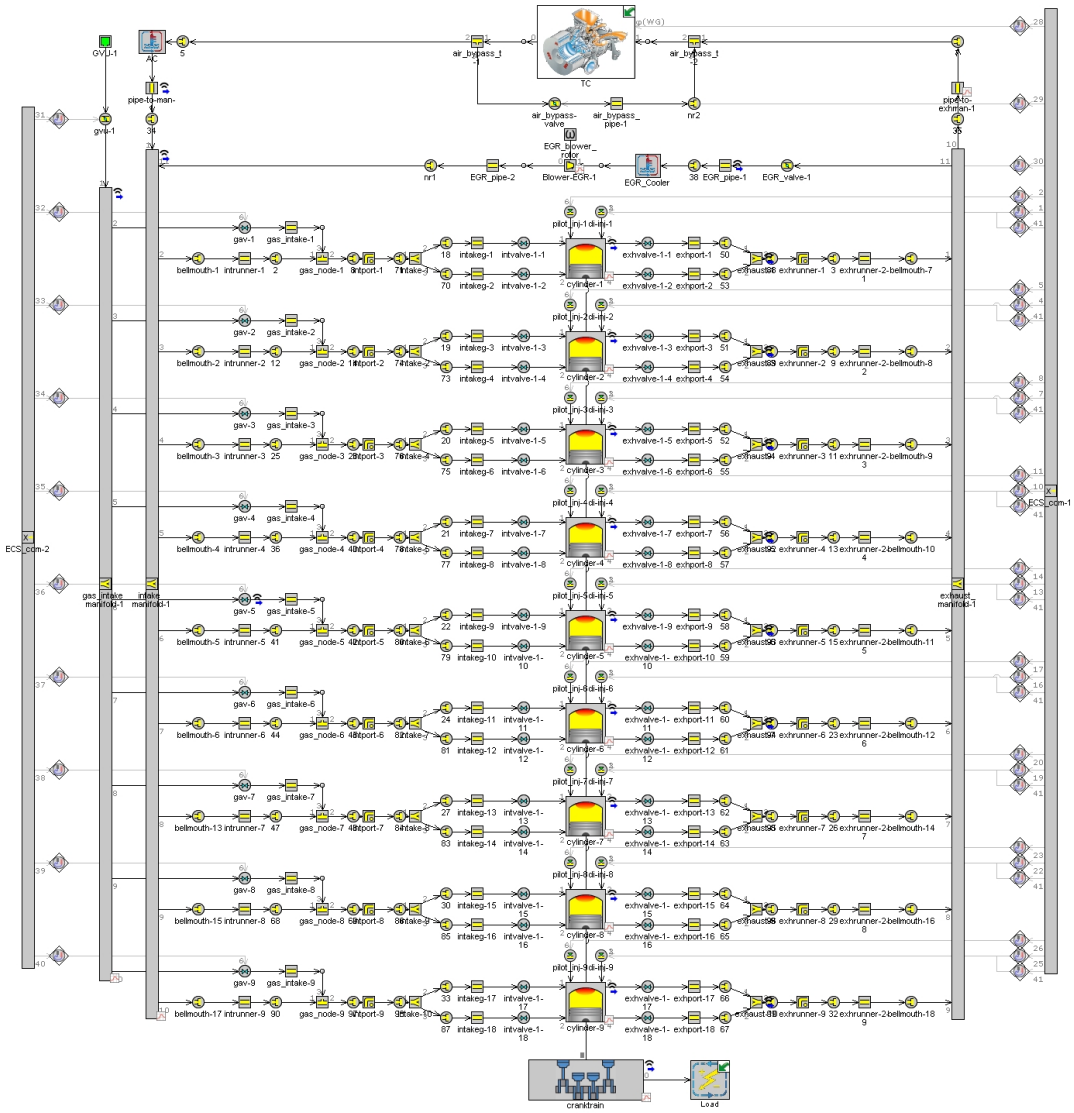

Figure 5.2 Engine thermodynamic model layout in GT-ISE environment

5.2.1.1 Turbocharger (TC) and Exhaust Waste Gate (EWG)

The turbocharger unit is modelled by using the compressor and turbine elements; the former is connected between the ambient and the air cooler (A/C), whereas the latter is connected between the exhaust pipe and the exhaust ambient. The compressor and turbine elements are mechanically connected with the T/C shaft element. The compressor and turbine models use the steady state maps of the respective elements in a digitised format, whereas the T/C compressor surging is modelled according to Theotokatos and Kyrtatos (2003) and Leufvén and Eriksson (2013). The exhaust waste

gate valve element is connected in the exhaust manifold for bypassing the turbine and is controlled by the boost pressure (acquired from the inlet manifold connected downstream the air cooler). The EWG valve dynamics are accounted by considering the opening/closing rates acquired from the technical datasheet (Woodward, 2015b).

5.2.1.2 Air cooler (A/C)

The engine air cooler element is modelled by employing an 1D approach by considering multiple pipes connected in parallel, where the heat transfer from the air to their walls is calculated considering the overall heat transfer coefficient. This heat transfer coefficient as well as the heat transfer area and the cooling water temperature are the model input parameters; the latter was considered constant for simulating both steady state and transient conditions.

5.2.1.3 Diesel and pilot injectors

The pilot fuel twin-needle injector (pilot injector is integrated to the main diesel injector) is modelled as two separate fuel injectors, directly connected to the engine cylinders. The diesel and pilot fuelling systems are not modelled. The fuel type (LFO) and its properties as well as the fuel temperature and/or pressure are considered input parameters, whereas the injection timing and duration vary based on the engine load and operating mode. The main diesel fuel injected amount is modelled as function of the engine load, whereas the pilot fuel amount is considered to be a function of the engine load and operating mode (diesel or gas). The diesel fuel governor dynamics are accounted by considered the actuator response as reported in the technical datasheet (Woodward, 2014).

5.2.1.4 Gas Valve Unit (GVU) and Gas Admission Valve (GAV)

The gas valve unit is modelled by considering a pre-set maximum pressure (6 bar) gas supply from the GVU to the gas (fuel) manifold , and a controlled valve regulating the gas (fuel) manifold pressure to the pre-set value for each load in the gas mode. However, the gas feeding system is not considered under the scope of this study.

The gas admission valve is modelled by using a solenoid valve element regulating the gas fuel amount from the gas (fuel) manifold entering the cylinder by adjusting the valve opening time. The GAV is connected in the cylinder inlet port (upstream the cylinder intake valves). The gas injection takes place during the respective cylinder induction process after the exhaust valves closing, so that all the injected gas remains into the engine cylinders. It must be noted that the methane slip effect is not considered within the scope of this study. The GAV are modelled by controlling the pulse width/duration (taking values in the region from 38 to 68°CA from low to high loads) considering that the respective fuel pressure linearly varies with the engine load. The gaseous fuel mass flow rate is calculated as function of the solenoid valve nozzle area, pressure ratio and the gaseous fuel properties upstream the GAV. The GAV dynamics are accounted by considering the opening/closing rates acquired from the GAV datasheet (Woodward, 2015a).

5.2.1.5 Intake and Exhaust valves

The inlet and exhaust valves use the respective valves profiles employing the quasi-steady adiabatic flow equation for calculating the respective flow rates. The intake valves employ the Miller timing closing before the cylinder bottom dead centre (BDC) (Wärtsilä, 2004, 2015a, 2020), which reduces the required compression work and the combustion temperature and results in higher engine efficiency and lower NO_x emissions (Wärtsilä, 2015a, 2020).

The geometry of the valves is obtained from the project guide of the engine, where detailed drawings are included (Wärtsilä, 2019b). Accordingly, the flow coefficients of the valves are calculated taking into account the geometry and the discharge coefficients from Heywood (2018). The valves lift profiles acquired from Schlick (2014) for a similar size engine were considered for estimating the investigated engine lift profiles.

5.2.1.6 Cylinders

Cylinder elements are connected upstream and downstream with the intake and exhaust valves, respectively. The engine cylinders are modelled by using a zero-dimensional method employing a two-zone approach for modelling the combustion and expansion

processes (one zone containing the combustion products and an unburned mixture zone), as well as a single-zone approach for the remaining of the cycle (Merker et al., 2005). The cylinders volume is calculated by using the engine kinematic mechanism geometry. The following mass and energy conservation equations were employed for modelling each zone along with the ideal gas equation and the cylinder volume time derivative equation:

$$\frac{dm}{dt} = \sum_i \dot{m} \tag{5-1}$$

$$\frac{d(me)}{dt} = -p\frac{dV}{dt} + \sum_i (\dot{m}\,H) - \dot{Q}_{ht} \tag{5-2}$$

where m and V denote the working medium mass and cylinder volume, respectively; $\dot{m}$ is the mass flow rate entering or exiting the cylinder: p denotes the cylinder pressure; e is the working medium total specific internal energy (internal energy plus kinetic energy per unit mass); H is the working medium total specific enthalpy; and $\dot{Q}_{ht}$ is the heat flow rate from the gas to the cylinder walls.

According to the employed two-zone approach (GT, 2019), the unburned gas zone consists of air and combustion products from the previous cycle, whereas the burned gas zone is generated after the start of combustion. At each time step, the amount of fuel and air is transferred from the unburned zone to the burned zone dictated by the burning rate, which is calculated by the employed combustion model. The chemical kinetics calculation considering dissociation effects is carried out in the burned gas zone taking into account the used fuel(s) combustion and the assumption that the combustion products consist of the following 13 species: N_2, O_2, H_2O, CO_2, CO, H_2, N, O, H, NO, OH, SO_2, and Ar. The gas properties are calculated by using the species mass fractions and the respective property, the latter is calculated as algebraic functions of temperature.

Combustion models

For calculating the fuel burning rate at the diesel operating mode, the single-Wiebe combustion model is employed along with the Sitkei equation for estimating the ignition delay (Sitkei, 1964, Merker et al., 2005). An aggregated approach which combined both diesel and pilot is used. For modelling the combustion process at the gas operating mode, a triple-Wiebe function is employed with each function representing the premixed combustion of a portion of the pilot fuel, the diffusive combustion of the remaining pilot fuel and the rapid burning of the gaseous fuel as well as the tail combustion of the cylinder residuals (Karim, 2015).

The ignition delay for the gas mode is approximated by using equation 5-3 and data reported in Christen and Brand (2013) and Sixel et al. (2016).

$$\tau_{ID} = C_0 \left[\tau_0 + \left(\frac{C_1}{p^{0.7}} + \frac{C_2}{p^{1.8}} \right) e^{C_3/T} \right] \quad 5\text{-}3$$

where C_0 denotes a correction factor introduced by ABB in order to match experimental results with different fuel properties (Christen and Brand, 2013); τ_0 denotes the Sitkei constant (considered 0.5) that represents a physical delay, C_1 to C_3 denote Sitkei constants (C_1 and C_2 terms represent the chemical delays of the cold and blue flames) (Sitkei, 1964); p and T denote average values of pressure and temperature respectively, from the start of injection until the start of combustion.

The cumulative fuel burnt for the gas mode is calculated according to the following equation:

$$x_{b,g}(\theta) = \sum_{i=1}^{3} \left[FF_{g,i} \; x_{b,g,i}(\theta) \right] \quad 5\text{-}4$$

where i denotes the Wiebe function; FF denotes the weight of each Wiebe function ($\sum_{i=1}^{3} FF_{g,i} = 1$); and θ denotes the crank angle (top dead centre (TDC) of the closed cycle is at 0^{o}CA).

Each individual Wiebe function is calculated by the following equation (Merker et al., 2005), which is also used for calculating the cumulative fuel burnt at the diesel operating mode:

$$x_{b,g,i}(\theta)=1-\exp\left[-a\left(\frac{\theta-\theta_{SC\_i}}{\Delta\theta_{g,i}}\right)^{m_{g,i}+1}\right]$$

5-5

where *i* denotes the Wiebe function; *a* is the Wiebe function parameter (considered 6.9); θ_{SC_i} is the start of combustion; $\Delta\theta_{g,i}$ is the combustion duration; and $m_{g,i}$ denotes the i-th Wiebe function shape factor.

The combustion heat release rate is calculated using the derived fuel burning rate, which is the time derivative of the cumulative fuel burnt from equation 5-6, and the total energy from all the injected fuels, according to the following equation:

$$\dot{Q}_b = \dot{x}_b E_{f,total} = \dot{x}_b \sum_{i=1}^{3} m_{f,i} LHV_i$$

5-6

where $\dot{x}_b$ denotes the fuel burning rate, $E_{f,total}$ is the total energy of all the injected fuels, m_f is the burnt fuel amount, LHV denotes the fuel lower heating value and *i* denotes the fuel (gas, diesel, pilot).

The single-Wiebe function can sufficiently capture the combustion processes in the diesel mode, as the maximum cylinder pressure, the brake specific fuel consumption (BSFC) and the indicated mean effective pressure (IMEP) were predicted with adequate accuracy. However, the triple-Wiebe function model was required to provide sufficient accuracy in the gas mode, as reported in the pertinent literature (Xu et al., 2014, Xu et al., 2016, Stoumpos et al., 2018, Theotokatos et al., 2018a). Hence, the Wiebe function modelling approach is also employed in this study, instead of a predictive combustion model; the latter requires a set of experimental data for the model constants calibration which was not available in this case (Sixel et al., 2016, Wenig et al., 2019).

The combustion models parameters (weights, start of combustion, combustion duration and shape factor for each Wiebe function), which determine the combustion profile, for both the diesel and the gas modes were calibrated at 25%, 50%, 75% and 100% loads (at steady state conditions), so that the predicted engine cylinder parameters (maximum pressure, IMEP and brake specific fuel/energy consumption) sufficiently match their respective experimental values. The calibrated values of the combustion model parameters (controlled parameters) are stored in a database in the format of three-dimensional matrices (or dependency templates) as functions of the following controlling parameters: (a) the engine load; and (b) the engine operating mode (diesel or gas).

The procedure illustrated in the flowchart of Figure 5.3 is employed for modelling the combustion process in each engine cylinder when the engine operates in transient conditions. The combustion model controlling parameters, which are taken from the engine control system model described in the following Chapter, include the engine load and the operating mode (diesel, gas, GTD mode switching, DTG mode switching) as well as the fuels injected amounts (the values of fuels amount are used only for the case of the DTG mode switching). For the engine operation in the diesel mode, the gas mode and the GTD mode switching, quadratic interpolation is used (considering the engine load as the controlling parameter) for calculating the values of the respective combustion model parameters for each engine cylinder (single-Wiebe function model for the diesel mode; triple-Wiebe function for the gas mode). It needs to be noted that during the GTD mode switching, the engine cylinders operate either in the gas mode for the cylinders in which combustion or injection processes already started prior to the implementation of the change, or the diesel mode for the cylinders in which combustion or injection processes started after the fuel change order (as in this case the gas fuel is cut off instantly and only diesel fuel is injected). Based on the combustion model parameters, the fuel burning rate and the heat release rate are calculated by using equation 5-4 and 5-6, respectively. This calculation procedure is depicted in the interior box shown in the left-hand side in Figure 5.3. The controlled combustion model parameters for each engine cylinder are updated at every cycle based on the controlling parameters derived from engine control system model.

The modelling of each cylinder combustion process for the DTG fuel change requires a more sophisticated approach as the engine cylinders operate for a considerable time period (around 2 minutes) with the main diesel fuel, the gas fuel and the pilot fuel. The employed calculation procedure is described in the flowchart included in the exterior box in Figure 5.3. First, the total burning rates at the specific engine load are calculated considering separately the diesel mode and the gas mode by employing the procedure described in the previous paragraph (the procedure illustrated by interior box flowchart in Figure 5.3). In addition, the fuels amounts (derived from the engine control system model) and the fuels lower heating values are used for calculating the fuels energy ratios for the diesel and gas modes according to the following equations:

$$ER_d = \frac{m_d LHV_d}{E_{f,total}},\ ER_g = \frac{m_g LHV_g + m_p LHV_g}{E_{f,total}} \quad 5\text{-}7$$

Subsequently, the total fuel burning rate is calculated by using equation 5-8, which provides an adequate approximation of the total heat release rate for gas-diesel engines as deduced from the analysis of the experimental results reported in (Ott et al., 2016). Finally, the heat release rate is calculated by using equation 5-6.

$$x_b = ER_d x_{b,d} + ER_g x_{b,g} \quad 5\text{-}8$$

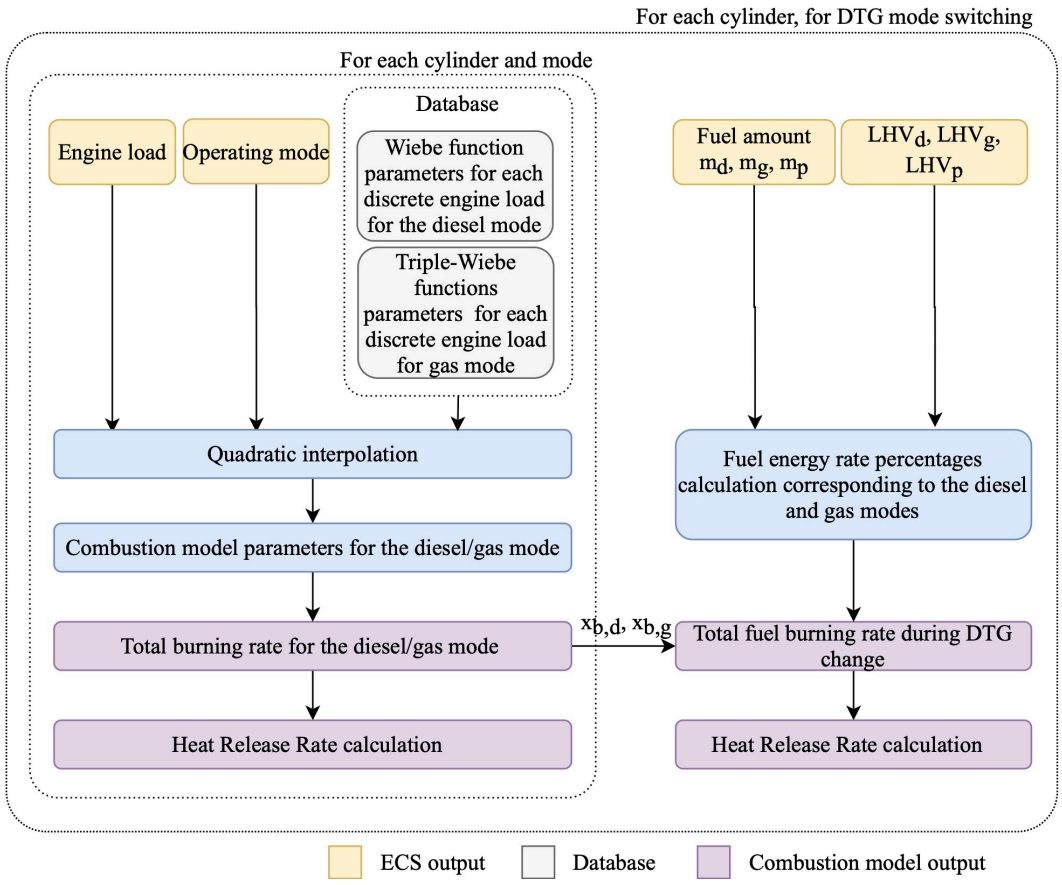

Figure 5.3 Combustion model procedure flowchart

Combustion models employed for the engine operation with EGR mode

For simulating the engine operation at the diesel mode with the EGR and ABP systems activated, the combustion models described in the preceding section are further extended. In reference to the literature review on the EGR systems analysed in Section 2.3.2, the reported effects include reduction in the fuel burning rate, the cylinder maximum pressure and the engine brake power when the EGR system is activated, whereas the ignition delay and the combustion duration increase due to the composition change of the trapped air-fuel mixture into the engine cylinders. Therefore, to counterbalance EGR system effects and maintain the engine power, the engine control system must order a fuel injection amount increase, resulting in a higher engine fuel consumption, as noted in the pertinent literature. In this respect, the variation of the cylinders composition must be accompanied by the variation of the combustion profile, in terms of the fraction of the burned fuels (diesel fuel) as well as the ignition delay and the combustion duration (Merker et al., 2005). Hence, the existing combustion model

parameters database previously developed is extended to consider the EGR system effects to the combustion model.

In specific, in the previous section, the combustion model parameters (controlled parameters) for the engine discrete loads, are stored in a database in the format of three-dimensional matrices (or dependency templates) as functions of the following three controlling parameters: (a) the engine load, and (b) the engine operating mode (diesel or gas). For modelling the diesel mode combustion with the EGR and ABP systems operation, this database is extended by considering an additional controlling parameter; the EGR/ABP systems operation status (activated/deactivated). Furthermore, The combustion model parameters are re-calibrated for the EGR system operation at 25%, 50%, 75% and 100% load considering 10%, 15% and 20% EGR rates at steady state conditions operation based on reported data deriving from the literature (Verschaeren et al., 2014, Fabio et al., 2015, Ma et al., 2016, Kaario et al., 2016). The Wiebe function parameters considering the EGR effect on the combustion process are then imported in an additional three-dimensional matrix in the database. It must be mentioned that due to lack of experimental data for EGR rates higher than 20%, the developed combustion model is designed to extrapolate the required combustion model parameters.

Heat transfer and friction models

Appropriate heat transfer and friction models are employed. In specific, for calculating the gas to wall heat transfer coefficient, the Woschni heat transfer model is used Woschni (1967). The Chen-Flynn friction model is employed for calculating the engine friction mean effective pressure (Rakopoulos and Giakoumis, 2007).

NO_x Emissions model

For estimating the NO_x emissions, the extended Zeldovich mechanism is employed (GT, 2019), which is described in detail by Lavoie et al. (1970), Hanson and Salimian (1984) and Heywood (2018). The model constants are calibrated for 25%, 50%, 75% and 100% load in diesel mode (EGR system deactivated) taking into account the temperature of the burned gas zone. It must be noted that the emissions weighting factor is estimated via trial and error method and used in the engine thermodynamic

model for calibrating the estimated NO_x emissions to match with the experimental values measured during the engine shop trials.

$$N_2 \text{ oxidation rate equation: } O + N_2 \rightleftarrows NO + N \quad (5\text{-}9)$$

$$N \text{ oxidation rate equation: } N + O_2 \rightleftarrows NO + O \quad (5\text{-}10)$$

$$OH \text{ reduction rate equation: } N + OH \rightleftarrows NO + H \quad (5\text{-}11)$$

The *k1*, *k2*, and *k3* rate constants that are used to calculate the reaction rates of the three equations above, respectively, are calculated by using the following equations.

$$k1 = F_1\ 7.6\ 10^{10}\ e^{-38000A_1/T_b} \quad (5\text{-}12)$$

$$k2 = F_2\ 6.4\ 10^{6}\ T_b\ e^{-3150A_2/T_b} \quad (5\text{-}13)$$

$$k3 = F_3\ 4.1\ 10^{10} \quad (5\text{-}14)$$

where F_1 denotes the N_2 Oxidation Rate Multiplier; F_2 denotes the N Oxidation Rate Multiplier; *F3* denotes the OH Reduction Rate Multiplier; *A1* denotes the N2 Oxidation Activation Energy Multiplier; *A2* denotes the N Oxidation Activation Energy Multiplier; and *Tb* denotes the burned zone temperature.

Air – Fuel equivalence ratio

The engine air–fuel equivalence ratio (also known as lambda or λ) (average considering all the engine cylinders) is calculated by using equation 5-15 (Zhou et al., 2014).

$$\lambda = \frac{m_{air}}{AFR_{st\_d}\ m_d + AFR_{st\_g}\ m_g} \quad (5\text{-}15)$$

where, AFR_{st} refers to the stoichiometric equivalence ratio of diesel and gaseous fuels (14.7 kg/kg and 17.25 kg/kg, respectively) (Zhou et al., 2014), m_{air} is the air mass flow rate, and m_d and m_g are the mass flow rates of the diesel and gas fuels.

5.2.1.7 Pipes and junctions

Pipes and junctions are used for modelling the inlet and exhaust manifolds as well as the gas (fuel) manifold. A one-dimensional approach is used to model the pipes and junction elements by solving the following momentum conservation equation along with the mass and energy conservation equations 5-1 and 5-2 in each discretised pipe element of the intake and exhaust manifolds (GT, 2019):

$$\frac{d\dot{m}}{dt} = \frac{A dp + \sum_i (\dot{m}u) - \left(\frac{4C_f dx}{D} + K_p\right)\left(\frac{1}{2}\rho u|u|A\right)}{dx} \quad 5\text{-}16$$

where $\dot{m}$ is the boundary mass flux ($\dot{m}=\rho Au$); ρ is the density; A is the pipe cross-sectional flow area; u denoted the velocity at the boundary; C_f is the friction factor; K_p is the pressure loss coefficient; D is the pipe equivalent diameter; dx is the discretization length; and dp: pressure differential acting across dx.

The pipe elements model solver employs an explicit time integration method, which provides a compromise between the required computational time and accuracy. The model variables include the working medium mass flow, density and internal energy. The pipe elements employed for representing the engine intake and exhaust manifolds are divided into a number of discrete elements considering a discretisation length of 0.4 to 0.55 times the cylinder bore diameter, respectively. The scalar variables (pressure, temperature, density, internal energy, enthalpy, species concentrations, etc.) are assumed to be uniform over each discrete element, whereas the vector variables (mass flux, velocity, mass fraction fluxes, etc.) are calculated for each discrete element boundary.

5.2.1.8 Exhaust Gas Recirculation (EGR) and Air Bypass (ABP) systems

The investigated HP-EGR system consists of the following components; (a) an exhaust gas cooler installed upstream the EGR blower; (b) an EGR blower driven by an electric

motor; (c) an EGR valve that regulates the EGR amount based on the charge air mass flow rate entering the engine; and (d) the required piping elements.

The HP-EGR system is modelled based on an existing investigated system layout reported in the literature for marine two-stroke (MAN, 2018) and four-stroke engines (Millo et al., 2013) and further extending it with the inclusion of the ABP system. The EGR cooler is modelled by employing an 1D approach by considering multiple pipes connected in parallel, similarly to the engine A/C model. Information on the input parameters of the EGR cooler were initially acquired from Florea et al. (2008). The EGR blower is modelled using its steady state map in a digitised format, which was acquired from (MAN, 2012c) and scaled accordingly to match the targeted/desired engine operating parameters.

An ABP system model is developed along with the EGR system model; the ABP system redirects a part of the compressed air flow (via a controlled air bypass valve) from the compressor outlet to the turbine inlet. The EGR and ABP systems piping is modelled by employing 1D approach, where the valves controlling modelling approach is described in the following Chapter.

5.2.2 Unified Digital System (UDS)

The Unified Digital System (UDS) consists of the Unified Engine Controls (UEC), the Faulty Operation Simulator (FOS) and the Engine Diagnostics System (EDS). The former system (UEC) represents part of the existing UNIC unit of the reference engine (W9L50DF), which includes the Engine Control System (ECS), the Alarms and Monitoring system (AMS) and the Engine Safety System (ESS), whereas the remaining systems (FOS and EDS) are proposed as additions to the UDS in this thesis. The above control systems are developed and integrated into the UDS, as shown in Figure 5.4. In-depth description of each individual sub-system, module and the UDS integration is presented in the following Sections.

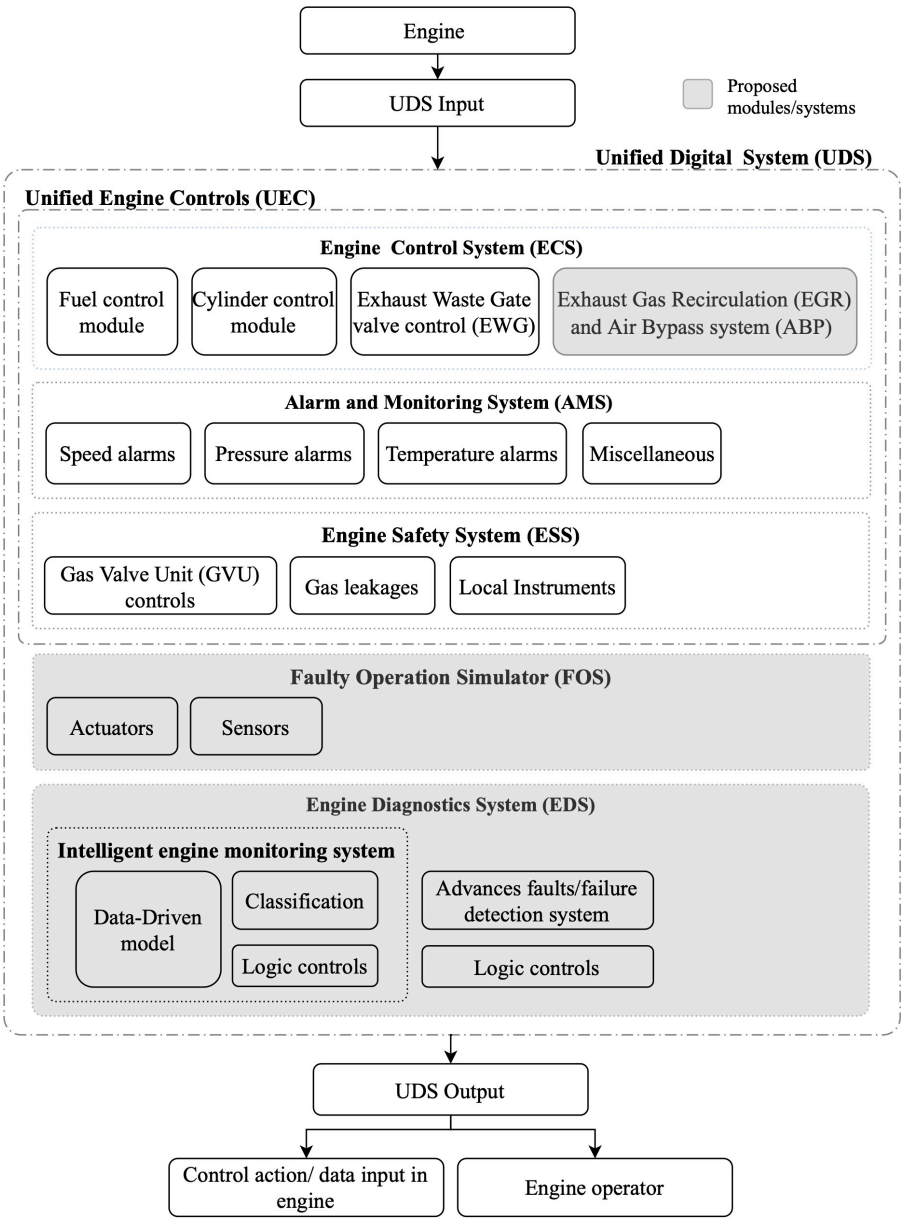

Figure 5.4 Unified Digital System structure

5.2.2.1 Engine Control System (ECS)

The developed ECS model assembly consists of the fuels (diesel main, diesel pilot and gas) and the cylinder control modules, the exhaust waste gate controller, as well as the EGR and ABP systems controllers. The developed ECS model is capable of operating at both steady state and transient conditions with modes switching or load changes. For the gas mode, the model is capable of identifying imposed step-wise load changes that exceed the maximum allowed load change (via comparison against the manufacturer

maximum step load increase limitations), and subsequently implementing a mode switching from gas to diesel as specified by the engine manufacturer requirements. In such scenarios, the engine operation is immediately switched to the diesel mode, via a fast-acting signal, for the fuels and the exhaust waste gate controls. In addition, requests for mode switching from diesel to gas above 80% engine load are not allowed as indicated by the manufacturer (Wärtsilä, 2019b). The ECS operating mode controller was modelled to identify either the engine load or the fuel transition (based on the manual input for ordered operation mode) and accordingly calculate the respective combustion model parameters.

A flowchart illustrating the modelling philosophy and the logical conditions of the developed ECS model is provided in Figure 5.5, whereas the structure and functionality of the developed fuel control system is illustrated by using the flow chart diagram presented in Figure 5.6.

Fuel control and cylinder control modules

The fuel control module employs two discrete control switches, which can be activated or deactivated though a logic controller based on the fuel or the fuels currently employed (i.e. diesel/gas and pilot). In specific, for a load change at any operating mode, only one of the two switches is activated based on the operating mode. However, during the modes switching operations, both switch controls are used in order to control the gas fuel, the pilot fuel and the diesel fuel injection timing. Additionally, the injection controllers for each engine cylinder were set to adjust the amount of all cylinder injected fuels and determine a suitable fuel change timing for each cylinder, based on each cylinder phase angle.

Upon an ordered operating mode, the developed fuel control system actuates the GAV, the diesel and the pilot fuels injectors via a set of controllers, so that the engine is able to operate at: (a) steady state conditions in the diesel or the gas modes (i.e. fixed load and no fuel change); (b) load changes (transient operations) in the diesel or the gas modes; and (c) modes switching (transient operations) from the diesel mode to the gas mode and vice versa. It must be noted that GT-ISE uses sensors elements, which acquire the simulated values of the engine parameters and feed them back to the ECS.

In specific, for the diesel mode simulation at steady state conditions, a PID controller (Diesel PID in Figure 5.5) adjusts the rack position of each cylinder diesel fuel pump that determines the fuel amount of the respective diesel fuel injector, based on the engine speed feedback signal. This controller employs a lambda limiter thus preventing the engine to operate with low air–fuel equivalence ratio values, which may cause incomplete combustion issues and high thermal loading. According to the engine manufacturer (Ott et al., 2013), the pilot fuel is always injected in both engine operating modes, so that wear and damage of the pilot injectors are avoided. Hence, the pilot fuel injection control (Pilot controller in Figure 5.5) is set to appropriately adjust the pilot fuel amount (the injected pilot fuel amount is assumed to remain unaffected when the EGR system is activated).

For the gas mode, the gas fuel supply pressure is assumed to linearly change as function of the engine load, whilst an additional PID controller (Gas PID in Figure 5.5) adjusts the duration of the gas admission valve opening based on the engine speed feedback signal, thus adjusting the mass of the gas fuel injected per cylinder. The pilot fuel pressure is considered constant and the pilot fuel injection amount is controlled for each cylinder. Moreover, the rack position of the diesel fuel pumps is set to its minimum position (i.e. no diesel fuel is injected). It is expected that the engine speed error signal (i.e. difference between the ordered and the actual average engine speed) is zero during the engine steady state operation in either the diesel or the gas modes, and as a result the employed controllers set the corresponding controlling parameters. The employed PID controllers settings were tuned by using the Ziegler-Nichols method according to the guidelines provided in Leigh (1987) and Graf (2013).

For controlling the engine transient operation with load changes in the diesel or the gas modes, the fuel control system follows a similar control strategy as described above for the steady state operation. The controllers use as input the engine speed error (ordered speed to actual speed difference) and eventually control the injected fuels amount depending on the operating mode aiming to the minimisation of the engine speed error; by adjusting either the rack position of each cylinder diesel fuel pump or the gas admission and the pilot fuel injection duration. Additionally, the fuel control system is also designed to immediately change the engine operation to the diesel mode in cases

where the ordered engine load change exceeds the investigated engine maximum load acceptance criteria when the engine operates in the gas mode. In this case, the transient operation involves both the load change and the fuel switching from the gas to the diesel modes. The fuel control system performs all the necessary control actions (described in the following paragraphs) to initially achieve the mode switching (i.e. gas to diesel) and subsequently to respond to the ordered engine load change.

For controlling the engine transient operation with a mode switching from diesel to gas (DTG), the actual engine control system controls both the gas and diesel fuels (gas fuel pressure and injection duration and diesel rack position), whilst the pilot fuel injection duration is also adjusted to control the amount of the pilot fuel injected per cylinder. However, for the modelled engine control system, the amount of the gas fuel injected per cylinder is controlled via an imposed profile with a positive rate of change (slope) depending on the engine load, whilst the pilot fuel amount is calculated by interpolation employing a lookup table with the measured values for each engine operating point. At the same time, the diesel PID controller adjusts the diesel fuel rack position based on the engine speed feedback signal, and thus, determines the mass of the diesel injected per cylinder and per cycle. It must be noted that the ECS model allows for the gas fuel injection only for the cylinders operating in their open cycle period.

In the case of an ordered gas to diesel mode switching (GTD), the rack position of each cylinder diesel fuel pump (determining the fuel amount of the respective diesel injector) is adjusted based on the feedback of the diesel PID controller. The gas admission valves of the engine cylinders, in which the injection has not started yet, are ordered to immediately close, based on an imposed step input signal, whilst a step change input signal governs the amount of pilot fuel injected in each cylinder.

In either the diesel or the gas modes, the fuel control system takes into account each cylinder phase angle during mode switching in order to determine if the ordered fuel change in each cylinder is permitted and, hence, define the timing for a cylinder fuel change to be implemented. This is considered in order to avoid a fuel change during the cylinders closed cycle or when the gas fuel injection is ongoing, which may lead to engine speed and power fluctuations. The fuel control system was set to perform the fuel change of each cylinder during the corresponding intake phase, prior to the gas fuel

injection start. The completion of the ordered engine fuel change is achieved when the fuel change is implemented to all the engine cylinders. In this respect, the injection controllers were set to serve the purpose of identifying whether the fuel change is permitted in each consecutive fired cylinder and whether the fuel change has been applied to all cylinders. If the fuel change is not permitted in a cylinder due to its ongoing operating phase, the initial fuel settings are applied until it reaches the intake phase of the next cycle. The fuel change control actions are repeated until the fuel change is applied to all the engine cylinders (Portin, 2010).

It must be noted that in the ECS model, the CA position information was taken from the engine crankshaft block whist considering the phase angle of each cylinder. The actual engine control system usually employs two crank angle (CA) (probe) sensors for measuring the crank angle via flywheel, whereas an optional sensor (encoder) may be installed at the free end of the engine on the crankshaft.

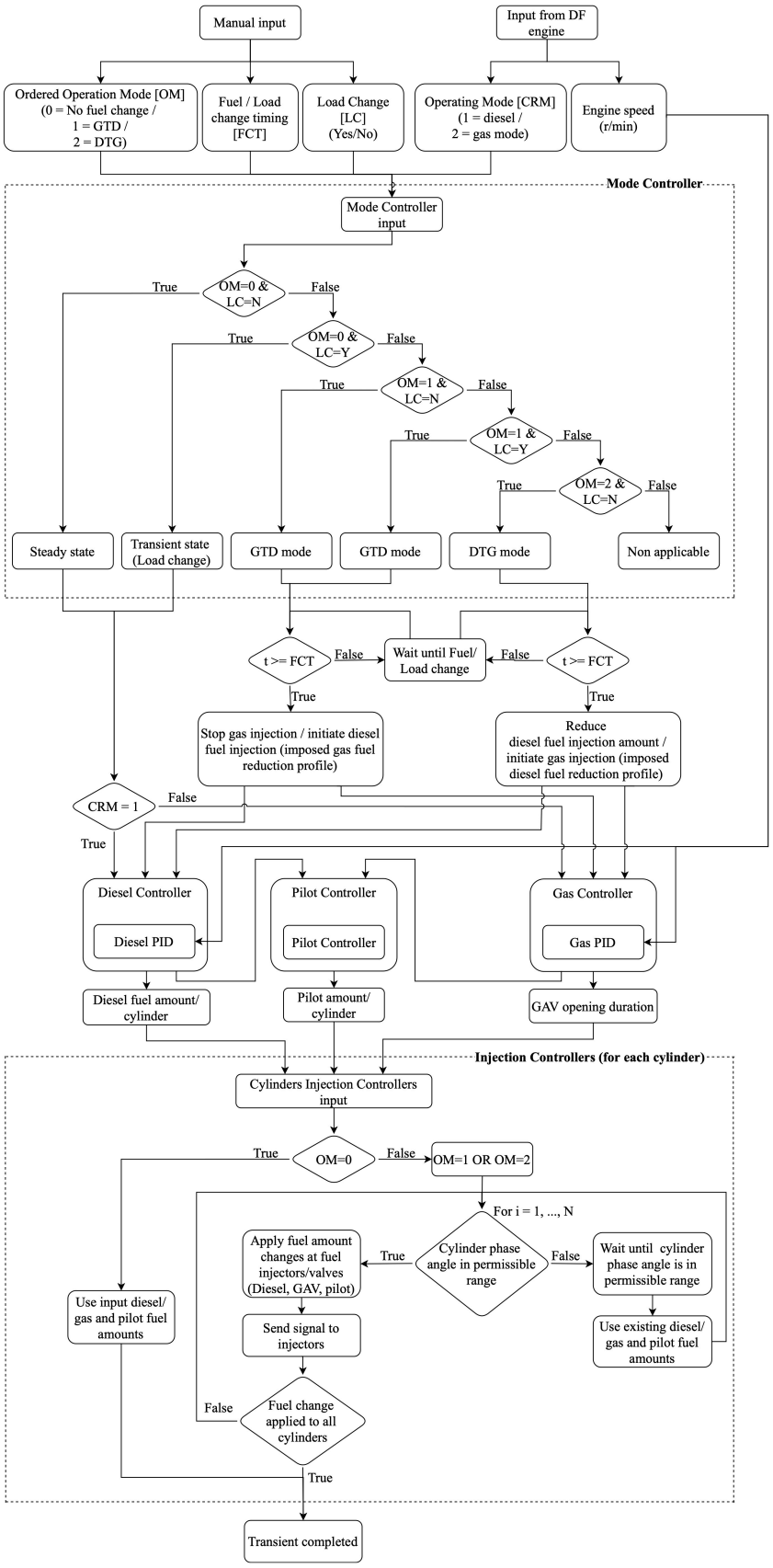

Figure 5.5 ECS model logical structure flowchart

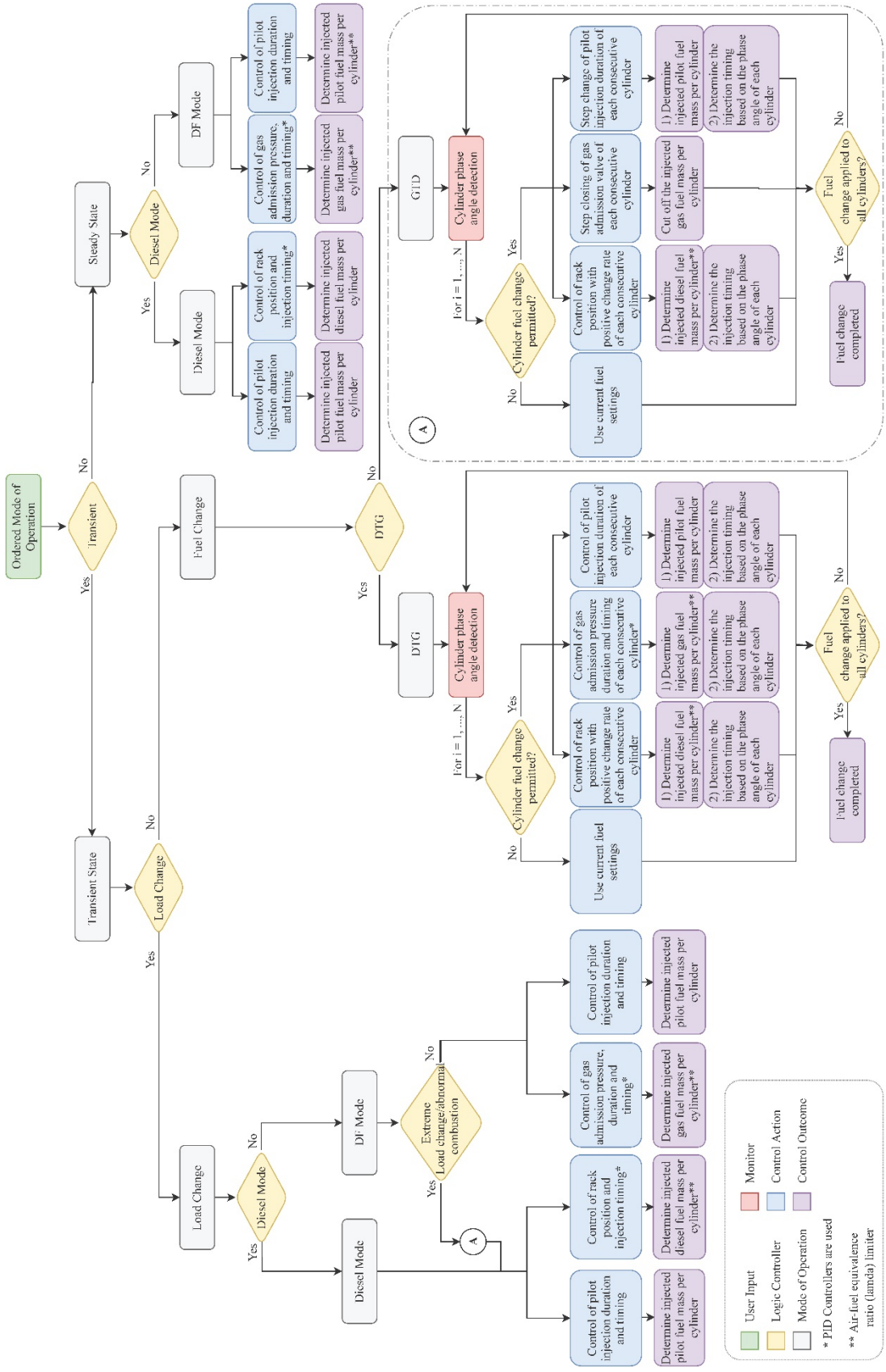

Figure 5.6 Fuel control system functional diagram

Exhaust Waste Gate (EWG)

The EWG valve employs a simplified PID controller with predefined proportional and integral constants for controlling the valve area, considering as input the engine boost pressure sensor. This PID controller settings, which affect the EWG valve response, were tuned by using the Ziegler-Nichols method according to the guidelines provided in Leigh (1987) and Graf (2013).

Exhaust Gas Recirculation (EGR) and Air Bypass Valve (ABP)

The EGR system operating settings control is essential for ensuring the safe and efficient engine operation within the engine design envelop and the defined manufacturer operation limitations. In this respect, the development of the EGR system control, especially for DF engines, is a crucial and challenging task that must consider the existing engine T/C matching for both diesel and gas operation, the engine design limitations related to the EGR system installation (T/C engine operating points with EGR, engine T/C re-matching process and additional design considerations such as the ABP system), as well as the engine manufacturer operational alarm limits (i.e. exhaust gas temperature, cylinders maximum pressure).

The EGR control system is developed by considering two discrete modules; namely the EGR control and the ABP control module. The former is responsible for controlling the EGR valve of the EGR system, whereas the latter is responsible for controlling the air bypass valve of the ABP system.

Furthermore, to model both the engine steady state and transient operations, the EGR and ABP control modules are developed to activate/deactivate the EGR and ABP systems during the diesel mode operation (similar to the EWG operation), in order to avoid potential engine safety implications, such as the T/C compressor surging effect. The EGR and ABP control systems functional diagram is presented in Figure 5.7.

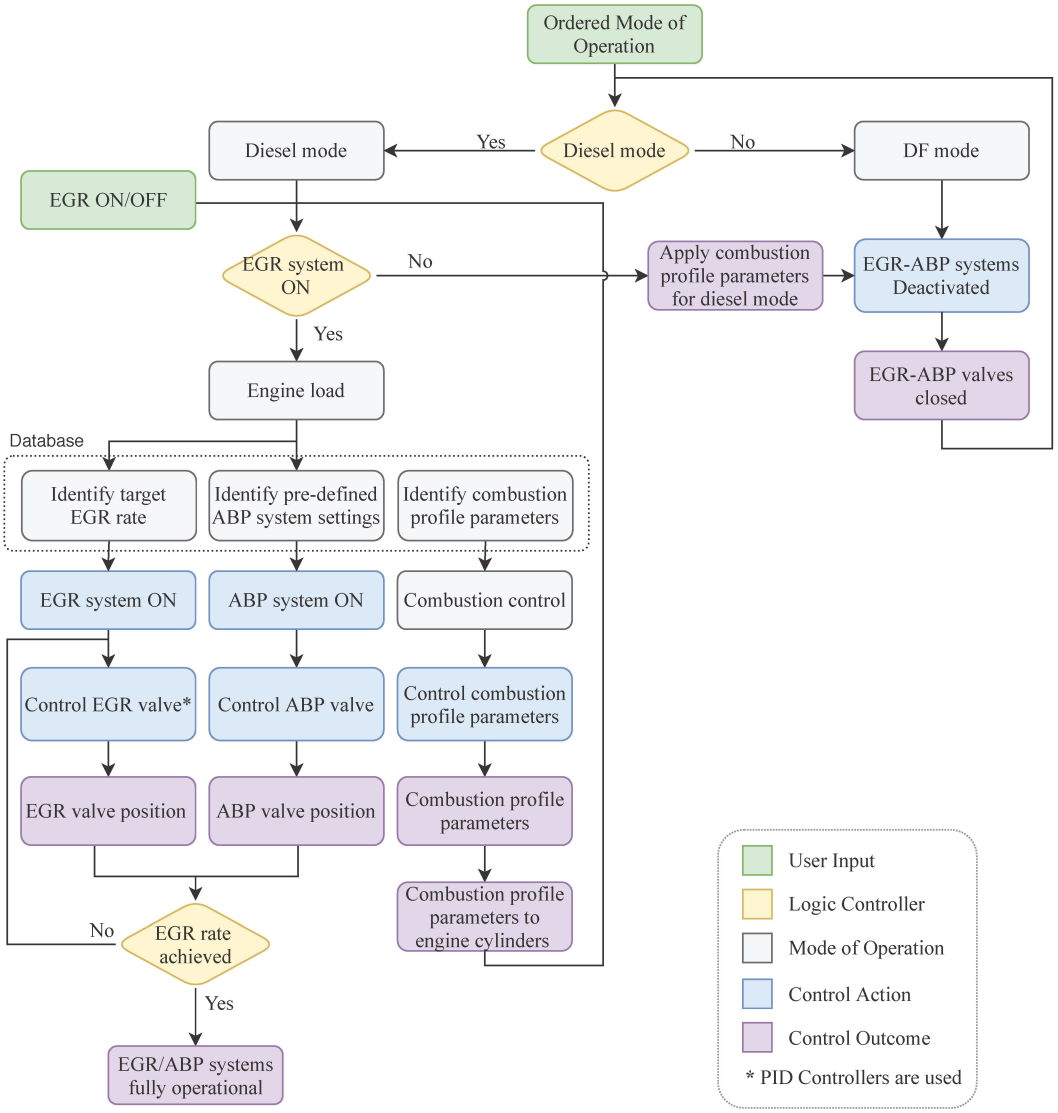

Figure 5.7 EGR and ABP control modules functional diagram

The EGR module consists of a PID controller and its settings were tuned by using the Ziegler-Nichols method according to the guidelines provided in Leigh (1987) and Graf (2013). The calculated EGR rate (mass fraction) is defined by equation 5-17 (Fabio et al., 2015).

$$x_{EGR} = \frac{\dot{m}_{EGR}}{\left(\dot{m}_{EGR} + \dot{m}_{charge\ air}\right)} \qquad 5\text{-}17$$

where $\dot{m}_{EGR}$ is the EGR exhaust gas mass flow rate and $\dot{m}_{charge\ air}$ is the charge air mass flow rate.

On the other hand, the ABP control module consists of a pre-determined profile element (2D lookup table) that orders a pre-set position to the ABP valve depending on the ordered engine load. The ABP valve position (as a function of engine load) is estimated during the optimisation phase of the ABP system settings that is described in detail in Section 7.4.2.

5.2.2.2 Alarms and monitoring system (AMS)

The developed AMS monitors the engine operating parameters fed from the engine sensors (e.g. engine speed, charge air pressure, exhaust temperature, etc.) and compare their values against the respective manufacturer limits/thresholds. In case these thresholds are exceeded during operation, respective alarms are activated. These limits are categorised to minor and major alarms, where appropriate actions are considered, respectively; i.e. engine slow down, shutdown or immediate trip to the diesel mode in case the engine operates in the gas mode. The modelling of these alarm actions is conducted via the use of logic expressions comparing the monitored parameters with the manufacturer alarm limits, by employing the available GT-ISE library elements, which that enable such a development.

5.2.2.3 Engine safety system (ESS)

Gas Valve Unit (GVU)

The gas valve unit (GVU) module is developed to control the gas fuel pressure in the gas (fuel) manifold (Wärtsilä, 2019b). To achieve this, the GVU control module is modelled to monitor the gas (fuel) manifold pressure (based on the gas (fuel) manifold pressure sensor) and regulate the GVU valve position accordingly to achieve the targeted gas (fuel) manifold pressure, as a function of engine load. The developed GVU control module consists of a PID controller, tuned by using the Ziegler-Nichols method according to the guidelines provided in Leigh (1987) and Graf (2013). The gas (fuel) manifold pressure data for the discrete engine loads in DF operation is reported in the engine project guide (Wärtsilä, 2019b).

5.2.2.4 Faulty Operation Simulator (FOS)

The faulty operation simulator (FOS) is developed to enable the digital twin simulation under faulty conditions related to the valves' actuators (e.g. EWG, GVU) or the engine pressure, temperature and speed sensors. In this respect, the FOS interacts between the ECS and the engine components (actuators or sensors) and handles the ECS and actuators/sensors feedback signals accordingly. Therefore, the FOS system is modelled with the following two discrete modules: (a) the sensors signals handling; and (b) the actuators signals handling. The former employs 'delay', 'gain' and 'offset' signal handling elements to simulate sensors faults and/or measurements bias, whereas the latter employs 'delay' and 'hold' signal handling elements to simulate actuators delays or null/non-responsive condition respectively.

5.2.2.5 Engine Diagnostics System (EDS)

The EDS model, developed as part of the UDS, comprises an innovative diagnostics system that offers intelligent engine monitoring and advanced faults/failure detection, irrespective of the engine load and operating mode. In this respect, the existing failure detection employed by the engine manufacturers is considerably expanded with logic controls, sensor measurements classification and a data-driven model. Moreover, the EDS is interconnected with engine sensors elements, which acquire the simulated values of the engine parameters and feed them back to the EDS, thus allowing the advanced faults diagnosis. Despite the simplistic modelling approach adopted, the development process of the EDS is proven to be relatively complex, as illustrated in the functional flowchart illustrated in Figure 5.10 and described in the following sub-Sections.

Intelligent engine monitoring system

Amongst the main novel capabilities of the developed EDS is the intelligent engine monitoring system, which aims at identifying and evaluating the sensors measurement uncertainty. In this respect, the modelling of this system is realised by developing a model capable of predicting the engine 'healthy' operating parameters (data-driven model) as well as the logic controls that will allow for the data processing and analysis in the EDS.

Data-Driven (DD) model

The digital twin described in the previous Chapters, can be used to provide the 'reference' or 'healthy' engine operating parameters for any possible combination of boundary conditions and engine operating conditions, therefore permitting the engine performance assessment and fault diagnosis. In this respect, following the developed engine model calibration, a large number of simulations for combinations of all the possible engine operating conditions are being performed a-priori. For the digital twin simulations design, the Design of Experiments (DoE) tool, which is integrated in the GT-ISE software, is employed. The digital twin simulations were performed for the engine steady state conditions in the gas and diesel modes at 25%, 50%, 75%, 85% and 100% loads considering the following engine operating parameters (factors) varying within the ranges provided in Table 5.1: (a) the ambient temperature; (b) the diesel fuel lower heating value (LHV); (c) the gas fuel LHV; (d) the GVU gas pressure; and (e) the A/C coolant temperature. The 'full factorial' DoE method is employed (Antony, 2014), in order to impose the minimum and maximum values for each parameter (factor), as well as the number of levels for each.

Table 5.1 DoE variable engine operating parameters

Parameter	Unit	NN input	Diesel mode	Gas mode
Load	[%]	u_1	25, 50, 75, 85, 100	25, 50, 75, 85, 100
Fuel (diesel:1/gas:2)	[-]	u_2	1	2
Ambient temperature	[K]	u_3	298.1, 304.8, 311.4, 318.1	298.1, 304.8, 311.4, 318.1
A/C temperature	[K]	u_4	298.1, 304.6, 306.8, 311.1	298.1, 304.6, 306.8, 311.1
GVU gas pressure	[bar]	u_5	5.92	5.92, 5.96, 6.00
Diesel fuel LHV	[MJ/kg]	u_6	42.0, 43.3, 44.6, 46.0	42.6
Gas LHV	[MJ/kg]	u_7	50.0	45.0, 46.6, 48.3, 50.0
No. of experiments	[-]	[-]	320	960

The upper and lower limits of the considered varying engine operating parameters were acquired from the engine record book. For the simulations in the diesel mode, gas fuel is not used, thus the GVU gas pressure and the gas lower heating value were disregarded during DoE simulations. Similarly, the simulation runs for the gas mode did not consider the diesel fuel lower heating value.

Furthermore, the engine operating parameters monitored by the EDS include: (a) the diesel fuel rack position; (b) the average maximum cylinder pressure; (c) the charge air inlet manifold pressure; (d) the charge air inlet manifold temperature; (e) the charge air mass flow rate; (f) the T/C speed; (g) the exhaust gas temperature at turbine inlet; (h) the exhaust gas temperature at turbine outlet; (i) the exhaust gas pressure upstream turbine; (j) the exhaust waste gate valve opening; (k) the gas injection duration; (l) the gas (fuel) manifold pressure; (m) the air−fuel equivalence ratio; (n) the NO_x emissions; (o) the CO_2 emissions; (p) the engine brake efficiency; (q) the BSFC (diesel mode); (r) the brake mean effective pressure; and (s) the engine brake power.

The mapping of these engine operating parameters is conducted with the aim to populate the available operational data from DoE simulations and use them to train a set of Neural Networks (NNs) (one NN for each EDS monitored parameter). In this respect, the embedded NNs form the data driven (DD) model, which is used to predict with adequate accuracy (as described in Section 5.3.2), the engine 'reference' operating parameters for any engine 'healthy' operation scenario. For training the NNs, the 90% of the populated data (DoE simulation results) is used, whereas a random 10% of the data is reserved for NNs validation.

The NNs training was examined by employing the following methods: (a) global polynomial; (b) self-organizing local linear; (c) self-organizing local non-linear; and (d) feedforward (GT, 2019). However, the GT-ISE software is capable of calculating and comparing the minimum errors between the given training methods and selecting the training method with the least error calculated, therefore, in the present development, the feedforward method is identified as the most accurate NNs training method to predict the engine operating parameters. The feedforward method is described below.

As aforementioned, GT software is capable of identifying the minimum errors between the given NNs training methods and automatically selecting the method resulting to the least error. For the case of the 'feed forward' method, the two-layer and three-layer layouts were examined (one input and one output layers/ two input and one output layers respectively). However, the 3-layer feedforward layout was proven to be more accurate for predicting the EDS monitored parameters, therefore it was selected for the NNs training. The input parameters of the NNs are presented in Table 5.1.

Hence, the developed NNs consist of two hidden layers and one output layer. The NNs output *y* is calculated by using equation 5-18, as follows:

$$y=f\{w\, g\,[z\, h(v\, u+a)+b]+c\} \tag{5-18}$$

where, *h* and *g* are the activation functions of the first and second layer, respectively; *v and a* are the weights and biases of the first hidden layer*; z and b* are the weights and biases of the second hidden layer*; w and c* are the weights and biases of the output layer.

$h(x)= -1+\frac{2}{1+e^{-2x}}$ *Activation function of the 1st hidden layer*

$g(x)= -1+\frac{2}{1+e^{-2x}}$ *Activation function of the 2nd hidden layer*

$f(x)=x$ *Activation function of the output layer*

u: input

The feedforward method calculates the weights and biases of the Neural Network in order to minimise the following objective function by employing the Levenberg-Marquardt optimisation method (Sharif Ahmadian, 2016, Kayri, 2016):

$$J=k_1 SSE+ k_2 SSW \tag{5-19}$$

where *SSE* denotes the sum of square errors and *SSW* the sum of square weights.

The objective function weights k_1 and k_2 can be dynamically calculated using the Bayesian regularisation algorithm (Kayri, 2016) or set as constant values. In the present study, the k_1 and k_2 are dynamically calculated.

The number of the neurons for the first and second hidden layer were determined considering the suggestions provided in the software manual (GT, 2019) and by trial and error. After training the NNs, those that produce the most promising output were saved. The basis of determining a promising network is the comparison of the DT parameter values (training data) to the output of the NNs (simulated data). The feedforward neural network settings are presented in Table 5.2.

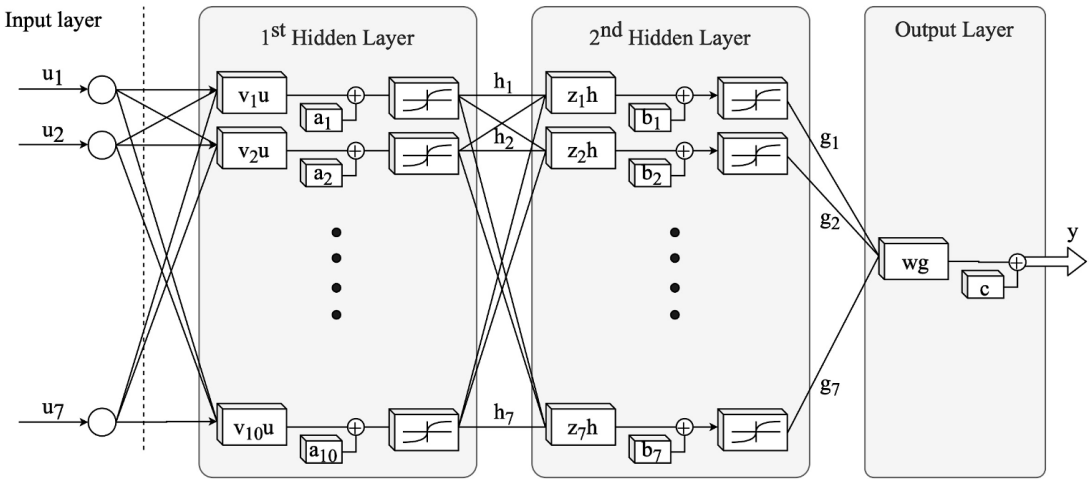

Figure 5.8 Feedforward Neural Network

Table 5.2 Feedforward method settings for NNs training

Parameter	**Value**
1st layer – number of Neurons	10
2nd layer – number of Neurons	7
Maximum training iterations	300
Target training error (SSE)	0.0
Percent of data used for validation	10%
Objective Coefficient	adjustable
SSE Coefficient	adjustable
SSW Coefficient	adjustable
Initial LM Factor (mu)	0.005
Mu update factor (beta)	3.0
Initialisation	random

As a result of the trained NNs, the response surface for each EDS monitored parameter is generated in GT-POST; an embedded GT-Suite tool. This software tool enables the assessment of the NNs fidelity (data linear regression analysis) (as presented in Section 5.3.2) as well as permits the graphical representation of the NNs algebraic equations to response surfaces.

EDS Sensors measurements uncertainty identification

The development of the intelligent engine monitoring system for the sensors measurements uncertainty is performed based on the following approach. During the simulation of the investigated engine operation, the EDS is fed with the engine

operational parameters measurements, as these are generated by the digital twin employing FOS (the data are acquired from the particular sensors included in the developed digital twin in GT-ISE). The digital twin acquired operating parameters measurements are compared in the EDS logic control with the 'reference' data, which are derived by simultaneously running the DD model. This allows the data processing and analysis in order to identify discrepancies between "expected/healthy" and "actual" behaviour of the EDS monitored operating parameters. Any deviation, between the digital twin measurements and the DD model values (at the same operating conditions) of the EDS monitored parameters is calculated and classified based on the EDS sensors measurements thresholds, according to Figure 5.9. It must be noted that the 'sensor error' region (normal operation) accounts for the deviations between the DD model and DT, where the engine operation is considered 'healthy'. The 'error margin' (EDS Warning) and 'alarm limits' (EDS Alarm) regions are defined considering engine manufacturer limits and the literature investigations, as presented in Section 2.4.3.

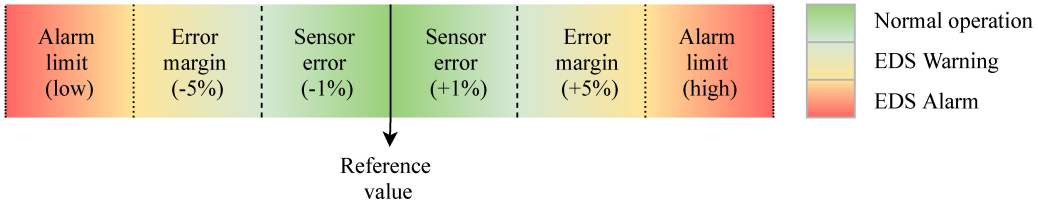

Figure 5.9 EDS sensors measurements thresholds

Each monitored parameter along with the recorded error from its 'reference' value is then imported in the EDS advanced faults/failure detection to proceed with the engine diagnostics.

Advanced faults/failure detection

Whilst the existing failure detection strategy currently adopted by the manufacturers can adequately diagnose a failure in sensors and actuators, the sensors measurements evaluation is based on testing measurements data. In this respect, the sensors measurements uncertainty is disregarded. The proposed advanced faults/failure detection system is developed by employing the existing strategy followed by the engine manufacturers, and further enhancing it to accommodate the sensors measurements uncertainty identification.

In principle, the EDS is primarily able to separate an actuator/sensor failure from a sensor fault. By employing the EDS functional control (Figure 5.10) for each monitored parameter, the EDS can identify the number of engine operating parameters deviating from their reference values, for the given boundary conditions (load, ambient temperature, A/C temperature, GVU gas pressure, and diesel/gas LHV). Moreover, the errors associated with these monitored parameters are provided by the intelligent engine monitoring system. Therefore, by considering both: (a) the number of EDS monitored parameters deviating from their 'reference' value; and (b) the sensor measurement error of each operational parameter, the EDS can separate a faulty/uncalibrated sensor from an actual engine mechanical failure (as described in Section 4.6.1). For example, if an EDS monitored operational parameter deviates from its 'reference' (healthy) value whilst the other parameters remain within ±1% error, this indicates that the sensor providing this measurement for this operational parameter is faulty or uncalibrated. Likewise, if all the monitored parameters demonstrate deviations of ±5% and above, that indicates most probably an engine mechanical failure. However, there are limited cases where most of the engine operational parameters can be affected by a single faulty sensor measurement. These are mainly sensors that have a major impact on the ECS controls, such as the speed and the boost pressure sensor. For this reason, the EDS is developed considering the so-called 'expert knowledge', correlating a number of key monitored operational parameters with specific sensors. Thus, this correlation makes the detection of these specific sensor faults intelligent by observing variations to the respective key operating parameters. However, this 'expert knowledge' is usually gained based on manufacturers vast experience that is reflected on the mapping tables interconnecting a number of observed issues with potential root causes. Nevertheless, for the cases where the diagnosis outcome is not definite (whether there is an engine mechanical failure or a sensor that the affect most of the engine parameters), the UDS functional model monitors the key operating parameters and implements corrective action(s) on the respective sensor(s). In this respect, the faulty or uncalibrated sensor(s) calculated deviation by the intelligent engine monitoring system, is used to correct the sensor(s) feedback signal from the engine to the ECS (i.e. the ECS input from the engine sensors). Lastly, the UDS informs the operator (with a warning message) to maintain appropriately the faulty/uncalibrated sensor.

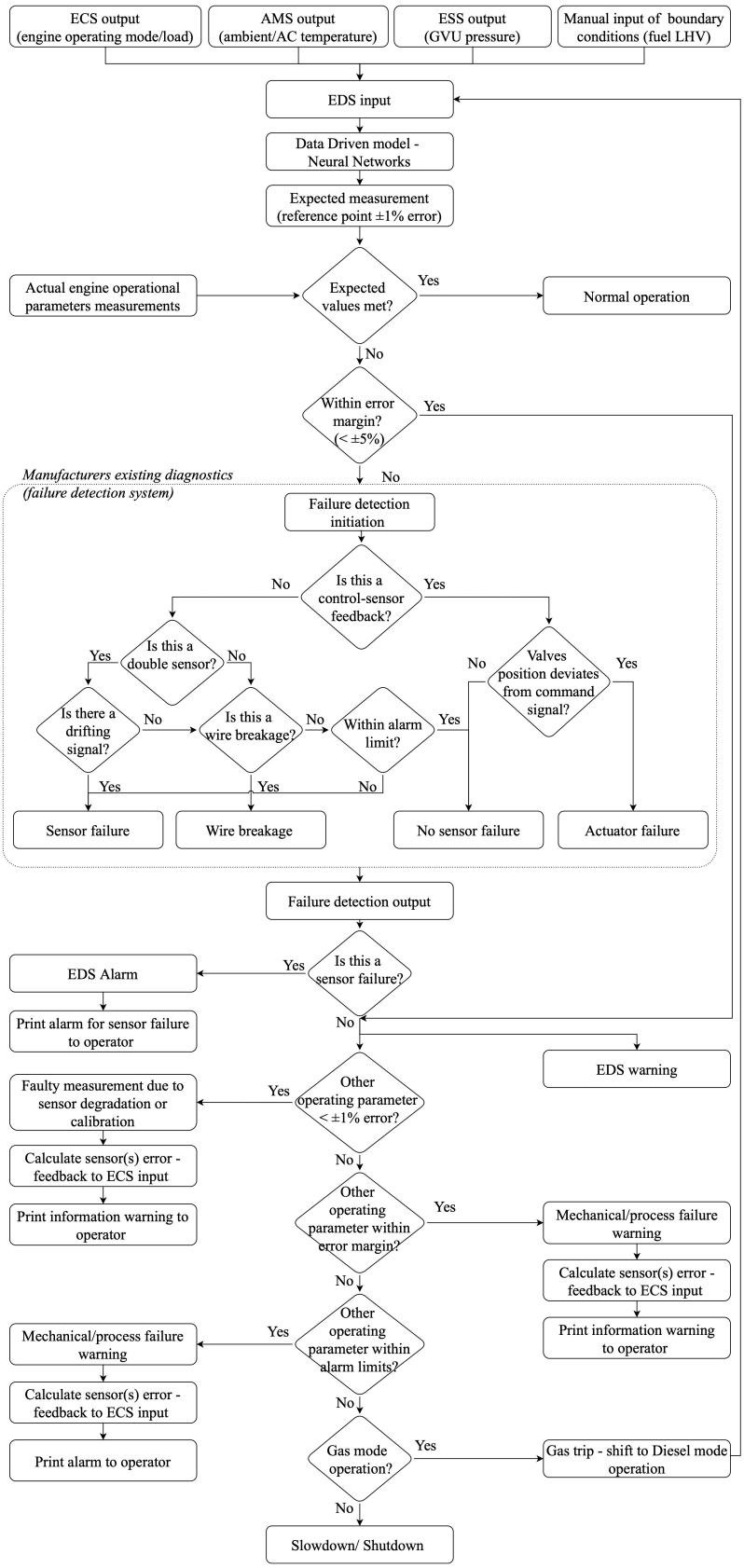

Figure 5.10 EDS control system event sequence flow chart diagram

5.3 Models validation

Further to the DT development, the operating parameters prediction accuracy of the engine thermodynamic and EDS models is validated. The percentage error of each investigated parameter is given by the equation 5-20.

$$\% \text{ Error} = \frac{V_2 - V_1}{V_1} 100 \qquad 5\text{-}20$$

where V_1 denotes the measured (reference) value and V_2 the predicted value of each parameter.

5.3.1 Reference cyber-physical system (CPS) Digital Twin (DT)

5.3.1.1 Steady State operation

The investigated marine DF engine steady state operation at both diesel and gas modes was examined by performing simulation runs in a load range from 25% to 100% and constant engine speed. The percentage errors between the available engine measured data from the engine shop trials and the predicted parameters are reported in Table 5.3. These include the brake power and BMEP/ IMEP, the BSFC/BSEC, the engine brake efficiency, the charged air pressure and temperature, the T/C operational parameters such as speed, EWG opening etc., the gas (fuel) manifold pressure and injection duration, the maximum (peak) cylinder pressure, the air–fuel equivalence ratio as well as the NO_x and CO_2 emissions. From the data given in Table 5.3, it is derived that the obtained accuracy for most of the engine parameters is adequate. Notably, the DT demonstrates no deviation with regards to the predicted charge air pressure in gas mode, whereas minor deviations are noted in diesel mode operation. However, this attributed to the EWG operation, where the EWG control adjust the EWG valve opening to achieve the targeted boost pressure. Therefore, the charge air pressure deviations are reflected via the EWG valve opening deviations.

Deviations beyond 5% are noted for the exhaust gas temperatures and mass flow rates (mainly in gas mode), which are attributed to a combination of model inaccuracies and

the measurements errors. With regard to the air−fuel equivalence ratio, the manufacturer provides a lambda window for the gas mode. Therefore, the margin from the permitted lambda window boundaries are provided in Table 5.3. By considering the justification on the calculated errors for the exhaust gas temperature and the mass flow rates as well as the minor errors calculated for the other engine operating parameters for both operating modes, it can be concluded that the developed model can be used to sufficiently represent the engine steady state behaviour.

Table 5.3 Percentage error between the available measured and the predicted values for engine steady state operation

	Diesel mode					**Gas mode**				
Load	**100**	**85**	**75**	**50**	**25**	**100**	**85**	**75**	**50**	**25**
Brake power	0.0	0.2	0.2	0.0	0.0	0.0	0.1	-0.1	-0.2	0.0
IMEP	0.4	-	-	-	-	0.2	-	-	-	-
BMEP	-0.1	-	-	-	-	-0.1	-	-	-	-
BSFC	1.0	0.8	1.4	1.4	1.5	n/a	n/a	n/a	n/a	n/a
BSEC	n/a	n/a	n/a	n/a	n/a	2.9	3.9	2.8	-0.4	0.1
Brake efficiency	0.5	0.6	0.1	0.1	0.0	-4.1	-5.1	-3.9	-0.5	-0.8
Charge air pressure	-0.5	-2.3	-1.9	1.6	-1.8	0.0	0.0	0.0	0.0	0.0
Charge air temperature	0.1	0.2	0.5	0.8	1.0	0.0	0.0	-0.2	0.0	-1.0
T/C speed	1.2	0.6	-0.1	2.1	0.1	1.2	0.5	-0.2	1.2	3.7
EWG opening	n/a	n/a	n/a	n/a	n/a	-2.2	5.2	2.0	5.9	5.5
Exhaust gas temperature – Turbine inlet	1.3	1.4	0.6	-0.8	0.4	4.4	5.3	5.5	6.0	12.4
Exhaust gas temperature – Turbine outlet	2.6	3.0	2.6	0.2	2.4	6.3	7.1	7.2	7.4	14.4
Mass flow rate compressor	-1.9	-	-	-	-	-5.6	-	-	-	-
Mass flow rate turbine	-2.0	-	1.9	2.0	-	-19.1	-	-20.9	-15.0	-
Gas (fuel) manifold pressure	n/a	n/a	n/a	n/a	n/a	-0.6	-0.7	-0.7	-0.9	-1.5
Gas injection duration	n/a	n/a	n/a	n/a	n/a	-1.5	1.4	4.5	6.6	14.2
Max. cylinder pressure	-1.2	-1.2	-0.4	2.7	-0.1	-3.0	-2.8	-3.2	-5.7	-5.1
Air—fuel equivalence ratio (% margin from manufacturer given lambda window)	-	-	-	-	from	-2.4	-0.3	0.8	-8.4	-10.7
					to	15.4	17.1	18.0	10.4	8.5
NO_x	0.9	-	2.3	2.6	1.2	-	-	-	-	-
CO_2	-1.1	-	-0.8	-0.7	-2.1	-	-	-	-	-

5.3.1.2 Transient operation

Following the engine simulation at steady state conditions, the developed digital twin was used for simulating the engine transient operation including load and modes switching. Three case studies, for which published experimental data are available, are investigated; in specific:

i. Case study V-1: the engine operation at 100% load in the gas mode and a mode switching to the diesel mode (Olander, 2006);

ii. Case study V-2: the engine operation at 80% load in the diesel mode and a mode switching to the gas mode (Olander, 2006); and

iii. Case study V-3: the engine operation at 40% load in the gas mode and a step-wise load increase to 80% engine load (Portin, 2010). For this case, due to the large ordered load increase, a mode switching from the gas mode to the diesel mode also takes place.

Due to availability of the published experimental data, the examined engine operating parameters are limited to: (a) the engine speed; (b) the air−fuel equivalence ratio; (c) the exhaust gas temperature (at T/C turbine inlet); and (d) the maximum cylinders pressure. For the three investigated case studies, the maximum percentage errors for the engine parameters with available experimental data are provided in Table 5.4. As it can be inferred from the presented results in Table 5.4, the developed model can predict the engine parameters response with an adequate accuracy. The derived errors were below 2.5% for the majority of the measured parameters apart from the boost pressure (for which deviations 5% and 10% were obtained for the two investigated transitions respectively), and the injected diesel fuel amount only for the diesel to gas transition (for which a maximum deviation of 13.7% was observed). However, as these maximum errors were obtained during the transition period and for only a short time, it can be deduced that the developed model accuracy is sufficient. As all the engine components and processes were accurately modelled, the prediction of the engine performance parameters is deemed satisfactory.

Table 5.4 Percentage error between the available measured and the predicted values for engine transient operation

	Case study V-1		Case study V-2		Case study V-3	
Error	min	max	min	max	min	max
Engine load	-0.3	0.6	0.1	2.1	-0.9	3.0
Engine speed	-0.9	-0.2	-0.5	1.4	0.0	2.8
Diesel fuel mass	-1.5	0.6	-13.7	11.6	-3.5	1.7
Gas mass	-	-	-	-	0.0	3.7
Charge air pressure	-0.7	4.6	-10.0	1.5	-	-

5.3.2 EDS model

As previously described in Section 5.2.2.5, the DD model was validated during the NNs training. Nevertheless, for the EDS model validation the developed digital twin is used to simulate steady state operations for 25%, 50%, 75%, 85% and 100% load, at the boundary conditions provided in

Table 5.5. The EDS monitored parameters of the digital twin are compared against the EDS model output and the calculated deviations are presented in Table 5.6.

Indicatively the NO_x emissions data linear regression of the DT (observed) and the EDS model (predicted) values is present in Figure 5.11. Linear regression curves of the remaining EDS monitored parameters are presented in Appendix C.

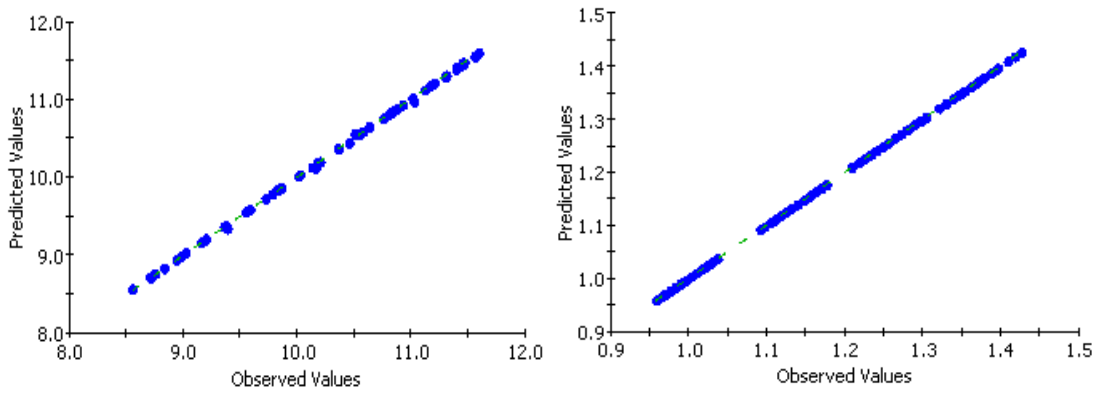

Figure 5.11 Example of predicted-observed NO_x emissions data linear regression for diesel (left) and gas (right) mode at 100% load

Table 5.5 Boundary conditions for the DT simulations

Parameter	**Unit**	**Value**
Ambient temperature	[K]	304.15
A/C coolant temperature	[K]	298.15
GVU gas pressure	[bar]	5.92
Gas LHV	[MJ/kg]	50
Diesel LHV	[MJ/kg]	42.6

Table 5.6 Percentage error between the digital twin and the EDS model predicted parameters for the engine steady state operation

	Diesel mode					**Gas mode**				
Load	**100**	**85**	**75**	**50**	**25**	**100**	**85**	**75**	**50**	**25**
Diesel fuel rack position	0.0	0.0	0.0	0.1	0.0	-	-	-	-	-
Max. cylinder pressure	0.2	-0.2	0.0	-0.2	-0.1	0.0	0.0	0.0	0.0	0.0
Charge air pressure	0.4	-0.3	0.0	-0.4	-0.2	0.0	0.0	0.0	0.0	0.0
Charge air temperature	0.0	0.0	0.0	0.0	0.0	0.0	0.0	0.0	0.0	0.0
Charge air mass flow rate	0.4	-0.3	0.1	-0.3	-0.1	0.0	0.0	0.0	0.0	0.0
T/C speed	0.4	0.2	0.5	0.3	0.3	0.5	0.8	0.5	0.5	0.5
Exhaust gas pressure – Turbine inlet	0.2	-0.3	0.0	-0.3	-0.1	-0.1	-0.1	0.0	0.0	0.0
Exhaust gas temperature – Turbine inlet	-0.4	0.1	-0.1	0.0	-0.1	0.0	0.0	0.0	0.0	0.1
Exhaust gas temperature – Turbine outlet	-0.5	0.1	-0.1	0.1	-0.1	0.0	0.0	0.0	0.0	0.1
EWG opening	-	-	-	-	-	0.9	0.7	0.1	0.0	0.1
Gas (fuel) manifold pressure	0.0	0.0	0.0	0.0	0.0	0.0	0.0	0.0	0.0	0.0
Gas injection duration	0.0	0.0	0.0	0.0	0.0	0.0	0.0	0.0	0.0	0.0
Air−fuel equivalence ratio	0.5	-0.4	0.1	-0.4	-0.2	0.0	0.0	0.0	0.0	0.0
Brake specific NO_x	-0.7	0.6	-0.1	0.5	1.1	-0.1	-0.1	0.4	0.2	0.7
Brake specific CO_2	-0.1	0.0	0.0	0.0	0.0	0.0	0.0	0.0	0.0	0.0
BSFC	-0.1	0.0	0.0	0.0	0.0	-	-	-	-	-
Brake efficiency	0.1	-0.1	0.0	-0.1	0.0	0.0	0.0	0.0	0.0	0.0
BMEP	0.0	0.0	0.0	0.0	0.0	0.0	0.0	0.0	0.0	0.0
Brake Power	0.0	0.0	0.0	0.0	0.0	0.0	0.0	0.0	0.0	0.0

As shown in Table 5.6, the percentage errors between the DT and the EDS model predicted engine performance and emissions parameters for the engine operation at steady state conditions are below 1.1%, with the calculated average absolute error being lower than 1%. Moreover, additional simulations were performed for 80% load in diesel and gas mode, in order to confirm the accuracy of the EDS model at the intermediate loads, demonstrating similar deviations. In specific, the percentage error for the EDS model predicted engine performance parameters are below 1%, whereas the NO_x emissions are below 2%. Therefore, it can be inferred that the EDS model can be used to accurately predict the monitored parameters at steady state conditions, providing the required fidelity for the UDS calculations. It must be mentioned that the operating parameters prediction under engine transient conditions is not considered, as the EDS model is not used under these conditions.

5.4 Chapter summary

In this Chapter, the digital twin modelling approach, methods, and tools are presented. In specific, the reference CPS engine thermodynamic model development, considering the engine sub-systems as well as the UDS and its sub-systems/modules functional modelling, are described in detail. In addition, the newly introduced FOS and EDS systems functional modelling is presented and their integration in the UDS is discussed. Lastly, the reference CPS digital twin and the DD model are validated against available published data, both found to sufficiently representing the engine response with adequate accuracy.

6 CASE STUDIES

6.1 Chapter outline

This Chapter focuses on the design of the case studies for the application of the engine digital twin and the other developed tools. The case studies described in this Chapter are strategically planned in order to reveal the engine design and operational limitations as well as the engine safety critical components and the potential effect that these may have in the engine operation; i.e. the performance, emissions and safety. In addition, this Chapter elaborates on the considered case studies for the engine performance optimisation and emissions reduction as well as the UDS verification.

6.2 Engine design and operational limitations

The engine design and operational limitations are investigated by using the verification case studies. These include three case studies, which were also used for the validation of the developed engine model and digital twin: (a) Case study V-1: the engine operation at 100% load in the gas mode and a mode switching to the diesel mode (Olander, 2006); (b) Case study V-2: the engine operation at 80% load in the diesel mode and a mode switching to the gas mode (Olander, 2006); and (c) Case study V-3: the engine operation at 40% load in the gas mode and a step-wise load increase to 80% engine load (Portin, 2010). For Case study V-3, due to the large ordered load increase, a mode switching from the gas to diesel mode also takes place. The case studies V-1 to V-3 are discussed and the engine parameters margin against the manufacturer limits are identified.

6.3 Performance and emissions

6.3.1 Engine settings optimisation − Gas mode

For the optimising the DF engine settings aiming to a simultaneous reduction of the CO_2 and NO_x emissions, a parametric study is performed via a DoE 'full factorial' method (integrated in GT-ISE). It must be noted that the CO_2 emissions are proportional to the engine specific energy consumption and therefore, a decrease of CO_2 emissions corresponds to a reduction of BSEC and an increase of the engine brake efficiency. The following DoE variables are considered: pilot fuel injection timing, inlet manifold boost pressure (as a function of EWG valve opening) and inlet valve closing. The parametric study simulations are performed for 50%, 75% and 100% engine load at steady state conditions (case studies P-1 to P-3). The reference values considered in the DoE optimisation for the CO_2 and NO_x emissions, were selected based on the generated emissions of engine in gas mode operation at 100% load. The DoE optimisation variables, constrains and objectives are summarised in Table 6.1

Table 6.1 DoE optimisation parameters

		Unit	Value	
			Min.	**Max.**
Variables	Load	[%]	50	100
	Pilot fuel injection timing	[°CA]	-2	2
	Inlet manifold boost pressure	[%]	-5	5
	Inlet valve closing	[°CA]	-5	5
Constrains	Air – fuel equivalence ratio	[-]	1.9	2.3
	CO_2 and NO_x emissions	[g/kWh]	Below reference values	
Objectives	CO_2 and NO_x emissions	[-]	CO_2/NO_x emissions trade-off minimisation	

6.3.2 EGR and ABP systems settings optimisation – Diesel mode

In order to reduce the engine NO_x emissions to the required levels (imposed by the IMO 'Tier III' requirements) and simultaneously ensure the optimal engine performance, it is essential to identify and optimise the EGR and ABP systems settings

affecting the engine response. In this respect, the following variables are considered in this optimisation phase: (a) the EGR and ABP valves opening – they can directly affect the EGR rate, and consequently the NO_x emissions, as well as the engine fuel consumption; (b) the EGR blower speed; and (c) the start of injection (SOI) – the reported impact of the SOI variation on the cylinders pressure, and consequently on the engine fuel consumption, renders SOI a crucial variable for the engine efficiency optimisation.

The optimisation phase is divided in two phases: (a) the optimisation of the EGR and ABP valves opening as well as the EGR blower speed; and (b) the SOI optimisation. The reasoning behind the discretisation into two phases is primarily to observe the BSFC improvements from SOI optimisation, and secondly improve the simulation time.

For the first optimisation phase, the built-in GT-ISE multi-objective genetic algorithm (MOGA) optimiser is employed. This method is selected due to the fact that it allows to maximize, minimize, or target a combination of responses (model parameter outputs) and study their competing objectives. In this respect, MOGA is considered one of the most sophisticated and robust optimisation algorithms (GT, 2019). The GT-ISE MOGA optimiser employs the NSGA-III genetic algorithm (Deb and Jain, 2014). The genetic algorithm settings are selected based on recommendations provided in the GT-ISE manual (GT, 2019) and by trial and error. The genetic algorithm settings are presented in Table 6.2.

Table 6.2 Genetic algorithm settings

Parameter	**Value**
Population size	40
Number of generations	10
Crossover rate	1
Crossover rate distribution index	15
Mutation rate	Calculated
Mutation rate distribution Index	20
Random seed	Random

The population size generally increases as the number of independent variables increases, where the counting of variables, *n*, is calculated by the following equation.

$$n = v\,c \tag{6-1}$$

where *v* denotes the number of variables and *c* the number of simulation cases.

Considering the MOGA settings, the optimiser runs a total number of generations (investigated designs) equal to the population size multiplied by the number of generations. The crossover distribution index determines the spread of the offspring solutions (ranging from 10 to 100). The mutation rate value is calculated from the number of independent variables, *n*, as follows:

$$\text{Mutation rate} = \frac{1}{n} \tag{6-2}$$

The mutation rate distribution index determines the spread of offspring solutions (ranging from 10 to 100).

As shown in Table 6.3, the MOGA optimiser objectives include the minimisation of; (a) the NO_x emissions; (b) the engine BSFC; and (c) the EGR blower power demand. The EGR and ABP systems settings (i.e. EGR and ABP valves openings) are optimised independently for each load, whereas the EGR blower speed is optimised for all the engine loads. The EGR and ABP valves opening ranges are assumed to be 10°-90° and 5°-90° respectively, considering integer steps intervals of 1° for the valves' opening. The EGR blower speed range is assumed 8500-9000 r/min with integer step intervals of 100 r/min. The imposed constrains considered for the MOGA optimisation included the acceptable ranges for the compressor surge and choke margins ranges, the EGR rate as well as the NO_x emissions limit (NO_x Technical Code (IMO, 2014a), E2 test cycle). The expected results from this optimisation stage include the sets of the optimal settings; i.e. the EGR and ABP valves openings, which demonstrate the minimum engine BSFC and the EGR blower power demand.

In the second optimisation phase, the BSFC reduction due to the SOI variations is investigated. The SOI parametric optimisation is performed via the GT-ISE DoE optimiser employing the 'full factorial' method. In reference to the existing literature, it is well reported that the SOI variation affects the maximum cylinder pressure, and consequently the engine power. Hence, simulation runs are performed for SOI values (20°-12°CA bTDC), in integer intervals of 1°CA. However, the increase of the maximum cylinder pressure is expected to be accompanied by a minor NO_x emissions increase. Thus, the EGR and ABP valves opening are also considered in the DoE parametric runs to compensate this NO_x emissions increase.

Both optimisation phases are performed at 25%, 50%, 75% and 100% engine loads for steady state conditions (case studies EM-1 to EM-4 and ED-1 to ED-4). The followed optimisation process flowchart is illustrated in Figure 6.1, whereas the optimisation process variables and their considered ranges are provided in Table 6.3.

Table 6.3 Optimisation process parameters

Load			**[%]**	**25**	**50**	**75**	**100**
MOGA optimisation	Settings (variables)	EGR Blower speed	[r/min]	8500-9000			
		EGR valve opening	[deg]	10-90			
		ABP valve opening	[deg]	5-90			
	Constrains	NO_x emissions limit	[g/kWh]	2.583			
		EGR rate	[%]	30-40			
		T/C compressor surge margin	[fraction]	0.15-0.35			
	Objectives	NO_x emissions	[g/kWh]	minimise			
		BSFC	[g/kWh]	minimise			
		EGR blower power	[kW]	minimise			
DoE optimisation	Settings (variables)	Start of injection (SOI)	[°CA bTDC]	20-12			
		EGR valve opening	[deg]	21-23	33-35	85-87	90
		ABP valve opening	[deg]	6-8	50-52	51-53	49-55
	Constrains	NO_x emissions limit	[g/kWh]	2.583			
	Objectives	BSFC	[g/kWh]	minimise			
		NO_x emissions	[g/kWh]	minimise			

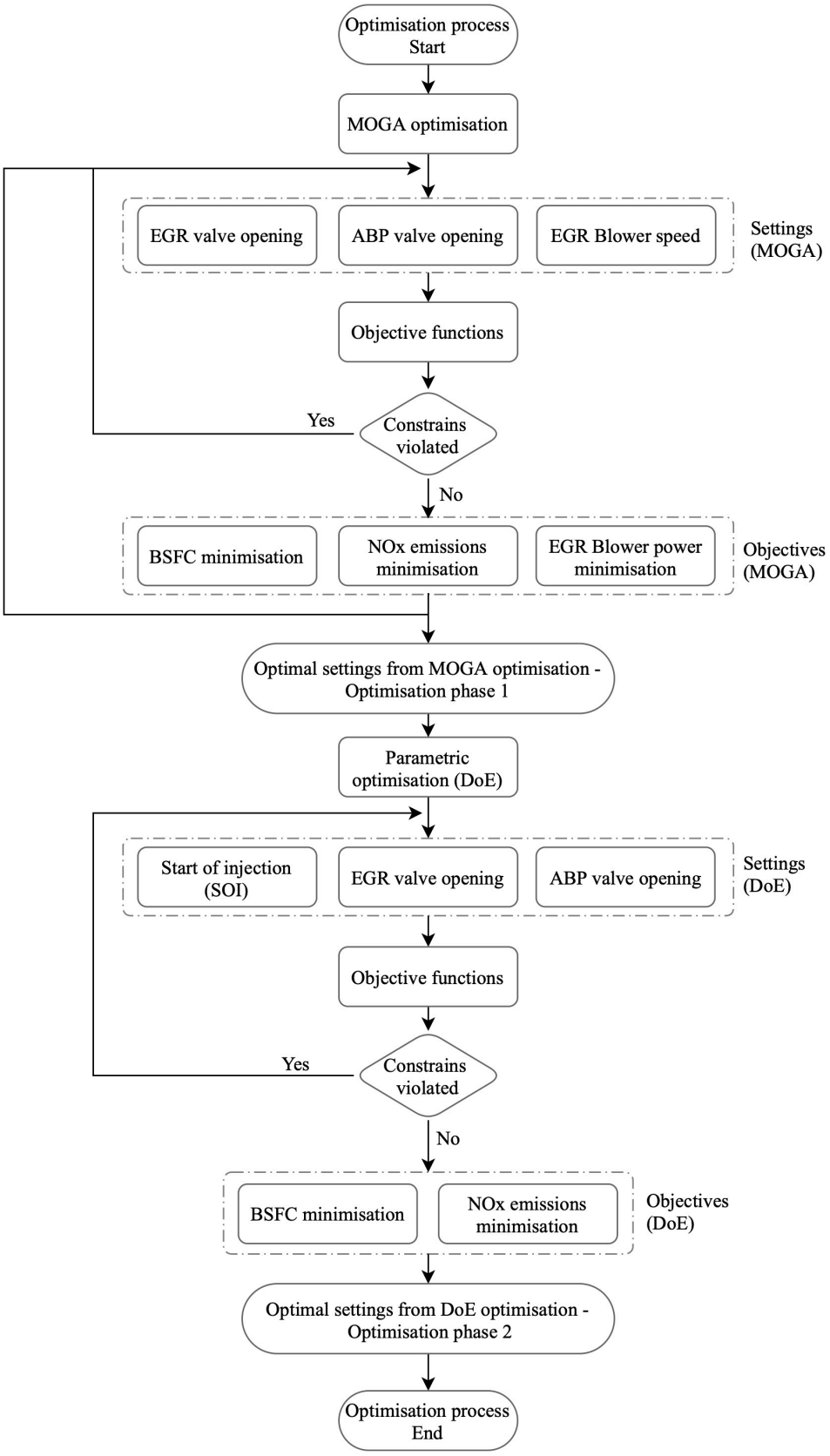

Figure 6.1 Optimisation phases process flowchart

Further to the preceding optimisation process, the developed digital twin is used to investigate the engine transient operation with the EGR and ABP systems. The case studies ET-1 to ET-3 are designed with the aim to simulate the engine operation in the diesel mode. The EGR and ABP systems are initially deactivated, and an activation input is ordered before the vessel enters an ECA, in order to comply with the NO_x requirements. Furthermore, once the vessel exits the ECA, a deactivation command for the EGR system is ordered. Therefore, the performed transient case studies provide insight for the EGR and ABP systems response and their effect on the engine operation during the transient conditions, as well as the engine operating limitations related to the EGR and ABP systems operation.

6.4 Safety

In order to investigate the engine safety, prior to the design of the engine simulation case studies, it is necessary to identify the DF engine safety critical systems/components as well as the most critical scenarios of the engine operation under faulty conditions. Therefore, the engine assessment in terms of components and systems criticality is required. This is carried out by using FMEA.

6.4.1 DF engine safety critical systems/components

The regulatory framework regarding the engine systems safety has led the engine manufacturers towards the identification of engine safety critical systems using FMEA or FMECA tools, in order to consider risk mitigation actions (redundancy, engine slowdown/shutdown etc.) in the engine design process. Engine malfunctions are usually grouped per system (e.g. ECS, AMS, ESS) with which the sensors and actuators are connected. The most crucial alarms and their related actions are primarily examined; i.e. the faults/failures of actuators/sensors that would trigger a gas trip, slowdown (SLD) or shutdown (SHD) by the ESS. Particularly in DF engines, the hazards involved with the engine operation are increased in number and in terms of consequences compared to the diesel engines, due to the hazards imposed by the handling and storage of the gas fuel as well as the additional equipment installed for the gas fuel control and utilisation when the engine operates in the gas mode. In this respect, the engine critical systems are

identified and ranked based on the impact of a potential component/system malfunction or fault on the engine.

In general, considering the diesel engines and based on the pertinent literature, the most critical systems safety-wise involve faults (demonstrating higher impact close to the engine MCR point operation), are associated either with the engine sensors and actuators or with the engine control software and/or hardware issues. In specific, these faults include: the pressure and/or temperature sensors for the charge air/exhaust gases, the sensors for the engine speed and crank angle, the pressure and/or temperature sensors for engine lube oil and charge air coolant as well as the diesel fuel oil, whereas with regards to the actuators and other components these involve the diesel fuel rack actuator, diesel fuel injectors (misfire issues) and valve clearance. Less common are the issues occurring due to software/hardware malfunction/failure on the engine ECS, however, their functionality has major impact on the engine operation under faulty conditions and must not be neglected.

Further to critical systems identified in the diesel engines, the utilisation of gas fuel in DF engines involves additional hazards. Therefore, the safety critical systems in DF engines is moderately increased due to the additional engine components employed to accommodate gas fuel. In this case, the misfiring and knocking sensors are essential to monitor the engine behaviour to allow the ECS to adjust the air–fuel ratio in the engine cylinders. In addition, the gas (fuel) pressure (controlled by the GVU) is considered a critical parameter that can affect the engine operation, whilst gas leakage sensors are necessary to avoid associated hazards. Moreover, the GVU valve actuator is considered a critical engine system, as a potential malfunction could correspond to gas built-up pressure in the gas (fuel) manifold and cylinders over-fuelling resulting in engine overspeeds, knocking and/or components failure. Similarly, the EWG system is also of vital importance, as an EWG valve actuator potential failure may lead to turbocharger overspeeds, generating, in turn, a domino effect on the engine response and operating parameters. Lastly, the engine manufacturers classify the ECS fuel control module as a crucial sub-system, due to its impact on the fuels controls. The DF engine safety critical components can be further expanded considering the pilot fuel injectors, the GAVs and the gas (fuel) manifold pressure sensor.

6.4.2 Failure Mode and Effects Analysis

FMEA is a method that is used to identify potential failure modes and to assess the impact of those failures on the system applicable to different system abstractions and system levels (BSI, 2006). In the present study, the engine critical components are identified and ranked based on the frequency and impact of a potential component malfunction. The FMEA worksheet proposed by IEC (2006) is employed, where the engine load and operating mode that the failure occurs were considered, in order to distinguish the consequences in each scenario. Moreover, during FMEA only the engine response is considered, disregarding any impact on the ship systems. For the analysis of the occurrence, severity and detectability indexes, the tables presented by (Zúñiga et al., 2020) are used as presented in Table 6.4 to Table 6.6. The ranking of faults is carried out based on the Risk Priority Number (RPN). A risk ranking table considering the RPN is provided by McCollin (1999), as presented in Table 6.7.

The engine systems considered in the FMEA of this thesis are: (a) the pilot injection system; (b) the GAV; (c) the GVU; (d) the diesel fuel system; (e) the EWG valve actuator; (f) the speed sensors, and; (g) the pressure sensors (including boost and gas (fuel) manifold pressure); and (h) temperature sensors.

It must be noted that the FMEA is based on the assumptions that the engine manufacturer maintenance procedures and intervals are followed, whereas the engine systems are operated and maintained by qualified personnel.

Table 6.4 Occurrence index scales

Occurrence (O)			
Ranking	**Description**	**Definition**	**$\lambda <$ [hours^{-1}]**
10	Extremely High	> 1 in 2	$5.00\ 10^{-1}$
9	Very High	1 in 3	$3.30\ 10^{-1}$
8	Repeated failures	1 in 8	$1.25\ 10^{-1}$
7	High	1 in 20	$5.00\ 10^{-2}$
6	Moderately high	1 in 100	$1.00\ 10^{-2}$
5	Moderate	1 in 400	$2.50\ 10^{-3}$
4	Relatively low	1 in 2000	$5.00\ 10^{-4}$
3	Low	1 in 15,000	$6.67\ 10^{-5}$
2	Remote	1 in 150,000	$6.67\ 10^{-6}$
1	Nearly impossible	< 1 in 1,500,000	$6.67\ 10^{-7}$

Table 6.5 Severity index scales

Severity (S)		
Ranking	**Description**	**Definition**
10	Hazardous without warning	The highest severity ranking of a failure mode, occurring without warning and with the consequent hazard.
9	Hazardous with warning	Higher severity ranking of a failure mode, occurring with a warning and the consequent hazardous.
8	Very high	Operation of the system is broken down without compromising safe
7	High	Operation of the system may be continued, but its performance is affected
6	Moderate	Operation of the system is continued, but its performance is degraded
5	Low	Performance of the system is affected seriously, and the maintenance is needed
4	Very low	Performance of the system is less affected, and the maintenance may not be needed
3	Minor	System performance and satisfaction with minor effect
2	Very Minor	System performance and satisfaction with a slight effect
1	None	No effect

Table 6.6 Detectability index scales

Detectability (D)		
Ranking	**Description**	**Definition**
10	Absolutely impossible	Design control does not detect a potential cause of failure mode, or there is no design control
9	Very remote	Very remote chance the design control will detect a potential cause of the failure or subsequent failure mode
8	Remote	Remote chance the design control will detect a potential cause of the failure or subsequent failure mode
7	Very Low	Very low chance the design control will detect a potential cause of the failure or subsequent failure mode
6	Low	Low chance the design control will detect a potential cause of the failure or subsequent failure mode
5	Moderate	Moderate chance the design control will detect a potential cause of the failure or subsequent failure mode
4	Moderately High	Moderately high chance the design control will detect a potential cause of the failure or subsequent failure mode
3	High	High chance the design control will detect a potential cause of the failure or subsequent failure mode
2	Very High	Very high chance the design control will detect a potential cause of the failure or subsequent failure mode
1	Almost Certain	Design control will almost certainly detect a potential cause of the failure or subsequent failure mode

Table 6.7 Risk ranking (McCollin, 1999)

O/S	1	2	3	4	5	6	7	8	9	10
1	N	N	N	N	N	N	N	N	C	C
2	N	N	N	N	N	N	10	8	C	C
3	N	N	N	N	10	7	6	5	C	C
4	N	N	N	8	6	5	4	4	C	C
5	N	N	10	6	5	4	3	3	C	C
6	N	N	7	5	4	3	3	2	C	C
7	N	10	6	4	3	3	2	2	C	C
8	N	8	5	4	3	2	2	2	C	C
9	N	7	5	3	3	2	2	1	C	C
10	N	6	4	3	2	2	1	1	C	C

Note: N (green) denoted that no corrective action is needed; C (red) denoted that correction action is needed and the yellow coloured boxed denote that corrective action is needed if the Detection rating is equal to or greater than the given number.

The Risk Priority Number (RPN) for each FMEA scenario is calculated by using equation 6-3.

$$RPN = O\ S\ D \tag{6-3}$$

where *O* denotes occurrence, *S* the severity and *D* the detectability of the failure modes.

6.4.3 Safety implications

According to the FMEA results, 329 different scenarios are identified. These correspond to potential simulation case studies. The most critical failures are interconnected to the EWG and GVU valves actuators, the diesel rack actuators and the GAV as well as the pilot fuel injector. In addition, the speed and boost pressure sensors as well as the gas (fuel) manifold pressure sensor are vital engine components, due to their impact on the ECS controls; potential faults occurring on these components will considerably affect on the engine response. Less common are the issues occurring due to software/hardware malfunction/failure on the engine ECS, however, their functionality has major impact on the engine operation under faulty conditions and must not be neglected.

From the FMEA potential simulation case studies, the 93 are identified with Risk Priority Number (RPN) over 36, or as critical (Table 6.8). However, by considering

failures that may lead to engine shut down as well as excluding similar failure modes, the critical modes are reduced to 8 case studies (S-1 to S-8), as presented in Table 6.9. The failure values identified based on the literature for the case studies S-1 to S-8 are presented Table 6.10.

Table 6.8 Simulated cases risk index ranking

Case ID (FMEA ID)	Occurrence (O)	Severity (S)	Detectability (D)	Risk Priority Number (RPN)
S-1 (11)	3	6	4	72
S-2 (43)	3	7	4	84
S-3 (82)	3	8	4	96
S-4 (170)	2	6	3	36
S-5 (200)	2	6	3	36
S-6 (220)	3	6	4	72
S-7a/b (266)	3	7	3	63
S-8 (272)	3	7	3	63

From the Table 6.8, it can be inferred that the RPN is generally low to moderate, as expected, implying that engine manufacturer has already taken appropriate risk mitigation measures such as increasing components (actuators/sensors) failure detectability to reduce the RPN. In addition, the RPN ranking reveals that the faulty components considered in the case studies S-2 and S-3 are defined as engine critical components due to their high severity index, which is interpreted as crucial components considerably affecting the engine operation.

Table 6.9 Selected failure modes for simulation

Case ID (FMEA ID)	Components and Functions		Failure mode and Failure cause		Oper. mode	Effects on the system	Failure detection method during design
S-1 (11)	Gas (fuel) manifold pressure sensor	Measurement of gas pressure at gas (fuel) manifold	Lower measurement	Degradation failure or non- calibrated equipment	Gas	Increase the gas (fuel) manifold pressure will result in increase in generated load and consequent loss of the DG set	More complex failure and it is more difficult to assess its impact
S-2 (43)	Speed sensor	Measurement of engine speed	Lower measurement		Diesel	Increase the fuel amount with potential overspeed	High chance that this issue is addressed during design – double sensors
S-3 (82)	Boost pressure sensor	Measurement of boost pressure	Erroneous measurement		DTG	Opening or closing of valve leading either to misfiring or knocking with T/C surging	More complex failure and it is more difficult to assess its impact
S-4 (170)	GVU valve actuator	Implement the control action	Null/ non-responsive	Degradation or mechanical failure	Gas	Failure to ensure proper load change	High chance that this issue is addressed during design -gas trip
S-5 (200)	GAV		Null/ non-responsive (no gas fuel injection)	Degradation or mechanical failure	Gas	Failure to achieve the load, inappropriate temperature, pressure	Safety functions will detect the effects associated with this failure mode -gas trip
S-6 (220)	Diesel fuel rack	Inject the desire amount of diesel fuel	Delayed response		GTD	Instability	High chance that this issue is addressed during design
S-7a/b (266)	Exhaust waste gate valve	Implement appropriate control for EWG valve	Delayed		GTD/ DTG	Surging of turbocharger	High chance that this issue is addressed during design
S-8 (272)			Null/ non-responsive		GTD	Surging of turbocharger	High chance that this issue is addressed during design

Table 6.10 Simulated failure values

Case ID (FMEA ID)	Component	Failure mode	Failure value	Source
S-1 (11)	Gas (fuel) manifold pressure	Lower measurement	-29%	(Balaban et al., 2009)
S-2 (43)	Speed sensor	Lower measurement	-5%	(Zidani et al., 2007, Heredia et al., 2008, Gaeid et al., 2012)
S-3 (82)	Boost pressure sensor	Erroneous measurement	-29%	(Balaban et al., 2009)
S-4 (170)	GVU valve actuator	Null/ non-responsive	Same value	[-]
S-5 (200)	GAV	Null/ non-responsive (no fuel injection)	Same value	[-]
S-6 (220)	Diesel fuel rack	Delayed response	1 sec	(Hountalas, 2000)
S-7a/b (266)	EWG valve	Delayed	1 sec	Assumed
S-8 (272)	EWG valve	Null/ non-responsive	Same value	[-]

Furthermore, as the FMEA results and the simulation case studies V-1 and V-2 indicate, the EWG valve and its control seems to be critical for the engine response, therefore special consideration is given with regards to the EWG and the case studies S-7a and S-7b are simulated to further investigate the potential engine safety implications. The FMEA case studies S-7a and S-7b are investigated for both the GTD and DTG modes switching and are further compared to the normal engine operation with the case studies V-1 and V-2, respectively.

The simulation case studies S-1 to S-8 are performed for transient conditions, where the engine initially operates under the normal/healthy state and for a given time the sensor/actuator demonstrates a faulty response. The alarm limits for a number of parameters are considered in order to identify responses that lead to potential safety implications for the engine.

6.5 Unified Digital System response

For the verification of the UDS model and for demonstrating its implementation advantages, both diesel and gas operating modes are considered during the simulation case studies design. As it can be inferred, the higher-end range of the engine loads renders the engine more prone to safety implications, therefore the 100% engine load is selected for conducting the engine operation simulations.

The UDS response is examined under faulty operation conditions of the speed sensor in combination with the boost pressure sensor (case studies U-1 and U-2). The rationale behind the strategic selection of the above, lies on the fact that these sensors are interconnected with the ECS controllers that can directly affect the engine response; i.e. the diesel and gas PID controllers as well as the EWG controller, in the respective operating modes. Hence, their faulty operation (in terms of their measurements uncertainty) has a considerable impact on the ECS output, and consequently, on the engine response. In addition, by considering potential faulty measurements of these sensors, the assessment of the engine response in such scenarios becomes a challenging task due to the processes complexity, therefore, establishing the measurements uncertainty identification of these sensors forms an apparent need for addressing the faults investigated in the case studies U-1 and U-2.

On the contrary, the exhaust gas temperature sensor is primarily installed in order to monitor the engine operation safety-wise (knocking situations) and prevent the prolonged operation beyond its designed alarm limits set by the manufacturer. Moreover, a potentially uncertain/deviated measurement from the gas (fuel) manifold pressure sensor can be compromised by an alteration in the gas injection duration of the GAV, as presented in the following Chapter. Nevertheless, the measurements uncertainty of these sensors can be intelligently identified considering the present development. With regards to the engine CA sensors, minor deviations in the CA measurements have limited impact in the engine operation in gas mode operation. In specific, the CA measurements are associated with the gas injection timing of the GAV, however, considering the intake valves profile, a minor drift of the CA measurement signal will result to early or delayed gas fuel injection that can be accommodated, due to

sufficient margins. Furthermore, considerable CA measurements deviations, sensor signal interruption/cut off and sensors failure are detectable by the existing manufacturer diagnostics system, so that corrective actions are imposed accordingly.

Notwithstanding the above, to realistically verify the UDS, the following assumptions are made; (a) the actuators delays or unresponsiveness as well as the sensors signal/wire breakage are identified by the existing diagnostics system; (b) sensors faulty response can occur either from the engine start or at a given random time; (c) the UDS diagnostics run only in steady state operating conditions; sensors faulty response during load transients or modes switching are identified when the engine converges back to its steady state conditions, and; (d) the engine response under faulty sensors measurements is expected to reach steady state conditions; unstable engine response due to hardware/software issues may be addressed by the existing diagnostics system and/or slowdown (SLD)/ shutdown (SHD) command may be ordered to avoid severe safety implications.

6.6 Case studies design summary

The case studies designed based on the discussion in the preceding Sections, are summarised as shown in Table 6.11.

Table 6.11 Case studies summary

Case ID	Description	Load [%]	Mode	Steady state/ transient
SS-1g/d	Steady State simulations (DT validation)	25	Gas/ diesel	Steady state
SS-2g/d		50		
SS-3g/d		75		
SS-4g/d		85		
SS-5g/d		100		
V-1	Gas to diesel modes switching	100	GTD	Transient
V-2	Diesel to gas modes switching	80	DTG	Transient
V-3	Step load increase from 40% to 80%	40 - 80	GTD	Transient
D-1g/d	DoE simulations for DD model development	25	Gas/ diesel	Steady state
D-2g/d		50		
D-3g/d		75		
D-4g/d		85		
D-5g/d		100		
P-1	DoE performance and emissions optimisation in gas mode	50	Gas	Steady state
P-2		75		
P-3		100		
EM-1	MOGA performance and emissions optimisation in diesel mode	25	Diesel	Steady state
EM-2		50		
EM-3		75		
EM-4		100		
ED-1	DoE performance and emissions optimisation in diesel mode	25		
ED-2		50		
ED-3		75		
ED-4		100		
ET-1	EGR/ABP systems transient operation	50	Diesel	Transient
ET-2		75		
ET-3		100		
S-1	Case studies identified from FMEA (Table 6.9)	100	Gas	Transient
S-2			Diesel	
S-3			DTG	
S-4			Gas	
S-5				
S-6			GTD	
S-7a				
S-7b		80	DTG	
S-8		100	GTD	
U-1	UDS verification simulations	100	Diesel	Transient
U-2			Gas	

6.7 Chapter summary

In this Chapter, the case studies design was presented. The considered simulation case studies were identified and an in-depth discussion and justification on their selection were provided. These case studies are simulated with the use of the developed digital twin and the generated results are presented and discussed in detail in the following Chapter.

7 RESULTS AND DISCUSSION

7.1 Chapter outline

This Chapter presents the case studies results that are generated from the digital twin simulations under steady state or transient conditions. The results related to the engine performance, emissions and safety are analysed, and the key findings are discussed. The reference values used for the results normalisation are presented in Appendix A.

7.2 Engine steady state and transient conditions operation

7.2.1 Steady state operation (Case studies S-1g/d to S-5g/d)

The measured and predicted simulation results generated during case studies S-1g/d to S-5g/d include: the brake power and BMEP/ IMEP; the BSFC/BSEC; the engine brake efficiency; the charged air pressure and temperature; the T/C operational parameters such as speed, EWG opening etc.; the gas (fuel) manifold pressure and injection duration, the maximum (peak) cylinder pressure; the cylinder maximum burned zone temperature; the air–fuel equivalence ratio as well as the NO_x and CO_2 emissions.

By considering the derived maximum cylinder pressure diagrams shown in Figure 7.1, it can be inferred that the diesel mode combustion starts closer to the cylinder top dead centre (TDC), whereas in the case of the gas mode the pilot injection and combustion starts earlier to avoid knocking problems. The gas mode operation also results in a longer ignition delay due to the natural gas presence in the combustion chamber as it is

also reported in Liu and Karim (1997), Christen and Brand (2013) and Sixel et al. (2016). The peak heat release rate (HRR) of the dual fuel combustion is slightly higher (Figure 7.1), and the main combustion ends earlier than that at the diesel mode. However, a slightly lower maximum pressure level is observed in the case of the gas mode, which is attributed to the engine turbocharger operation at lower speed due to the exhaust waste gate valve opening. As the boost pressure is lower in the case of the gas mode, the cylinder pressure during the compression process is also lower; however due to the advanced start of combustion and the shorter combustion duration, the lower maximum pressure and the resultant lower friction, the engine brake power is retained at the same level as in the diesel mode.

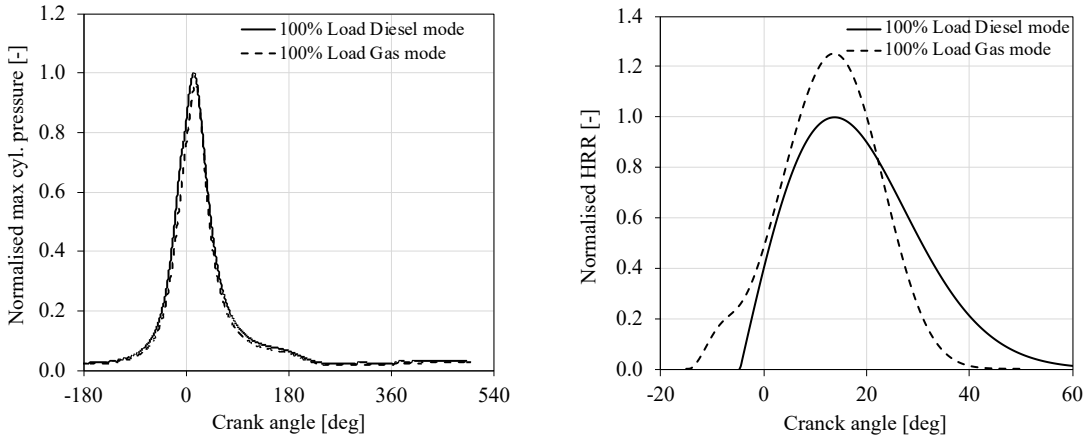

Figure 7.1 Maximum cylinder pressure (left) and HRR (right) for diesel and gas operating modes at 100 engine load (case studies SS-5g/d)

Therefore, in terms of the engine power output and mean effective pressures, it can be observed from Figure 7.2 that similar values were obtained in each operating mode; the indicated mean effective pressure of the diesel mode seems to be only slightly greater, however the brake mean effective pressures in both modes are exactly the same as the difference is compensated by the slightly higher friction mean effective pressure (due to the greater maximum pressure of the diesel mode).

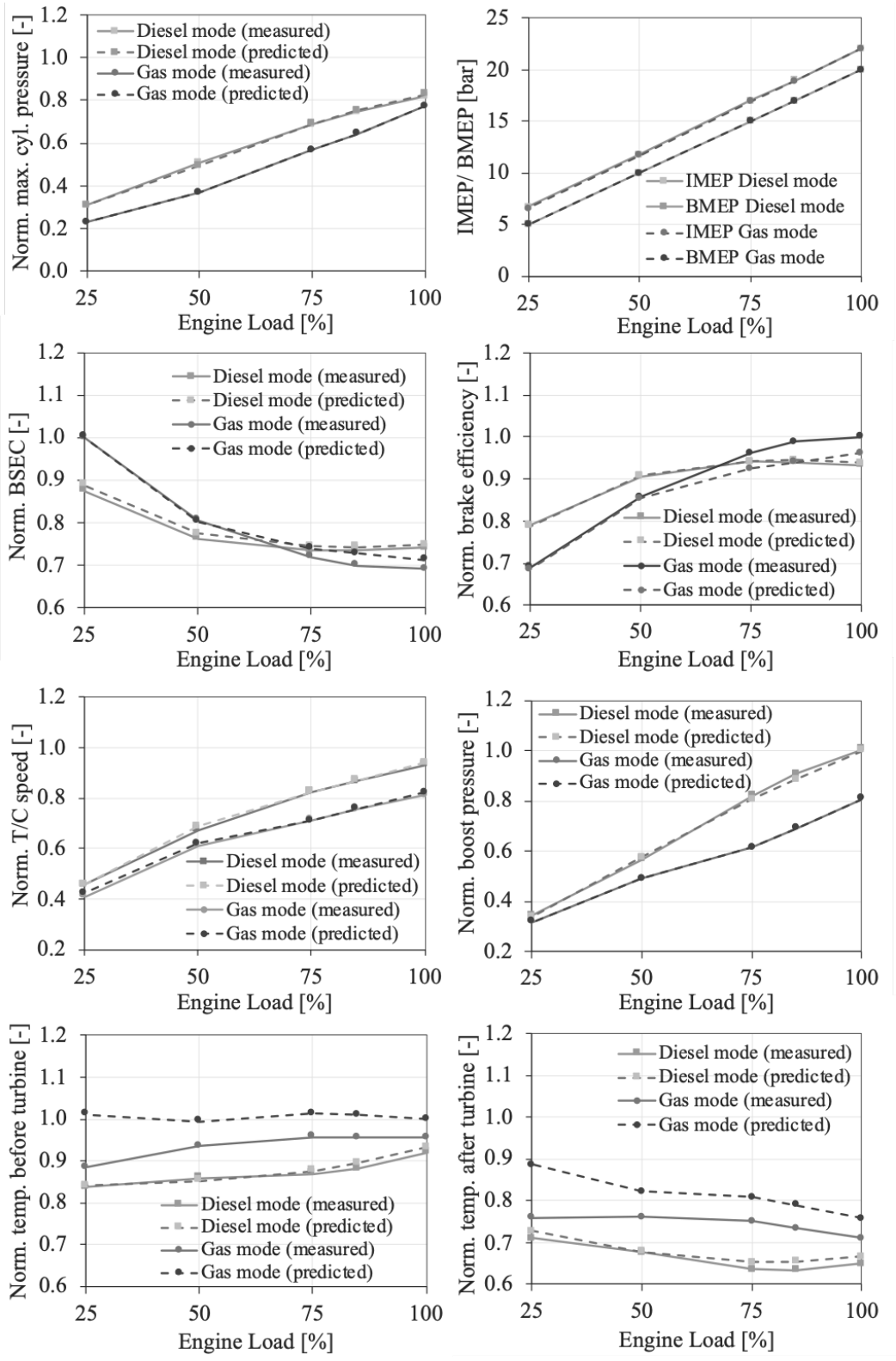

Figure 7.2 Simulation results and comparison with available experimental data

In terms of the engine efficiency at the two operating modes, it can be observed that the gas mode is more efficient at the high loads region obtaining values up to 47% at 100% load. When operating in the diesel mode, the engine obtains its highest efficiency at 75% load, whereas the engine efficiency only slightly varies in the load region from 70% to 100%. For the gas mode, the efficiency decreases at a steeper gradient as the load decreases reaching its lowest value at 25% load; the engine obtains much higher efficiency at 25% load when operating at the diesel mode. This is attributed to the specific characteristics of diesel and gas operating modes as well as to the opening of the exhaust waste gate valve that results in lower turbocharger speed and pressure levels for the gas mode. Similar conclusions can be derived by analysing the brake specific energy consumption, which is the reciprocal of engine brake efficiency. The energy provided by the pilot diesel fuel accounts for 0.3% to 2.3% of the totally supplied fuel energy (the values increase with decreasing load).

In terms of the air−fuel equivalence ratio (lambda), it is observed from Figure 7.3 that in the gas mode the engine operates within a narrow lambda window with values between 1.9 and 2.1 (2.1 was observed at the low loads whilst approx. 2.0 was obtained at medium and high loads). For the diesel mode, the obtained values for lambda are slightly higher (in the range from 2.5 to 2.8), which means that more air passes through the engine cylinders in the latter case. For the gas operation, the exhaust waste gate opening affects (actually reduces) the turbocharger speed, which in turn controls the boost pressure and as a result, the engine air flow and lambda. The obtained exhaust waste gate opening values were estimated in the range from 23% to 38% of the exhaust waste gate cross-sectional area depending on the engine load (100% represents a fully-open EWG valve).

Considering the calculated NO_x and CO_2 emissions, the following remarks can be noted. The specific NO_x emissions are lower for the case of the gas mode operation; the NO_x emissions for the diesel mode comply with 'Tier II' limits, whereas the IMO 'Tier III' limit requirements are satisfied for the gas mode. In addition, the lower specific NO_x emissions value is obtained at 100% load whilst higher values of the specific NO_x emissions are obtained at lower loads. In the gas operating mode, the NO_x emissions

slightly reduce at lower loads due to the premixed combustion of natural gas at greater values of air−fuel ratio.

The NO_x differences between the engine operating modes can be explained by considering the in-cylinder burnt zone temperature plots in conjunction with the cylinder pressure diagrams and maximum cylinder pressure. As it can be inferred from Figure 7.3, at the diesel mode, the combustion occurs at greater pressure levels and the maximum temperature values of the burnt zone are greater than the respective values obtained for the gas mode; therefore, higher NO_x emissions are produced. In average, a reduction of 85% in NO_x emissions is obtained when changing the operating mode from diesel to gas.

The CO_2 emissions of the gas mode are also reduced (by 25% in average) due to the lower carbon to hydrogen ratio of the natural gas compared to the respective one of diesel fuel. Larger reduction is obtained at the high loads region where the efficiency difference between the gas mode and diesel mode is greater. However, considering the methane slip in marine four-stroke DF engines (5.5 g CH_4/kWh for the Wärtsilä 50DF engines) (Pavlenko et al., 2020), and by applying an CO_2 equivalence factor of 25 for CH_4, as reported by (Trivyza et al., 2020), it is observed that the CO_2 emissions are slightly reduced for 100% and 75% load compared to the diesel operation, whereas they remain at the same levels for 50% load and marginally increase at 25% load. Nevertheless, the methane emissions could not have been predicted in the present DT, as the combustion model is of the 0D type.

As it can be observed from Figure 7.4, the turbocharger speed, pressure ratio and flow rate are considerably reduced in the gas mode when the engine operates at high loads. Smaller reductions can be observed at the lower loads (25% and 50%). This denotes that the T/C matching needs special attention for a DF engine compared to the respective process for diesel or gas engines, as in the former case, the requirements for the two discrete modes need to be satisfied. Especially for the compressor selection, a number of parameters (usually contradictory) have to be considered including targeting operation in the high efficiency area and providing adequate margins to avoid the compressor surging and the turbocharger overspeed.

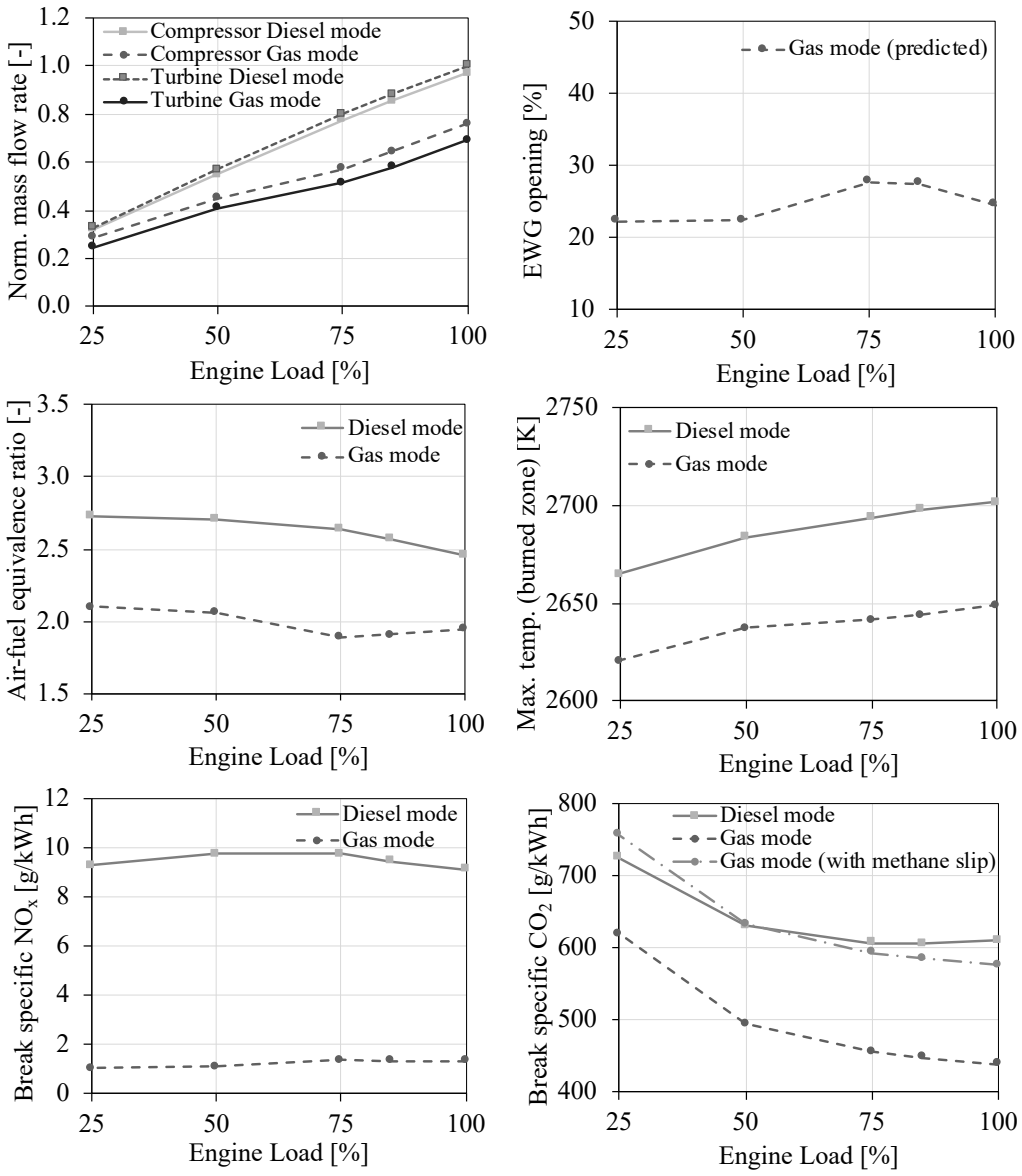

Figure 7.3 Predicted simulation results in steady state conditions

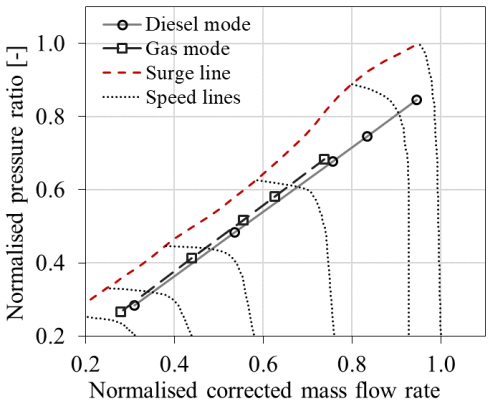

Figure 7.4 T/C compressor operating points superimposed on the compressor map

7.2.2 Transient operation (Case studies V-1 to V-3)

For the investigated case studies V-1 to V-3, the predicted variations of the engine parameters including the normalised rotational speed, the engine load and the normalised fuels amount (for the gas and diesel fuels), the engine boost pressure, the exhaust gas temperature before the T/C turbine, the T/C shaft speed, the EWG opening, the air−fuel equivalence ratio, as well as the T/C compressor operating point superimposed on the compressor map, are presented in Figure 7.5 to Figure 7.7, respectively. In these figures, the available experimentally measured parameters variations are also presented for serving the purpose of the developed model validation. All the parameters except for the exhaust gas EWG valve opening were normalised by using their corresponding values at 100% load for the diesel mode, whereas the EWG valve opening was normalised by using its maximum area. It can be inferred from the presented results that the model can predict the engine parameters response with an adequate accuracy.

7.2.2.1 Case study V-1 – 100% load and GTD mode switching

For the investigated case study V-1, the engine parameters variations are sufficiently predicted as illustrated in Figure 7.5. Both the simulation and experimental results show that the change of the engine operating mode from gas to diesel took place within 1 s, whereas the engine recovery time was less than 3 s after the ordered fuel change. The maximum engine speed and load drops from their initial values were approximately 3% and 4%, respectively. The gas fuel was cut off within 1 s in the consecutive firing cylinders with a simultaneous fast increase of the injected diesel fuel, which exhibited an overshoot (obtaining its maximum value at the 11^{th} s of the simulation run) and a subsequent gradual reduction till reaching its steady state value at the 14^{th} s of the simulation run. This is attributed to the PID diesel fuel governor sub-model that detected and appropriately responded to an increased error between the ordered and the actual speed (due to the engine speed drop). Based on the above, it can be concluded that the engine operation complies with the manufacturer specifications/requirements, according to which, the mode switching must occur within 1 s, the acceptable maximum

speed drop must be less than 10% and the acceptable maximum recovery time must be 5 s.

It can be observed that a considerable reduction of the exhaust gas temperature before T/C turbine occurred immediately after the gas fuel cut off between the 10.5th s and the 11th s of the simulation run. This is attributed to the fact that the gas fuel was immediately cut off, whilst the diesel fuel rack position response was not as fast (i.e. the diesel fuel cannot instantly reach its required value). This, in turn, resulted in the under-powering of a number of engine cylinders for a number of engine cycles after the gas full cut off at the 10.5th s associated with a temporary considerable increase of the air−fuel equivalence ratio between the 10.5th s and 11th s of the simulation run, as well as the temporary loss of the engine power, which reached its minimum value at the 11th s of the simulation run. The gradually increasing injection of the diesel fuel (following the gas fuel cutting off) resulted in the recovery of the engine power within 1 s after the time of its minimum value (the engine load almost reached its steady state value at the 12th s of the simulation run), however it caused a notable decrease of the air−fuel equivalence ratio to 1.5 at the 11.5th s. The latter is attributed to the fact that the EWG valve was open in the gas mode operation, and therefore, the air mass flow rate was less that the one required for the engine to operate in the diesel mode. The lower exhaust gas energy at the T/C turbine resulted in corresponding reductions of the T/C speed and the boost pressure, which in turn, moved the compressor operating point closer to the surge line of the compressor map. For this investigated case study, compressor surge did not occur as the surge margin was adequate; however careful consideration is required during the engine-T/C matching procedure to account for the fast-transient phenomena taking place during the GTD mode switching. It must be noted that the predicted temporary engine boost pressure drop is also observed in the experimental results (Olander, 2006) indicating that the simulation effectively captures this feature of the engine operation during the GTD mode switching.

The fast increase of the injected diesel fuel in conjunction with the air−fuel equivalence ratio drop resulted in a peak of the exhaust gas temperature (due to the diesel combustion with less air). Following the fuel change order, the engine control system reacted by closing the EWG valve, thus increasing the exhaust gas flow rate (hence the

energy rate) entering the T/C turbine, which in turn, increased the T/C shaft speed. The T/C shaft speed gradual increase resulted in a respective increase of the engine boost pressure (hence the engine air flow), which as a consequence gradually increased the engine air−fuel equivalence ratio and reduced the exhaust gas temperature before the T/C turbine. All the engine performance parameters reached their steady state values approximately 8 s after the fuel change order; therefore, the engine restored its operation at steady conditions in the diesel mode in the 18th s of the simulation run.

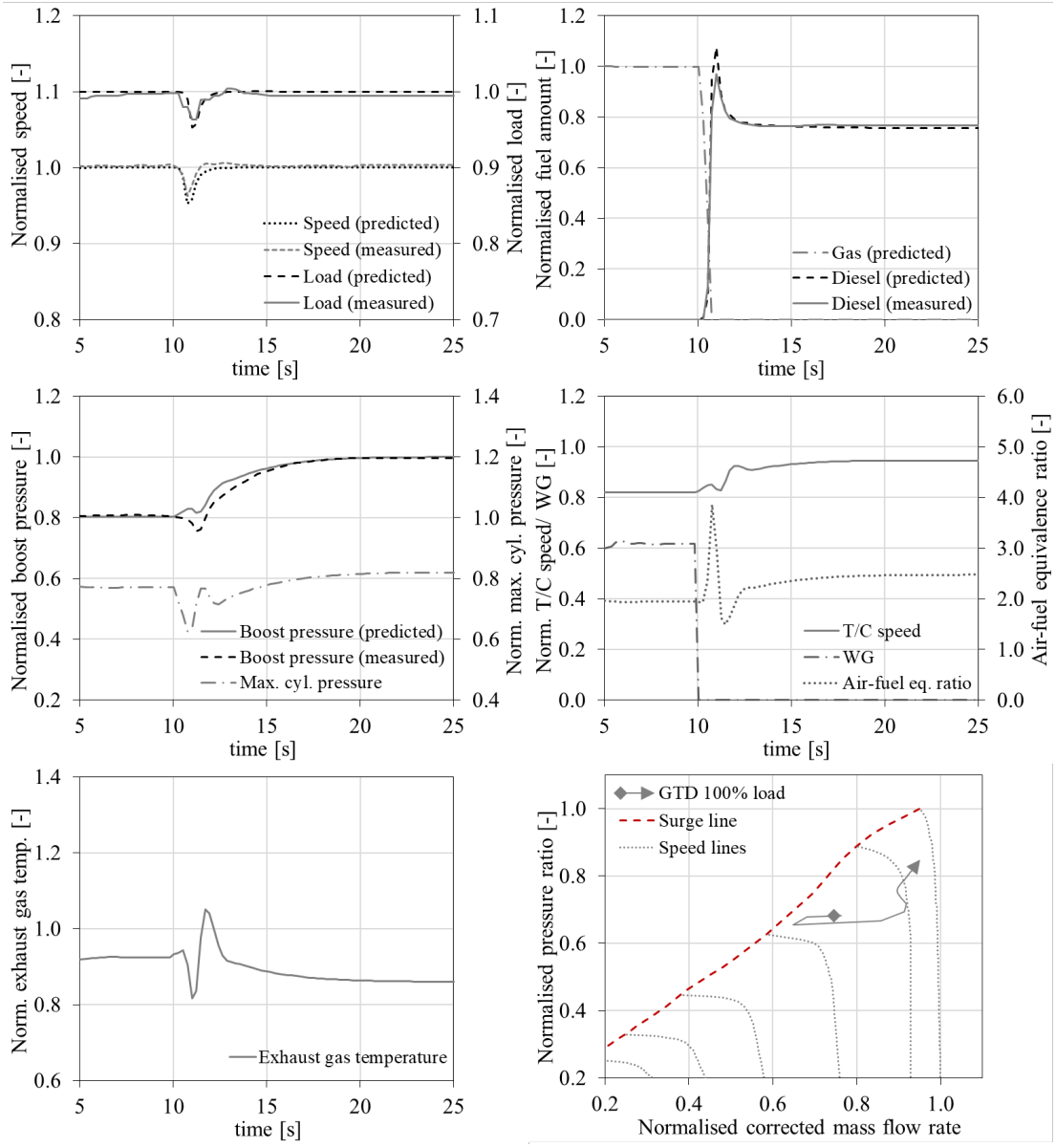

Figure 7.5 Case study V-1 — GTD mode switching at 100% load; predicted engine parameters and comparison with experimental data taken from (Olander, 2006)

Based on the above analysis, the following points must be noted: (a) a GTD mode switching takes place in a very short time (within 1 s) and therefore, it is quite challenging for the engine and its control system; (b) the EWG valve control along with the engine T/C matching are critical parameters for the successful completion of the GTD mode switching, as they affect the compressor normal operation and the T/C response time (compressor surging and incomplete combustion at the diesel fuel operation must be avoided) with implications to the engine air flow rate, the combustion conditions, and the engine thermal loading; (c) considering that gas fuel operation takes place only for the cylinders initially operating in either the closed cycle or gas injection phase, knocking or misfiring do not seem as an issue during the GTD mode switching.

7.2.2.2 Case study V-2 – 80% load and DTG mode switching

For the investigated case study V-2 where the engine operates at 80% load, it can be observed from the respective plots of Figure 7.6 that the engine speed and load are also predicted with sufficient accuracy. However, fluctuations are observed both in the engine speed and load from the experimental measurements, which are attributed to the more considerable cycle to cycle variations of the engine gas mode operation. A notable deviation in the prediction of the diesel fuel amount during this fuel change is observed; however, this can be justified based on the employed method for the gas fuel amount estimation in the modelled engine control system. In the actual engine control system, the gas (fuel) manifold pressure and the gas valve opening duration are controlled. Similarly, in the model the latter is controlled by the gas PID controller, whereas the gas (fuel) manifold pressure is adjusted by the GVU controller. In this respect, the fuel transition is gradually performed within 2 min where the gas, diesel and pilot fuels are controlled. Based on the above, it can be concluded that the engine operation complies with the manufacturer specifications, according to which, the mode switching must occur within 2 min, the acceptable maximum speed drop should be less than 10% and the acceptable maximum recovery time should be 10 s.

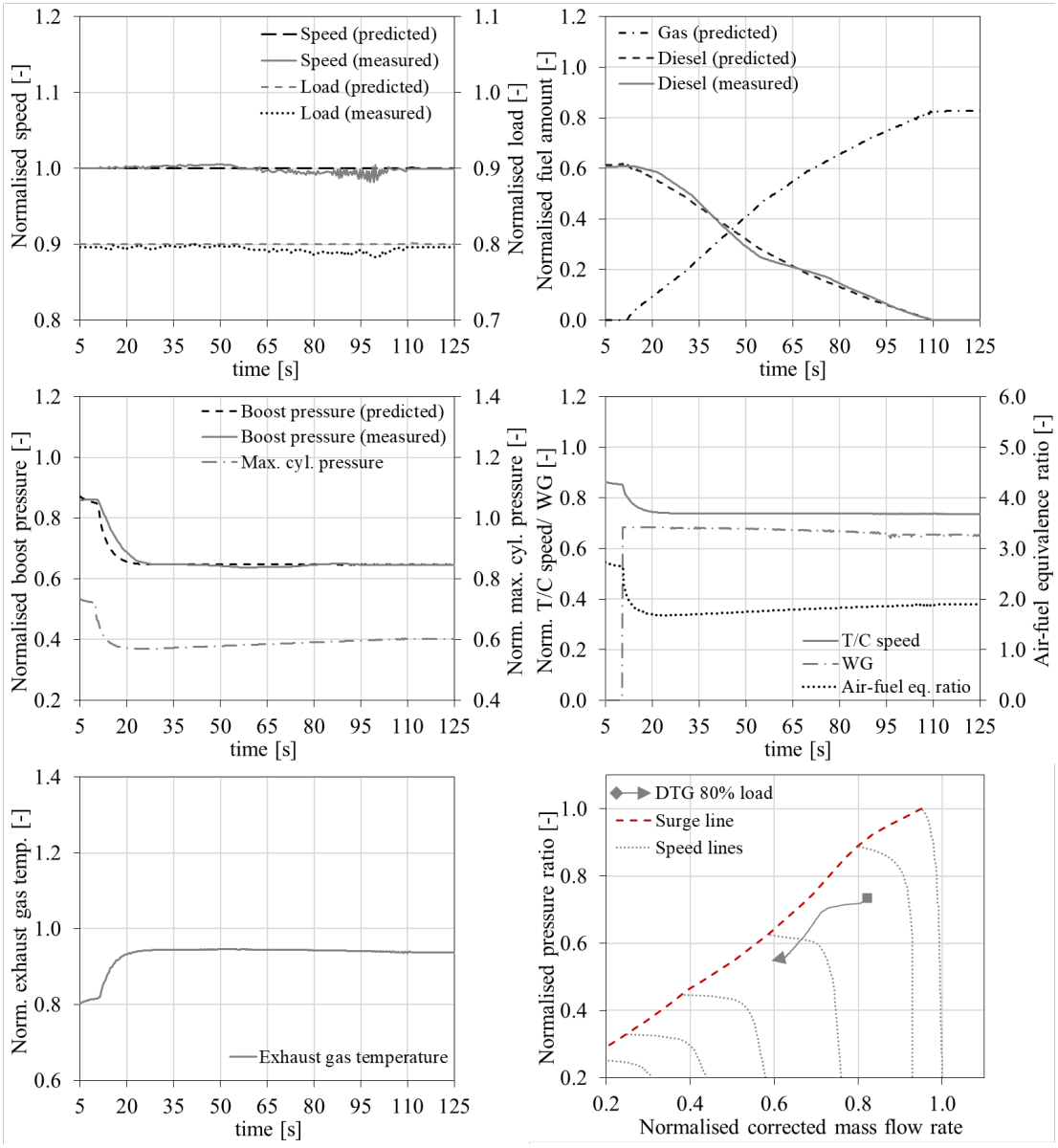

Figure 7.6 Case study V-2 — DTG mode switching at 80% load; predicted engine parameters and comparison with experimental data taken from (Olander, 2006)

In this case, the DTG mode switching is completed within 2 min and as a result, the transition from the diesel engine mode to the gas mode is much slower and smoother compared with the GTD mode switching. In the diesel mode, the engine operates with closed the EWG valve, which results in greater values of the boost pressure, the T/C shaft speed, as well as the air−fuel equivalence ratio and lower exhaust gas temperature before the T/C turbine in comparison with the respective values of these parameters at the gas operating mode. Following the fuel change order, the engine control system reacted by increasing the EWG valve opening to its maximum value (considering a

EWG valve opening limiter in order to avoid compressor surging) at the 11th s of the simulation run; subsequently, the EWG valve opening was gradually reduced reaching its steady state value at the end of the fuel change (at the 112th s of the simulation run). The EWG valve opening resulted in a decrease of the T/C shaft speed, and as a consequence, the boost pressure drop, as also can be observed in the experimental results reported in (Olander, 2006). In turn, this reduced the air flow into the engine cylinders, thus decreasing the air−fuel equivalence ratio whilst increasing the exhaust gas temperature before the T/C turbine. The challenges for the engine operation during the DTG mode switching include the knocking conditions avoidance due to the change of the air−fuel equivalence ratio as well as the compressor surging avoidance. Therefore, it can be inferred that the EWG valve control is quite critical for the smooth engine DTG mode switching.

7.2.2.3 Case study V-3 – Step load increase from 40% to 80%

For the investigated case study V-3, the engine parameters response is examined under a rather abnormal step-wise load increase from 40% to 80% load in the gas mode. As this ordered load change is not permitted in the gas mode according to the engine manufacturer (the maximum allowed step-wise load increase is 20% for the case where the engine operates at 40% load in the gas mode), the engine control system orders a fuel transition from gas to diesel. The measured parameters were taken from (Portin, 2010), where it is reported that they acquired from a plant with two generator sets initially operating at 40% load. One of these two units exhibited an emergency shutdown, so that all the electric load was transferred to the generator set in operation, thus resulting in its almost instantaneous load increase. These engines are of the same type as the investigated engine in this study, however the number of cylinders and their power are double the respective values of the investigated engine herein. Thus, a greater inertia and a relatively slower response is expected in the measured data, as also verified by the results presented in Figure 7.7. However, as (Portin, 2010) is the only available study in the open literature with published measured results of such a considerable load increase that induces a GTD mode switching, it was decided to be used for validating the developed model herein.

The comparison of the derived engines parameters response with the respective experimentally measured variations, demonstrates that the model can adequately predict the engine response during this transient operation. In specific, the results show that the fuel change from gas to diesel took place within 1 s, whereas the engine recovery time was found to be slightly higher than 5 s. The maximum engine speed drop was found to be 4% and 6% in the simulated and experimental cases, respectively. However, the engine speed response is sufficiently captured. Similarly, to the investigated case study V-1, the gas fuel was cut within 1 s with a simultaneous rapid increase of the injected diesel fuel that retains its maximum value for approximately 3 s due to the PID diesel fuel governor response following the detected increased error between the ordered and the actual speed. The diesel fuel amount started reducing from the 14^{th} s of the simulation run obtaining its steady state value corresponding to 80% load almost after 2 s. An additional characteristic of this case (in comparison with the investigated case study V-1) is the activation of the lambda limiter to confine the injected diesel fuel for values of air−fuel equivalence ratio lower than 1.1. This resulted in the slight drop of the injected diesel fuel amount between the 10.7^{th} and 11^{th} s of the simulation run. Based on the above discussion, it can be concluded that the engine response complies with the engine manufacturers specifications.

Similarities of the plotted engine parameters variations with the ones presented and discussed for the investigated case study V-1 are observed. The rapid reduction of the gas fuel along with the slower increase of the injected diesel fuel resulted in the temporary considerable increase of the air−fuel equivalence ratio (slightly above 3) as well as the considerable decrease of the exhaust gas temperature before the T/C turbine and the corresponding decreases of the T/C shaft speed and the boost pressure. Due to the almost instantaneous increase of the engine load and the respective increase of the injected diesel fuel amount, the air−fuel equivalence ratio reduced to very low values close to 1 at the 11^{th} s of the simulation run denoting that the engine operation temporarily reaches the limits for incomplete combustion and smoke appearance.

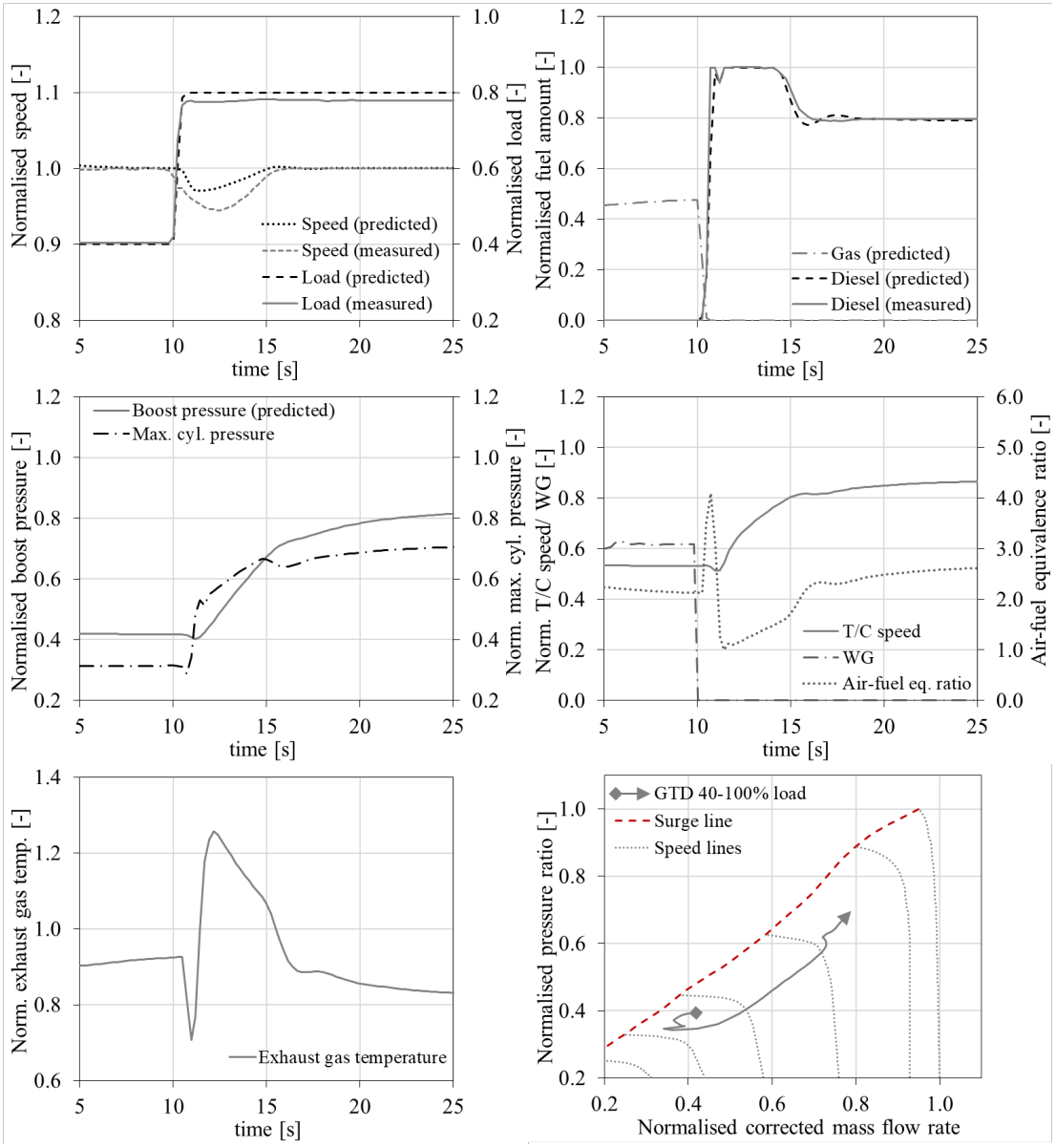

Figure 7.7 Case study V-3 — 40%-80% load change in the gas mode including a GTD mode switching; predicted engine parameters and comparison with experimental data taken from (Portin, 2010)

As explained above, the lambda limiter was engaged slightly reducing the injected diesel fuel amount. The air−fuel equivalence ratio increased after the 11th s of the simulation run as a result of the effect of the EWG valve closing and the increase of the exhaust gas temperature (due to the diesel fuel combustion), which resulted in the increase of the exhaust gas energy in the T/C turbine and the corresponding increases of the T/C shaft speed and the boost pressure (also leading to the reduction of the exhaust gas temperature after the 12th s of the simulation run). The engine speed was restored to its

original value at the 15th s of the simulation run, which, in turn, caused the decrease of the injected fuel to its steady state value and the corresponding changes of the engine parameters slopes variations. The engine operation obtained steady state conditions around the 25th s (7 s longer than what was required for the investigated case study V-1). Similarly to the investigated case study V-1, this run is also quite demanding for both the fuels control system (due to the fast mode switching) and the smooth compressor operation (compressor surging avoidance).

7.3 Engine design and operational limitations

In order to identify and map the engine operational limitations for the investigated case studies V-1 to V-3, a number of engine performance parameters were considered along with their limits (upper or lower) as proposed by the engine manufacturer (Wärtsilä, 2009). These parameters were the following: engine speed, air−fuel ratio equivalence ratio, exhaust gas temperature before the T/C turbine, maximum cylinders EWG valve opening/closing area change rate. The employed metrics to characterise the criticality of the engine operation include the percentage difference of each parameter from the respective limit and are provided in Table 7.1. From Table 7.1 results, it can be inferred that, in all the investigated case studies, the engine speed drops were within the allowed limits ranges, the cylinders maximum pressure was below its upper limit, whereas the T/C shaft speed was kept below its maximum allowed value. On the other hand, the exhaust gas temperature exceeded the respective upper alarm limit for a very limited time period for the investigated case studies with the GTD mode switching, however the engine shut down limit conditions (alarm limit and duration) were not exceeded. Specifically, for the GTD mode switching in 100% engine load (Case study V-1) the exhaust gas temperature (before the T/C turbine) exceeded the manufacturer limit for 3 s with its maximum value being 7% above the limit. For Case study V-3 (GTD mode switching and load increase from 40% to 80%), the exhaust gas temperature exceeded the limit for 4.5 s with its maximum value being above the limit value by 36%. For the GTD mode switching, the air-fuel equivalence ratio in the diesel mode exceeded the corresponding lower limit; for Case study V-1, the lambda exceeded the respective smoke limit for less than 1 s with its minimum value being 6% below this limit; for Case study V-3, the lambda exceeded the respective smoke (lower) limit for approximately 3 s

with its minimum value being 27% below this limit. It must be noted that the usage of an EWG valve controller with a slower response or stricter lambda limiter for the diesel fuel can be considered an option to mitigate this operational issue; however, greater speed and power drops are expected in these cases. For the DTG mode switching, the lower air–fuel equivalence ratio limit for the gas mode (knocking limit) was critically approached with the lambda value being 6% above this limit. The compressor surge line was also approached for all the investigated case studies as shown in Figure 7.5 to Figure 7.7 and the surge margin values presented in Table 7.1. The most critical cases for compressor surging were the case studies V-1 and V-2 as the engine operates at high loads. This is connected with the EWG valve area change rate, which controls how quickly the EWG valve opens or closes. In this respect, it can be inferred that, the EWG valve almost instant closing is needed for avoiding compressor surging issues and lambda values below the smoke limit for the GTD mode switching, whereas for the DTG mode switching, a slower EWG valve opening is required, so that compressor surging and lambda mismatch (leading to knocking or misfiring) are avoided. In cases where the EWG valve control fails to provide the specified opening/closing area rates, compressor surging is highly likely to occur.

Table 7.1 Engine operating parameters deviations compared to the respective manufacturer limits

	Case study V-1	**Case study V-2**	**Case study V-3**
Engine speed	Within limits minimum value 5.3% above the lower limit	Within limits minimum value 9.9% above the lower limit	Within limits minimum value 7% above the lower limit
Air−fuel equivalence ratio	For the diesel mode: below the lower limit for less than 1 s; minimum value 6% below the smoke (lower) limit	For the gas mode: minimum value 6% above the knocking (lower) limit	For the diesel mode: below the lower limit for 3 s; minimum value 27% below the smoke (lower) limit
Exhaust gas temperature before Turbine	Above the upper limit for 3 s; maximum value 5% above the upper limit; engine shut down limit was not exceeded	Within limits maximum value 5% below the upper limit	Above the upper limit for 4.5 s; maximum value 26% above the upper limit; engine shut down limit was not exceeded
Maximum cylinders pressure	Within limits Maximum value 18% below the upper limit	Within limits Maximum value 27% below the upper limit	Within limits Maximum value 29% below the upper limit
T/C speed	Within limits Maximum value 5% below the upper limit	Within limits Maximum value 14% below the upper limit	Within limits Maximum value 13% below the upper limit
T/C compressor surge margin	Minimum value: 5.8% Surge did not occur	Minimum value: 10.5% Surge did not occur	Minimum value: 15.2% Surge did not occur

The identification of these limitations metrics is quite useful to investigate solutions for mitigating the potential engine safety and operational implications by considering both design measures and engine settings optimisation. Examples of such solutions, which have been adapted by the engine manufacturer in recent engine versions for reducing the likelihood for compressor surging, include the modification of the engine manifolds design to introduce an air bypass loop and a bypass valve for controlling the air flow from the compressor outlet to the turbine inlet (Wärtsilä, 2019a), as well as the replacement of the EWG valve electric actuators by fast acting hydraulic actuators (Kalax, 2018).

7.4 Performance and emissions

7.4.1 Engine settings optimisation for the gas mode (Case studies P-1 to P-3)

The simulation results for the engine settings optimisation for the gas mode considering the NO_x and CO_2 emissions, the air–fuel equivalence ratio, the inlet valve closing and the boost pressure for the case P-2 are presented in Figure 7.8 and Figure 7.9, whereas the respective results for the case studies P-1 and P-3 are shown in Figure 7.10. The summary of all these case studies results is included in Table 7.2.

As it can be inferred from Figure 7.8 and Figure 7.9, the simultaneous reduction of CO_2 and NO_x emissions can be obtained by operating the engine in higher values of air−fuel equivalence ratio. However, the considered permissible lambda window from 1.9 to 2.3 (to avoid knocking and misfiring, respectively) resulted in the exclusion of a number of the performed parametric runs points. The used start of injection (at the reference point) provides a compromise between the CO_2 and the NO_x emissions. Retarding the injection results in increased CO_2 emissions and reduced NO_x emissions and vice versa. Therefore, the reference value for the start of injection was only considered for the parametric runs for 50% and 100% loads presented below (case studies P-1 and P-3).

As indicated in the bottom plots of Figure 7.9, the engine operation with increased air−fuel equivalence ratio values can be achieved either by increasing the boost pressure (by closing the exhaust waste gate valve that results in higher exhaust gas mass flow through the turbine and therefore, increasing the turbocharger speed) or retarding the inlet valve closing that results in more air trapped in the engine cylinder. A greater reduction potential, for both CO_2 and NO_x emissions, is obtained by increasing the boost pressure as shown in the right-middle plot of Figure 7.9. The trade-off between the CO_2 and the NO_x emissions as well as with the derived air−fuel equivalence ratio values are presented in Figure 7.8. By excluding the points outside the considered lambda window as well as the points with CO_2 and NO_x emissions higher than the respective reference values, a limited number of points can be identified for a potential engine optimisation.

In Table 7.2, the optimised points are provided for the following cases: (a) maximum simultaneous reduction of the CO_2 and NO_x emissions; (b) maximum CO_2 emissions reduction and (c) NO_x emissions equal or less than the respective reference point value. For the former, point No.2 is the optimised point with 5% greater boost pressure, 5°CA inlet valve closing retard and no change in the pilot injection start, which results in reductions by 0.9% and 6.5% in the CO_2 and NO_x emissions, respectively and an air−fuel equivalence ratio value equal to 2.21. Point No.3 having an additional pilot injection start advance of 2°CA (compared to point No 2) results in slightly greater air−fuel equivalence ratio (2.22) and reductions by 1.6% and 2.8% of the CO_2 and NO_x emissions, respectively. If lower lambda values are needed, point No.1 can be considered with increased boost pressure by 5% compared to the reference point, resulting in lambda equal to 2.09 and reductions by 0.6% and 3.8% in the CO_2 and NO_x emissions, respectively.

From the results presented in Figure 7.9 and Table 7.2 (the slopes of the respective curves), the relative significance of the three parameters used in the parametric runs can be identified. The inlet manifold boost pressure can be characterised as the main engine parameter for reducing both NO_x and CO_2, whilst, inlet valve closing can be considered of lower significance. The pilot fuel injection timing is also a parameter that considerably affects the emissions as shown in Figure 7.9, however, it exhibits a contradictory influence on the CO_2 and NO_x emissions, as when the one increases, the other decreases and vice versa.

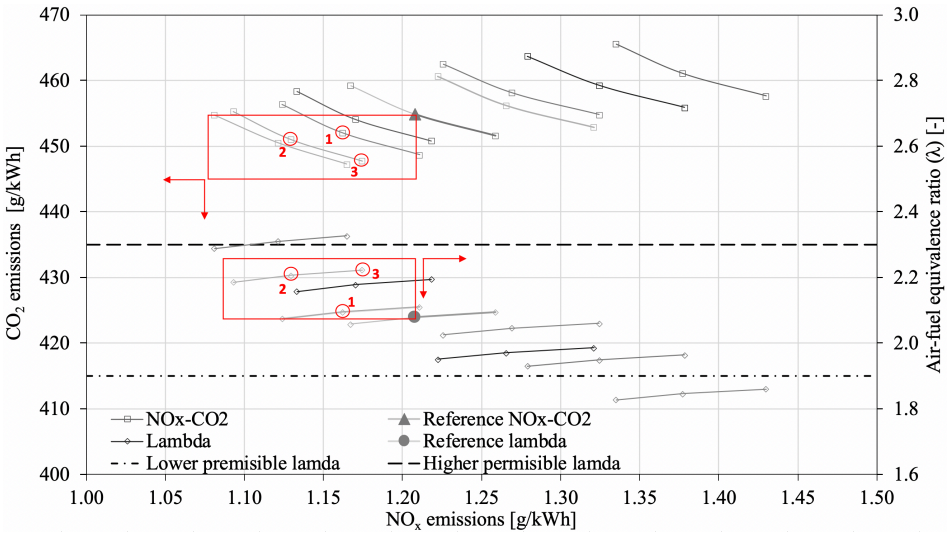

Figure 7.8 Parametric study results for the gas mode at 75% load (case study P-2)

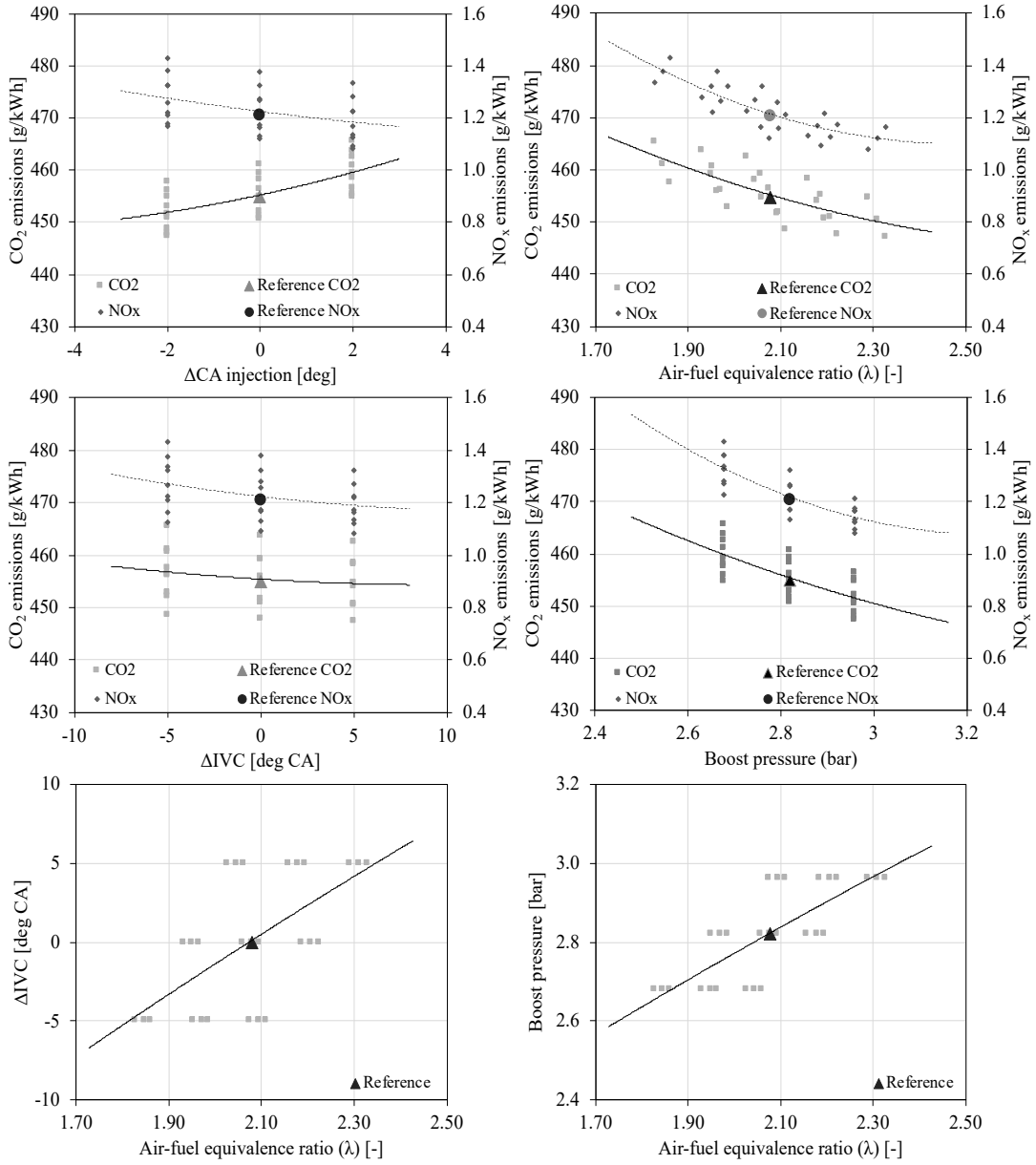

Figure 7.9 Parametric study results for engine gas mode operation at 75% load (case study P-2) showing potential for CO_2 and NO_x emissions reduction

Furthermore, additional parametric runs were performed for 50% and 100% loads (case studies P-1 and P-3) considering the reference point pilot start of injection and varying the boost pressure and the inlet valve closing. The derived CO_2−NO_x emissions trade-off and the air−fuel equivalence ratio values are presented in Figure 7.10. The permissible air−fuel equivalence ratio window for the case of 50% load was considered to be wider (1.5-2.3) in comparison with that at 100% load (2.0-2.3). The green marks represent points with the same settings as the points No.1 and No.2 at 75% load.

As it can be inferred from the analysis of the results in Figure 7.10, there is potential for simultaneously reducing the CO_2 and NO_x emissions. A greater reduction can be obtained in the NO_x emissions (4.4 and 7.2% at 50% load, 3.8 and 5.7% at 100% load), whereas the CO_2 emissions reduction is in the range of 0.7 to 0.8%. However, the resulting lambda values are considerably high (2.31 and 2.41) at 50% load, whereas the respective values are 2.17 and 2.28 at 100% load. Therefore, a boost pressure increase, less than 5%, might be used for the other load points to avoid misfiring, thus resulting in lower emissions reduction.

Another important parameter that needs to be considered in the engine optimisation study is the unburnt hydrocarbon emissions and in specific, the methane slip for the DF engines (Järvi, 2010). This was not considered in this study as the 0D models cannot provide accurate results for the HC emissions, which apart from the thermodynamic and thermochemistry parameters are greatly influenced by the combustion chamber design. However, the parametric investigation study presented herein is quite useful in the preliminary stage of the engine design process as it provides insight information for the engine performance and emission parameters trade-offs.

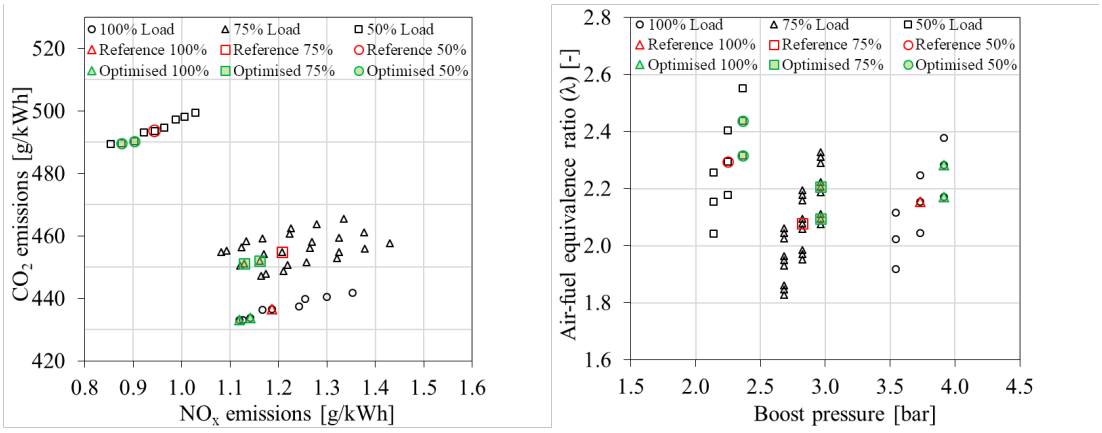

Figure 7.10 Parametric study results in the gas mode at 50% (case study P-1) and 100% (case study P-3) load along with the respective results for 75% load (case study P-2)

A summary of the investigated variables optimal values for the parametric runs of the case studies P-1 to P-3, is presented in Table 7.2.

Table 7.2 Optimised points from parametric runs in gas mode operation (case studies P-1 to P-3)

Load	[%]	**50**		**75**			**100**	
Case ID		**P-1**		**P-2**			**P-3**	
Point No.	[-]	-	-	1	2	3	-	-
Optimisation objective	[-]	Minimise NO_x and CO_2	Minimise NO_x and CO_2	Minimise NO_x and CO_2	Minimise NO_x	Minimise CO_2	Minimise NO_x and CO_2	Minimise NO_x and CO_2
ΔIVC	[ºCA]	0	5	0	5	5	0	5
ΔBoost pressure	[%]	5	5	5	5	5	5	5
ΔPilot Injection timing	[ºCA]	0	0	0	0	-2	0	0
Lambda	[-]	2.31	2.44	2.09	2.21	2.22	2.17	2.28
NO_x	[g/kWh]	0.90	0.88	1.16	1.13	1.17	1.14	1.12
CO_2		490.3	489.5	452.0	451.0	447.8	433.6	433
ΔNO_x	[%]	-4.4	-7.2	-3.8	-6.5	-2.8	-3.8	-5.7
ΔCO_2	[%]	-0.7	-0.8	-0.6	-0.9	-1.6	-0.7	-0.8

7.4.2 EGR and ABP systems settings optimisation for diesel mode (Case studies EM-1 to EM-4, ED-1 to ED-4 and ET-1 to ET-3)

The optimal EGR and ABP systems settings derived from the two discrete optimisation phases (case studies EM-1 to EM-4 and ED-1 to ED-4) are presented in Table 7.3. The derived results (normalised BSFC against normalises NO_x emissions) from the MOGA optimisation results and the DoE parametric investigation results for the 100% engine load are presented in Figure 7.11. In the same figure, the points of the Pareto front are shown with the square symbol, whereas failed designs correspond to the cases where the simulation did not achieve steady state conditions. The MOGA optimisation results, in specific the derived Pareto front points, were employed to select the EGR and ABP systems settings ranges, so that the engine operation marginally complies with the 'Tier III' limits whilst achieving the minimum possible BSFC value. For the DoE parametric investigation, it is noted that negligible variation of BSFC was achieved for SOI values greater than 15ºCA bTDC, therefore this value is chosen as the optimal SOI value for the 50%, 75%, and 100% loads. At 25% load, the reference value (12ºCA bTDC) is selected due to insignificant variation of BSFC in the range between 20ºCA and 12ºCA bTDC. Nevertheless, it must be mentioned that the model limitations described in Section 8.4 should also be considered.

As it is presented in Table 7.3, the EGR blower speed resulted in the optimal EGR/ABP systems performance for the range of 25% to 100% engine load is 9000 r/min. The EGR blower power requirements range from 0.7% to 2.3% of the engine brake power in the investigated engine loads. Furthermore, the EGR system valve opening increases as the engine load increases from 25% to 100%, in order to achieve the required EGR rate as the charge air mass flow rate increases. On the other hand, the ABP valve opening demonstrates a low value (almost 0.2 where 1 represents the fully opening) at 25% load, which is attributed to the low charge air mass flow rate, whilst is accounted for adjusting the T/C compressor operating point to avoid the T/C surging effect. However, for engine loads of 50% and higher, it is observed that the ABP valve opening remains at the same levels (due to increased charge air mass flow rate), providing the required charge air mass flow at the inlet manifold to achieve the targeted EGR rate. In this respect, it is inferred that the ABP has a direct impact on the charge air mass flow rate, and thus the EGR rate as well as the mitigation of the potential safety implications related to the T/C surging effect.

From the steady state simulations results presented in Table 7.3 and Figure 7.12, it can be inferred that the engine, in the diesel mode operation with EGR and ABP systems activation, is capable of complying with the IMO 'Tier III' requirements, achieving a 73% reduction in NO_x emissions for EGR rates ranging from 31% to 35%. However, the NO_x emissions reduction is associated with an increase in the BSFC ranging from 8.4% to 9.9% considering the respective EGR blower electrical power requirements (the respective BSFC numbers without considering the EGR blower power requirements were found to be 6.1% to 8.7%). This is found to be in accordance with the reported findings in the available literature (Fabio et al., 2015, Kaario et al., 2016). As shown in Figure 7.12 top right graph, the implementation of an advanced SOI offers BSFC reduction from 0.3% up to 1.8%, as the load increases, with the highest BSFC reduction noted at 100% load. Moreover, a moderate increase in the CO_2 emissions is observed, ranging from 5.5% to 7.8%, which is attributed to the higher BSFC. With regard to the exhaust gas temperature, in all case studies the manufacturer alarm limit was not exceeded. For the 50%, 75% and 100% loads the exhaust gas temperature demonstrates a reduction ranging from 0.6% to 2.9%, whereas for the 25% load an increase of 9% is noted. This occurs due to the increased EGR rate at the respective engine load in

combination with the reduced charge air mass flow rate, as shown in Figure 7.12 (bottom right graph). The maximum cylinder pressure and the boost pressure demonstrated similar descending trends, with reductions ranging from 11% to 18.7% and 6.9% to 35% respectively. The reductions observed in these engine operating parameters are attributed to the lower exhaust gas thermal power to the T/C turbine due to the EGR operation, which results in lower T/C speed, lower boost pressure and eventually reduced charged air mass flow rate.

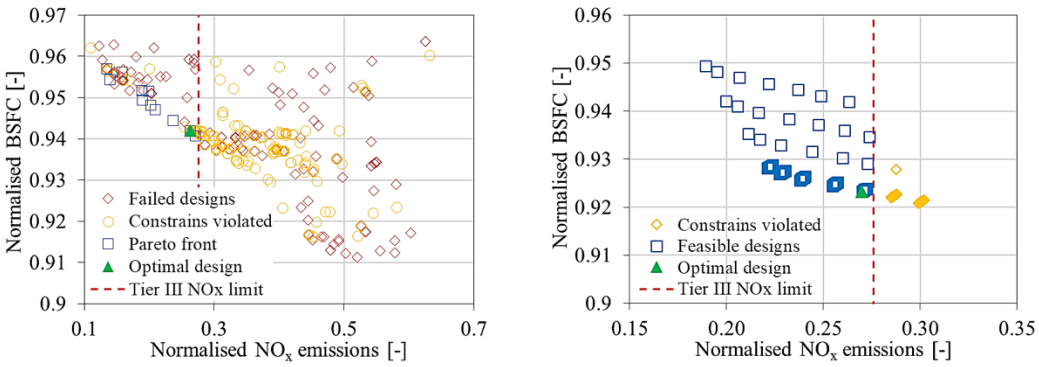

Figure 7.11 MOGA (left) (Case study EM-4) and DoE (right) (case study ED-4) optimisation of the engine parameters in gas mode operation at 100% load

Table 7.3 EGR and ABP systems optimisation results summary (case studies EM-1 to EM-4 and ED-1 to ED-4)

		Load	[%]	25	50	75	100
		Case study ID		**EM-1**	**EM-2**	**EM-3**	**EM-4**
MOGA optimisation	Settings (variables)	EGR Blower speed	[r/min]	9000	9000	9000	9000
		EGR valve opening	[deg]	21	33	85	90
		ABP valve opening	[deg]	6	50	51	49
	Output parameters	NO_x emissions	[g/kWh]	2.62	2.57	2.49	2.46
		BSFC	[g/kWh]	249.1	221.3	212.1	214.9
		EGR blower power/ P_E	[%]	0.76	1.17	1.82	2.32
		Case study ID		**ED-1**	**ED-2**	**ED-3**	**ED-4**
DoE optimisation	Settings (variables)	Start of injection (SOI)	[°CA bTDC]	-12	-15	-15	-15
		EGR valve opening	[deg]	21	33	85	90
		ABP valve opening	[deg]	6	50	51	51
	Output parameters	BSFC	[g/kWh]	249.1	220.7	209.6	210.6
		NO_x	[g/kWh]	2.62	2.41	2.59	2.52
		EGR blower power/ P_E	[%]	0.76	1.14	1.78	2.32
ΔBSFC ($BSFC_{without\ EGR}$ - $BSFC_{with\ EGR}$)			[%]	8.4	10.2	9.9	10.2
ΔBSFC ($BSFC_{without\ EGR}$ - $BSFC_{with\ EGR\ and\ SOI}$)			[%]	8.4	9.9	8.8	8.4

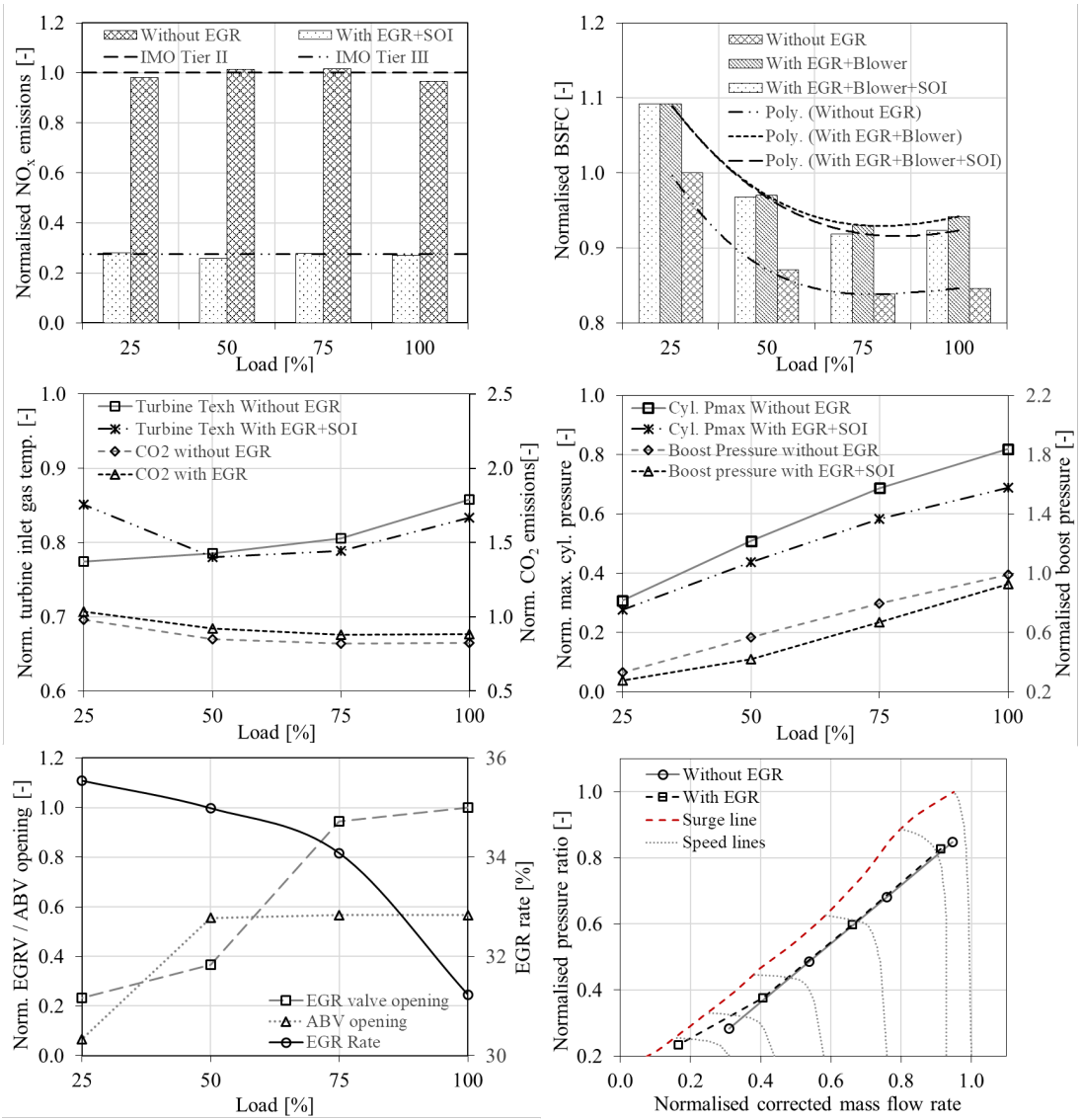

Figure 7.12 Predicted engine parameters with EGR and ABP systems operation under steady state conditions (Case studies EM-1 to EM-4 and ED-1 to ED-4)

In addition to the preceding optimisation case studies, engine transient simulations (ET-1 to ET-3) under the EGR and ABP systems operation in the diesel mode were performed for 50%, 75% and 100% engine loads, as described in Section 6.3.2. Indicatively, the simulation run results at 50% load are presented in Figure 7.13. However, similar engine response is observed in the investigated case studies ET-2 and ET-3, as presented in Figure 7.14 and Figure 7.15 respectively.

For the investigated case studies ET-1 to ET-3, it is assumed that the engine initially operates in the diesel mode with the EGR and ABP systems deactivated, and the EGR

and ABP systems are manually activated at the 10th s, so that the engine complies with the 'Tier III' requirements, whereas the EGR and ABP systems are manually deactivated at the 40th s. It must be noted that the ABP system valve is driven from its control to a predetermined position/opening identified during the EGR/ABP optimisation process (Table 7.3) and the EGR system valve is controlled by the EGR controller, with the aim to achieve the target EGR rate resulted from the optimisation process. The engine operating parameters time variations for the BFSC, the boost pressure, the maximum cylinder pressure, exhaust gas temperature as well as the NO_x and CO_2 emissions between the EGR/ABP activation and deactivation are found to align with the findings observed for the steady state operation (Table 7.3 and Figure 7.12). In all the case studies (ET-1 to ET-3) the engine alarm limits are not exceeded.

For the investigated case study ET-1 at 50% load, the engine recovery time for the engine to reach steady state conditions after the EGR/ABP activation is estimated to 20 s, whereas in the case of the EGR/ABP deactivation this period is predicted to 15 s. However, the respective required time for the remaining case studies ET-2 and ET-3, are reduced to 15 s and 10 s / 10 s and 5 s, respectively. Justification on the noted differences on the recovery time and its effects amongst the examined case studies is provided herein. In specific, as shown in the top right graph of Figure 7.13, the EGR and ABP valves open in approximately 1 s from the activation order, in order to prevent the T/C compressor surging (bottom right graph of Figure 7.13). The EGR controller responds gradually reducing the EGR valve opening till it reaches its steady state value after 20 s to 25 s from the EGR/ABP systems activation. This is a fairly slow response comparing to the other investigated case studies (ET-2 and ET-3). However, this can be justified considering that the T/C compressor operating points on the EGR/ABP OFF/ON operation are more distant than in the other investigated case studies (ET-2 and ET-3), therefore the T/C requires more time to shift from the 'EGR/ABP OFF' operating point to the 'EGR/ABP ON' operating point, hence resulting is slower T/C speed convergence to the respective steady state conditions, which is obtained at the 35th s. This, in turn, has an impact to the boost pressure reduction slope/rate which gradually decreases reaching a 35% reduction from its initial value at 35th s. Nevertheless, the boost pressure reduction is attributed to the EGR system operation and its effects on the exhaust gas amount entering the T/C turbine, and thus the T/C

speed. Similar projection is noted in the maximum cylinder pressure which also demonstrates a progressive reduction of 16% at the 35th s. However, it must be noted that the maximum cylinder pressure decrease is also interconnected with the lower oxygen content of the working medium trapped in the engine cylinders. The BSFC exhibits an increase owing to the EGR system operation, reaching a maximum at the 35th s (8.8% increase from its initial BSFC value without considering the EGR blower power requirements). This BSFC penalty is attributed to the delayed combustion start as well as the slower combustion during the EGR system operation, which are directly interconnected to the O_2 content in the working medium. With regard to the air–fuel equivalence ratio, a considerable reduction from 3 to almost 1.1 is observed due to the diesel fuel amount increase and the charge air amount decrease. This is acceptable lambda range according to Llamas and Eriksson (2014), however it may potentially lead to incomplete combustion and the associated high soot and smoke emissions levels. In terms of the derived emissions in the engine operation with the EGR system activated (EGR/ABP ON), the CO_2 emissions increase by 7.8% due to the BSFC increase, whilst the NO_x emissions are reduced by 75%, rendering the engine to achieve the 'Tier III' compliance. The minor fluctuations noted following the EGR and ABP systems activation/deactivation in the BSFC, boost pressure, emissions and exhaust gas pressure are attributed to engine and systems dynamics in this fast transient operation.

Notwithstanding the above, it can be summarised that the engine transient operation with the EGR/ABP systems activation/deactivation is relatively smooth, yet demanding operation, due to the required fast EGR and ABV valves response in order to avoid the T/C compressor surging effect. The EGR and ABP systems operation in the diesel mode is capable of achieving the IMO 'Tier III' requirements, however, its operation is associated with a considerable BSFC penalty, as also reported in the pertinent literature. The identified design/operational limitations of this engine operation with the EGR system activated are associated with the T/C unit matching (a new T/C unit is required if an EGR system without the ABV valve is installed), and the EGR cooler. In specific, the application of the ABP system has proven to be a feasible solution to overcome the T/C compressor surging effect and thus negating the need for a new T/C unit installation in an existing engine. The EGR cooler effectively decreased the temperature of the exhaust gas, therefore, maintaining the working medium temperature at the inlet

manifold within the manufacturer alarm limits. Therefore, it can be inferred that the proposed system is capable of mitigating potential safety implications by considering the existing system's design/operational limitations.

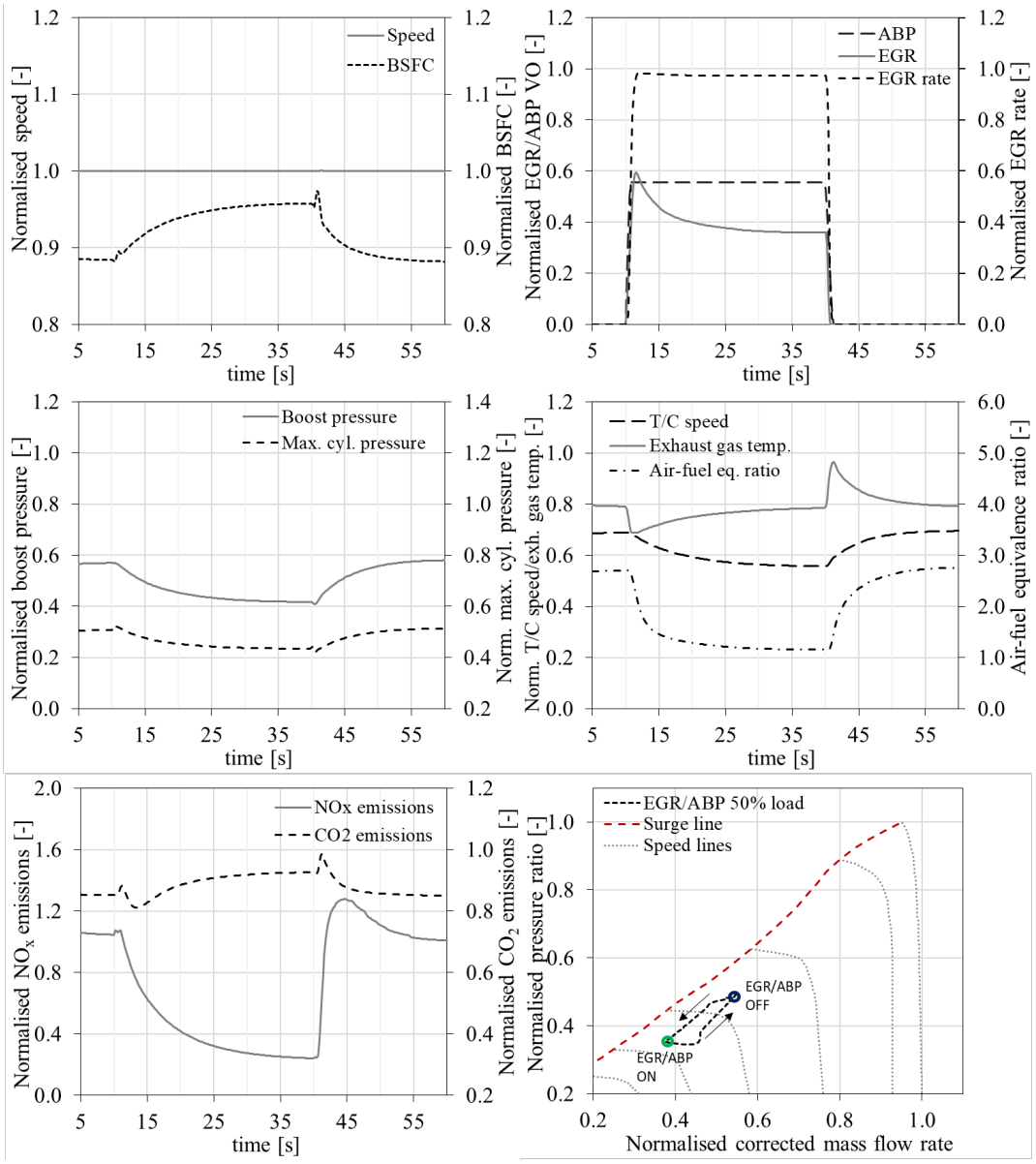

Figure 7.13 Predicted engine parameters with EGR and ABP systems operation under transient conditions (case study ET-1)

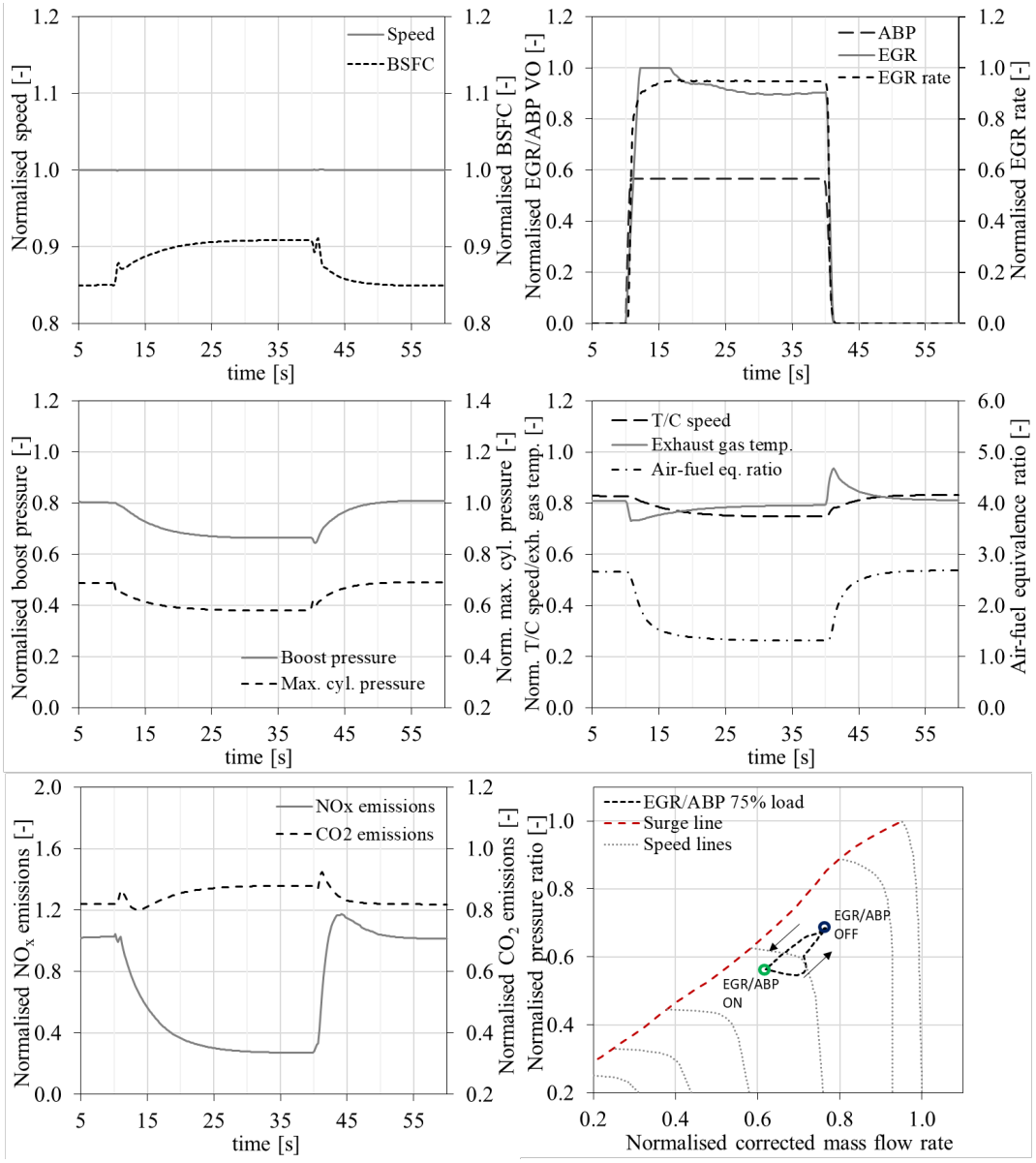

Figure 7.14 Predicted engine parameters with EGR and ABP systems operation under transient conditions (case study ET-2)

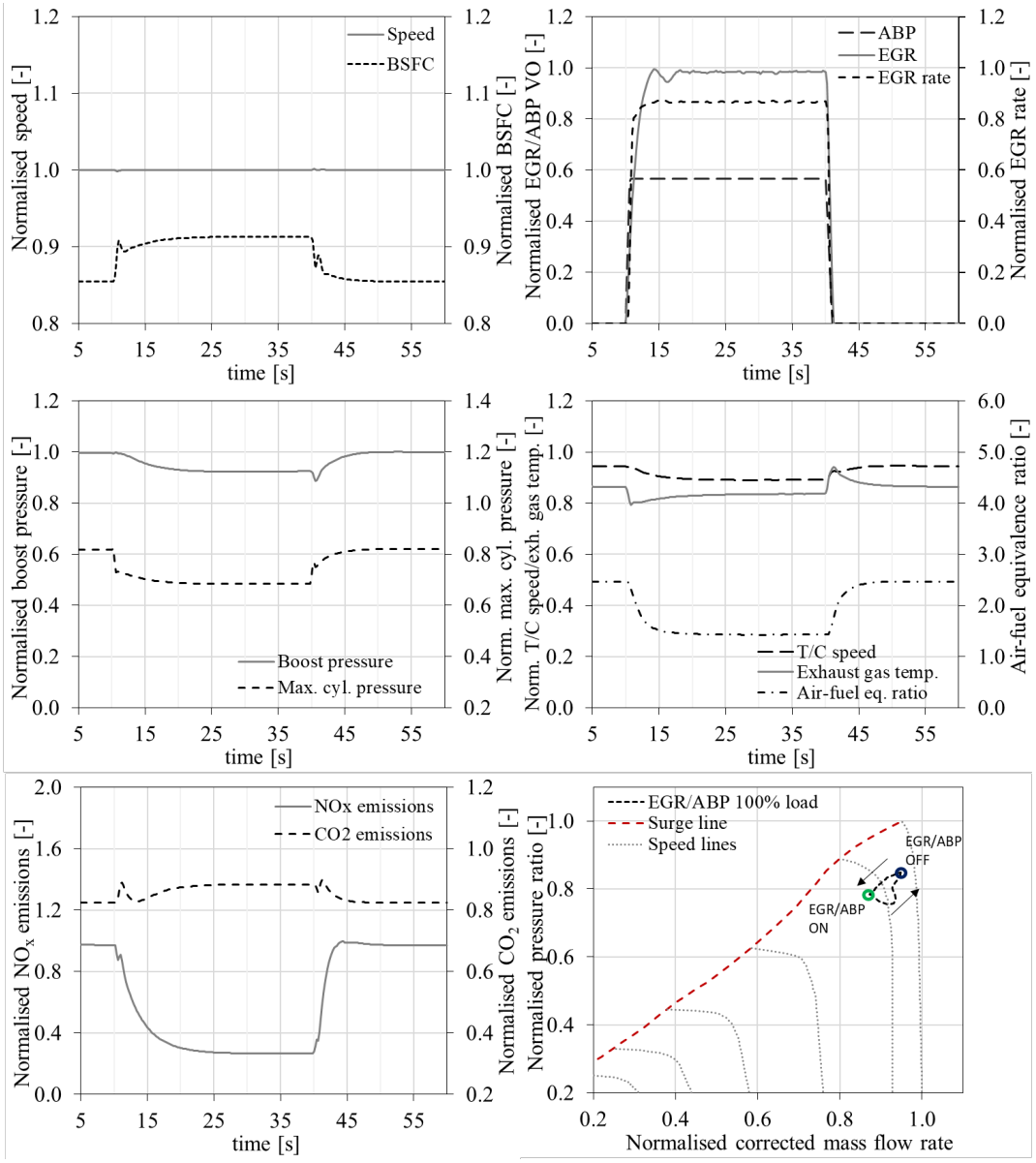

Figure 7.15 Predicted engine parameters with EGR and ABP systems operation under transient conditions (case study ET-3)

7.5 Safety implications (Case studies S-1 to S-8)

The generated results of the simulation cases studies S-1 to S-8 that resulted from FMEA, as described in Chapter 6.4.3, are presented in Table 7.4. As shown in Table 7.4, the engine control system response as well as the faults effects on the engine response are identified, whereas the potential safety implications, which were derived by taking

into account the engine manufacturer design and alarm limits, are reported for all the case studies.

Summarising the findings of Table 7.4, the gas (fuel) manifold pressure sensor related faults in gas mode operation (case study S-1) may be associated with potential misfiring issues due to lambda values exceeding 2.4 as well as exhaust gas temperature surpassing the alarm limits (2.3%) for approximately 1 s. It should be noted that the gas fuel controller (gas fuel PID controller) is able to identify gas (fuel) manifold pressure discrepancies noted in the gas (fuel) manifold (via the speed sensor feedback) and counterbalance this safety implication by reducing the gas injection duration at the GAV. For the case study S-2, speed sensor faulty operation in diesel mode seems to have a major effect on the T/C speed, in the case of engine over-fuelling, with the T/C speed and the exhaust gas temperature exceeding the alarm limits by 4.3% and 0.5% respectively, for a duration of 1 s to 3 s. Special consideration should be given on the fact that the speed sensor has a direct and critical impact on diesel fuel controller (diesel PID controller), and thus to the diesel governor and the delivered diesel fuel amount into the engine cylinders. In case study S-3, a boost sensor fault is investigated under DTG mode switching, exhibiting increased boost pressure and T/C speed due to its impact on the EWG valve controls. The lambda values recorded are relatively higher than expected after the mode switching (in gas mode), which may lead to potential misfiring issues. Therefore, it can be inferred that boost sensor related faults are critical for the engine operation due to the considerable impact on the EWG controller (especially in gas mode), and consequently the effects to the engine response. Furthermore, the engine response captured in the case studies S-4 and S-5 is found within the set alarm limits, where the gas controller countermeasures for the introduced faults in each case (GVU valve and GAV respectively); gas trip may occur in the former. On the contrary, diesel rack and EWG valve faults introduced in the case studies S-6 and S-8 respectively under GTD mode switching, demonstrate that the engine response can be greatly affected. Specifically, for the case study S-6, for a period of 1 s to 2 s the speed reaches the lower limit, the exhaust gas temperature exceeds the alarm limits by 13% and T/C compressor surging effect occurs. In addition, considerable oscillations are observed in maximum cylinder pressure, exhaust gas temperature and lambda, which may be associated with mechanical and thermal stresses as well as knocking/misfiring

issues respectively. Case study S-7 exhibits similar engine response with the exhaust gas temperature exceeding the alarm limits by 7.4%. Hence, it can be concluded from case studies S-6 and S-7 that the diesel rack and the EWG valve along with their controllers are of crucial importance for the engine smooth operation. Potential faults in these components or their control and feedback sensor can have severe impact on the engine response with considerable safety implications. Lastly, with regards to the case studies S-7a and S-7b, the key findings are discussed separately in detail below.

Table 7.4 Case studies simulation results from FMEA

Case ID (FMEA ID)	Component	Operation mode/ actual value	Sensors measur.[1]/ actuator status	Control system response	Engine effects	Safety implications and margin from alarm limit
S-1 (11)	Gas (fuel) manifold pressure	Gas mode/ 4.77 bar (static)	3.34/3.74 bar (static) (imposed/predicted)	The reduced gas (fuel) manifold pressure sensor measurement is fed in the ECS (GVU PID controller) and as a result a gradual increase in the GVU valve opening is ordered (8° to 90°) – The actual gas (fuel) manifold pressure is maximised (5.92 bar), however, the gas pressure sensor feeds the GVU PID controller with the faulty measurement (4.14 bar), therefore the controller orders the GVU valve to fully open to achieve the target value (4.77 bar). The gas PID controller orders a reduction in gas injection timing.	The ordered GVU valve opening increase is associated with higher gas (fuel) manifold pressure; (3.77/5.92 bar). This in turn results to a reduction in the GAV opening timing (21.5 ms to 16.6 ms) from the gas PID controller. The GAV injection duration reduction counterbalances the faulty gas pressure sensor measurement; no changes in the engine operating parameters – minor fluctuations during transient.	**For <1 s** – Max. engine speed (4.8% below max. limit) – Max. cyl. pressure (15.2% below max. limit) – Max. lambda 2.4 (from 1.94) – potential misfiring issues – Max. exhaust gas temperature (2.3% above max. limit)

Case ID (FMEA ID)	Component	Operation mode/ actual value	Sensors measur.[1]/ actuator status	Control system response	Engine effects	Safety implications and margin from alarm limit
S-2 (43)	Speed sensor	Diesel mode/ 514 r/min	488/494 r/min (imposed/predicted)	The reduced engine speed sensor measurement is fed in the ECS (diesel PID controller) and as a result an increase in the injected diesel fuel is ordered (rack shift from 0.72 to 1 for 1 s and then to 0.74).	The ordered diesel fuel increase is associated with higher engine speed (514/541 r/min); power (8775/9236 kW); BSFC (193.2/197.9 g/kWh); NO_x and CO_2 emissions (9.1/9.5 g/kWh and 609/624 g/kWh); exhaust gas temperature (795/823 K); T/C speed (19026/19500 r/min); as well as reduced max. cyl. pressure (139/134.8 bar); and air−fuel equivalence ratio (2.45/2.34).	– Max. engine speed (3.6% below max. limit) **For <1 s** – Max. cyl. pressure (8.6% below max. limit) – Max. exhaust gas temperature (0.5 above max. limit) **For approx. 3 s** – Max. T/C speed (reaches max. speed and EWG opens)
S-3 (82)	Boost pressure sensor	DTG/ 4.0/3.02 bar (diesel/gas mode)	2.80/2.76 bar (diesel mode) 2.11/2.70 bar (gas mode)	When operating in diesel mode EWG is closed. Once the mode switching is ordered and the boost pressure sensor faulty measurement is fed to the EWG controller, the controller reads that the targeted boost pressure is not achieved, therefore the EWG is not ordered to open.	**For the diesel mode;** – actual boost pressure 3.95 bar – lambda 2.63 **During mode switching;** – increased boost pressure – increased T/C speed **For the gas mode;** – closed EWG results in higher boost pressure; (3.02/3.87 bar) – increased T/C speed – increased lambda (2.55)	– Lambda 2.55 – misfiring issues may occur
S-4 (170)	GVU valve actuator	Gas mode/ valve opening: 8°	Null/ non-responsive	The gas (fuel) manifold pressure is fed to the GVU PID controller, which provides feedback to the null actuator. The GAV PID controller orders a reduction in gas injection timing.	The null GVU valve actuator in combination with the reduced gas injection duration in the 85% load (compared to 100% load), leads to an increase in gas pressure (4.77/5.12 bar). However, the GAV injection duration reduction counterbalances the faulty actuator effects. Engine load transient as expected.	**For approx. 3 s** – Max. engine speed (6.5% below max. limit) – Max. lambda 2.12 (from 1.95) Gas trip may occur

Case ID (FMEA ID)	Component	Operation mode/ actual value	Sensors measur.[1]/ actuator status	Control system response	Engine effects	Safety implications and margin from alarm limit
S-5 (200)	GAV (Cylinder No.1)	Gas mode/ 21.5 ms	Null/ non-responsive	The gas PID controller reads the speed drop (509 r/min) and orders an increase in the gas injection duration at the GAVs. The gas fuel amount increase results in nominal engine speed.	The cylinder no.1 operates without any gas fuel in the cylinder (compression pressure 90.85 bar). The increase in the gas injection duration results in higher max. cyl. pressure of the remaining cylinders; (131/138.4 bar). The above are associated with an increase in BSEC, NO_x and CO_2 emissions (1.32/1.56 g/kWh and 437/444 g/kWh) and exhaust gas temperature (853/862 K) as well as a minor reduction in the air−fuel equivalence ratio (1.95/1.92).	**For approx. 3 s** – Max. engine speed (8.6% above min. limit)

Case ID (FMEA ID)	Component	Operation mode/ actual value	Sensors measur.[1]/ actuator status	Control system response	Engine effects	Safety implications and margin from alarm limit
S-6 (220)	Diesel fuel rack	GTD/ instant response	Delayed response (1 s)	The diesel PID controller orders the rack to open; rack actuator opens with 1 s delay.	The engine speed drops to 469 r/min during the delay as there is no diesel fuel injected in the consecutive cylinders firing order. The diesel PID controller orders the rack actuator to maximum opening for 1 s so as to recover engine speed and then gradually decreases. **For gas mode;** – max. cyl. pressure 131 bar – exhaust gas temperature 853 K – lambda 1.94 **During mode switching;** – max. cyl. pressure drops to 91 bar and increases to 148.3 bar – exhaust gas temperature drops to 633 K and then increases up to 1060 K – max. lambda increases to 9 and drops to 1.23 **For diesel mode;** – max. cyl. pressure 140 bar – exhaust gas temp. 792 K – lambda 2.47	**For 1-2 s** – Max. engine speed drop (0.4% above min. limit) – Considerable max. cyl. pressure oscillations associated with mechanical stresses – Considerable exhaust gas temperature oscillations associated with thermal stresses – Considerable lambda oscillations associated with knocking and misfiring – Max. exhaust gas temperature (13.8% above max. limit) – T/C compressor surging
S-7a (266) S-7b (266)	EWG valve	GTD/DTG/instant response	Delayed response (opening/closing rate)	*S-7a (266) GTD mode switching* *S-7b (266) DTG mode switching* Please refer to the description below		

Case ID (FMEA ID)	Component	Operation mode/ actual value	Sensors measur.[1]/ actuator status	Control system response	Engine effects	Safety implications and margin from alarm limit
S-8 (272)	EWG valve	GTD/ instant response	Null/ non-responsive	The EWG operation in diesel model results to reduced boost pressure (3.9 bar). This in turn, and in combination with the mode switching effects, results in engine speed drop (495 r/min). The diesel PID controller reads the engine speed drop and orders an increase in the diesel fuel injected.	**During mode switching;** – boost pressure drops from 3.74 bar (in gas mode) to 3.5 bar due to open EWG, and then gradually increases up to 3.9 bar (diesel mode) – Lambda increases from1.94 (gas mode) to 3.4, followed by a drop to 1.8 and then converging to 2.0 (diesel mode) **For diesel mode;** – reduced max. cyl. pressure (140/124 bar) – reduced T/C speed (18700/17000 r/min) – higher exhaust gas temperature (785/864 K) – higher BSFC (191.4/196.5 g/kWh) – increased NO_x and CO_2 emissions (9.03/10.06 g/kWh and 616/620 g/kWh)	**For 1-2 s** – Max. exhaust gas temperature (7.7% above max. limit) – Considerable exhaust gas temperature oscillations associated with thermal stresses – Lambda oscillations associated with knocking/misfiring issues; lean mixture for diesel mode – lambda 2.0 associated with potential knocking issues – Considerable max. cyl. pressure oscillations associated with mechanical stresses – T/C compressor surging

[1]Variations from the imposed and predicted sensor measurements are noted due to the rapid response of the PID controllers.

Indicatively, the simulated case studies S-7a and S-7b are described herein to demonstrate the safety implications investigation approach. For the investigated case studies S-7a and S-7b, a set of the derived simulation parameters time variations including the normalised speed and load, the diesel and gas fuels amount, the boost pressure, the maximum cylinder pressure, the exhaust gas temperature after turbine, the T/C speed, the EWG valve opening, the air–fuel equivalence ratio, the engine CO_2 and NO_x emissions as well as the compressor operating points trajectory superimposed on the compressor map are presented.

For the investigated case study S-7a, where the EWG valve responds in a slower rate in GTD mode switching, the engine response significantly deteriorates as for few cycles of the engine operation, the compressor surging can be observed. This is a critical engine operation, which apart from the effect discussed in the following paragraph, it also induces significant torsional vibrations of the turbocharger shaft (Theotokatos and Kyrtatos, 2003, Leufvén and Eriksson, 2013). As it can be observed from Figure 7.16 (bottom-right plot), the compressor operating point enters the compressor unstable area (left to the compressor surge line) resulting in the occurrence of one compressor surging cycle. The following compressor operating phases are identified; (a) the instant reversal of the compressor air mass flow (from positive flows to negative flows), i.e. air flows from the engine manifold to the ambient via the compressor and the air filter; (b) the mass flow rate increases towards zero flow (the absolute flow reduces); (c) an instant reversal of the flow to positive flows; (d) a restoration period during which the compressor operating point remains within the compressor stable operating area, and; (e) the engine/compressor operation continues till restoring the targeted steady state conditions.

Due to the air flow reversal, the boost pressure further reduces after the mode switching order (in comparison with the respective variation of case study V-1), which, in turn, leads to lower lambda values (down to 1.25 at 11.5^{th} s) and greater exhaust gas temperature (its peak is observed at 11.7^{th} s). In this lambda range, the engine operation at the diesel mode is associated with considerable smoke. The peak in the exhaust gas temperature also increases considerable exceeding the respective manufacturer limit, which indicates higher thermal loading of the engine components and may cause the engine emergency shout down. This phase of the engine operation is also associated with greater NO_x emissions values (its peak was observed at 11.5^{th} s with a value of 2.8 times the NO_x emissions of the 100% load engine operation at the diesel mode) and a slightly greater peak value for the CO_2 emissions.

Based on the preceding discussion, it can be concluded that: (a) the GTD modes switching results in a very fast transient, which proves to be challenging for the engine and its systems operation; (b) the engine control systems (components, functions, hardware and software) need to be appropriately designed to satisfy the engine

operation requirements, and; (c) the turbocharging system matching as well as the EWG valve control, which affect the variation of the engine operating parameters, are crucial for avoiding the turbocharger compressor instabilities and the turbocharger lag effect during engine operation at transient conditions.

For the case study S-7b, where the EWG valve opened more slowly in DTG mode switching, delayed responses (of around 4 s) are exhibited form the engine and turbocharger performance parameters, which also caused small delays in obtaining the respective parameters steady state values (Figure 7.17). The slower opening of the EWG valve resulted in the slower reduction of the exhaust gas energy entering the turbocharger turbine, thus retaining for a longer period the engine turbocharger speed and consequently the engine boost pressure. However, following the EWG valve opening, the exhaust gas energy to the turbine considerable reduced, causing the reduction of the turbocharger speed and the engine boost pressure as well as the observed variations of the other performance and emission parameters. Similarly to the case study V-2 results, smooth parameters variations were predicted (after the opening of the EWG valve), which indicates that the DTG transition does not result in arising additional safety implications. However, malfunctions in the ECS and actuators may result in incorrect fuel amounts supplied to the engine cylinders leading to uneven cylinders load sharing, which can be exacerbated during transients, and thus should be further examined.

Based on the preceding discussion, it can be inferred that; (a) knocking may occur if lambda value is not properly controlled; (b) the DTG modes switching is a smooth relatively stable and other implications to the engine safety are not expected unless other engine component failures are present.

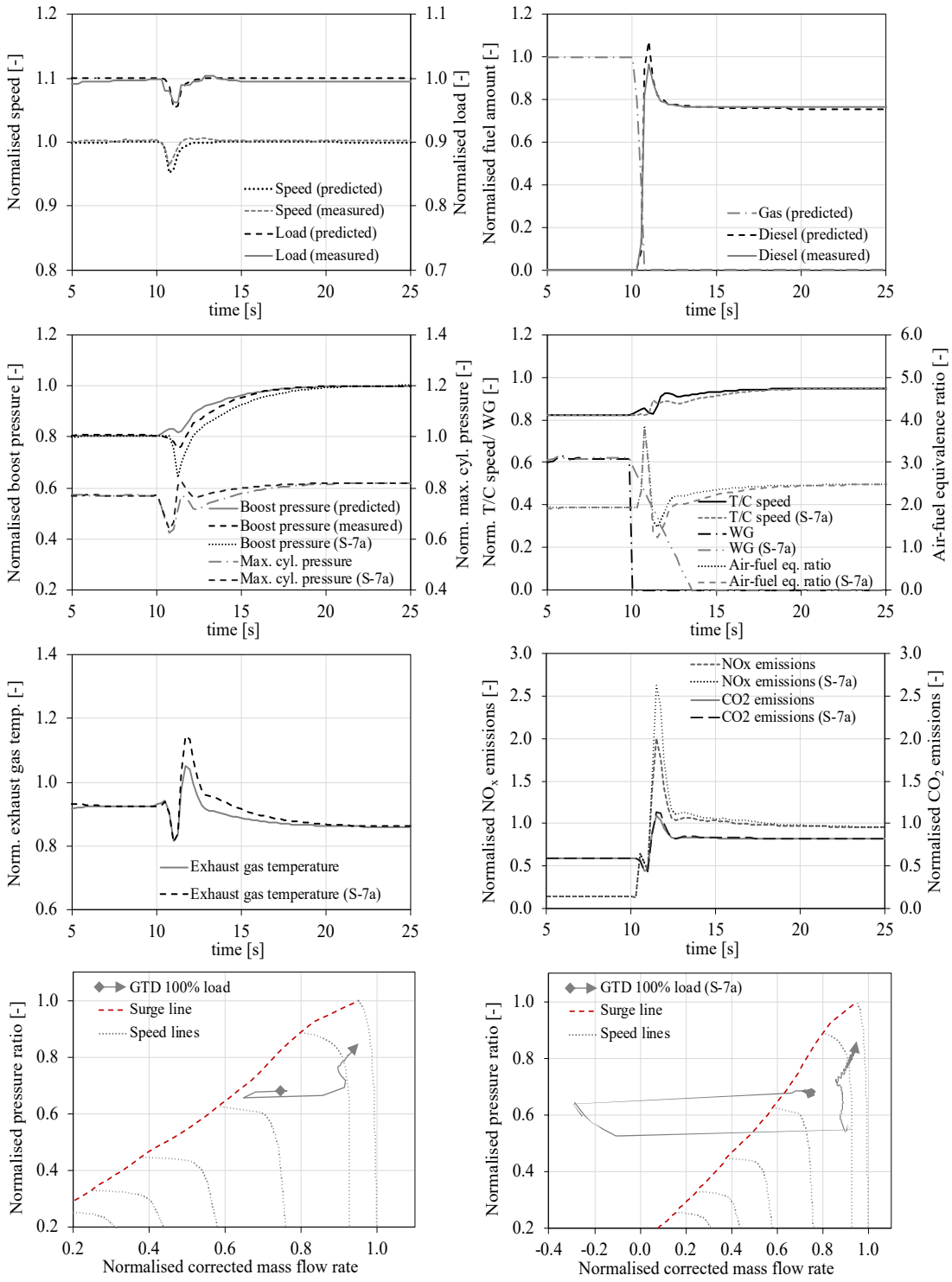

Figure 7.16 Predicted engine response parameters for GTD modes switching at 100% load with normal and delayed EWG valve operation (Case study S-7a)

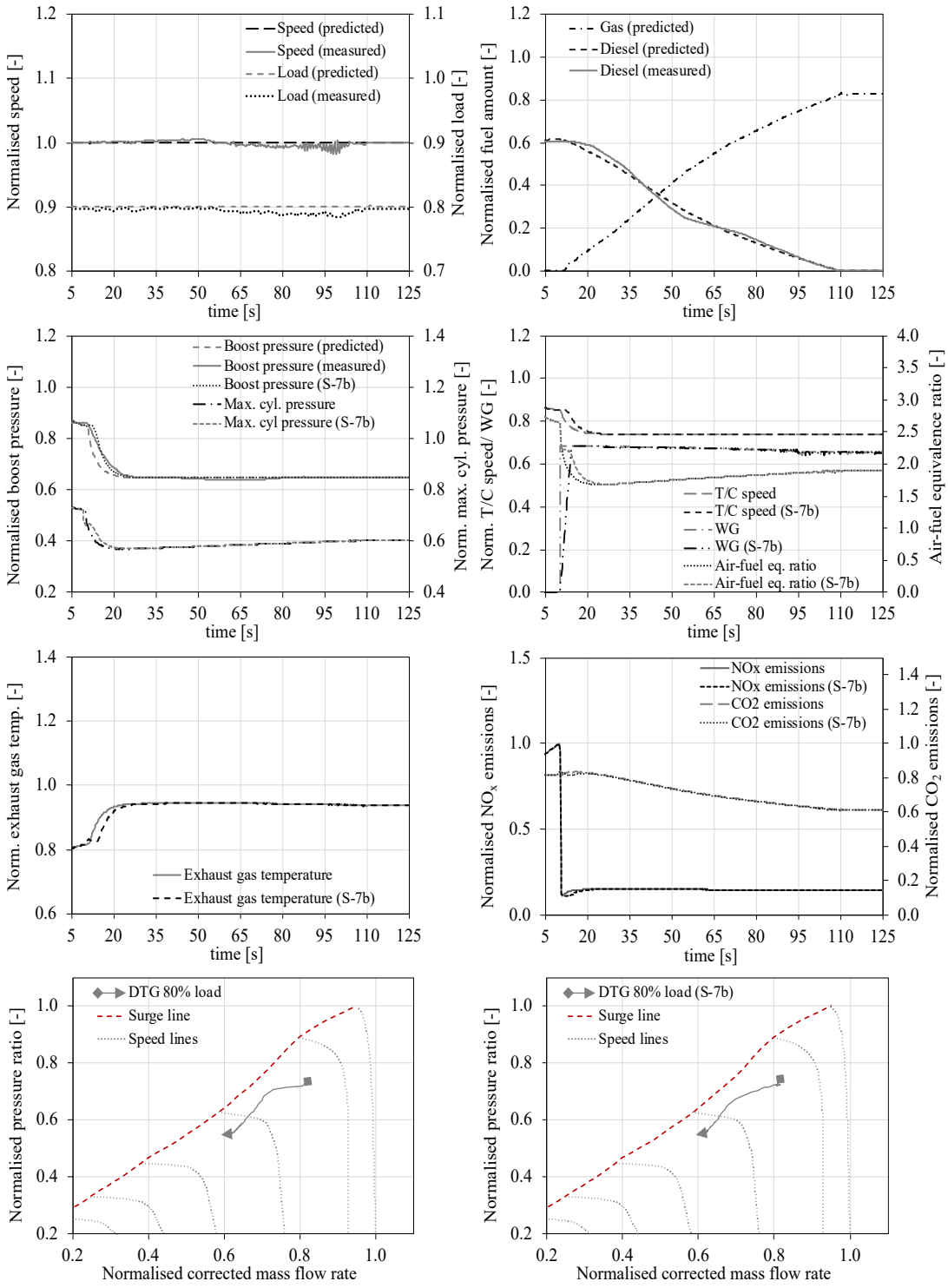

Figure 7.17 Predicted engine response parameters for DTG modes switching at 80% load with normal and delayed EWG valve operation (Case study S-7b)

The previous simulation results and their analysis support the identification of the potential safety implications, which are presented in Table 7.5 on a similar approach to a

PHA format followed in (Vincoli, 2014), that can arise during the investigated engine transient runs. The results demonstrate that during the GTD modes switching, the number of potential hazards is significantly higher than the one in the case of the DTG modes switching. In the former case, the most critical situation is associated with the T/C compressor surging as the GTD engine modes switching involves much faster dynamics. During the DTG transition, the potential hazards are associated with low lambda values, which can lead to knocking in the engine cylinders.

Table 7.5 Potential safety implications during transient for the investigated case studies S-7a and S-7b

ID	Hazard	Caused by	Effect	Recommendation
Case S-7a — GTD modes switching	Compressor surging	T/C lag / matching at different conditions in the gas and diesel model with EWG valve open/close, respectively	Lower air entering the cylinders / lower lambda values and greater exhaust gas temperature / smoke and engine thermal loading Fluctuating T/C shaft torque/ T/C shaft torsional vibrations	Proper design of EWG valve control Appropriate T/C matching Appropriate fuel injection timing
	High smoke emissions	Low lambda values	Deposits formation leading to increased wearing of engine components	Proper design of EWG valve control Appropriate T/C matching Appropriate fuel injection timing
	Oscillatory thermal and mechanical stresses	Lambda fluctuations	Fatigue problems	Proper control of injection timing
	D/G set Tripping	High exhaust gas temperature	Power unavailability leading to ship level hazards	Monitoring of engine parameters Selecting alarm settings ignoring temporal temperature variations
	Piston rings blow-by and potential crank case explosion	High maximum cylinder pressure	Damage to the engine and cylinder components	Proper control of injection timing
Case S-7b — DTG modes switching	Knocking	Low lambda values	Damage to the engine cylinders	Appropriate T/C matching EWG valve opening limiter

In conclusion, the developed DT proved to be a useful tool for obtaining a better understanding of the engine processes and components interactions as well as for investigating potential engine safety implications. It supported the identification of criticality systems, such as the EWG valve control, which are required for enhancing the engine safety.

7.6 Unified Digital System (UDS)

The developed UDS model verification results are divided into two parts; the EDS data-driven model results and the UDS validation results through the simulation case studies U-1 and U-2. The former incorporates the generation of the response surfaces for each monitored engine operational parameter by the EDS, whilst the latter entails the UDS capability of identifying faulty or uncertain measurements from faulty/uncalibrated sensors. The derived results for both parts are presented in this Section followed by an in-depth discussion on the key findings.

7.6.1 EDS Data-driven model

As the developed EDS is a part of the UDS serving the intelligent monitoring of the engine operation (through the sensors measurement uncertainty identification) and the advanced faults/failures detection, the generated response surfaces for each monitored engine operating parameter is an important output. In this respect, the developed response surfaces, which were derived by the developed data-driven model based on NNs, are employed by the EDS to acquire the 'reference' engine operating parameters (corresponding to healthy conditions) for a given set of boundary conditions (the ambient temperature; the diesel fuel lower heating value; the gas fuel LHV; the GVU gas pressure; and the A/C coolant temperature). These reference values are compared to the actual values measured from the engine sensors to identify the respective deviations. As stated in the Section 5.2.2.5, this serves the EDS intelligent engine monitoring functionality and the sensors measurements uncertainty identification, which is subsequently used for the advanced sensors faults detection. This is turn, allows the UDS to proceed to corrective actions based on the EDS results, as discussed in the following Section.

Indicatively, the response surfaces generated from the developed data-driven NNs model (case studies D-1g/d to D-5g/d) for the NO_x emissions in the diesel and gas modes for 100% load are presented in Figure 7.18. The T/C speed response surfaces for the diesel and the gas mode operation for the range of 25% to 100% is presented in Figure 7.19.

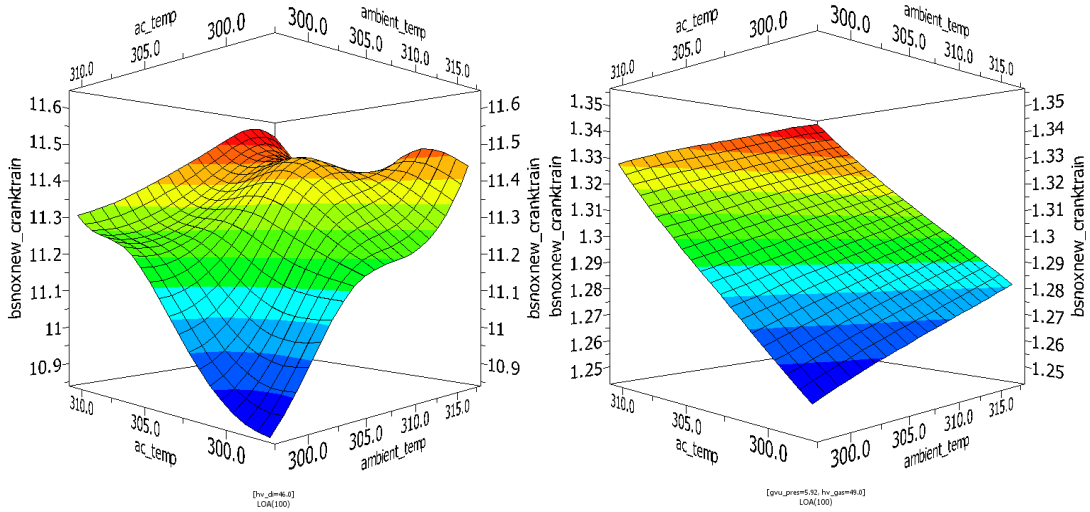

Figure 7.18 Example of NOx emissions response surfaces for diesel (left) and gas (right) mode at 100% load

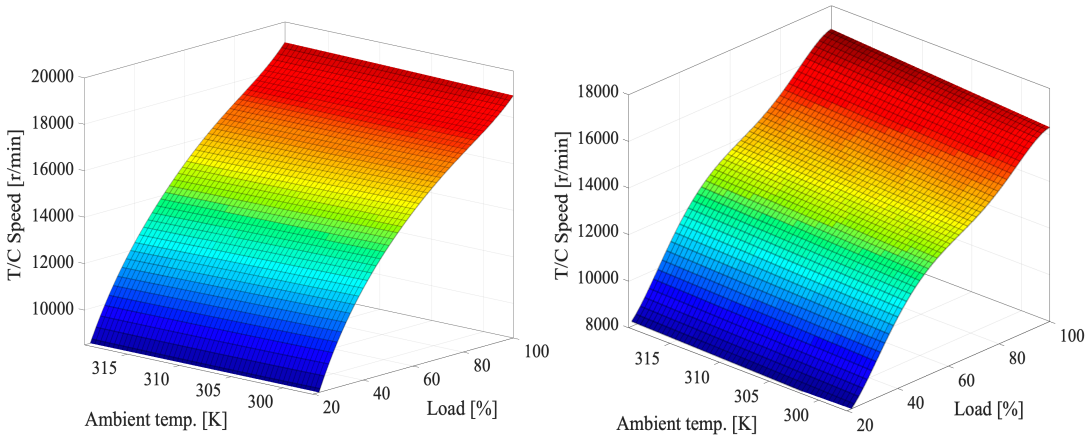

Figure 7.19 Example of T/C speed response surfaces for diesel (left) and gas (right) mode

As it can be inferred from Figure 7.19, the DD model demonstrate the expected continuity between the discrete loads (design grid) for the intermediate engine loads. Additional response surfaces for the 100% load for a set of boundary conditions is presented in Appendix C.

7.6.2 UDS verification (Case studies U-1 and U-2)

The UDS functionality and novel capabilities are verified via the assessment of the generated results for the investigated case studies U-1 and U-2. The UDS implementation in these simulation case studies aims to demonstrate the benefits from the UDS system application as described below.

The case studies U-1 and U-2 investigate the engine response considering faulty conditions/measurements (with respect to the sensors measurements uncertainty) from the speed and boost pressure sensors in the diesel and gas operating modes, respectively. For the case studies (U-1 and U-2) simulations, the DT model is considered as the actual engine, whereas the UDS is assumed to be the actual control system of the engine. The terminology 'actual' in the results analysis and figures, denotes the actual engine operational parameters values during sensors faulty operation, and the 'predicted' signifies the faulty sensors measurements of the operational parameters.

Furthermore, the following assumptions are made for the case studies U-1 and U-2. Firstly, it is assumed that the electric load control system can adjust the number of electric power consumers to match the DF engine generation set electric power output. Nevertheless, considering a ship power plant includes a number of gen-sets, in case of power deficit, the load difference is expected to be covered by another gen-set. Secondly, it is assumed that the engine brake power is calculated by using the measured electrical power and the electric generator efficiency.

The U-1 and U-2 transient simulation case studies overview is presented in Figure 7.20. For both case studies, an initialisation phase is established, where the engine operates faults-free, followed by the introduction the faulty sensors status that provide faulty measurements (engine speed and boost pressure) in the ECS (as part of the UDS) at the 10^{th} s. At this stage, the faulty sensors impact to the actual engine operational parameters is evaluated via the EDS intelligent engine monitoring system and the UDS initiates the engine diagnostics in the EDS advanced faults/failure detection system. Upon the engine operation with faulty sensors reaching steady state conditions, the UDS proceeds with a set of consecutive corrective actions (described below) and informs the operator with a warning information message. Once the corrective response

phase is completed, the UDS monitors the engine response to identify any engine operational parameters deviations against the 'healthy' data. When all the EDS monitored operating parameters obtain deviations (from their respective reference values predicted by the data-driven NN model) less than 1%, the UDS ultimately confirms the sensors faults and generates an information message to the operator. In this respect, the engine 'healthy' performance is ensured, and any safety implications are mitigated.

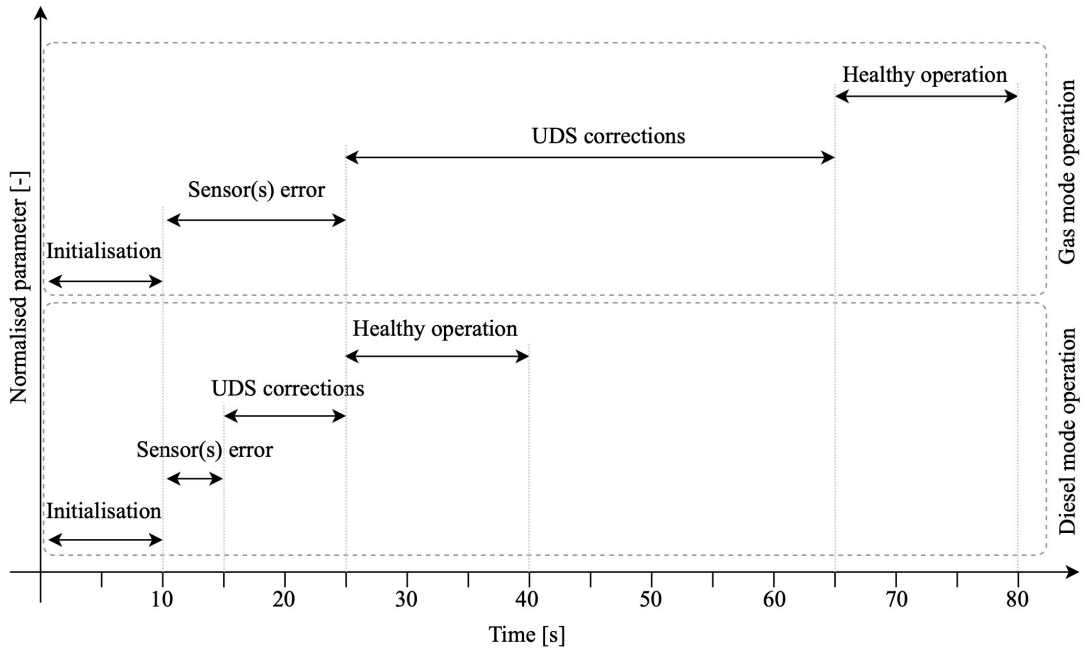

Figure 7.20 UDS verification cases overview in engine transient conditions operation; diesel mode (case study U-1) and gas mode (case study U-2)

The results for the case studies U-1 and U-2 are presented in Figure 7.21 and Figure 7.22 respectively. Both case studies focus on the representation and investigation of the engine operation in the diesel/gas mode assuming that after the 10^{th} s, the faulty speed sensor measurement is increased by 5%, whereas the faulty boost pressure sensor provides measurements decreased by 10% (both from their respective values at healthy conditions). The top graphs in Figure 7.21 and Figure 7.22 illustrate the faulty (predicted) engine speed and boost pressure signals from the sensors fed back to the ECS versus the actual values of these parameters over time, whereas the two bottom graphs present the actual engine brake power, T/C speed, EWG opening and air–fuel equivalence ratio. It must be mentioned that when both the speed and boost pressure

sensors are faulty and the UDS system is not employed, the engine response is according to the variations presented in Figure 7.21 and Figure 7.22 between the 10th and 15th s in the diesel mode and 10th and 25th in the gas mode, respectively.

In specific for case study U-1, the faulty speed sensor signal fed in the ECS (as part of the UDS) (providing input to the diesel PID controller) after the 10th s results in a decrease of the diesel fuel injected amount into the engine cylinders. This in turn has a direct impact on the delivered engine brake power as the engine actually operates in a reduced speed (5%) for the period between the 10th and the 15th s (before the UDS apply corrective actions). The fuel control is based on the faulty speed sensor input. The manufacturer engine diagnostics system is not capable of identifying this sensor measurements deviation. In the diesel mode operation, the boost pressure sensor is only used for monitoring purposes; although the boost pressure sensor is interconnected with the EWG controller, it is only in gas mode operation that can affect the engine response, as discussed in case study U-2. Nevertheless, the reduced diesel fuel injected amount (as an effect of the faulty speed sensor measurement) also has a negative impact to the boost pressure (resulting in a 17% maximum drop from its initial value) exhibiting a 13% error from the actual boost pressure at the 11th s, which is attributed to the T/C speed reduction. With regard to the air–fuel equivalence ratio, the instantaneous diesel fuel injected amount drop in combination with the T/C lag and the delayed boost pressure decrease, lead to lambda fluctuations between the 10th and 11th s ranging from 2.2 to 3.9. However, the fluctuations noted in the diesel fuel amount and the air–fuel equivalence ratio in the region of 10th to 12th s, occur due to the introduction of sensors faults during the simulation. Moreover, it is observed that these fluctuations are associated with safety implications, including the T/C compressor surge effect as well as misfiring issues due to high air–fuel equivalence ratio.

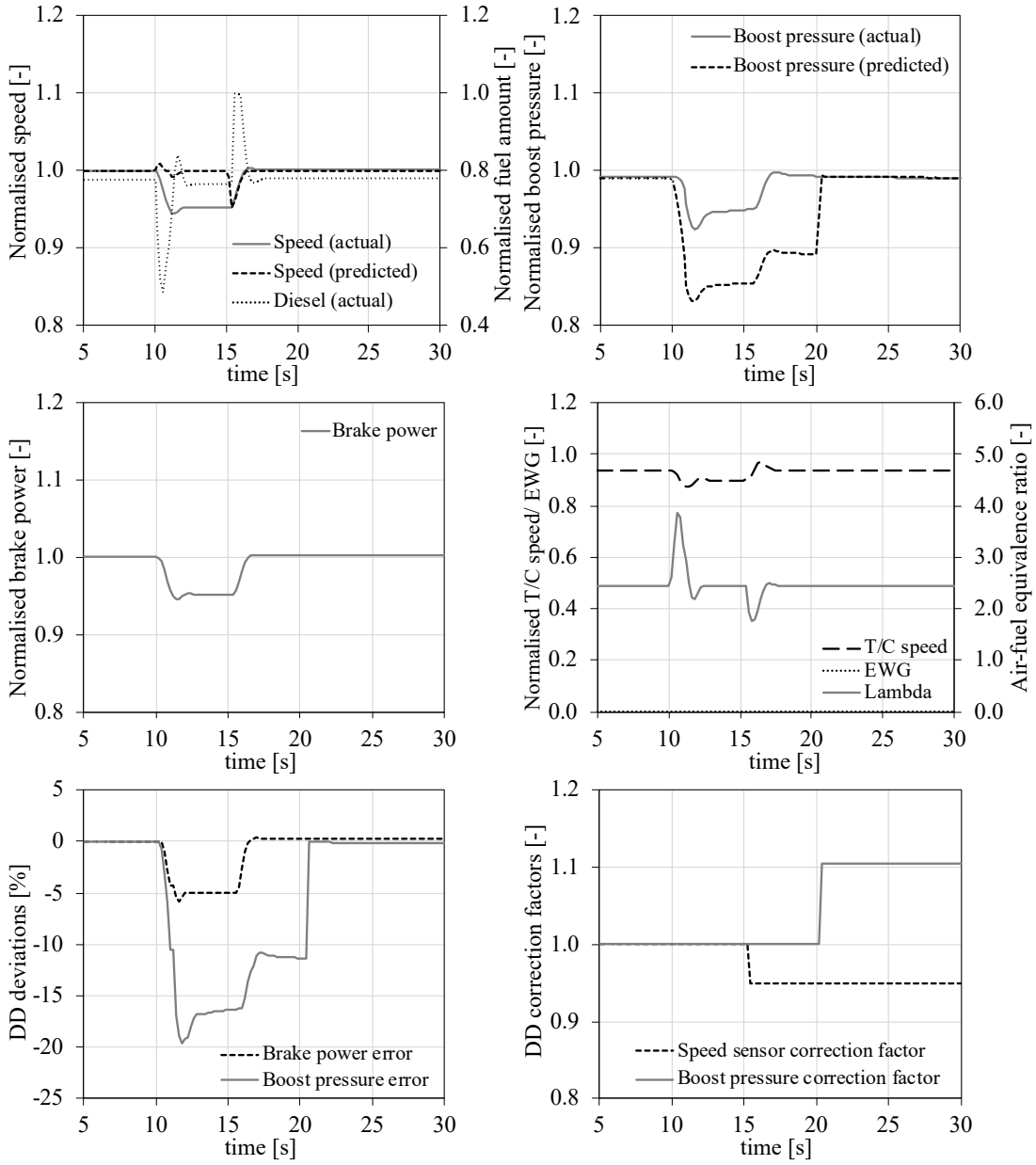

Figure 7.21 Case study U-1 results; actual and predicted engine response parameters in the diesel mode with faulty speed and boost pressure measurements

Focusing on the UDS response in case study U-1, it is divided into two sequential actions, which include the signals correction factors calculation and implementation; first for the speed sensor implemented at the 15th s; and second for the boost pressure sensor implemented at the 20th s. Considering that any deviations in the speed sensor measurements are reflected in the delivered engine brake power (due to ECS response adjusting the injected fuel amount), the later parameter was used to quantify the speed

sensor measurement error. This was achieved by comparing the actual brake power against its reference (expected) value derived from the DD model employed in the EDS system. As shown in Figure 7.21, the UDS successfully identified the speed sensor error and implemented the calculated correction factor to the speed signal fed to the ECS (diesel PID controller), thus recovering the actual engine speed to the nominal levels. This can also be confirmed by the recovery of the engine brake power observed between 15th and 17th s. Likewise, for the boost pressure sensor correction, the boost pressure demonstrates a 3% rise between 15th and 17th s, aligning with the observed T/C speed increase. The air–fuel equivalence ratio drop noted at the 16th s is attributed to the fast diesel rack response and the T/C lag. Following the first UDS corrective response, the UDS was also capable of evaluating the remaining EDS monitored signals and identify only a boost pressure sensor signal error (10%) during 17th to 20th s. Therefore, a second corrective action on the boost pressure sensor signal was imposed by the UDS at the 20th s, leading to the actual measurement prediction with adequate accuracy.

Moving to the investigated case study U-2, the faulty speed sensor measurement fed in the ECS (gas fuel PID controller) results in a response of the GAV to reduce the gas fuel injection duration, and thus, the injected gas fuel amount at each cylinder inlet port. This in turn has a negative impact on the delivered engine brake power from the 10th to the 25th s, exhibiting its maximum reduction by 4.8% from its initial value at 25th s when the UDS orders a corrective action, as shown in Figure 7.22. It can be observed that the engine operates in a lower speed compared with its nominal value in the period between the 10th to 25th s, due to the imposed speed sensor fault. With regard to the boost pressure, the observed engine response differentiates from the response of the case study U-1, as the EWG in gas mode is open and is adjusted by the ECS respective PID controller. In this sense, the process under investigation becomes more complex. In specific, the boost pressure sensor output is fed in the EWG controller in order to adjust the EWG valve opening. The latter has an immediate effect on the exhaust gas amount entering the T/C turbine, and hence the T/C speed. Therefore, the EWG controller reacts on the faulty boost pressure drop at the 10th s and orders a decrease of the EWG valve opening. This eventually leads to the EWG valve closure at the 11th s, to achieve the targeted boost pressure (the targeted boost pressure values for the engine discrete load are stored in the EWG PID controller in a form of a lookup table; for

intermediate loads linear interpolation is performed). However, as the boost pressure recovers at the 15th s, the EWG controller readjusts the EWG opening, obtaining convergence to a steady opening value at around the 22nd s (which is 49% lower than its reference value). It must be noted that in the period between the 15th and 25th s the actual boost pressure exhibits a 10.9% increase from its reference (and predicted by DD model) value. The effects of the EWG controller and the EWG valve opening are also noted in the T/C speed variation; a 5.4% increase from the reference T/C speed value is observed for the period 15th s to 25th s. In addition, the air–fuel equivalence ratio increases from 2 to 2.3 at 20th s, which is attributed to the lower gas fuel amount and (actual) boost pressure increase, the latter resulting in the charge air flow increase. This lambda range is associated with potential misfiring issues.

The first UDS correction action on the speed sensor measurement is implemented in the period between the 25th to 40th s (as discussed below), resulting in the accurate prediction (from the UDS) of the actual engine speed, which in turn leads to the engine brake power recovery to the reference value. Minor fluctuations are observed in both the engine speed power, which are attributed to the actions of the ECS system PID controllers. The boost pressure and the T/C speed are slightly affected by the gas fuel amount change due to the speed sensor correction, whereas the EWG valve opening demonstrates a 28% deviation (decrease) from its reference value. The air–fuel equivalence ratio is reduced to 2.2. Furthermore, the second UDS correction action (described below) is related to the EWG valve opening and is introduced in the time period from the 40th to 55th s. As it is observed, the EWG valve opening by the UDS has a direct effect on the boost pressure, the T/C speed and the air–fuel equivalence ratio. At the end of this period, the reference values of these parameters are obtained. Lastly, the third UDS correction action is implemented on the boost pressure sensor measurements in the period from the 55th to 70th s, resulting in the recovery of the engine response to its "expected/healthy" conditions. The oscillations observed in the EWG valve during this time period are described below. It must be noted that similarly to case study U-1, the fluctuations noted in the gas fuel amount and air–fuel equivalence ratio in the region of 10th to 25th s, occur due to the introduction of sensors faults during the simulation, and they are associated with safety implications, including the T/C compressor surge effect as well as misfiring issues due to high air–fuel equivalence ratio.

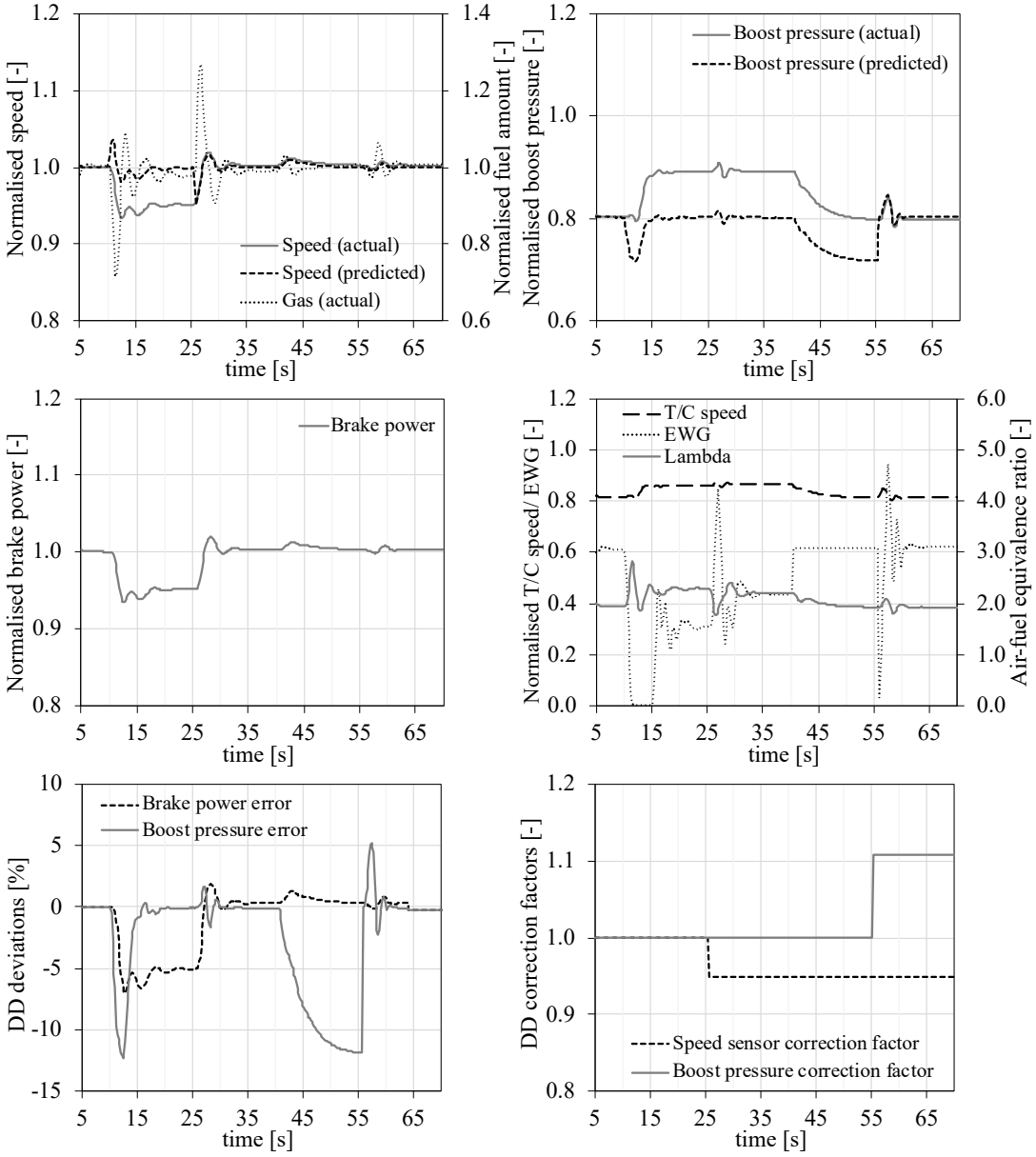

Figure 7.22 Case study U-2 results; actual and predicted engine response parameters in the gas mode with faulty speed and boost pressure measurements

With regard to the UDS corrective response in the case study U-2, it is divided into three sequential actions; (a) speed sensor signal correction factor implementation; (b) EWG imposed valve opening; and (c) boost pressure sensor correction factor implementation. The first action takes place at the 25th s, the second at the 40th s and the third at the 55th s. Similar to case study U-1, considering that any deviations in the speed sensor are reflected in the delivered engine brake power (due to the injected fuel amount variations); the brake power deviation was used to quantify the speed sensor

measurement error. This was achieved by comparing the actual brake power against its reference (expected) value estimated by employing the DD model of the EDS system. As shown in Figure 7.22, the UDS was capable of successfully identifying the speed sensor error (via the brake power calculated deviation from its reference value) and implementing the calculated correction factor to the speed signal fed to the ECS (gas fuel PID controller), hence recovering the actual engine speed to its 'healthy' conditions. This can also be confirmed by the engine brake power recovery observed between 25th and 35th s. The second UDS corrective action is related to the EWG valve operation and it is implemented based on the following approach. In order to accurately define the boost pressure sensor error, the EWG valve is driven to its reference value opening identified from the DD model of the EDS for the specific load, operating mode and boundary conditions. The imposed EWG valve opening is expected to result to a (faulty) boost pressure measurement drop, as illustrated in Figure 7.22, revealing the boost pressure sensor measurement error (calculated in the UDS based on its expected 'reference' value estimated from the DD model). At the same time, the UDS evaluates the remaining EDS monitored operating parameters of the engine, and once deviations below 1% in all parameters are obtained, the UDS triggers the third corrective action. The latter includes the implementation of the calculated correction factor to the boost sensor measurement fed in the ECS as well as the activation of the EWG valve controller adjusting the EWG valve opening based on the corrected boost pressure signal. During the reactivation of the EWG controller, oscillations in the EWG valve opening are observed with minor impact on the boost pressure, however the controller is able to reach steady state conditions after 5 s.

The sensors faults effects on the engine response, as revealed from the investigated case studies (U-1 and U-2) results analysis and the UDS process development are summarised in a concise mapping presented in Table 7.6., where the sensor faulty measurements are interconnected to the affected engine operating parameters. Likewise to Table 7.6, the engine manufacturers, based on their vast experience, usually interconnect the engine components faults (e.g. fuel injectors, exhaust valves, cylinders O-rings and liners, bearings etc.) with a number of engine operating parameters,. The manufacturers assessment on the components' faults and their potential effects on the engine operational parameters is commonly included in the engine maintenance manual

as part of the troubleshooting, however, this process is not considered under the scope of the present thesis.

Table 7.6 Mapping table interconnecting sensor(s) faults with engine operational parameters affected

Sensor	Impact on UDS	Main parameter(s) affected	Other key parameters affected
Speed sensor	Diesel/gas PID controller	Brake power	Diesel fuel rack position Gas injection duration Boost pressure T/C speed T/C exhaust gas inlet pressure T/C exhaust gas inlet temperature Lambda Brake specific NO_x/CO_2 BSFC/BSEC Brake efficiency
Boost pressure sensor	EWG controller	EWG valve opening (gas mode) Charge air pressure Charge air mass flow rate Lambda	Max. cylinder pressure Charge air temperature T/C speed T/C exhaust gas inlet pressure T/C exhaust gas inlet/outlet temperature Gas injection duration Brake specific NO_x/CO_2 BSFC/BSEC Brake efficiency

It must be noted that the manufacturer's engine diagnostics system is capable of identifying faults related to the valves' actuators (e.g. EWG valve, GVU valve) and GAVs, therefore these items are disregarded from this research.

Having completed the UDS verification, the FMEA of the failure modes investigated in cases U-1 and U-2 were re-evaluated considering the UDS application. In this respect, the FMEA metrics (occurrence, severity and detectability) for the investigated case studies are revised as presented in Table 7.7. Considering the initial (manufacturer) and revised (proposed UDS) system, the percentage reduction in the Risk Priority Number (RPN) is calculated by using equation 7-1.

$$\text{RPN reduction [\%]} = \frac{\text{RPN}_i - \text{RPN}_r}{\text{RPN}_i} \quad 7\text{-}1$$

where *i* denotes the initial system and *r* the revised system (with UDS).

Table 7.7 RPN percentage reduction with UDS

	Case ID (FMEA ID)	Occurrence (O)	Severity (S)	Detectability (D)	RPN (RPN reduction)
Initial	S-2 (43)	3	7	4	84
	S-3 (82)	3	8	4	96
With UDS	S-2 (43)	2	7	2	14 (-83% from initial)
	S-3 (82)	2	8	2	16 (-83% from initial)

Notwithstanding the above, the UDS application establishes a novel approach to the engine monitoring, the sensors measurements uncertainty identification and the faults diagnosis. In specific, in both investigated case studies, the UDS was capable of identifying the sensor measurements deviations and implementing corrective actions that recovered the engine operation to its "healthy" conditions. Hence, the UDS application offers: (a) intelligent engine monitoring capabilities in terms of sensors measurements uncertainty identification, via the novel DD model implementation, as well as advanced faults/failure detection that can guarantee the 'healthy' engine performance and mitigate any potential safety implications, as demonstrated from the reduced RPN; (b) elimination of redundant (double) sensors, which will result in a reduced number of the installed sensors, as well as an extra layer of assurance for the personnel supervised sensors; and (c) UDS automated virtual calibration of the uncalibrated/faulty sensors via the UDS corrective response in order to ensure engine 'healthy' operation until maintenance actions are implemented.

7.7 Chapter summary

In this Chapter the results generated for the designed Case studies under investigation were presented and discussed in detail. The engine design and operational limitations identified during transient conditions were presented and their impact on the engine performance, emissions and safety results was assessed. The performance and emissions optimisation results for steady state and transient conditions were reviewed and the key findings were discussed. The potential safety implication due to engine systems/components faulty operation were addressed and the most critical components were used for the UDS verification. Lastly, the UDS response was assessed during the investigated faulty scenarios.

8 FINAL REMARKS AND RESEARCH CONCLUSIONS

8.1 Chapter outline

In this Chapter, first the accomplishment of the aim and objectives of this research are discussed. Subsequently, the novelty of this research is summarised and reflections on the developed framework and the key findings are presented. The implications of this work for the academia and the maritime industry are demonstrated. Finally, recommendations for future work are outlined.

8.2 Review of research objectives

As it was stated in Chapter 1, the question that drove this research is the following.

How can the dual fuel engines be further improved/enhanced in terms of performance and safety, considering future environmental regulatory requirements and digitalisation capabilities?

The research question is answered by the development of the presented novel framework that can be employed in newbuilt and existing marine (DF) engines, to optimise their performance-emissions trade-offs and enhance their safety, whilst delineating the involved interactions and their effect on the performance and safety.

This work was intended to address the following literature gaps identified in the critical review reported in Chapter 2:

Gap no.1: A lack of a Digital Twin (DT) to adequately represent the marine four-stroke DF engines behaviour along with their control system functionalities.

Gap no.2: A lack of reporting the marine four-stroke DF engines processes during transient operations, including modes switching, as well as mapping the engine systems/components design and operational limitations.

Gap no.3: A lack of optimisation studies on DF engines to optimise performance-emissions trade-offs at gas mode operation, whilst considering the engine operational limitations.

Gap no.4: A lack of a methodology that aims to optimise the performance and emissions trade-off and consists the marine four-stroke DF engines operating in diesel mode, compliant with the IMO 'Tier III' requirements, whilst considering the systems/components design and operational limitations related to the EGR and ABP systems and their associated control system functionalities.

Gap no.5: A lack of a methodology that aims to enhance the marine four-stroke DF engines safety, by introducing ML capabilities to provide intelligent engine monitoring and advanced faults/failure detection, whilst considering safety implications and sensors measurements uncertainty.

The research aim was accomplished through the research objectives that were discussed in Chapter 1 and in this Section, it is outlined how these objectives were achieved.

Objective no.1: Perform a comprehensive literature review on the DF engines performance, emissions and safety context for revealing the research gaps

This objective was achieved in two stages, as described in Chapter 2. Firstly, the marine dual fuel engines categories, technology and operation modes were identified. Previous numerical and experimental investigations and state-of-the-art industry/commercial developments in marine engines related to the performance optimisation and/or emissions reduction were identified and reviewed to provide a detailed background on the modelling and optimisation approaches, methods and tools commonly used. The technologies that have the potential to reduce the marine engines generated airborne emissions were reviewed, with special emphasis on the NO_x emissions reduction.

Special focus was given on the EGR technology along with the potential installation layouts and their impact on the engine response. In addition, previous investigations on marine engines control development were reviewed to identify design strategies, methods and tools for fuel controlling, combustion simulation and EGR control approaches. Secondly, investigations on the marine engines' safety implications were reviewed to address hazards related to the engine components/systems and their effects on the engine operation. Safety evaluation methods and tools employed in commercial applications by the engine designers to analyse and control all the safety concerns during the design phase were outlined. Furthermore, previous investigations on faults and failures diagnosis and prognosis were identified and analysed to identify state-of-the-art methods and tools employed in this area. In subsequence, the most significant part of the critical literature review, was the identification of the key findings and research gaps, which were used to select the reference cyber-physical system (CPS) under investigation as well as the methods and tools of the followed research approach that led to the proposed framework development.

Objective no.2: Research approach development

The first part of this objective included the reference CPS selection, which was achieved based on the literature review gaps and by considering the limited number of investigations on the marine four-stroke DF engines (compared to the marine two-stroke diesel/DF engines), as reported in Chapter 2. As a result, the Wärtsilä 9L50DF engine was identified as the reference CPS under investigation for the present study. The second part of this objective, incorporated the proposed framework development, as presented in Chapter 3. This framework, which incorporates two methodologies to address (a) the performance improvement and emissions reduction and (b) the safety enhancement, was described in detail in Chapter 3, where the methodological steps for its implementation were discussed. The selected state-of-the-art technologies, methods and tools of each methodological step were supported by appropriate justification based on the literature review. The framework development in this objective, partially satisfies the research gaps no.3 to no.5, whereas the DT development carried out in Objective no.4 and the framework verification carried out in the Objective no.5 fully address these research gaps.

Objective no.3: Reference cyber-physical system (CPS) Digital Twin (DT) development

This objective was achieved by initially identifying, analysing and mapping the investigated reference CPS (W9L50DF) along with its sub-systems/components including the Unified Engine Controls (UEC), as described in Chapter 4. The reference CPS detailed analysis laid the basis for the reference CPS digital twin development in GT-ISE, employing the modelling approach and tools identified in Chapter 3 and described in Chapter 5. The developed reference CPS DT was validated against available test data, in order to ensure the DT fidelity. Consequently, as the main outcome of this objective is the state-of-the-art reference CPS DT that can adequately represent the marine four-stroke DF engine behaviour along with its control system functionalities, the research gap no.1 is addressed. The reference CPS DT development achieved in this objective, paved the way for addressing the research gap no.2 in Objective no.5.

Objective no.4: Digital Twin development with integrated Unified Digital System (UDS)

The first part of this objective, related to the development of the extended digital twin considering the developed framework, was achieved by employing the technologies, modelling approach and state-of-the-art methods and tools for each proposed system, as identified in Chapter 3 and described in Chapter 5. The EDS data-driven model developed, as part of the UDS, was calibrated and validated by employing the DT simulation results, in order to ensure the DD model fidelity. Furthermore, the second part of this objective, comprising the Engine Diagnostics System (EDS) and Faulty Operation Simulator (FOS) integration with the Engine Control System (ECS), Engine Safety System (ESS) and Alarms and Monitoring System (AMS) of the reference CPS into the UDS, was also accomplished in Chapter 5. The development of the integrated DT with the UDS, contributed towards addressing the research gaps no.3 to no.5 in Objective no.5.

Objective no.5: Case studies design – optimisation/ verification

This objective was achieved by initially designing the case studies under investigation in Chapter 6. The cases studies design process employed methods and tools selected in Chapter 3, as identified from the literature review. In subsequence, the simulations runs for these case studies were conducted, and the derived results were presented and

discussed in Chapter 7. These results addressed the following; (a) the reference CPS response during transients and the identifications of the engine design and operational limitations; (b) the framework verification to improve the engine performance and reduce emissions; (c) the identification of the most critical DF engine systems, examination of potential safety implications and evaluation of the engine manufacturer failure diagnosis method; and (d) the verification the UDS response and framework verification for the engine safety performance enhancement. Therefore, considering the outcome of the previous objectives and the generated results of this objective, the research gaps no.2 to no.5 are fully addressed.

8.3 Research novelty

The novelty of this research lies in the framework developed for enhancing both marine engines environmental and safety performance, via the development and implementation of digital twins (DT). In this respect, the main novelty stems from the combination of methods and tools into the proposed methodologies, and therefore the resulted framework, as well as its application on the marine four-stroke DF engines. This framework can be adopted for newbuilt and existing marine engines, where operational/test data is required to define the engine "reference/healthy" condition in each case.

In specific, this research introduces and describes in-detail a digital twin of a marine four-stroke DF engine, delineating the involved interactions between performance and safety. In comparison with the pertinent literature that reveals a lack of studies on marine four-stroke DF engines operating in transient conditions, the present study provides a detailed analysis on the processes during transient operations, including modes switching, as well as mapping the engine systems/components design and operational limitations. Both the reference CPS (W9L50DF) and the integrated DTs (including UDS), developed during the framework implementation, are considered as novel outcome of this research.

Furthermore, the proposed framework presented in this research study demonstrates a set of novel outputs for each methodology. With regard to the performance-emissions trade-offs optimisation, the novel output includes: (a) the optimal DF engine/systems

settings in both the gas and diesel operating modes; and (b) the development of the integrated Digital Twin (DT) with the EGR and ABP systems. On the other hand, considering the proposed methodology for safety performance enhancement, the novel output includes: (a) the development of the Data Driven (DD) model for engine operating parameters prediction under healthy engine operation; (b) the Engine Diagnostics System (EDS) including intelligent engine monitoring system and advanced faults/failure detection system for diesel/gas mode; and (c) the integrated DT with the Unified Digital System (UDS). Furthermore, the exclusive benefits from the implementation of the UDS include: sensors measurements uncertainty identification, mitigation of potential safety implications, elimination of redundant sensors resulting in a reduced number of the installed sensors, as well as an extra layer of assurance for the personnel supervised sensors, and UDS automated virtual calibration of the uncalibrated/faulty sensors via the UDS corrective response.

Lastly, the most relevant studies on the respective investigated areas are acknowledged (Dimopoulos et al., 2014, Zymaris et al., 2016, Mavrelos and Theotokatos, 2018, Lei et al., 2019, Meier et al., 2019). These studies may use similar methods and tools, such as ML models, however, the aim and scope of the present research thesis is deemed to deviate from the pertinent literature. The fundamental variations of the present research work to the existing studies lies under the investigated engine type, the systems investigated (EGR system with ABP system, the UDS etc.), the focus on the faults/failures diagnosis (sensors and actuators) considering sensors measurements uncertainty identification as well as the introduction of a system (UDS) that demonstrates corrective response capabilities.

8.4 Reflections

In this section, reflection on the framework boundaries, the DT modelling as well as the required data challenges and the case study findings are presented.

8.4.1 Considered boundaries and limitations

The boundaries and limitations of this research are related to the DT development, including the technologies under consideration, the modelling approach as well as the methods and tools employed.

In specific, for the combustion modelling of the engine thermodynamic model, the 'semi-predictive' combustion model was selected due to lack of combustion calibration data. It must be noted that by the term 'semi-predictive', as defined in (GT, 2019), it is implied that the combustion model parameters are imposed for the engine discrete loads and predicted for intermediate loads. In this respect, a 'predictive' (phenomenological) combustion model for the DF engine combustion prediction in a wide operating envelope can be employed in future research studies, providing combustion calibration data is available. In addition, the methane emissions generated by the investigated DF engine could not have been predicted in the present DT, as the combustion model is of the 0D type. However, considering the methane slip in marine four-stroke DF engines and by applying an CO_2 equivalence factor an estimation on the CO_2 emissions is provided. Furthermore, the develop DT does not take into account any knocking and/or misfiring effects. Particularly, the developed engine thermodynamic model does not accommodate engine knocking and/or misfiring prediction, whereas the engine knocking and misfiring detection and controls are not included in the Engine Control System (ECS) model.

Moreover, the present research study focuses on the EGR technology, in combination with an ABP system, and elaborates on its application on the marine four-stroke DF engines. Other exhaust after-treatment technologies, such as the SCR are not considered under this investigation.

The developed UDS capabilities are limited to the sensors and actuators faults/failures detection and diagnosis. Hence, the developed UDS is not designed to predict the engine components mechanical failures. Finally, the UDS functional processes do not take into account the engine mechanical components degradation, which can affect the engine response, and thus the actual engine operational parameters. The application of the UDS model in variable speed engines in not investigated.

Lastly, the systems capital expenditure (CAPEX) and operational expenses (OPEX) or any other related costs as well as systems' volume and mass footprint are not considered in this work. In specific, the impact that the selected technologies have on the cargo capacity, the resources that are carried by the ship, the machinery space design and the structural ship design is not discussed.

8.4.2 Digital Twin modelling and required data challenges

The digital twin development required access to relevant input data, the accuracy of which was of great importance due to their influence on the simulation results. This data entails detailed engine geometrical and operational data as well as functional diagrams of the control components, in order to model the engine processes accurately. In this respect, the acquisition of this information is usually quite challenging, as partial data sets are usually available during the model development stages.

Likewise, in this research, partial information was available. A characteristic example is that of the EGR system model development. Since the current number of engines built with EGR systems is limited and the engine testing is expensive, a powerful alternative for developing EGR controllers for such engines is to use simulation models. However, the same reasons that motivate the use of simulation models, also lies the challenges to obtain sufficient measurement data for developing the EGR system model. To overcome this challenge, the required information was either estimated based on experience or acquired by elaborating available published data for similar engines.

In this research study, different sources of data were used including online sources, the existing literature, technical reports (i.e. engine project guide) and engine shop trials. It is evident though that the inclusion of technical reports and engine shop trials were crucial in order to develop, calibrate and validate a DT.

In addition to the data challenges, the DT development requires a considerable amount of time and skills for the engine and controls modelling. In addition, the DT development is related to combination of various research areas (thermodynamics, controls, safety etc.), therefore requiring a multi-disciplinary approach. Although these

challenges, the best attention was paid to provide a solid and technically correct model, which is demonstrated from the results validation.

Lastly, more of a time constrain rather than a challenge, the DT simulations time is an important factor. Simulation time is usually interconnected with the available computational power. In this study, the developed DT computational time on a modern desktop computer with a single processing (due to software licence limitations) is approximately 20-25 times the real-time. The simulation time can be significantly reduced by using a parallel computing approach. It must also be noted that the GT-ISE offers a tool to transform the existing 1D model to a real-time model, which can be used in future work for developing the real-time digital twin of the investigated engine.

8.5 Discussion on the case studies findings

8.5.1 Steady state and transient conditions operation and models validation

The integrated modelling (including the engine thermodynamic model and the control system functional model) of a large marine DF four-stroke engine and its control system was developed in GT-ISE to allow for the simulation of the engine transient operation with fuel switching and load changes. The engine control system and components functions were analysed based on the engine manufacturer requirements, thus allowing for the development of the ECS model (also in GT-ISE environment) to adjust the employed fuels (gas, diesel and pilot) and the EWG valve under both steady state and transient operating conditions.

The developed integrated DT was validated against available test data (engine shop trials) for five cases studies (case studies SS-1g/d to SS-5g/d) at steady state conditions operation. The main findings of the validation are summarised as follows.

It is observed that the gas mode is more efficient than the diesel mode at the high load region, however, less efficient operation was observed at the lower load region The engine in the gas mode operates with almost constant air−fuel equivalence ratio in a narrow window from 1.9 to 2.3, whereas slightly higher values of the air−fuel

equivalence ratio are used for the diesel mode corresponding to greater air flow rates. This is obtained by controlling EWG opening (in gas mode) to adjust the engine air flow and therefore the air−fuel equivalence ratio. Moreover, in the gas mode, the engine operates at lower receivers and in-cylinder pressure level. However, the mean effective pressure and power output is kept at the diesel mode levels due to the shorter combustion duration and the earlier start of combustion.

The NO_x emissions reduced by 85% in average in the gas mode compared with the diesel mode. The diesel mode complies with the 'Tier II' limits, whereas IMO 'Tier III' limits are met when the engine operated in the gas mode. The derived results verify that the CO_2 emissions in the gas mode reduced approximately 25% in average due to the natural gas low carbon to hydrogen ratio. Larger reduction is obtained when the engine operates at the high load region where the efficiency is greater than that of the diesel mode.

The developed integrated DT was used for the investigation of three representative engine operating cases studies (case studies V-1 to V-3) with fuel and load changes for which experimental results were published. The main findings of the validation are summarised as follows.

The combustion modelling was challenging needed to accommodate the combustion process of the employed engine fuels (gas, diesel and pilot) during the mode switching. The followed approach for representing the engine combustion performance during transients, which included a database for storing the Wiebe functions parameters, validated at steady state conditions, and the use of quadratic interpolation for predicting the combustion characteristics during the fuel and load changes, proved to be sufficient for capturing the involved phenomena.

The developed engine control system realistically represented the actual ECS operation. However, it was a demanding task requiring attention to all the engine control sub-systems and components as well as their interactions, the sequence of the involved processes and the engine manufacturer requirements. In addition, the EWG valve control was identified as a crucial part of the sophisticated and complex ECS for

ensuring the smooth and reliable marine DF engine transient operation with fuel and changes.

From the performed validation, it was inferred that the developed DT is capable of sufficiently predicting the engine parameters response during steady state and transient operating conditions, including fuel and load changes, and can be used in the preliminary stage of the engine design process for optimising the engine settings. Even for the almost instantaneous GTD mode switching, which modelling and simulation are quite demanding tasks, the developed DT provided sufficient predictions. Therefore, the developed DT provided the required accuracy and fidelity for investigating both the engine steady state and transient conditions operation.

The engine response for the investigated operating cases were found to satisfy the engine manufacturer requirements. The mode switching from gas to diesel (GTD) is rapid and must be completed within 1 s; therefore, it is demanding for both the engine and its control system operation. The quick gas fuel cut off in conjunction with the slower diesel fuel increase resulted in a temporary loss of power, associated with a slight reduction in the TC shaft speed and the engine boost pressure. The subsequent reduction of the air−fuel equivalence ratio and the increase of the exhaust gas temperature can result in smoke and engine components thermal loading, respectively. The mode switching from diesel to gas (DTG) has to be completed in a longer period (within 2 min), and as a result, smoother engine parameters variations were observed. Considering that the investigated engine in the present study is a marine dual fuel engine, the T/C needs to match for both dual fuel and diesel mode operations requirements. For that reason, the T/C matching is primarily performed in the diesel mode based on the targeted boost pressure whereas in dual fuel mode operation the EWG valve is employed to regulate the boost pressure and consequently to allow the turbocharging matching in both mode operations. Therefore, the EWG valve control is critical for avoiding compressor surging issues as well as air−fuel equivalence ratio mismatching between the diesel and the gas operating modes. Hence, careful consideration is required during the engine-T/C matching and the engine control system design to accommodate the contradictory requirements for the GTD and DTG fuel changes.

Further to the DT validation at steady state and transient conditions, the developed DD model of the EDS was validated at steady state conditions operation. The NNs incorporated in the developed EDS data-driven (DD) model, were trained for the discrete engine loads (25%, 50%, 75%, 85%, 100%) for a given range of boundary conditions. The NNs results demonstrated high accuracy in all the main predicted parameters for both the discrete and intermediate loads (max error < ±1%; NO_x emissions < ±2%). Hence, the data-driven (DD) model was found to predict with high fidelity the expected 'reference/heathy' value of each engine operational (EDS) monitored parameter (Section 5.2.2.5), in order for the EDS to calculate any deviations of the actual to the 'reference' value by comparing them.

In conclusion, the developed DT adequately captures the engine steady state and transient response indicating the effectiveness for the engine thermodynamic modelling as well as the engine control system functional modelling. The derived analysis results revealed the engine and its systems characteristics during transients with fuel and load changes enlightening the involved processes and associated phenomena. Furthermore, the DD model of the EDS was able to accurately predict the engine 'reference/healthy' response, demonstrating the UDS capability to accommodate the EDS for the engine safety performance investigation.

8.5.2 Engine design and operational limitations

The case studies used for DT validation purposes (case studies V-1 to V-3), were also analysed to identify the engine design and operational limitations, under demanding transient conditions operations. Based on the results analysis, the engine and its control system operation were delineated, and the engine operational limitations were discussed considering the engine performance parameters difference from the manufacturer alarm limits. The investigated transient operation case studies demonstrated that the engine operates in the within the manufacturer alarm limits even in the most demanding transient conditions (case study V-3) for all the examined operational parameters. However, the investigated case studies V-1 to V-3 indicated that main focus must be given in the engine components/systems related to the air–fuel equivalence ratio control and the T/C compressor surge effects, due to the tight margins observed in these

parameters. It can be inferred that the EWG; containing the EWG valve and its control system, is a critical engine component, whose response have an immediate effect on both lambda and the T/C operational parameters. For this reason, for mitigating the potential engine safety and operational implications, the engine manufacturers investigate different solutions, including the replacement of the EWG valve electric actuators by fast acting hydraulic actuators (Kalax, 2018) as well as the introduction of the ABP system for controlling the air flow from the compressor outlet to the turbine inlet (Wärtsilä, 2019a).

8.5.3 Performance and emissions

8.5.3.1 Engine settings optimisation for the gas mode

The performance-emissions trade-off optimisation in the gas mode was achieved by performing parametric runs for steady state conditions (case studies P-1 to P-3) and identifying the engine setting that provide a simultaneous reduction of CO_2 and NO_x emissions considering the engine operational limitations. The main findings of the case studies P-1 to P-3 are summarised as follows.

Increasing the engine boost pressure and/or retarding the Miller timing inlet valve closing can result in NO_x and CO_2 emissions reduction. Compared to the reference point engine settings, the engine NO_x and CO_2 emissions can be reduced up to 6% and 1.6%, respectively by increasing the inlet boost pressure by 5% and/or by retarding the Miller timing inlet valve closing by 5 ºCA. However, limitations apply due to air−fuel ratio operation window and the potential hydrocarbon emissions (methane slip) increase.

8.5.3.2 EGR and ABP systems settings optimisation for diesel mode

The performance-emissions trade-offs optimisation in the diesel mode operation was achieved by realising the EGR and ABP systems and optimising both EGR/ABP systems and engine settings. The investigated case studies (EM-1 to EM-4, ED-1 to ED-4 and ET-1 to ET-3) findings for steady state and transient conditions are summarised as follows.

The engine generated NO_x emissions can be reduced by almost 73%, when using an EGR in combination with an ABP system, demonstrating compliance with the 'Tier III' requirements. The required EGR rates range from 31% to 35% as a function of the engine load. However, the obtained NO_x emissions reduction is associated with a BSFC increase from 8.4% to 9.9% considering the respective EGR blower electrical power requirements, in comparison to the diesel mode operation without EGR/ABP systems activation. The respective BSFC penalty without considering the EGR blower power requirements were found to be 6.1% to 8.7%. The advance of SOI offered fuel savings ranging from 0.3% up to 1.8% as the load increases, with the highest BSFC reduction obtained at 100% load.

8.5.4 Safety implications

For investigating the safety implications during engine operation, a FMEA was conducted to identify the most critical engine operation scenarios under engine components faulty conditions. The derived results for the investigated case studies (S-1 to S-8) were employed to discuss the engine safety implications and operational limitations. Special attention was paid in the potential safety implications that may arise during the engine GTD and DTG operating mode switching for the cases of normal and delayed EWG valve control (case studies S-7a and S-7b). The main findings of this research are summarised as follows.

The GTD mode switching is a rapid transient that must be completed within 1 s and therefore, has a profound effect on all the engine operational parameters resulting in a number of potential hazards including compressor surging, smoke, fluctuating mechanical and thermal stresses in the various engine components. For the GTD mode switching, the turbocharger compressor surging can occur due to delayed response of the EWG valve caused by a faulty controller operation or a degraded/faulty performance of the EWG valve actuator and/or its electric motor.

As the DTG mode switching is slower (compared with the GTD transition) taking place within 2 min, the engine operating parameters demonstrated a smooth time variation. However, knocking in various engine cylinders may occur due to the air-fuel ratio variation and limitations of the engine operation within a window. Although the EWG

valve control has only slight influence to the engine operation at the DTG mode switching, the EWG valve opening limiter is deemed as essential for avoiding compressor surging.

The following safety recommendations were provided and can be used during the design and operation phases of marine DF engines.

To avoid problems with compressor surging during the engine modes switching, the EWG valve control system must be designed considering the optimal EWG valve response rate to accommodate both the GTD and DTG transitions. It is important to ensure the appropriate matching of the turbocharger with the engine for both operating modes for minimising the turbocharger lag effect during modes transitions and avoiding the compressor surging and its effects when faults in the EWG valve control are present. Furthermore, appropriate monitoring of the engine components health status including the EWG valve, the turbocharger fouling and the engine cylinders condition is required for avoiding the engine tripping and emergency shut down especially during the GTD modes switching. The engine alarm settings must be able to ignore temperature spikes in measurements before tripping the engine during the GTD transition.

Although faster diesel fuel injection control cannot be achieved due to the limitations of the diesel fuel system mechanical components, the complete engine control may be revisited and improved to reduce the combustion instabilities during the GTD modes switching (in this way, mitigating the effects of the mechanical and thermal stresses fluctuations as well as the deposits formation).

Lastly it must be mentioned that the engine control system must keep the air−fuel ratio values at adequately high levels during the DTG transition to avoid potential knocking in the engine cylinders.

8.5.5 UDS model verification

The developed DT integrated with the UDS model, were further used in simulation runs for the case studies U-1 and U-2 in order to demonstrate the benefits from UDS

application. Two sensors faulty operational scenarios were investigated in the diesel and gas operating modes at 100% load, where the speed and the boost pressure sensors were assumed faulty/uncalibrated. The key findings from the case studies U-1 and U-2 are summarised as follows.

Both speed and boost pressure sensors have a profound effect on the ECS response to the engine due to the fact that these sensors are providing feedback from the engine to the fuel control and the EWG control modules, respectively. Moreover, for both case studies U-1 and U-2, the speed sensor faulty measurements (+5%) was associated with an immediate negative effect on the engine brake power due to reduced actual engine speed. The boost pressure sensor faulty measurement (-10%) was not found to have an impact to the engine response in the case study U-1, due to the fact that the EWG is deactivated (remains closed) in the diesel mode. However, in the case study U-2, where the gas mode operation is investigated, the boost pressure sensors faulty measurements affected the EWG control output (EWG valve opening), and thus, the engine response and its operational parameters.

The developed UDS managed to successfully capture the abnormal engine operation and detect the faulty sensors measurements in both the diesel and gas operating modes. Furthermore, the UDS implemented sequential corrective actions for addressing the speed and boost pressure sensors faults or measurements uncertainty were verified, as the engine operating parameters were recovered to their 'reference' values. Lastly, considering the UDS application, the calculated RPN for the investigated case studies is reduced by 83%.

From the UDS application, the following outcomes were achieved: (a) intelligent engine monitoring capabilities in terms of sensors measurements uncertainty identification, via the novel DD model implementation, as well as advanced faults/failure detection that can guarantee the 'reference/healthy' engine performance and mitigate any potential safety implications; (b) elimination of redundant sensors and an extra layer of assurance for the personnel supervised sensors; and (c) UDS automated virtual calibration of the uncalibrated/faulty sensors via the UDS corrective response in order to ensure 'reference/healthy' engine performance until maintenance actions are implemented.

8.6 Research contribution

This section discussed the contribution and implications of this research to the theory and the industry.

8.6.1 Theoretical implications

The significant contribution of the present study to knowledge steps from the novel framework developed in this thesis for enhancing the environmental and safety performance of the marine DF engines.

In specific, this study introduces in the pertinent literature a validated digital twin of a marine DF four-stroke engine, which includes a detailed thermodynamic model of the engine along with an extensive control system functional model. Furthermore, the developed DT is able to simulate the engine performance/emission and response at both steady state and transient operation, including mode switching. It must be mentioned that in comparison with the existing literature in marine DF engines, neither the DF engine DT nor the control system functional analysis and modelling is currently presented or discussed. The detailed investigation of a large four-stroke marine DF engine transient operation by the use of the developed DT, empowered the better understanding of the involved processes, the interactions between the engine components and the analysis of the control system response effects on the engine components operation. Therefore, this allowed the mapping the engine systems/components design and operational limitations.

Furthermore, this study presents a marine DF engine performance and emissions trade-offs optimisation investigation by using an integrated DT with EGR/ABP system and their controls to simulate both steady state and transient conditions operations. Comparing to the existing literature, this work investigates a marine four-stroke DF engine with the aim to reduce emissions and optimise performance in both diesel and gas mode operations considering the engine design and operational limitations in both modes. Moreover, the potential of EGR system application on marine four-stroke DF engines in combination with the ABP system (and advanced SOI) is addressed in the present research study. The combined effects of the EGR and ABP systems to the engine response in order to

achieve 'Tier III' emissions requirements in marine four-stroke DF engines when operating is diesel model has not been previously examined. Likewise, this study addresses T/C operational limitations interconnected with the EGR system application. Finally, this investigation employs the state-of-the-art tools, such as the MOGA optimisation method, to improve the performance-emissions trade-offs of marine four-stroke DF engines with EGR and ABP systems, whilst considering engine design and operational limitations; a combination which makes the application of this tool unique.

The unique contributions related to the engine safety in the present work, involve the DT-based investigation of the engine faulty operating scenarios that may result in safety issues for the engine and its sub-systems/components, as well as the identification of hazards and their causes. Special interest attracted the analysis the DF engine operation that leads to turbocharger compressor surging due to issues related to the EWG valve and its controls during engine mode switching. Provision of safety recommendations for the engine design by considering the derived simulation results, was provided and discussed. Hence, by considering the existing literature review, the safety contributions addressed in this work, have not been previously reported, consisting this study unique.

Furthermore, the introduction of the developed EDS model (including a state-of-the-art DD model with NNs) is developed based on a distinctive methodology to realise intelligent engine monitoring and actuators/sensors advanced faults/failure detection on marine DF engines that has not been previously established. In addition, the integrated DT incorporating the developed EDS and the existing engine controls into a novel UDS, all thoroughly presented and discussed in this thesis, paves a unique way towards innovative DT-based investigations for enhancing marine DF engines.

8.6.2 Industrial implications

The digitalisation is the technological opportunity to increase engine and ship efficiency, improve the asset availability and create more effective business models. In this respect, the marine industry implications of this work have a direct impact to the engine manufacturers, the ship owners/operators and the classification societies.

8.6.2.1 Engine manufacturers

The digitalisation and AI/ ML tools capabilities has already drawn the attention of the engine manufacturers in order to strengthen their competitiveness in the marine market by offering more reliable and efficient products, with the aims to cover the industry needs and remain profitable. Therefore, the engine manufacturers continuously seek for opportunities to develop their products and provide effective services that will offer savings to the ship owners/operators whist complying with the established regulatory framework.

The proposed framework has proven to offer a number of apparent benefits that would be of interest for the engine manufacturers. Amongst these benefits, is the high-level intelligent engine performance monitoring and real-time engine performance parameters optimisation that can be achieved by implementing the developed UDS. Furthermore, the UDS exhibits advanced sensors diagnostics obtaining sensors measurement uncertainty minimisation, resulting in detailed diagnostics of engine sensors/actuators faults along with recommended corrective actions. Considering the existing manufacturer approach on the diagnostics systems, the benefits of the developed UDS application can be realised. Lastly, the application of the proposed framework offers effective analysis on a number of engine monitored parameters and indicates deviations from the engine 'healthy' state for a number of measured parameters. In this respect, the engine performance optimisation, the control of measurement uncertainties as well as the engine risk mitigation (or safety enhancement) can be obtained.

8.6.2.2 Ship-owners and operators

The ship owners and/or operators is another major group that could be impacted by the proposed framework implementation.

By employing the first methodology of the proposed framework, it can be inferred that the ship owners/operators can resolve the "Tier III" compliance issue for diesel engines or DF engines (operating in diesel mode). Nevertheless, due to the established decarbonisation strategy, the utilisation of the Very Low Sulphur Fuel Oil (VLSFO) and Ultra-Low Sulphur Fuel Oil (ULSFO) is imminent.

Furthermore, as machine learning algorithms gain greater levels of intelligence, ship owners who have invested in AI will find competitive advantages. Thus, by employing the proposed framework (and specifically the UDS) the ship owners/operators are expected to experience improved maintenance costs based on the advance sensors and actuators faults/failure detection, as well as reduced down-time due to failures.

The use of the collected data when combined with the proposed tools/methods can detect and quickly solve issues, optimise the engine settings, provide operational recommendations, and coordinate further technical support. Performance-wise, ship operators can also benefit by the UDS application via the intelligent engine monitoring and UDS correction actions, as the engine will continue to operate at its 'healthy' levels, whereas the operator will be advised to proceed to the necessary maintenance actions. Lastly, by comparing the actual engine operational parameters to the reference/ healthy values in UDS (as specifically EDS), the operators can acquire the engine health status for further assessment and consider, if necessary, maintenance actions to ensure the engine 'healthy' performance.

8.6.2.3 Classification Societies

Considering the influence of the digitalisation as an outcome of the fourth industrial revolution (Industry 4.0), the classification societies have already adjusted to the forthcoming changes in the maritime industry. Indicatively LR (2018) has established a 'Digital Compliance Framework' to provide DT assurance services and digital compliance. Digital compliance is the independent evaluation, involving a number of verification and validation activities, to improve confidence in digital twins and supporting algorithms. This 'Digital Compliance Framework' relies on a DT approved provider (by the Class) and the asset owner/operator employing the DT. The DT approved provider is responsible for the DT review and approval, whereas the Class approves the DT commissioning and monitors the DT function and performance in the field over time. In this respect, the marine four-stroke DF engine DT developed under this research study provides extensive knowledge on the modelling principles, the functional processes of a DT that can be considered during the approval process as well as reveals the challenges that can be introduced by the use of a DT.

8.7 Future research recommendations

Through this research, a number of topics for improvement and future investigation were identified. The following areas are recommended for research:

- The engine knocking and misfiring phenomena can be addressed via extending the developed DT combined with AI tools and control techniques.
- Methane slip consideration; this can be achieved by integrating the developed engine thermodynamic model with a detailed chemical kinetics software/tools for predicting the unburned HC emissions and other incomplete combustion species with adequate accuracy.
- Phenomenological combustion model; development and customisation of a phenomenological combustion model that takes into account the varying DF engine conditions and EGR rates.
- Develop the control system modules considering modern control techniques such as optimal controls and the 'multiple-input multiple-output' (MIMO) method whist considering stability and robustness.
- The DT and UDS can be further extended to include identification of engine mechanical failures (e.g. exhaust valves, diesel injectors etc.) as well as engine components degradation.
- Engine components dynamic risk monitoring via DT and AI tools to provide decision support for risk control options to the crew and operators.

8.8 Chapter summary

In this Chapter, the realisation of this work research objectives and set aim was discussed and justified. The research novelty as well as the research contribution to the academia and the maritime industry were demonstrated. Lastly, the recommendations for future work were outlined.

9 REFERENCES

Aaltonen, P., Järvi, A., Vaahtera, P. & Widell, K. 2016. New DF Engine Portfolio (Wärtsilä 4-Stroke). Proceedings of the 28th CIMAC World Congress on Combustion Engine Technology, 6–10 June 2016, Helsinki, Finland.

Abadie, L. M. & Goicoechea, N. 2019. Powering newly constructed vessels to comply with ECA regulations under fuel market prices uncertainty: Diesel or dual fuel engine? *Transportation Research Part D: Transport and Environment,* 67**,** 433-448, DOI: https://doi.org/10.1016/j.trd.2018.12.012.

ABS 2013. Ship Energy Efficiency Measures - Status and Guidance. Available: https://ww2.eagle.org/content/dam/eagle/advisories-and-debriefs/ABS_Energy_Efficiency_Advisory.pdf.

Ahmed, S. & Gu, X.-C. 2020. Accident-based FMECA study of Marine boiler for risk prioritization using Fuzzy expert system. *Results in Engineering***,** 100123, DOI: https://doi.org/10.1016/j.rineng.2020.100123.

Alegret, G., Llamas, X., Vejlgaard-Laursen, M. & Eriksson, L. 2015. Modeling of a Large Marine Two-Stroke Diesel Engine with Cylinder Bypass Valve and EGR System. *IFAC-PapersOnLine,* 48**,** 273-278, DOI: https://doi.org/10.1016/j.ifacol.2015.10.292.

Amr, I. & Saiful, B. 2008. Optimization of a natural gas SI engine employing EGR strategy using a two-zone combustion model. *Fuel,* 87**,** 1824-1834, DOI: https://doi.org/10.1016/j.fuel.2007.10.004.

Antony, J. 2014. 6 - Full Factorial Designs. *In:* ANTONY, J. (ed.) *Design of Experiments for Engineers and Scientists (Second Edition).* Oxford: Elsevier, Available: http://www.sciencedirect.com/science/article/pii/B9780080994178000067.

Attfield, M. D., Schleiff, P. L., Lubin, J. H., Blair, A., Stewart, P. A., Vermeulen, R., Coble, J. B. & Silverman, D. T. 2012. The Diesel Exhaust in Miners Study: A Cohort Mortality Study With Emphasis on Lung Cancer. *JNCI: Journal of the National Cancer Institute,* 104**,** 869-883, DOI: https://doi.org/10.1093/jnci/djs035.

Ayhan, V., Çangal, Ç., Cesur, İ., Çoban, A., Ergen, G., Çay, Y., Kolip, A. & Özsert, İ. 2020. Optimization of the factors affecting performance and emissions in a diesel engine using biodiesel and EGR with Taguchi method. *Fuel,* 261**,** 116371, DOI: https://doi.org/10.1016/j.fuel.2019.116371.

Balaban, E., Saxena, A., Bansal, P., Goebel, K. & Curran, S. 2009. Modeling, detection, and disambiguation of sensor faults for aerospace applications. *IEEE Sensors Journal,* 9, DOI: https://doi.org/10.1109/JSEN.2009.2030284.

Baldi, F., Theotokatos, G. & Andersson, K. 2015. Development of a combined mean value–zero dimensional model and application for a large marine four-stroke Diesel engine

simulation. *Applied energy,* 154**,** 402-415, DOI: https://doi.org/10.1016/j.apenergy.2015.05.024.

Banck, A., Sixel, E. & Rickert, C. 2016. Dual Fuel Engine optimized for marine applications. Proceedings of the 28th CIMAC World Congress on Combustion Engine Technology, 6–10 June 2016, Helsinki, Finland.

Banks, J., Hines, J., Lebold, M., Campbell, R. & Begg, C. 2001. Failure modes and predictive diagnostics considerations for diesel engines.

Barroso, P., Ribas, X., Pita, M., Dominguez, J., De Seia, E. & Maria Garcia, J. 2013. Study of dual-fuel (diesel and natural gas) particle matter and CO2 emissions of a heavy-duty diesel engine during transient operation. *Combustion Engines,* R. 52, nr 2**,** 3-11, DOI, http://www.combustion-engines.eu/entityfiles/files/articles_published/PTNSS-2013-201.pdf

Benvenuto, G., Laviola, M. & Campora, U. 2014. *Simulation model of a methane-fuelled four stroke marine engine for studies on low emission propulsion systems.*

Boeckhoff, N., Heider, G. & Hagl, P. 2010. Operational experience of the 51/60 DF from MAN Diesel SE. Proceedings of the 26th CIMAC World Congress on Combustion Engine Technology, 14-17 June 2010, Bergen, Norway.

Bolbot, V., Theotokatos, G., Boulougouris, E. & Vassalos, D. 2019a. Comparison of diesel-electric with hybrid-electric propulsion system safety using System-Theoretic Process Analysis. Propulsion and Power Alternatives, 2019a, London, United Kingdom. Royal Institute of Naval Architects, 55-61.

Bolbot, V., Theotokatos, G., Bujorianu, L. M., Boulougouris, E. & Vassalos, D. 2019b. Vulnerabilities and safety assurance methods in Cyber-Physical Systems: A comprehensive review. *Reliability Engineering & System Safety,* 182**,** 179-193, DOI: https://doi.org/10.1016/j.ress.2018.09.004.

Bolbot, V., Theotokatos, G. & Vassalos, D. 2018. Using system-theoretic process analysis and event tree analysis for creation of a fault tree of blackout in the Diesel-Electric Propulsion system of a cruise ship. International Marine Design Conference XIII, 2018, Helsinki, Finland. CRC Press, 691-699.

Bolton, A., Butler, L., Dabson, I., Enzer, M., Evans, M., Fenemore, T., Harradence, F., Keaney, E., Kemp, A., Luck, A., Pawsey, N., Saville, S., Schooling, J., Sharp, M., Smith, T., Tennison, J., Whyte, J., Wilson, A. & Makri, C. 2018. Gemini Principles. CDBB. Available: https://doi.org/10.17863/CAM.32260.

Bondarenko, O. & Fukuda, T. 2020. Development of a diesel engine's digital twin for predicting propulsion system dynamics. *Energy,* 196**,** 117126, DOI: https://doi.org/10.1016/j.energy.2020.117126.

Bouman, E. A., Lindstad, E., Rialland, A. I. & Strømman, A. H. 2017. State-of-the-art technologies, measures, and potential for reducing GHG emissions from shipping–a review. *Transportation Research Part D: Transport and Environment,* 52**,** 408-421, DOI: https://doi.org/10.1016/j.trd.2017.03.022.

Bows–Larkin, A., Mander, S., Gilbert, P., Traut, M., Walsh, C. & Anderson, K. 2014. High Seas, High Stakes (High Seas Final Report). Available: http://www.lowcarbonshipping.co.uk/files/ucl_admin/High_Seas_High_Stakes_High_Seas_Project_Final_Report.pdf.

Brynolf, S., Fridell, E. & Andersson, K. 2014. Environmental assessment of marine fuels: liquefied natural gas, liquefied biogas, methanol and bio-methanol. *Journal of Cleaner Production,* 74**,** 86-95, DOI: https://doi.org/10.1016/j.jclepro.2014.03.052.

BSI 2006. Analysis techniques for system reliability - Procedure for failure mode and effects analysis (FMEA). London: British Standards Instituition, Available.

Cameretti, M. C., Tuccillo, R., De Simio, L., Iannaccone, S. & Ciaravola, U. 2016. A numerical and experimental study of dual fuel diesel engine for different injection timings. *Applied Thermal Engineering,* 101**,** 630-638, DOI: https://doi.org/10.1016/j.applthermaleng.2015.12.071.

Castillo Buenaventura, F., Witrant, E., Talon, V. & Dugard, L. 2015. Air Fraction and EGR Proportion Control for Dual Loop EGR Diesel Engines. *Ingeniería y Universidad,* 19**,** 115-133, DOI: http://dx.doi.org/10.11144/Javeriana.iyu19-1.aegr.

Center, N. S. W. 2011. *Handbook of reliability prediction procedures for mechanical equipment,* West Bethesda, Maryland, United States, Naval Surface Warfare Center.

Černík, F. 2018. *Phenomenological Combustion Modeling for Optimization of Large 2-stroke Marine Engines under both Diesel and Dual Fuel Operating Conditions.* Ph.D, Czech Technical University in Prague, Available: https://dspace.cvut.cz/handle/10467/75564.

Chai, Y., Peng, X., Xu, L. & Shi, J. Research on Fault Diagnosis of Marine Diesel Engine Based on Integrated Similarity. *In:* ZHANG, J., ed. Applied Informatics and Communication, 2011// 2011 Berlin, Heidelberg. Springer Berlin Heidelberg, 678-685.

Christen, C. & Brand, D. 2013. IMO tier 3: gas and dual fuel engines as a clean and efficient solution. Proceedings of the 27th CIMAC World Congress on Combustion Engine Technology, 13–16 May 2013, Shanghai, China.

Cicek, K. & Celik, M. 2013. Application of failure modes and effects analysis to main engine crankcase explosion failure on-board ship. *Safety science,* 51**,** 6-10, DOI: https://doi.org/10.1016/j.ssci.2012.06.003.

Cicek, K., Turan, H. H., Topcu, Y. I. & Searslan, M. N. Risk-based preventive maintenance planning using Failure Mode and Effect Analysis (FMEA) for marine engine systems. Engineering Systems Management and Its Applications (ICESMA), 2010 Second International Conference on, 2010. IEEE, 1-6.

Cichowicz, J., Theotokatos, G. & Vassalos, D. 2015. Dynamic energy modelling for ship life-cycle performance assessment. *Ocean Engineering,* 110**,** 49-61, DOI: https://doi.org/10.1016/j.oceaneng.2015.05.041.

Coble, A. R., Smallbone, A., Bhave, A., Mosbach, S., Kraft, M., Niven, P. & Amphlett, S. 2011. Implementing detailed chemistry and in-cylinder stratification into 0/1-D IC engine cycle simulation tools. SAE 2011 World Congress & Exhibition April 12 2011, United States. SAE International.

Deb, K. & Jain, H. 2014. An Evolutionary Many-Objective Optimization Algorithm Using Reference-Point-Based Nondominated Sorting Approach, Part I: Solving Problems With Box Constraints. *IEEE Transactions on Evolutionary Computation,* 18**,** 577-601, DOI: 10.1109/TEVC.2013.2281535.

Dikis, K. 2017. *Establishment of a novel predictive reliability assessment strategy for ship machinery.* Doctor of Philosophy, University of Strathclyde, Available: https://pureportal.strath.ac.uk/en/studentTheses/establishment-of-a-novel-predictive-reliability-assessment-strate.

Dimopoulos, G., Georgopoulou, C., Stefanatos, I., Zymaris, A. & Kakalis, N. 2014. A general-purpose process modelling framework for marine energy systems. *Energy Conversion and Management,* 86**,** 325-339, DOI: https://doi.org/10.1016/j.enconman.2014.04.046.

DNV-GL. 2019. *LNG as ship fuel - A focus on the current and future use of LNG as fuel in shipping* [Online]. Available: https://www.dnvgl.com/maritime/lng/index.html [Accessed 14 June].

Duan, X., Liu, Y., Liu, J., Lai, M.-C., Jansons, M., Guo, G., Zhang, S. & Tang, Q. 2019. Experimental and numerical investigation of the effects of low-pressure, high-pressure and internal EGR configurations on the performance, combustion and emission characteristics in a hydrogen-enriched heavy-duty lean-burn natural gas SI engine. *Energy Conversion and Management,* 195**,** 1319-1333, DOI: https://doi.org/10.1016/j.enconman.2019.05.059.

Easterby-Smith, M., Thorpe, R. & Jackson, P. R. 2012. *Management research*, Sage.

EC. 2019. *Equipment for potentially explosive atmospheres (ATEX)* [Online]. Available: https://ec.europa.eu/growth/sectors/mechanical-engineering/atex_en [Accessed 13/11/2019].

EGCSA. 2014. NOx Reduction by Exhaust Gas Recirculation – MAN explains. *Technologies.* Available: https://www.egcsa.com/exhaust-gas-recirculation-explained/ [Accessed 17 June 2019].

EMSA. 2015. *Environment - Air Emissions* [Online]. European Maritime Safety Agency (EMSA). Available: http://emsa.europa.eu/main/air-pollution.html [Accessed 13 June].

EPA 2010. Control of Emissions From New Marine Compression-Ignition Engines at or Above 30 Liters per Cylinder. *In:* (EPA), U. S. E. P. A. (ed.) *Federal Register Volume 75, Issue 83.* Office of the Federal Register, National Archives and Records Administration, Available: https://www.govinfo.gov/content/pkg/FR-2010-04-30/pdf/FR-2010-04-30.pdf, [Accessed 13 June 2019].

Fabio, B., Vincenzo, D. B. & Luigi, T. 2015. EGR Systems Employment to Reduce the Fuel Consumption of a Downsized Turbocharged Engine at High-load Operations. *Energy Procedia,* 81**,** 866-873, DOI: https://doi.org/10.1016/j.egypro.2015.12.134.

Fathi, M., Jahanian, O. & Shahbakhti, M. 2017. Modeling and controller design architecture for cycle-by-cycle combustion control of homogeneous charge compression ignition (HCCI) engines – A comprehensive review. *Energy Conversion and Management,* 139**,** 1-19, DOI: https://doi.org/10.1016/j.enconman.2017.02.038.

Feng, L., Tian, J., Long, W., Gong, W., Du, B., Li, D. & Chen, L. 2016. Decreasing NOx of a Low-Speed Two-Stroke Marine Diesel Engine by Using In-Cylinder Emission Control Measures. *Energies,* 9, DOI: https://doi.org/10.3390/en9040304.

Fiedler, M., Fiedler, H. & Boy, P. 2013. Experimental Experience Gained with a Long-Stroke Medium-Speed Diesel Research engine using Two Stage Turbo Charging and Extreme Miller Cycle. Proceedings of the 27th CIMAC World Congress on Combustion Engine Technology, 13-17 May 2013, Shanghai, China.

Florea, R., Taraza, D., Henein, N. A. & Bryzik, W. 2008. Transient Fluid Flow and Heat Transfer in the EGR Cooler. DOI: https://doi.org/10.4271/2008-01-0956.

Gaeid, K. S., Ping, H. W., Khalid, M. & Masaoud, A. 2012. Sensor and sensorless fault tolerant control for induction motors using a wavelet index. *Sensors (Basel),* 12**,** 4031-4050, DOI: https://doi.org/10.3390/s120404031.

García Valladolid, P., Tunestål, P., Monsalve-Serrano, J., García, A. & Hyvönen, J. 2017. Impact of diesel pilot distribution on the ignition process of a dual fuel medium speed marine engine. *Energy Conversion and Management,* 149**,** 192-205, DOI: https://doi.org/10.1016/j.enconman.2017.07.023.

Gautier, P., Albrecht, A., Chasse, A., Moulin, P., Pagot, A., Fontvieille, L. & Issartel, D. 2009. A Simulation Study of the Impact of LP EGR on a Two-Stage Turbocharged Diesel Engine. *Oil & Gas Science and Technology - Rev. IFP,* 64**,** 361-379, DOI: https://doi.org/10.2516/ogst/2009019.

Geertsma, R. D., Visser, K. & Negenborn, R. R. 2018. Adaptive pitch control for ships with diesel mechanical and hybrid propulsion. *Applied Energy,* 228**,** 2490-2509, DOI: https://doi.org/10.1016/j.apenergy.2018.07.080.

Georgescu, I., Stapersma, D. & Mestemaker, B. T. W. 2016. Dynamic Behaviour of Gas and Dual-Fuel Engines: Using Models and Simulations to Aid System Integration. Proceedings of the 28th CIMAC World Congress on Combustion Engine Technology, 6–10 June 2016, Helsinki, Finland.

Graf, J. 2013. *PID Control: Ziegler-Nichols Tuning*, CreateSpace Independent Publishing Platform.

Grøne, O. 2016. IMO Tier III strategies under the light of changes in the oil market. *In:* MAN (ed.). CIMAC, Available: https://www.cimac.com/cms/upload/events/circles/circle_2016_SMM/MAN_K_Aabo_CIMA_Circle_Emission_Tier_III_sep_2016_MDT1.pdf, [Accessed 17 June 2019].

GT 2019. GT-ISE Manual. Gamma Technologies, Available.

GT. 2020. *Gamma Technologies* [Online]. Available: https://www.gtisoft.com [Accessed 07/04/2020].

Gunton, P. 2019. Scrubber orders boom but alternative fuels show promise. Available: https://shipinsight.com/articles/scrubber-orders-boom-but-alternative-fuels-show-promise?_lrsc=7e286be8-d629-4337-a62c-4df593d580fd [Accessed 30/11/2019].

Hanson, R. K. & Salimian, S. 1984. *Survey of Rate Constants in the N/H/O System,* New York, United States, Springer.

Hegab, A., La Rocca, A. & Shayler, P. 2017. Towards keeping diesel fuel supply and demand in balance: Dual-fuelling of diesel engines with natural gas. *Renewable and Sustainable Energy Reviews,* 70**,** 666-697, DOI: https://doi.org/10.1016/j.rser.2016.11.249.

Hendrik, L., Andreas, B. & Eike, S. 2016. Investigation of alternative dual fuel engine concepts. Proceedings of the 28th CIMAC World Congress on Combustion Engine Technology, 6–10 June 2016, Helsinki, Finland.

Herdzik, J. 2011. LNG as a Marine Fuel - Possibilities and Problems. *Journal of KONES Powertrain and Transport,* 18, DOI, https://kones.eu/ep/2011/vol18/no2/22.pdf

Heredia, G., Ollero, A., Bejar, M. & Mahtani, R. 2008. Sensor and actuator fault detection in small autonomous helicopters. *Mechatronics,* 18**,** 90-99, DOI: https://doi.org/10.1016/j.mechatronics.2007.09.007.

Heywood, J. B. 2018. *Internal combustion engine fundamentals,* New York, McGraw-Hill Education.

Higashida, M., Nakamura, T., Onishi, I., Yoshizawa, K., Takata, H. & Hosono, T. 2013. Newly Developed Combined EGR & WEF System to comply with IMO NOx Regulation Tier 3 for Two-stroke Diesel Engine. Proceedings of the 27th CIMAC World Congress on Combustion Engine Technology, 13-17 May 2013, Shanghai, China.

Hiraoka, N., Miyanagi, A., Kuroda, K., Ito, K., Nakagawa, T. & Ueda, T. 2016a. The World's First Onboard Verification Test of UE Engine with Low Pressure EGR complied with IMO's NOx Tier III Regulations. Mitsubishi Heavy Industries, Available: http://www.dieselduck.info/machine/06%20safety/2016%20MHI%20LP%20EGR.pdf, [Accessed 17 June 2019].

Hiraoka, N., Ueda, T., Nakagawa, T. & Ito, K. 2016b. Development of Low Pressure Exhaust Gas Recirculation system for Mitsubishi UE Diesel Engine. Proceedings of the 28th CIMAC World Congress on Combustion Engine Technology, 6-10 June 2016b, Helsinki, Finland.

Hiroyasu, T. 2004. Diesel Engine Design using Multi-Objective Genetic Algorithm. Japan/US Workshop on Design Environment, 26 February 2004.

Hountalas, D. T. 2000. Prediction of marine diesel engine performance under fault conditions. *Applied Thermal Engineering,* 20**,** 1753-1783, DOI: https://doi.org/10.1016/S1359-4311(00)00006-5.

Hountalas, D. T. & Kouremenos, A. D. 1999. Development and application of a fully automatic troubleshooting method for large marine diesel engines. *Applied Thermal Engineering,* 19**,** 299-324, DOI: https://doi.org/10.1016/S1359-4311(98)00048-9.

IACS 2014. Recommendation for the FMEA process for diesel engine control systems. *In:* MACHINERY (ed.). International Association of Classification Societies (IACS), Available: www.iacs.org.uk/download/1938, [Accessed 14 June 2019].

IACS. 2019. *Unified Requirements* [Online]. IACS. Available: http://www.iacs.org.uk/publications/unified-requirements/ [Accessed 13/11/2019].

Ibrahim, A. & Bari, S. 2008. Optimization of a natural gas SI engine employing EGR strategy using a two-zone combustion model. *Fuel,* 87**,** 1824-1834, DOI: https://doi.org/10.1016/j.fuel.2007.10.004.

IEC 2006. IEC 60812—Analysis Techniques for System Reliability—Procedure for Failure Mode and Effects Analysis (FMEA) *In:* COMMISSION, I. E. (ed.). Geneva, Switzerland, Available.

IEC. 2019. *International standards for all electrical, electronic and related technologies* [Online]. Available: https://www.iec.ch [Accessed 13/11/2019].

IMO. 2014a. *NOx Technical Code 2008 (as ammended by resolution MEPC.251.(66))* [Online]. 4 Albert Embankment, London SE1 7SR. Available:

http://www.imo.org/en/KnowledgeCentre/IndexofIMOResolutions/Marine-Environment-Protection-Committee-%28MEPC%29/Documents/MEPC.251%2866%29.pdf [Accessed 13/11/2019].

IMO. 2014b. *Third IMO GHG Study 2014* [Online]. 4 Albert Embankment, London SE1 7SR. Available: http://www.imo.org/en/OurWork/Environment/PollutionPrevention/AirPollution/Documents/Third%20Greenhouse%20Gas%20Study/GHG3%20Executive%20Summary%20and%20Report.pdf [Accessed 13/11/2019].

IMO. 2018. *Inintial IMO strategy on reduction of GHG emissions from ships* [Online]. Available: http://www.imo.org/en/KnowledgeCentre/IndexofIMOResolutions/Marine-Environment-Protection-Committee-%28MEPC%29/Documents/MEPC.304%2872%29.pdf [Accessed 13/11/2019].

IMO. 2019a. *Energy Efficiency Measures* [Online]. Available: http://www.imo.org/en/OurWork/Environment/PollutionPrevention/AirPollution/Pages/Technical-and-Operational-Measures.aspx [Accessed 13/11/2019].

IMO. 2019b. *International Code of Safety for Ship Using Gases or Other Low-flashpoint Fuels (IGF Code)* [Online]. Available: http://www.imo.org/en/OurWork/Safety/SafetyTopics/Pages/IGF-Code.aspx [Accessed 13/11/2019].

IMO. 2019c. *International Code of the Construction and Equipment of Ships Carrying Liquefied Gases in Bulk* [Online]. Available: http://www.imo.org/en/OurWork/Safety/Cargoes/CargoesInBulk/Pages/IGC-Code.aspx [Accessed 13/11/2019].

IMO. 2019d. *International Convention for the Prevention of Pollution from Ships - MARPOL Annex VI - Regulations for the Prevention of Air Pollution from Ships* [Online]. Available: http://www.imo.org/en/OurWork/Environment/PollutionPrevention/AirPollution/Pages/Air-Pollution.aspx [Accessed 13/11/2019].

IMO. 2019e. *International Convention for the Safety of Life at Sea (SOLAS), 1974* [Online]. Available: https://ec.europa.eu/growth/sectors/mechanical-engineering/atex_en [Accessed 13/11/2019].

IMO. 2019f. *Marine Environment Protection Committee (MEPC), 74th session, 13-17 May 2019* [Online]. IMO. Available: http://www.imo.org/en/MediaCentre/MeetingSummaries/MEPC/Pages/MEPC-74th-session.aspx [Accessed 13/11/2019].

Jacobs, P. 2012. *LNG engine technology* [Online]. Wärtsilä. Available: http://www.glmri.org/downloads/focusAreas/presentations/jacobs2-2012.pdf [Accessed 24/12/2019].

Jafarian, K., Mobin, M., Jafari-Marandi, R. & Rabiei, E. 2018. Misfire and valve clearance faults detection in the combustion engines based on a multi-sensor vibration signal monitoring. *Measurement,* 128**,** 527-536, DOI: https://doi.org/10.1016/j.measurement.2018.04.062.

Jaliliantabar, F., Ghobadian, B., Najafi, G., Mamat, R. & Carlucci, A. P. 2019. Multi-objective NSGA-II optimization of a compression ignition engine parameters using biodiesel fuel and exhaust gas recirculation. *Energy,* 187**,** 115970, DOI: https://doi.org/10.1016/j.energy.2019.115970.

Jarf, C. & Sutkowski, M. 2009. The Wärtsilä 32GD engine for heavy gases. DOI, http://www.combustion-engines.eu/entityfiles/files/articles_published/PTNSS-2009-SS2-C015.pdf

Järvi, A. 2010. Methane slip reduction in Wärtsilä lean burn gas engines. Proceedings of the 26th CIMAC World Congress on Combustion Engine Technology, 14–17 June 2010, Bergen, Norway.

Jean-Michel, H. 2012. Retrofit Moteur Diesel Wärtsilä en Dual fuel. ENSM, Marseille, France: Wärtsilä, Available: https://cdnimg.supmaritime.fr/wp-

content/uploads/2018/11/Retrofit_moteur_diesel_Wartsila.pdf, [Accessed 13 June 2019].

Jeong, B., Suk Lee, B. & Zhou, P. 2017. Quantitative risk assessment of fuel preparation room having high-pressure fuel gas supply system for LNG fuelled ship. *Ocean Engineering,* 137**,** 450-468, DOI: https://doi.org/10.1016/j.oceaneng.2017.04.002.

Jeppesen, M. 2016. Tier III service experience. *In:* TURBO, M. D. (ed.). SNAME, Athens, Greece, Available: https://higherlogicdownload.s3.amazonaws.com/SNAME/a09ed13c-b8c0-4897-9e87-eb86f500359b/UploadedImages/2016-2017/jeppesen.TIER_III_service_2.2016.SECP.pdf, [Accessed 17 June 2019].

Ji, W., Li, A., Lu, X., Huang, Z. & Zhu, L. 2019. Numerical study on NOx and ISFC co-optimization for a low-speed two-stroke engine via Miller cycle, EGR, intake air humidification, and injection strategy implementation. *Applied Thermal Engineering,* 153**,** 398-408, DOI: https://doi.org/10.1016/j.applthermaleng.2019.03.035.

Jiang, Z., Mao, Z., Wang, Z. & Zhang, J. 2017. Fault Diagnosis of Internal Combustion Engine Valve Clearance Using the Impact Commencement Detection Method. *Sensors,* 17**,** 2916, DOI: https://doi.org/10.3390/s17122916.

Jo, Y., Min, K., Jung, D., Sunwoo, M. & Han, M. 2019. Comparative study of the artificial neural network with three hyper-parameter optimization methods for the precise LP-EGR estimation using in-cylinder pressure in a turbocharged GDI engine. *Applied Thermal Engineering,* 149**,** 1324-1334, DOI: https://doi.org/10.1016/j.applthermaleng.2018.12.139.

Jung, M., Niculita, O. & Skaf, Z. 2018. Comparison of Different Classification Algorithms for Fault Detection and Fault Isolation in Complex Systems. *Procedia Manufacturing,* 19**,** 111-118, DOI: https://doi.org/10.1016/j.promfg.2018.01.016.

Kaario, O., Sarjovaara, T., Larmi, M. & Wik, C. 2016. Zero NOx emission in large-bore medium speed engines with exhaust gas recirculation. Proceedings of the 28th CIMAC World Congress on Combustion Engine Technology, 6–10 June 2016, Helsinki, Finland.

Kalax, J. 2018. Wärtsilä - Small changes, big results. *in detail - Wärtsilä Technical Journal.* Available: https://www.wartsila.com/twentyfour7/in-detail/wartsila-20-small-changes-big-results [Accessed 14 June 2019].

Kaltoft, J. & Preem, M. 2013. Development of integrated EGR system for two-stroke diesel engines. Proceedings of the 27th CIMAC World Congress on Combustion Engine Technology, 13-17 May 2013, Shanghai, China.

Karim, G. A. 2015. *Dual-fuel diesel engines*, CRC Press.

Kayri, M. 2016. Predictive Abilities of Bayesian Regularization and Levenberg–Marquardt Algorithms in Artificial Neural Networks: A Comparative Empirical Study on Social Data. *Mathematical and Computational Applications,* 21, DOI: https://doi.org/10.3390/mca21020020.

Kindt, S. & Sørensen, O. 2016. MAN B&W Two-stroke Engines Latest design development within engine types, Tier III and multiple gas fuels. Proceedings of the 28th CIMAC World Congress on Combustion Engine Technology, 6–10 June 2016, Helsinki, Finland.

Kowalski, J., Krawczyk, B. & Woźniak, M. 2017. Fault diagnosis of marine 4-stroke diesel engines using a one-vs-one extreme learning ensemble. *Engineering Applications of Artificial Intelligence,* 57**,** 134-141, DOI: https://doi.org/10.1016/j.engappai.2016.10.015.

Krishnan, S. R., Biruduganti, M., Mo, Y., Bell, S. R. & Midkiff, K. C. 2002. Performance and heat release analysis of a pilot-ignited natural gas engine. *International Journal of Engine Research,* 3**,** 171-184, DOI: https://doi.org/10.1243/14680870260189280.

Kumaraswamy, A. & Prasad, B. D. 2012. Performance Analysis of a Dual Fuel Engine Using LPG and Diesel with EGR System. *Procedia Engineering,* 38**,** 2784-2792, DOI: https://doi.org/10.1016/j.proeng.2012.06.326.

Kyrtatos, A., Spahni, M., Hensel, S., Züger, R. & Sudwoj, G. 2016a. The Development of the Modern Low-Speed Two-Stroke Marine Diesel Engine. Proceedings of the 28th CIMAC World Congress on Combustion Engine Technology, 6-10 June 2016a, Helsinki, Finland.

Kyrtatos, P., Bolla, M., Lee, Y., Yoon, W. & Boulouchos, K. 2019. Combustion Modeling of a Medium- Speed Dual-Fuel Engine Using Double Vibe Function. Proceedings of the 29th CIMAC World Congress on Combustion Engine Technology, 10-14 June 2019, Vancouver, Canada.

Kyrtatos, P., Herrmann, K., Hoyer, K. & Boulouchos, K. 2016b. Combination of EGR and Fuel-Water Emulsions for Simultaneous NOx and Soot Reduction in a Medium Speed Diesel Engine. Proceedings of the 28th CIMAC World Congress on Combustion Engine Technology, 6-10 June 2016b, Helsinki, Finland.

Ladommatos, N., M. Abdelhalim, S. & Zhao, H. 2000. The Effects of Exhaust Gas Recirculation on Diesel Combustion and Emissions. *International Journal of Engine Research,* 1**,** 107-126, DOI: https://doi.org/10.1243/1468087001545290.

Lavoie, G. A., Heywood, J. B. & Keck, J. C. 1970. Experimental and Theoretical Study of Nitric Oxide Formation in Internal Combustion Engines. *Combustion Science and Technology,* 1**,** 313-326, DOI: https://doi.org/10.1080/00102206908952211.

Lazakis, I., Raptodimos, Y. & Varelas, T. 2018. Predicting ship machinery system condition through analytical reliability tools and artificial neural networks. *Ocean Engineering,* 152**,** 404-415, DOI: https://doi.org/10.1016/j.oceaneng.2017.11.017.

Lei, S., Kangyao, D., Yuehua, Q., Yong, G. & Bo, L. 2019. Research and Optimization of Low-Speed Two-Stroke Engines Using High Pressure EGR with Cylinder Bypass. Proceedings of the 29th CIMAC World Congress on Combustion Engine Technology, 10-14 June 2019, Vancouver, Canada.

Leigh, J. 1987. *Applied control theory,* London, The Institution of Engineering and Technology.

Leufvén, O. & Eriksson, L. 2013. A surge and choke capable compressor flow model—Validation and extrapolation capability. *Control Engineering Practice,* 21**,** 1871-1883, DOI: https://doi.org/10.1016/j.conengprac.2013.07.005.

Li, J., Wu, B. & Mao, G. 2015. Research on the performance and emission characteristics of the LNG-diesel marine engine. *Journal of Natural Gas Science and Engineering,* 27**,** 945-954, DOI: https://doi.org/10.1016/j.jngse.2015.09.036.

Li, J., Yu, X., Xie, J. & Yang, W. 2020. Mitigation of high pressure rise rate by varying IVC timing and EGR rate in an RCCI engine with high premixed fuel ratio. *Energy,* 192**,** 116659, DOI: https://doi.org/10.1016/j.energy.2019.116659.

Li, Y. 2016. Research on the influence of diesel injection law to combustion process of micro ignition dual fuel engine. Proceedings of the 28th CIMAC World Congress on Combustion Engine Technology, 6–10 June 2016, Helsinki, Finland

Li, Y., Wang, P., Wang, S., Liu, J., Xie, Y. & Li, W. 2019. Quantitative investigation of the effects of CR, EGR and spark timing strategies on performance, combustion and NOx emissions characteristics of a heavy-duty natural gas engine fueled with 99% methane content. *Fuel,* 255**,** 115803, DOI: https://doi.org/10.1016/j.fuel.2019.115803.

Li, Z., Yan, X., Yuan, C. & Peng, Z. 2012. Intelligent fault diagnosis method for marine diesel engines using instantaneous angular speed. *Journal of Mechanical Science and Technology,* 26**,** 2413-2423, DOI: https://doi.org/10.1007/s12206-012-0621-2.

Ling, D., Huang, H.-Z., Song, W., Liu, Y. & Zuo, M. J. Design FMEA for a diesel engine using two risk priority numbers. Reliability and Maintainability Symposium (RAMS), 2012. IEEE, 1-5.

Liu, Z. & Karim, G. A. 1997. Simulation of combustion processes in gas-fuelled diesel engines. *Proceedings of the Institution of Mechanical Engineers, Part A: Journal of Power and Energy,* 211**,** 159-169, DOI: https://doi.org/10.1243/0957650971537079.

Livanos, G., Theotokatos, G. & Pagonis, D.-N. 2014. Techno-economic investigation of alternative propulsion plants for Ferries and RoRo ships. *Energy Conversion and Management,* 79**,** 640-651, DOI: https://doi.org/10.1016/j.enconman.2013.12.05.

Llamas, X. & Eriksson, L. 2014. Optimal Transient Control of a Heavy Duty Diesel Engine with EGR and VGT. *IFAC Proceedings Volumes,* 47**,** 11854-11859, DOI: https://doi.org/10.3182/20140824-6-ZA-1003.01520.

LR. 2018. *Class goes digital - LR Digital Compliance Framework* [Online]. Lloyd's Register website. Available: https://www.lr.org/en-gb/latest-news/class-goes-digital/ [Accessed 16/04/2020].

Ludu, A., Engelmayer, M., Thomas, B. & Lustgarten, G. 2007. Emission compliance strategy for multiapplication medium speed engines. Proceedings of the 25th CIMAC World Congress on Combustion Engine Technology, 21-24 May 2007, Hofburg, Vienna.

Ma, X., Li, Y., Qi, Y., Xu, H., Shuai, S. & Wang, J. 2016. Optical study of throttleless and EGR-controlled stoichiometric dual-fuel compression ignition combustion. *Fuel,* 182**,** 272-283, DOI: https://doi.org/10.1016/j.fuel.2016.05.021.

Maiboom, A. & Tauzia, X. 2011. NOx and PM emissions reduction on an automotive HSDI Diesel engine with water-in-diesel emulsion and EGR: An experimental study. *Fuel,* 90**,** 3179-3192, DOI: https://doi.org/10.1016/j.fuel.2011.06.014.

MAN 2012a. Costs and Benefits of LNG as Ship Fuel for Container Vessels. Copenhagen, Denmark: MAN Diesel & Turbo, Available: https://marine.mandieselturbo.com/docs/librariesprovider6/technical-papers/costs-and-benefits-of-lng.pdf?sfvrsn=18, [Accessed 17 June 2019].

MAN 2012b. SFOC Optimization Methods for MAN B&W Two-Stroke IMO Tier II Engines. Copenhagen, Denmark.

MAN 2012c. Tier III Two-Stroke Technology. Copenhagen, Denmark: MAN Diesel & Turbo, Available: https://marine.mandieselturbo.com/docs/librariesprovider6/technical-papers/tier-iii-two-stroke-technology.pdf?sfvrsn=18, [Accessed 17 June 2019].

MAN 2015. ME-GI Gas-ready Ship. Copenhagen, Denmark. Available: https://marine.man-es.com/docs/librariesprovider6/test/me-gi-gas-ready-ship-low.pdf?sfvrsn=706909a2_6.

MAN 2018. Emission project guide. *MAN Energy Solutions. Future in the making.* Copenhagen, Denmark: MAN Diesel & Turbo, Available.

Masaki, K., Yusuke, H. & Akihiro, T. 2019. Advanced Combustion Strategy for Medium-Speed Dual-Fuel Engine. Proceedings of the 29th CIMAC World Congress on Combustion Engine Technology, 10-14 June 2019, Vancouver, Canada.

Mavrelos, C. & Theotokatos, G. 2018. Numerical investigation of a premixed combustion large marine two-stroke dual fuel engine for optimising engine settings via parametric runs. *Energy conversion and management,* 160**,** 48-59, DOI: https://doi.org/10.1016/j.enconman.2017.12.097.

Mayr, P., Pirker, G., Wimmer, A. & Krenn, M. 2017. Simulation-Based Control of Transient SCE Operation. WCX™ 17: SAE World Congress Experience 28 March 2017, United States. SAE International.

McCollin, C. 1999. Working around failure. *Manufacturing Engineer.* Available: https://digital-library.theiet.org/content/journals/10.1049/me_19990114.

Meier, M., Sudwoj, G., Theodossopoulos, P., Tzanos, E. & Karakas, I. 2019. A Real Time Comprehensive Analysis of the Main Engine and Ship Data for Creating Value to Ship Operators. Proceedings of the 29th CIMAC World Congress on Combustion Engine Technology, 10-14 June 2019, Vancouver, Canada.

Menage, A., Gruand, A., Berg, P. & Golloch, R. 2013. The New Dual Fuel Engine 35/44 DF from MAN Diesel & Turbo SE. In: International Council on Combustion Engines Proceedings of the 27th CIMAC World Congress on Combustion Engine Technology 13–16 May 2013, Shanghai, China.

Merker, G. P., Schwarz, C., Stiesch, G. & Otto, F. 2005. *Simulating Combustion: Simulation of combustion and pollutant formation for engine-development*, Springer Science & Business Media.

Millo, F., Bernardi, M. G., Servetto, E. & Delneri, D. 2013. Computational Analysis of Different EGR Systems,Combined with Miller Cycle Concept for a Medium Speed Marine Diesel Engine. Proceedings of the 27th CIMAC World Congress on Combustion Engine Technology, 13-17 May 2013, Shanghai, China.

Mohr, H. & Baufeld, T. 2013. Improvement of Dual-Fuel-Engine Technology for Current & Future Applications. Proceedings of the 27th CIMAC World Congress on Combustion Engine Technology, 13–17 May 2013, Shanghai, China.

Moriyoshi, Y., Xiong, Q., Takahashi, Y., Kuboyama, T., Morikawa, K., Yamada, T., Suzuki, M., Tanoue, K. & Hashimoto, J. 2016. Combustion Analysis in a Natural Gas Engine with Pre-Chamber to Improve Thermal Efficiency. Proceedings of the 28th CIMAC World Congress on Combustion Engine Technology, 6–10 June 2016, Helsinki,Finland.

Nielsen, K., Blanke, M., Eriksson, L. & Vejlgaard-Laursen, M. 2018. Marine diesel engine control to meet emission requirements and maintain maneuverability. *Control Engineering Practice,* 76**,** 12-21, DOI: https://doi.org/10.1016/j.conengprac.2018.03.012.

NSF 2020. Cyber-Physical Systems (CPS) *Program Solicitation* National Science Foundation, Available: https://www.nsf.gov/pubs/2020/nsf20563/nsf20563.pdf.

Ntonas, K., Aretakis, N., Roumeliotis, I., Pariotis, E., Paraskevopoulos, Y. & Zannis, T. 2020. Integrated Simulation Framework for Assessing Turbocharger Fault Effects on Diesel-Engine Performance and Operability. *Journal of Energy Engineering,* 146**,** 04020023, DOI: doi:10.1061/(ASCE)EY.1943-7897.0000673.

Nylund, I. 2007. Field Experience with the Wärtsilä 50DF Dual Fuel Engine. Proceedings of the 25th CIMAC World Congress on Combustion Engine Technology, 21–24 May 2007, Vienna, Austria.

Nylund, I. & Ott, M. 2013. Development of a Dual Fuel technology for slow-speed engines. Proceedings of the 27th CIMAC World Congress on Combustion Engine Technology, 13–17 May 2013, Sanghai, China.

Olander, K. 2006. *Dual-fuel-electric for LNGC-Wärtsilä* [Online]. Korea, Daewoo Shipbuilding and Marine Engineering (DSME): Wärtsilä. Available: https://www.wartsila-hyundai.com/filedown?alias=adpds&file=Wartsila%2B50%2BDF%2BDual%2Bfuel%2Bengine%2Breference%2Bfor%2BLNGC%2B04%2B01%2B07%2Bppt.pdf. [Accessed 24/12/2019].

Ott, M., Nylund, I., Alder, R., Hirose, T., Umemoto, Y. & Yamada, T. 2016. The 2-stroke Low-Pressure Dual-Fuel Technology: From Concept to Reality. Proceedings of the 28th CIMAC World Congress on Combustion Engine Technology, 6–10 June 2016, Helsinki, Finland.

Ott, T., Zurbriggen, F., Onder, C. & Guzzella, L. 2013. Cylinder Individual Feedback Control of Combustion in a Dual Fuel Engine. *IFAC Proceedings Volumes,* 46**,** 600-605, DOI: https://doi.org/10.3182/20130904-4-JP-2042.00080.

Ozcan, H. & Yamin, J. A. A. 2008. Performance and emission characteristics of LPG powered four stroke SI engine under variable stroke length and compression ratio. *Energy Conversion and Management,* 49**,** 1193-1201, DOI: https://doi.org/10.1016/j.enconman.2007.09.004.

Pakarinen, R. 2012. IMO tier III and beyond. *Wärtsilä - Environment.* Available: https://www.wartsila.com/twentyfour7/environment/imo-tier-iii-and-beyond [Accessed 17 June 2019].

Papagiannakis, R. G., Rakopoulos, C. D., Hountalas, D. T. & Rakopoulos, D. C. 2010. Emission characteristics of high speed, dual fuel, compression ignition engine operating in a wide range of natural gas/diesel fuel proportions. *Fuel,* 89**,** 1397-1406, DOI: https://doi.org/10.1016/j.fuel.2009.11.001.

Park, H., Park, J., Park, M., Ghal, S. & Kim, S. 2013. NOx Reduction by Combination of Charge Air Moisturizer and Exhaust Gas Recirculation on Medium Speed Diesel

Engines. Proceedings of the 27th CIMAC World Congress on Combustion Engine Technology, 13-16 May 2013, Shanghai, China.

Park, J., Song, S. & Lee, K. S. 2015. Numerical investigation of a dual-loop EGR split strategy using a split index and multi-objective Pareto optimization. *Applied Energy,* 142**,** 21-32, DOI: https://doi.org/10.1016/j.apenergy.2014.12.030.

Pathirage, C., Amaratunga, R. & Haigh, R. 2007. The role of philosophical context in the development of theory: Towards methodological pluralism. *The Built and Human Environment Review,* 1, DOI,

Pavlenko, N., Comer, B., Zhou, Y., Clark, N. & Rutherford, D. 2020. The climate implications of using LNG as a marine fuel. The International Council on Clean Transportation, 2020, https://theicct.org/sites/default/files/publications/Climate_implications_LNG_marinefuel_01282020.pdf.

Perera, L. P. 2016a. Marine Engine Centered Localized Models for Sensor Fault Detection under Ship Performance Monitoring. *IFAC-PapersOnLine,* 49**,** 91-96, DOI: https://doi.org/10.1016/j.ifacol.2016.11.016.

Perera, L. P. 2016b. Statistical Filter based Sensor and DAQ Fault Detection for Onboard Ship Performance and Navigation Monitoring Systems. *IFAC-PapersOnLine,* 49**,** 323-328, DOI: https://doi.org/10.1016/j.ifacol.2016.10.362.

Pirker, G., Losonczi, B., Fimml, W., Wimmer, A. & Chmela, F. 2010. Predictive Simulation of Combustion and Emissions in Large Diesel Engines with Multiple Fuel Injection. Proceedings of the 26th CIMAC World Congress on Combustion Engine Technology, 14–17 June 2010, Bergen, Norway.

Portin, K. 2010. Wartsila dual fuel (DF) engines for offshore applications and mechanical drive. Proceedings of the 26th CIMAC World Congress on Combustion Engine Technology, 14–17 June 2010, Bergen, Norway.

Pueschel, M., Buchholz, B., Fink, C., Rickert, C. & Ruschmeyer, K. 2013. Combination of post-injection and cooled EGR at a medium-speed diesel engine to comply with IMO Tier III emission limits. Proceedings of the 27th CIMAC World Congress on Combustion Engine Technology, 13-16 May 2013, Shanghai, China.

Rakopoulos, C. D. & Giakoumis, E. G. 2007. Prediction of friction development during transient diesel engine operation using a detailed model. *International Journal of Vehicle Design,* 44, No.1/2**,** 143-166, DOI: https://doi.org/10.1504/IJVD.2007.013223.

Raptotasios, S., Sakellaridis, N., Papagiannakis, G. & Hountalas, D. 2015. Application of a multi-zone combustion model to investigate the NOx reduction potential of two-stroke marine diesel engines using EGR. *Applied Energy,* 157**,** 814-823, DOI: https://doi.org/10.1016/j.apenergy.2014.12.041.

Rickert, C., Banck, A., Ruschmeyer, K. & Ernst, S. 2016. Pros and Cons of Exhaust Gas Recirculation for Emission Reduction of Medium Speed Diesel Engines. Proceedings of the 28th CIMAC World Congress on Combustion Engine Technology, 6–10 June 2016, Helsinki, Finland.

Ritzke, J., Andree, S., Theile, M., Henke, B., Schleef, K., Nocke, J. & Hassel, E. 2016. Simulation of a Dual-Fuel Large Marine Engines using combined 0/1-D and 3-D Approaches. Proceedings of the 28th CIMAC World Congress on Combustion Engine Technology, 6–10 June 2016, Helsinki, Finland.

Roecker, R., Sarlashkar, J. & Anderson, G. 2016. State-Based Diesel Fuelling for Improved Transient Response in a Dual-Fuel Engine. Proceedings of the 28th CIMAC World Congress on Combustion Engine Technology, 6–10 June 2016, Helsinki, Finland.

Rudrabhate, S. D. & Chaitanya, S. V. 2017. Comaprision between EGR & SCR Technologies. Proceedings from the International Conference on Ideas, Impact and Innovation in Mechanical Engineering (ICIIIME), 2017. 856 – 861.

Samokhin, S., Sarjovaara, T., Zenger, K. & Larmi, M. 2014. Modeling and Control of Diesel Engines with a High-Pressure Exhaust Gas Recirculation System. *IFAC Proceedings Volumes,* 47**,** 3006-3011, DOI: https://doi.org/10.3182/20140824-6-ZA-1003.02231.

Saunders, M. N. K., Lewis, P. & Thornhill, A. 2009. *Research methods for business students,* New York, Prentice Hall.

Schlick, H. 2014. *AVL - Potentials and challenges of gas and dual-fuel engines for marine application* [Online]. Busan: CIMAC. Available: https://www.cimac.com/cms/upload/events/cascades/cascades_2014_busan/presentations/Presentation_Session2_AVL_CASCADES_Busan_Oct2014_Harald_Schlick.pdf [Accessed 24/12/2019].

Schmid, K. 2016. Cylinder Individual Combustion Control of Gas and Dual Fuel Engines. Proceedings of the 28th CIMAC World Congress on Combustion Engine Technology, 6–10 June 2016, Helsinki, Finland.

Sharif Ahmadian, A. 2016. Chapter 4 - Theories and Methodologies. *In:* SHARIF AHMADIAN, A. (ed.) *Numerical Models for Submerged Breakwaters.* Boston: Butterworth-Heinemann, Available: http://www.sciencedirect.com/science/article/pii/B9780128024133000043.

Shinsuke, M., Thomas, K., Robert, S., Michael, Z., Ingo, K. & Andrei, L. 2016. Holistic approach for performance and emission development of high speed gas and dual fuel engines. Proceedings of the 28th CIMAC World Congress on Combustion Engine Technology, 6–10 June 2016, Helsinki, Finland.

Singh, S., Kong, S.-C., Reitz, R. D., Krishnan, S. R. & Midkiff, K. C. 2004. Modeling and experiments of dual-fuel engine combustion and emissions. SAE 2004 World Congress & Exhibition, March 8 2004, United States. SAE International, 124-133.

Singh, S. & Subramanian, K. A. 2016. Experimental investigations of effects of EGR on performance and emissions characteristics of CNG fueled reactivity controlled compression ignition (RCCI) engine. *Energy Conversion and Management,* 130**,** 91-105, DOI: https://doi.org/10.1016/j.enconman.2016.10.044.

Sitkei, G. 1964. *Kraftstoffaufbereitung und Verbrennung bei Dieselmotoren*, Springer-Verlag Berlin Heidelberg.

Sixel, E. J., Hiltner, J. & Rickert, C. 2016. Use of 1-D simulation tools with a physical combustion model for the development of Diesel-Gas or Dual Fuel engines. Proceedings of the 28th CIMAC World Congress on Combustion Engine Technology, 6–10 June 2016, Helsinki, Finland.

Srinivasan, K. K., Krishnan, S. R. & Midkiff, K. C. 2006. Improving low load combustion, stability, and emissions in pilot-ignited natural gas engines. *Proceedings of the Institution of Mechanical Engineers, Part D: Journal of Automobile Engineering,* 220**,** 229-239, DOI: https://doi.org/10.1243/09544070JAUTO104.

Stefana, E., Marciano, F. & Alberti, M. 2016. Qualitative risk assessment of a Dual Fuel (LNG-Diesel) system for heavy-duty trucks. *Journal of Loss Prevention in the Process Industries,* 39**,** 39-58, DOI: https://doi.org/10.1016/j.jlp.2015.11.007.

Stork, M., Eisenbach, S., Spengler, S. & Toshev, P. 2019. Turbocharger Innovations for Compliance with Tier III Emission Limits. Proceedings of the 29th CIMAC World Congress on Combustion Engine Technology, 10-14 June 2019, Vancouver, Canada.

Stoumpos, S., Theotokatos, G., Boulougouris, E., Vassalos, D., Lazakis, I. & Livanos, G. 2018. Marine dual fuel engine modelling and parametric investigation of engine settings effect on performance-emissions trade-offs. *Ocean Engineering,* 157**,** 376-386, DOI: https://doi.org/10.1016/j.oceaneng.2018.03.059.

Stoumpos, S., Theotokatos, G., Mavrelos, C. & Boulougouris, E. 2020. Towards Marine Dual Fuel Engines Digital Twins—Integrated Modelling of Thermodynamic Processes and Control System Functions. *Journal of Marine Science and Engineering,* 8**,** 200, DOI: https://doi.org/10.3390/jmse8030200.

Sun, X., Liang, X., Shu, G., Lin, J., Wang, Y. & Wang, Y. 2017. Numerical investigation of two-stroke marine diesel engine emissions using exhaust gas recirculation at different

injection time. *Ocean Engineering,* 144**,** 90-97, DOI: https://doi.org/10.1016/j.oceaneng.2017.08.044.

Tay, S., Te Chuan, L., Aziati, A. & Ahmad, A. N. A. 2018. An Overview of Industry 4.0: Definition, Components, and Government Initiatives. *Journal of Advanced Research in Dynamical and Control Systems,* 10**,** 14, DOI,

Thangaraja, J. & Kannan, C. 2016. Effect of exhaust gas recirculation on advanced diesel combustion and alternate fuels - A review. *Applied Energy,* 180**,** 169-184, DOI: https://doi.org/10.1016/j.apenergy.2016.07.096.

Theotokatos, G. & Kyrtatos, N. P. 2003. Investigation of a Large High-Speed Diesel Engine Transient Behavior Including Compressor Surging and Emergency Shutdown. *Journal of Engineering for Gas Turbines and Power,* 125**,** 580-589, DOI: http://dx.doi.org/10.1115/1.1559903.

Theotokatos, G., Stoumpos, S., Bolbot, V. & Boulougouris, E. 2020. Simulation-based investigation of a marine dual-fuel engine. *Journal of Marine Engineering & Technology,* 19**,** 5-16, DOI: https://doi.org/10.1080/20464177.2020.1717266.

Theotokatos, G., Stoumpos, S., Bolbot, V., Boulougouris, E. & Vassalos, D. Marine Dual Fuel Engine Control System Modelling and Safety Implications Analysis. INEC/iSCSS – 14th International Naval Engineering Conference and Exhibition / International Ship Control System Symposium, October 2018a Glasgow.

Theotokatos, G., Stoumpos, S., Bolbot, V., Boulougouris, E. & Vassalos, D. 2018b. Marine Dual Fuel Engine Control System Modelling and Safety Implications Analysis. 14th International Naval Engineering Conference, 2018b, Glasgow, United Kingdom.

Theotokatos, G. & Tzelepis, V. 2015. A computational study on the performance and emission parameters mapping of a ship propulsion system. *Proceedings of the Institution of Mechanical Engineers, Part M: Journal of Engineering for the Maritime Environment,* 229**,** 58-76, DOI: https://doi.org/10.1177/1475090213498715.

Tinschmann, G., Thum, D., Schlueter, S., Pelemis, P. & Stiesch, G. 2010. Sailing towards IMO Tier III - Exhaust Aftertreatment versus Engine-Internal Technologies for Medium Speed Diesel Engines. Proceedings of the 26th CIMAC World Congress on Combustion Engine Technology, 14-17 June 2010, Bergen, Norway.

Trivyza, L. N., Rentizelas, A. & Theotokatos, G. 2020. A Comparative Analysis of EEDI Versus Lifetime CO2 Emissions. *Journal of Marine Science and Engineering,* 8, DOI: 10.3390/jmse8010061.

Tsaganos, G., Papachristos, D., Nikitakos, N., Dalaklis, D. & Ölcer, A. 2018. Fault Detection and Diagnosis of Two-Stroke Low-Speed Marine Engine with Machine Learning Algorithms. Proceeding of 3rd International Symposium on Naval Architecture and Maritime, 2018, Turkey, Instanbul.

Tsalaptis, D. 2015. Tier III Considerations. *Safety for Sea.* Available: https://safety4sea.com/wp-content/uploads/2015/01/5.4-D.Tsalapatis-COSTAMARE.pdf [Accessed 20/11/2019].

Tse, Y. L. & Tse, P. W. 2014. A low-cost and effective automobile engine fault diagnosis using instantaneous angular velocity evaluation. *International Journal of Strategic Engineering Asset Management,* 2**,** 2-21, DOI: https://doi.org/10.1504/IJSEAM.2014.063884.

US-DOE 2017. Clean Cities Alternative Fuel Price Report. Washington, United States. Available: https://afdc.energy.gov/files/u/publication/alternative_fuel_price_report_jan_2017.pdf.

Vera-García, F., Pagán Rubio, J. A., Hernández Grau, J. & Albaladejo Hernández, D. 2019. Improvements of a Failure Database for Marine Diesel Engines Using the RCM and Simulations. *Energies,* 13**,** 104, DOI, https://www.mdpi.com/1996-1073/13/1/104

Verschaeren, R., Schaepdryver, W., Serruys, T., Bastiaen, M., Vervaeke, L. & Verhelst, S. 2014. Experimental study of NOx reduction on a medium speed heavy duty diesel engine by

the application of EGR (exhaust gas recirculation) and Miller timing. *Energy,* 76**,** 614-621, DOI: https://doi.org/10.1016/j.energy.2014.08.059.

Vincoli, J. W. 2014. *Basic guide to system safety,* USA, New Jersey, John Wiley & Sons.

Vuollet, T., Hyvönen, J., Kaas, T., Lasén, F., Lendormy, E. & Vettenranta, N. 2019. Engine Controls as Part of a Smart Marine Ecosystem. Proceedings of the 29th CIMAC World Congress on Combustion Engine Technology, 10-14 June 2019, Vancouver, Canada.

Walker, T. R., Adebambo, O., Del Aguila Feijoo, M. C., Elhaimer, E., Hossain, T., Edwards, S. J., Morrison, C. E., Romo, J., Sharma, N., Taylor, S. & Zomorodi, S. 2019. Chapter 27 - Environmental Effects of Marine Transportation. *In:* SHEPPARD, C. (ed.) *World Seas: an Environmental Evaluation (Second Edition).* Academic Press, Available: http://www.sciencedirect.com/science/article/pii/B9780128050521000309.

Wang, B., Li, T., Ge, L. & Ogawa, H. 2016a. Optimization of combustion chamber geometry for natural gas engines with diesel micro-pilot-induced ignition. *Energy conversion and management,* 122**,** 552-563, DOI: https://doi.org/10.1016/j.enconman.2016.06.027.

Wang, H., Kolmanovsky, I., Sun, J. & Ozaki, Y. 2015. Feedback control during mode transition for a marine dual fuel engine. *IFAC-PapersOnLine,* 48**,** 279-284, DOI: https://doi.org/10.1016/ j.ifacol.2015.10.293.

Wang, L., Chen, Z., Yang, B., Zeng, K., Zhang, K. & Jin, Z. 2016b. Control Strategy Development of Natural Gas/Diesel Dual Fuel Engine for Heavy Duty Vehicle. SAE 2016 World Congress and Exhibition 5 April 2016b, United States. SAE International.

Wang, Z., Zhou, S., Feng, Y. & Zhu, Y. 2017. Research of NOx reduction on a low-speed two-stroke marine diesel engine by using EGR (exhaust gas recirculation)–CB (cylinder bypass) and EGB (exhaust gas bypass). *International Journal of Hydrogen Energy,* 42**,** 19337-19345, DOI: https://doi.org/10.1016/j.ijhydene.2017.06.009.

Wärtsilä 2004. 27 - Wärtsilä. *In:* WOODYARD, D. (ed.) *Pounder's Marine Diesel Engines (Eighth Edition).* Oxford: Butterworth-Heinemann, Available: http://www.sciencedirect.com/science/article/pii/B9780750658461500286.

Wärtsilä. 2009. *Wärtsilä 50DF Engine Technology* [Online]. Wärtsilä. Available: https://cdn.wartsila.com/docs/default-source/power-plants-documents/wärtsilä-50df.pdf [Accessed 08.2007].

Wärtsilä. 2015a. The Dual Fuel Technology. Available: https://www.onthemosway.eu/wp-content/uploads/2015/10/5.pdf [Accessed 08/04/2020].

Wärtsilä 2015b. Improving engine fuel and operational efficiency. Finland. Available: https://cdn.wartsila.com/docs/default-source/services-documents/white-papers/wartsila-bwp---improving-engine-fuel-and-operational-efficiency.pdf?sfvrsn=b1fcc345_10.

Wärtsilä 2017. LNG shipping solutions. Wärtsilä Available: https://cdn.wartsila.com/docs/default-source/oil-gas-documents/brochure-lng-shipping-solutions.pdf?utm_source=engines&utm_medium=dfengines&utm_term=dfengines&utm_cont, [Accessed 14 June 2019].

Wärtsilä 2019a. Wärtsilä 31DF Product Guide. Finland Oy: Wärtsilä, Available: https://cdn.wartsila.com/docs/default-source/product-files/engines/df-engine/product-guide-o-e-w31df.pdf, [Accessed 14 June 2019].

Wärtsilä. 2019b. *Wärtsilä 50DF Information (Product guide, Drawings and 3D models)* [Online]. Wärtsilä. Available: https://www.wartsila.com/marine/build/engines-and-generating-sets/dual-fuel-engines/wartsila-50df [Accessed 13/11/2019].

Wärtsilä. 2020. *Miller Timing* [Online]. Wärtsilä. Available: https://www.wartsila.com/encyclopedia/term/miller-timing [Accessed 08/04/2020].

Wenig, M., Roggendorf, K. & Fogla, N. 2019. Towards Predictive Dual-Fuel Combustion and Prechamber Modeling for Large Two-Stroke Engines in the Scope of 0D/1D Simulation. Proceedings of the 29th CIMAC World Congress on Combustion Engine Technology, 10-14 June 2019, Vancouver, Canada.

Wenzheng, Z., YuShan, J., Feixiang, S., Feng, W., Li, H. & Tao, P. 2019. Tier III Emission Development of a Marine Medium-Speed Diesel Engine Based on Virtual Calibration Method. Proceedings of the 29th CIMAC World Congress on Combustion Engine Technology, 10-14 June 2019, Vancouver, Canada.

WinGD. 2017. *SCF Group chooses WinGD's X-DF technology for the first ever gas-powered Aframax tanker* [Online]. Available: https://www.wingd.com/en/news-media/media/press-releases/scf-group-chooses-wingd%E2%80%99s-x-df-technology-for-the-first-ever-gas-powered-aframax-tanker/ [Accessed 14/06/2019].

WinGD. 2019. *2-stroke dual fuel engine safety concept* [Online]. Available: https://www.wingd.com/en/documents/concept-guidances/dg9727-df-safety-concept/ [Accessed 13/11/2019].

Wingrove, M. 2019. AI will be the next maritime technology growth sector. *Riviera.* Available: https://www.rivieramm.com/news-content-hub/ai-will-be-the-next-maritime-technology-growth-sector-22009 [Accessed 13/11/2019].

Wirth, K. 2010. Emissions Reduction Opportunities on MaK Engines. Proceedings of the 26th CIMAC World Congress on Combustion Engine Technology, 14-17 June 2010, Bergen, Norway.

Woodward. 2014. *PG - EG Actuator Hydraulic Powered Electric Actuator for Engine Control* [Online]. Available: https://www.google.com/url?sa=t&rct=j&q=&esrc=s&source=web&cd=1&cad=rja&uact=8&ved=2ahUKEwjupZei373pAhWCgVwKHZ1ECLYQFjAAegQIBRAC&url=https%3A%2F%2Fwww.woodward.com%2FWorkArea%2FDownloadAsset.aspx%3Fid%3D2147483831&usg=AOvVaw2eNioPpQbC6RmdSGuoOUkt [Accessed 18/05/2020].

Woodward. 2015a. *Product Specification 03316 - Solenoid Operated Gas Admission Valve (SOVAG) 250* [Online]. Available: https://www.pmcontrol.com.au/attachments/PMControl/products/46/SOGAV%20250.pdf [Accessed 18/05/2020].

Woodward. 2015b. *Product Specification 03413 - R - 11 and R - 30 R - Series Electric Actuators with Integral Driver* [Online]. Available: https://www.turner-ecs.com/cms/product/pdf/03413%20R11-30.pdf [Accessed 18/05/2020].

Woodyard, D. 2009. *Pounder's Marine Diesel Engines and Gas Turbines (Ninth Edition),* Oxford, Butterworth-Heinemann.

Woschni, G. 1967. A Universally Applicable Equation for the Instantaneous Heat Transfer Coefficient in the Internal Combustion Engine. 1967-02-01 1967. SAE International.

Wu, H. W., Hsu, T. Z. & Lai, W. H. 2018. Dual Fuel Turbocharged Engine Operated with Exhaust Gas Recirculation. *Journal of Mechanics,* 34**,** 21-27, DOI: https://doi.org/10.1017/jmech.2016.32.

Xi, W., Li, Z., Tian, Z. & Duan, Z. 2018. A feature extraction and visualization method for fault detection of marine diesel engines. *Measurement,* 116**,** 429-437, DOI: https://doi.org/10.1016/j.measurement.2017.11.035.

Xin, Q. 2013. Durability and reliability in diesel engine system design. *In:* XIN, Q. (ed.) *Diesel Engine System Design.* Woodhead Publishing, Available:

Xu, S., Anderson, D., Hoffman, M., Prucka, R. & Filipi, Z. 2016. A phenomenological combustion analysis of a dual-fuel natural-gas diesel engine. *Proceedings of the Institution of Mechanical Engineers, Part D: Journal of Automobile Engineering,* 231**,** 66-83, DOI: https://doi.org/10.1177/0954407016633337.

Xu, S., Anderson, D., Singh, A., Hoffman, M., Prucka, R. & Filipi, Z. 2014. Development of a phenomenological dual-fuel natural gas diesel engine simulation and its use for analysis of transient operations. SAE 2014 International Powertrain, Fuels & Lubricants Meeting, October 13 2014, United States. SAE International Journal of Engines, 1665-1673.

Yang, B., Xi, C., Wei, X., Zeng, K. & Lai, M.-C. 2015. Parametric investigation of natural gas port injection and diesel pilot injection on the combustion and emissions of a turbocharged common rail dual-fuel engine at low load. *Applied Energy,* 143**,** 130-137, DOI: https://doi.org/10.1016/j.apenergy.2015.01.037.

Yasin, M., Hafizil, M., Perowansa, P., Rizalman, M. & Mohd Hafiz, A. 2015. Fundamental Study of Dual Fuel on Exhaust Gas Recirculation (EGR) Operating with a Diesel Engine. *Applied Mechanics and Materials,* 773-774**,** 415-419, DOI: https://doi.org/10.4028/www.scientific.net/AMM.773-774.415.

Yin, B., Wang, J., Yang, K. & Jia, H. 2014. Optimization of EGR and split injection strategy for light vehicle diesel low temperature combustion. *International Journal of Automotive Technology,* 15**,** 1043-1051, DOI: 10.1007/s12239-014-0108-5.

Zamboni, G. & Capobianco, M. 2013. Influence of high and low pressure EGR and VGT control on in-cylinder pressure diagrams and rate of heat release in an automotive turbocharged diesel engine. *Applied Thermal Engineering,* 51**,** 586-596, DOI: https://doi.org/10.1016/j.applthermaleng.2012.09.040.

Zhang, Q., Li, N. & Li, M. 2016. Combustion and emission characteristics of an electronically-controlled common-rail dual-fuel engine. *Journal of the Energy Institute,* 89**,** 766-781, DOI: https://doi.org/10.1016/j.joei.2015.03.012.

Zhao, Z., Yang, Y., Zhou, J., Li, L. & Yang, Q. 2018. Adaptive fault-tolerant PI tracking control for ship propulsion system. *ISA transactions,* 80**,** 279-285, DOI: https://doi.org/10.1016/j.isatra.2018.07.004.

Zhou, J. H., Cheung, C. S. & Leung, C. W. 2014. Combustion, performance and emissions of a diesel engine with H2, CH4 and H2–CH4 addition. *International Journal of Hydrogen Energy,* 39**,** 4611-4621, DOI: https://doi.org/10.1016/j.ijhydene.2013.12.194.

Zidani, F., Diallo, D., Benbouzid, M. E. H. & Berthelot, E. Diagnosis of Speed Sensor Failure in Induction Motor Drive. 2007 IEEE International Electric Machines & Drives Conference, 3-5 May 2007 2007. 1680-1684.

Zúñiga, A. A., Baleia, A., Fernandes, J. & Branco, J. P. 2020. Classical Failure Modes and Effects Analysis in the Context of Smart Grid Cyber-Physical Systems. *Energies,* 13, DOI: https://doi.org/10.3390/en13051215.

Zymaris, A., Alnes, Ø., Knutsen, K. E. & Kakalis, N. 2016. Towards a model-based condition assessment of complex marine machinery systems using systems engineering. European Conference of the PHM Society 2016, Bilbao, Spain.

10 APPENDICES

APPENDIX A – RESULTS NORMALISATION

All the presented parameters are provided in a normalised basis by using the corresponding values of the parameters presented in Table 10.1. The exhaust gas temperature was normalised by using [K].

Table 10.1 Parameters reference values for results normalisation

Parameter	**Unit**	**Normalisation**
Engine load	[%]	Engine MCR (100% load)
Engine speed	[rpm]	Engine nominal speed as per manufacturer
Diesel fuel mass	[g/cyl/cycle]	Diesel fuel amount in diesel mode for 110% load
Gas fuel mass	[g/cyl/cycle]	Gas fuel amount in gas mode for 100% load
BSFC	[g/kWh]	BSFC at 25% load in diesel mode
BSEC	[kJ/kWh]	BSEC at 25% in gas mode
Charge air pressure	[bar]	Charge air pressure in diesel mode for 100% load
T/C speed	[rpm]	Maximum T/C speed from T/C manufacturer (alarm limit)
EWG opening angle	[deg]	EWG valve opening angle
Temperature before/after T/C turbine	[K]	Maximum temperature as per manufacturer alarm limit
Max. cylinder pressure	[bar]	Maximum cylinder pressure as per manufacturer alarm limit
Brake efficiency	[%]	Brake efficiency at 25% at gas mode
NO_x	[g/kWh]	NO_x weighted value as per emissions report (in accordance with NO_x Technical Code (IMO, 2014a), E2 test cycle)
CO_2	[g/kWh]	CO_2 emissions for 100% load

APPENDIX B – MODEL CONSTANTS

The model PID controller constants, tuned by using the Ziegler-Nichols method according to the guidelines provided in Leigh (1987), Graf (2013) and (GT, 2019), are presented in Table 10.2. The single (diesel mode) and triple-Wiebe (gas mode) function parameters for 100% engine load are presented Table 10.3 and Table 10.4 respectively.

Table 10.2 PID controllers constants

Controller	Description	Parameter value
Diesel fuel	Proportional Gain	0.0278
	Integral Gain	0.0483
	Derivative Gain	—
Gas fuel	Proportional Gain	0.2711
	Integral Gain	0.1254
	Derivative Gain	—

Table 10.3 Single-Wiebe function parameters (diesel mode 100% load)

Description	Units	Parameter value	
		Without EGR	With EGR
Start of combustion	[deg]	4.2	6.5
Main Duration	[°CA]	56	67
Main Exponent/ function shape factor	[-]	1	1

Table 10.4 Triple-Wiebe function parameters (gas mode, 100% load)

Description	Units	Parameter value		
		Premix	Main	Tail
Fraction of Fuel per Wiebe Curve	[deg]	0.025	0.95	0.025
Start of combustion	[°CA]	-16.7	-16.7	8
Duration (10% Burned to 90% Burned)	[°CA]	15.3	56.3	30
Wiebe Exponent/ function shape factor	[-]	1.5	2.5	2

APPENDIX C – DATA-DRIVEN MODEL NNS DATA LINEAR REGRESSION AND RESPONSE SURFACES

This appendix presents the linear regression of the measured DT data compared against the DD model predicted values as well as the generated response surfaces from the NNs for each EDS monitored operational parameter of the engine. The results presented herein, were generated for a range ambient and A/C coolant temperatures in the diesel and gas modes at 100% load. In addition, the results presented in the following figures represent only one GVU gas pressure value (5.92 bar) and one LHV of diesel and gas fuels (46 and 49 MJ/kg respectively) from the investigated range of these parameters.

Table 10.5 Data-driven model parameters

Engine parameter	**Model parameter name**
Load	loa
Diesel fuel rack position	output1 (in diesel mode)
Max. cylinder pressure	cylpmax
Charge air pressure	pav
Charge air temperature	tav0
Charge air mass flow rate	favl
T/C speed	trb_rpma
Exhaust gas pressure – T/C inlet	trb_pia0
Exhaust gas temperature – T/C inlet	trb_tia0
Exhaust gas temperature – T/C outlet	trb_tot
EWG opening	trb_dwga
Gas (fuel) manifold pressure	gpav0
Gas injection duration	output1 (in gas mode)
Air−fuel equivalence ratio	ealambda
Brake specific NO_x	bsnoxnew
Brake specific CO_2	bsCO2
BSFC	bsfc_sys
Brake efficiency	Beff_sys
BMEP	bmep_sys
Brake Power	bpower_sys

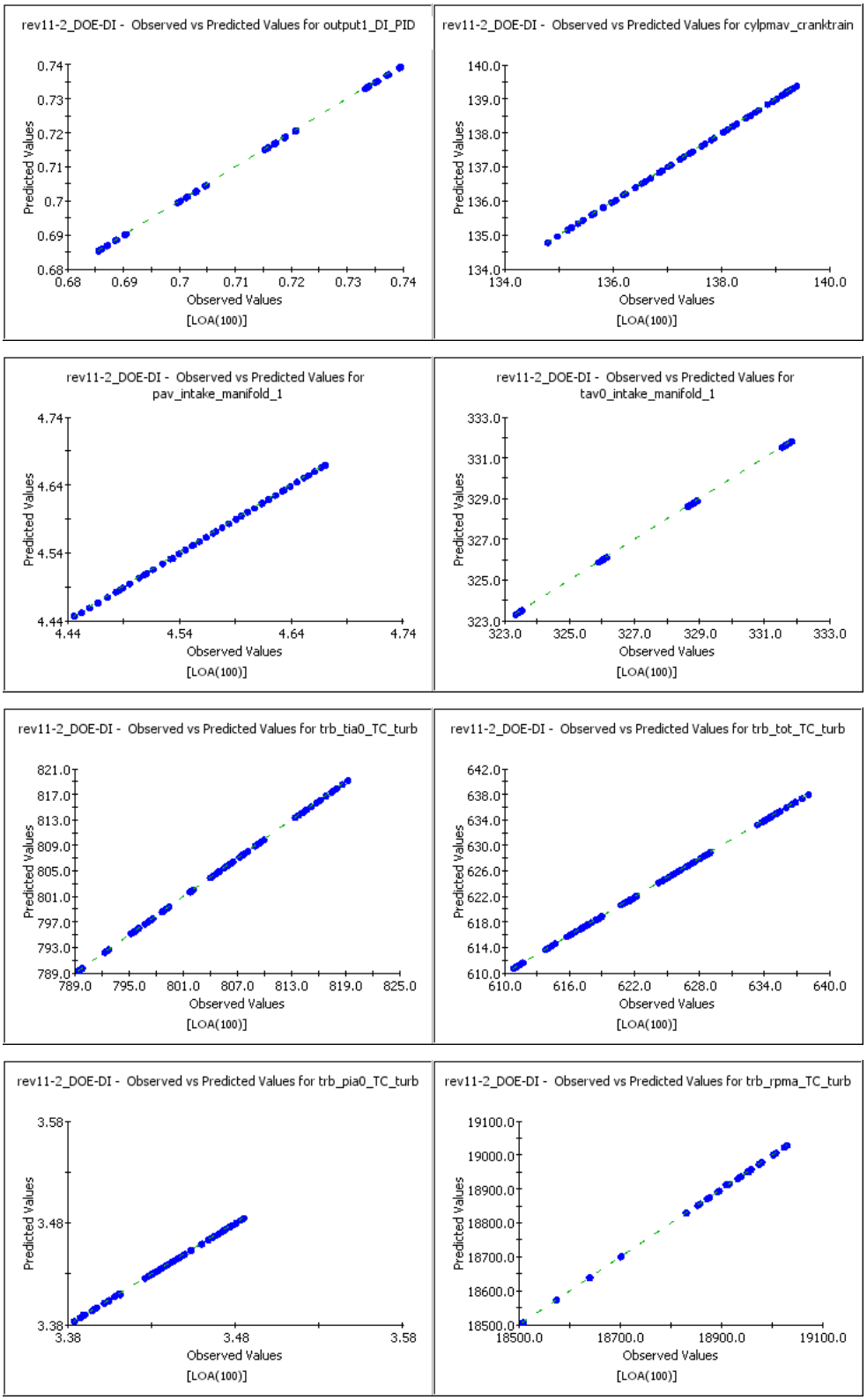

Figure 10.1 Data linear regression for 100% load; diesel mode

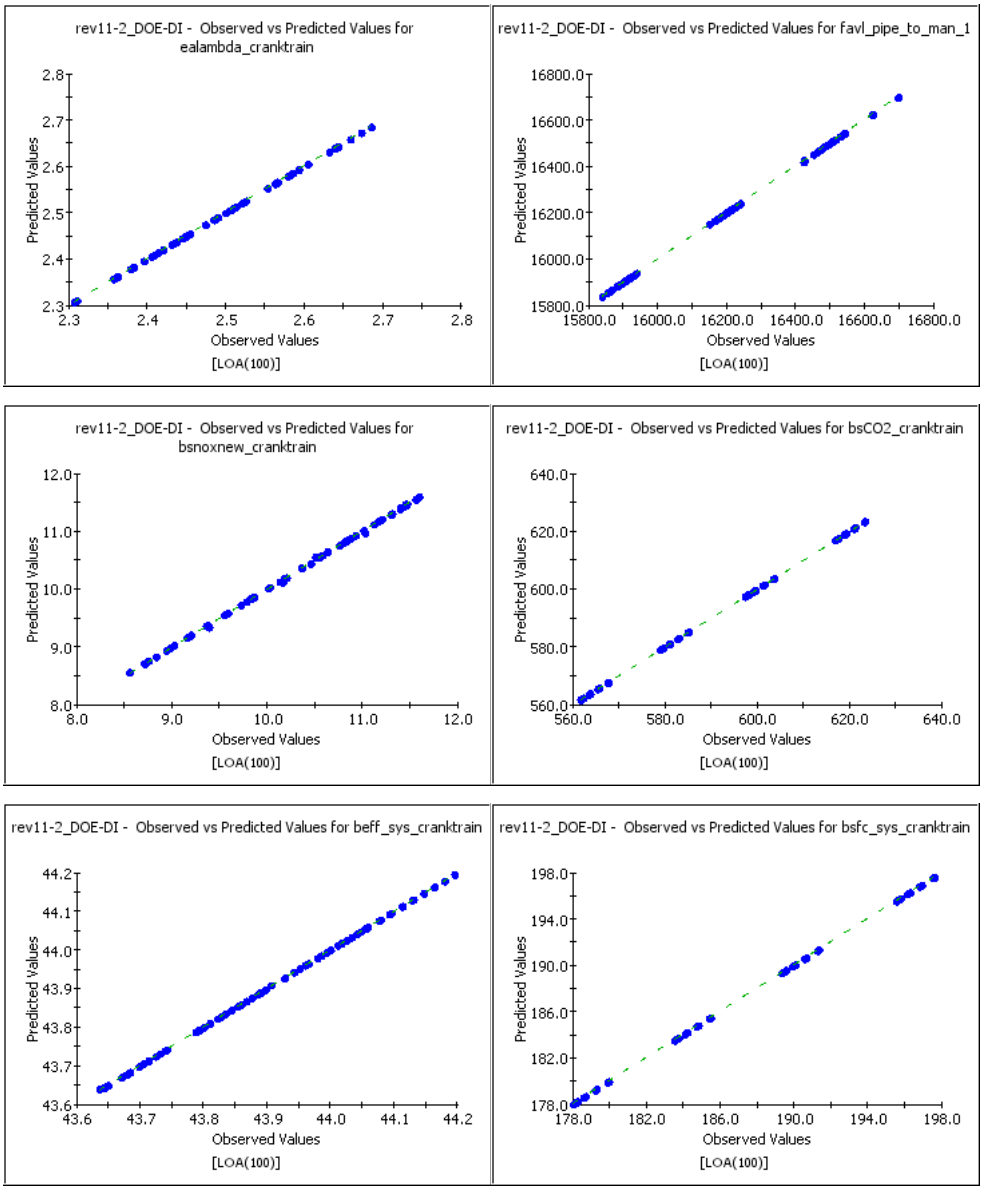

Figure 10.2 Data linear regression for 100% load in diesel mode

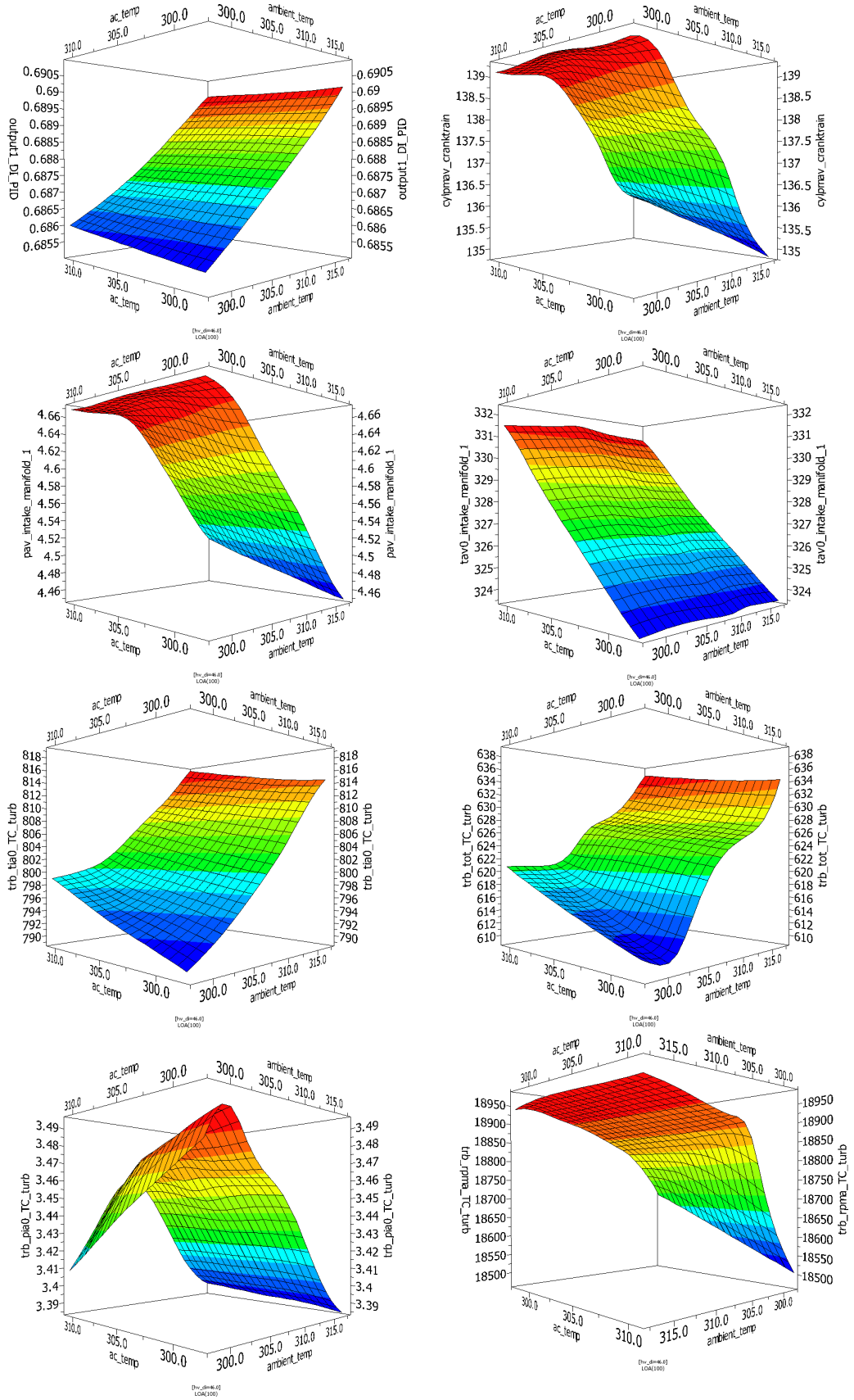

Figure 10.3 DD response surfaces for 100% load in diesel mode

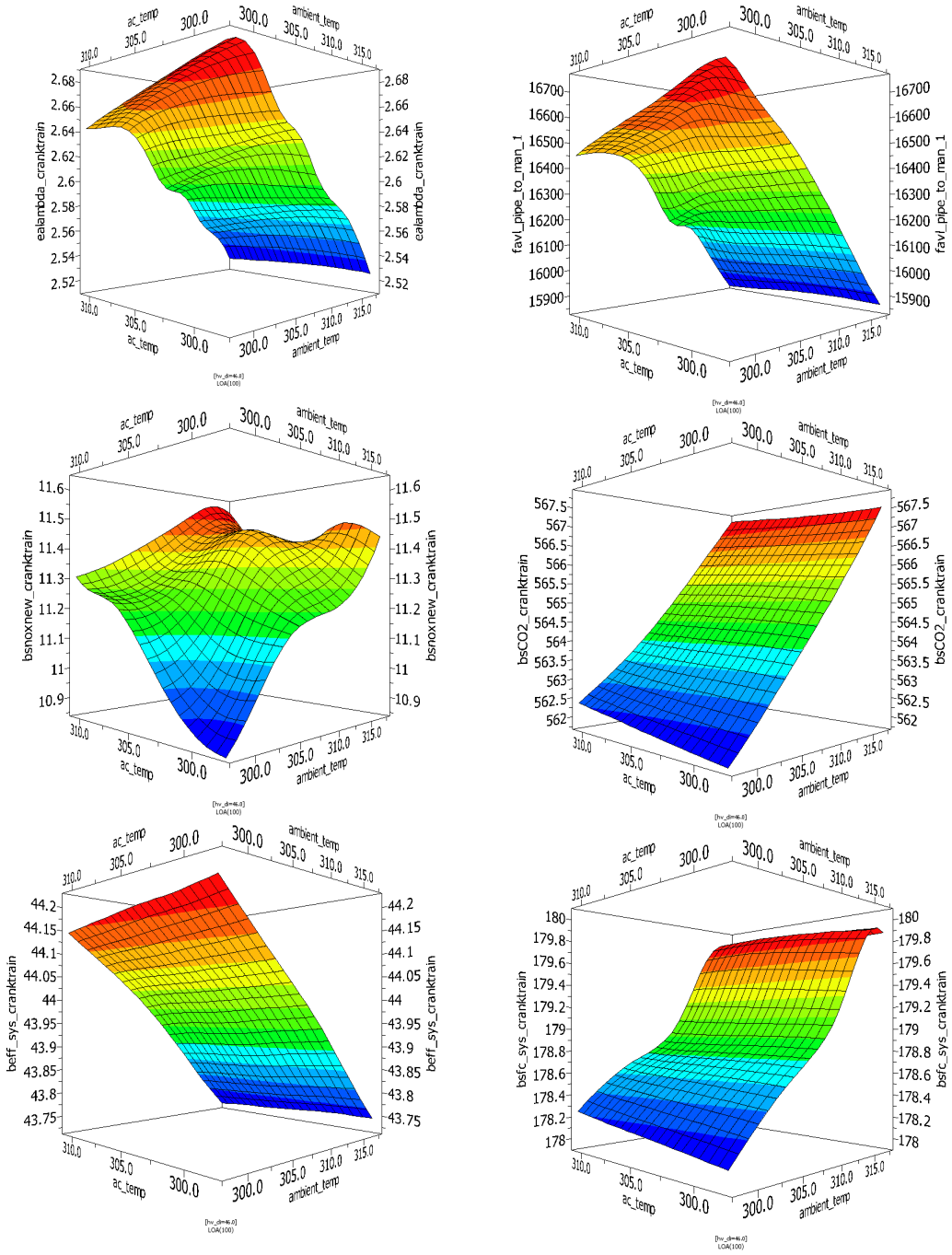

Figure 10.4 DD response surfaces for 100% load in diesel mode

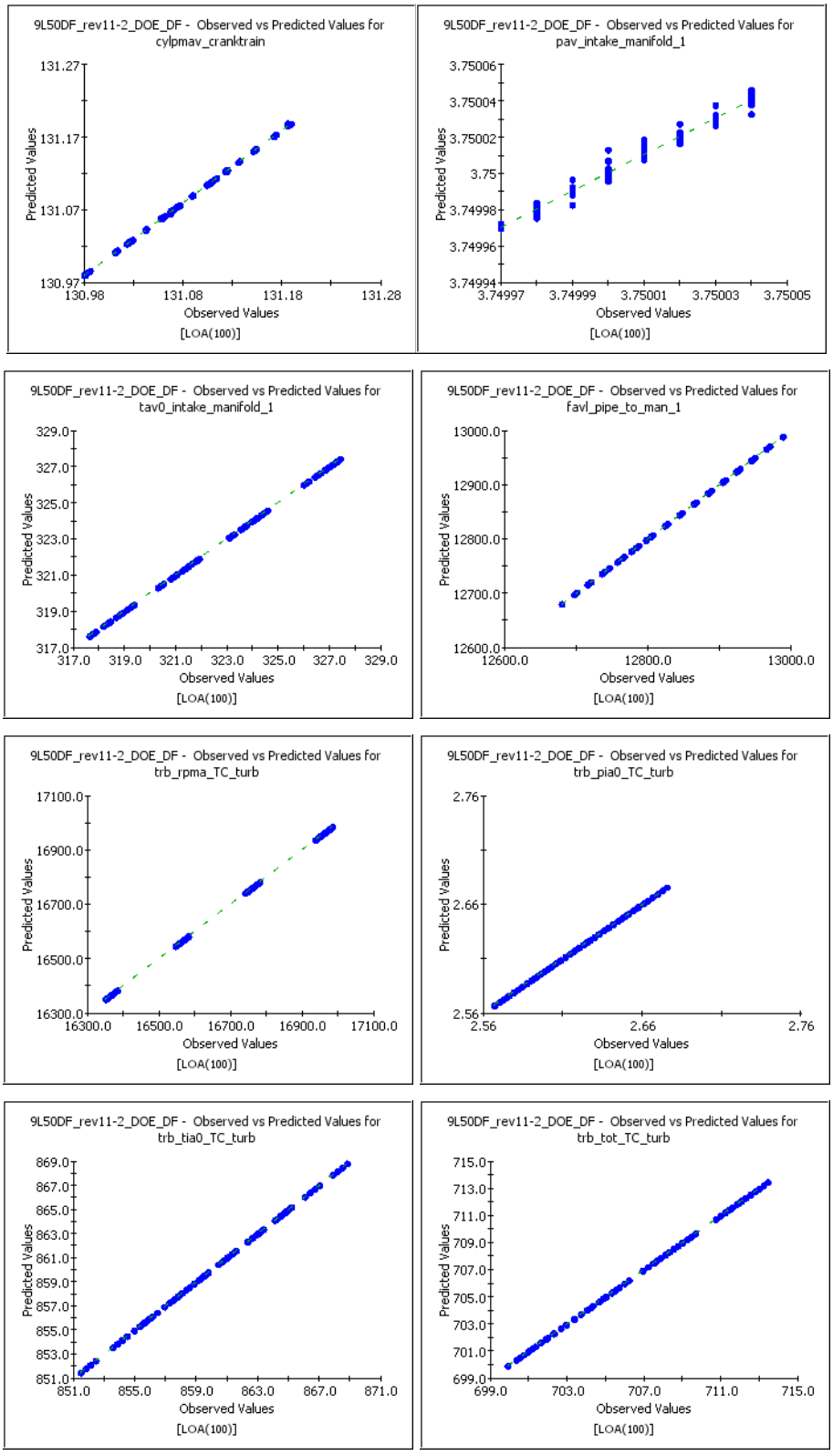

Figure 10.5 Data linear regression for 100% load in gas mode

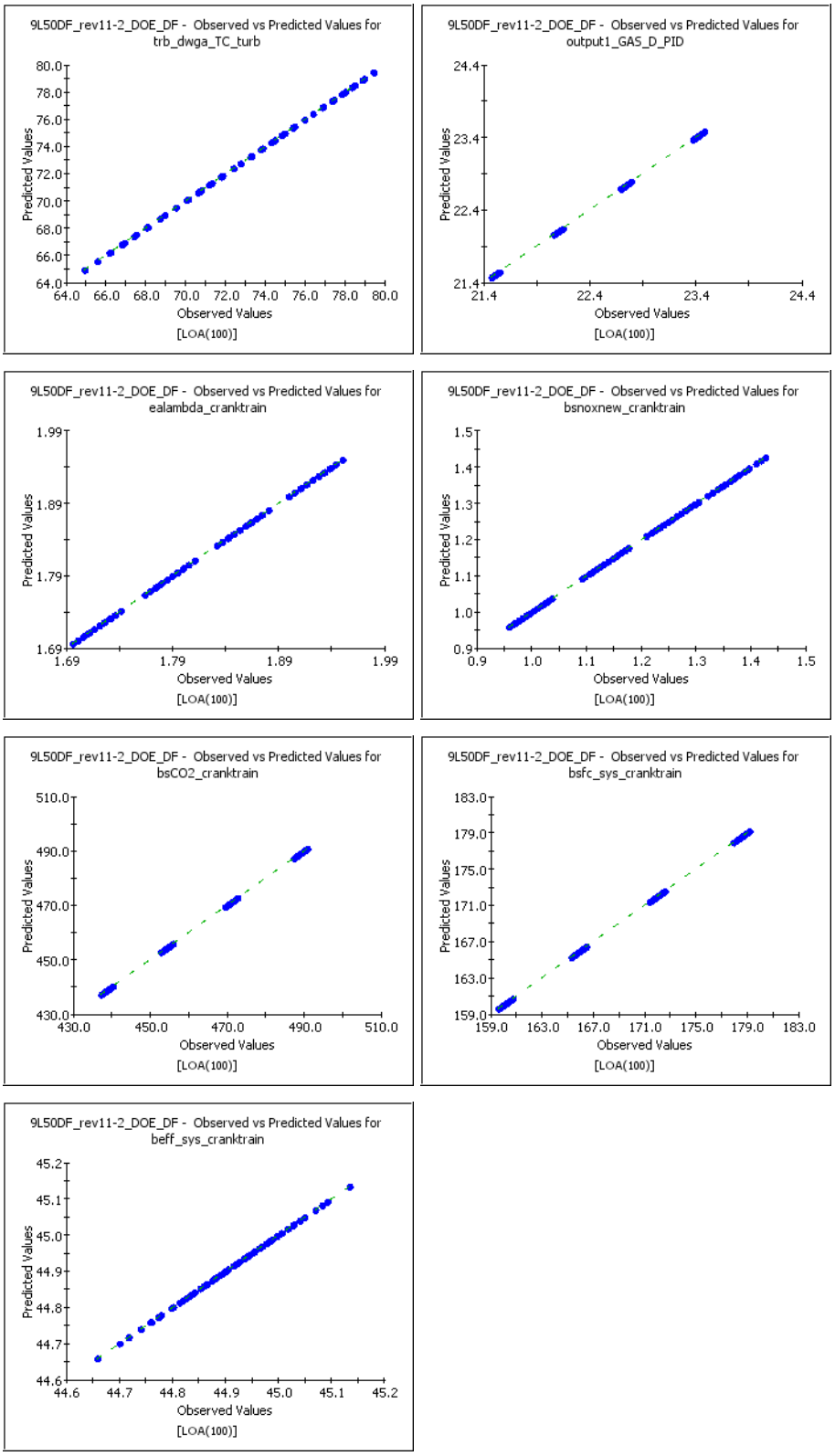

Figure 10.6 Data linear regression for 100% load in gas mode

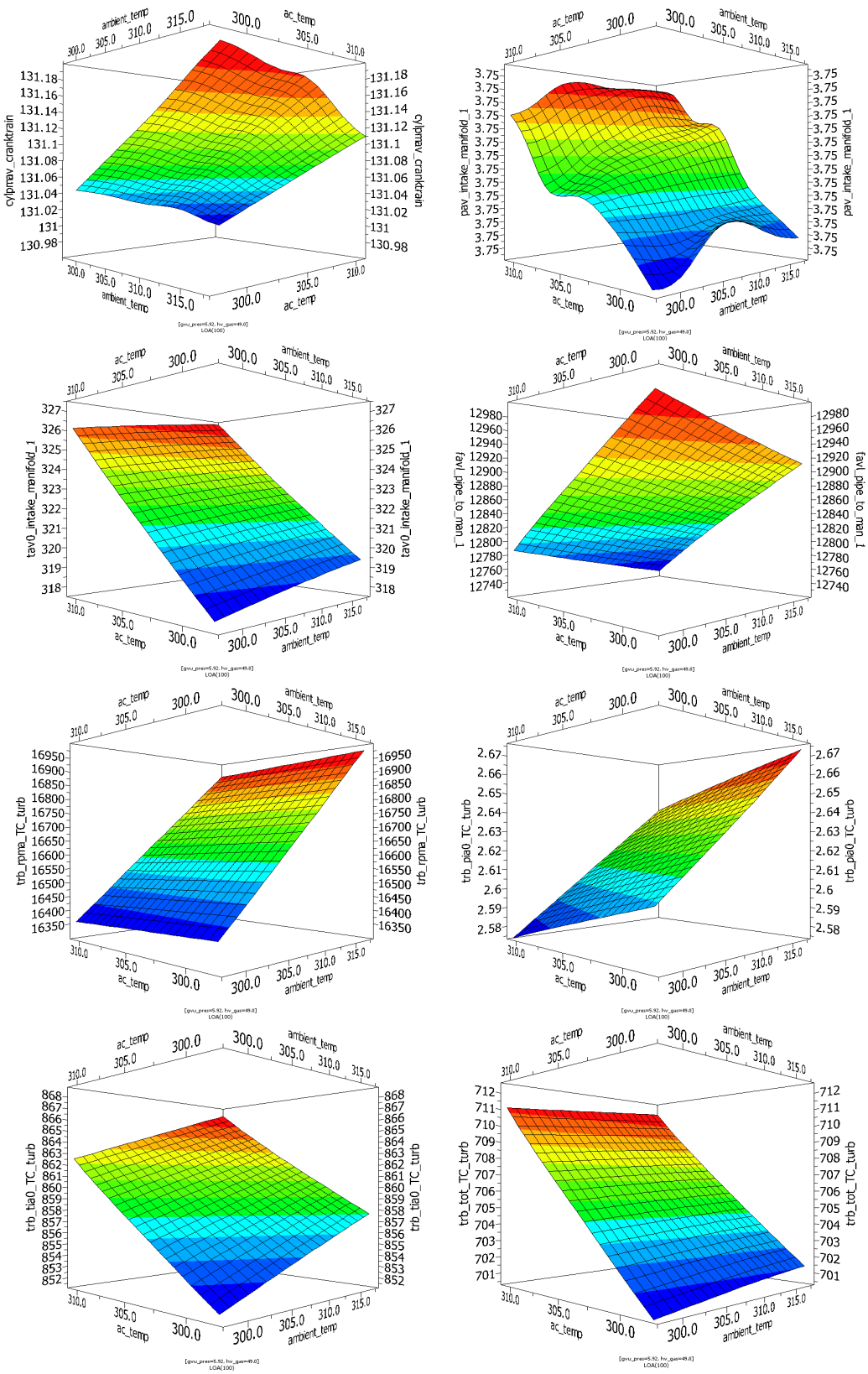

Figure 10.7 DD response surfaces for 100% load in gas mode

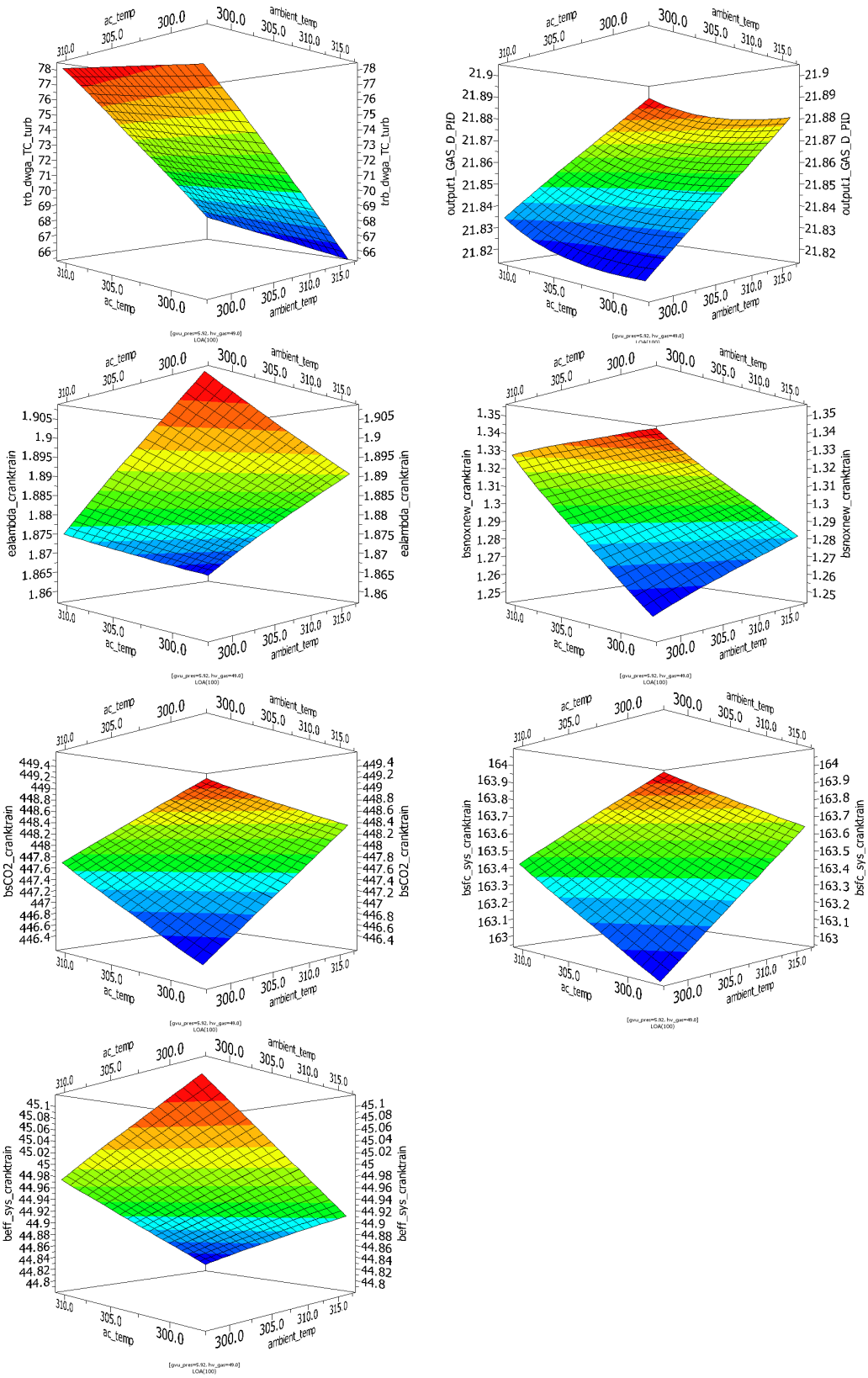

Figure 10.8 DD response surfaces for 100% load in gas mode